**THESE**

Pour l'obtention du titre de

**Docteure de l'Université de Lille**

Discipline : Aspects moléculaires et cellulaires de la biologie

Présentée et soutenue par

**Hala MANSOUR**

Le 17 Novembre 2023

# Characterization of GEXP15 as a Potential Regulator of Protein Phosphatase 1 in *Plasmodium falciparum*

**Composition du jury :**

Professeur Benoit FOLIGNE, Président

Professeur Marie-France DELAUW, Rapporteur

Professeur Philippe GRELLIER, Rapporteur

Docteur Alejandro CABEZAS-CRUZ, Examinateur

**Docteur Jamal KHALIFE, Directeur de thèse**

# Résumé

Le paludisme est l'une des maladies infectieuses les plus répandues, menaçant 40% de la population mondiale, provoquant environ 300 millions de cas et 450 000 décès chaque année, touchant principalement les enfants de moins de 5 ans. En l'absence d'un vaccin efficace et face à l'émergence de la résistance aux médicaments, il y a un besoin urgent pour mieux comprendre la biologie du parasite afin de proposer des traitements innovants. Le parasite du paludisme, *Plasmodium*, responsable de la maladie, présente un cycle de vie complexe et un processus de division cellulaire unique. Par rapport aux systèmes bien étudiés, la connaissance limitée de la biologie du *Plasmodium* empêche le développement thérapeutique. La phosphorylation des protéines, un mécanisme de régulation important, est moins comprise dans *Plasmodium* que dans les cellules mammifères ou de levure. Les kinases et les phosphatases impliquées dans la phosphorylation et la déphosphorylation respectivement sont des cibles potentielles de médicaments. La sous-unité catalytique de la protéine phosphatase de type 1 (PP1c) (PF3D7_1414400) opère en combinaison avec diverses protéines régulatrices pour diriger et contrôler spécifiquement son activité phosphatase. Cependant, peu d'informations sont disponibles sur cette phosphatase et ses régulateurs dans le parasite du paludisme humain, *Plasmodium falciparum*. Pour combler cette lacune de connaissances, nous avons mené une étude approfondie sur les caractéristiques structurelles et fonctionnelles d'un régulateur spécifique du *Plasmodium* appelé, Gametocyte EXported Protein 15, GEXP15 (PF3D7_1031600). Par analyses in silico, nous avons identifié trois régions d'intérêt significatives dans GEXP15 : une région N-terminale couvrant un motif RVxF interagissant avec PP1, un domaine conservé dont la fonction est inconnue, et un domaine de type GYF qui facilite potentiellement des interactions spécifiques protéine-protéine. Pour élucider davantage le rôle de GEXP15, nous avons réalisé des études d'interaction in vitro qui ont démontré une interaction directe entre GEXP15 et PP1 via le motif de liaison RVxF. Cette interaction avec PfGEXP15 a été montrée capable d'augmenter l'activité phosphatase de PP1 *in vitro*. De plus, en utilisant une lignée transgénique de *P. falciparum* exprimant la GEXP15-GFP, nous avons observé une forte expression de GEXP15 dans les stades asexués tardifs du parasite, avec une localisation principalement dans le noyau. Des expériences d'immunoprécipitation suivies d'analyses en spectrométrie de masse ont révélé l'interaction de GEXP15 avec des protéines de liaison aux ribosomes et à l'ARN. De plus, grâce à des analyses de capture de domaines fonctionnels recombinants de GEXP15 marqués avec un tag His, nous avons confirmé sa liaison avec PfPP1 et au complexe ribosomal via le domaine GYF. Dans l'ensemble, notre étude éclaire l'interaction PfGEXP15–PP1–ribosome, qui joue un rôle crucial dans la traduction des

protéines. Ces découvertes suggèrent que PfGEXP15 pourrait être une cible potentielle pour le développement de médicaments contre le paludisme.

**Mots clé :** Protéine Phosphatase de type 1; *Plasmodium*; Paludisme; GEXP15; CD2BP2; GYF; ribosomes

# Abstract

Malaria is one of the most prevalent vector-borne infectious diseases threatening 40% of the global population, causing around 300 million cases and 450,000 deaths annually, mostly affecting children under 5. With no effective vaccine and drug resistance emerging, there is an urgent need for innovative treatments. The malaria-causing *Plasmodium* parasite has a complex life cycle and unique cell division process. Compared to well-studied systems, limited knowledge of *Plasmodium* biology hampers therapeutic development. Protein phosphorylation, a key regulatory mechanism, is less understood in *Plasmodium* than in mammalian or yeast cells. Kinases and phosphatases involved in phosphorylation and dephosphorylation processes respectively are potential drug targets. The Protein Phosphatase type 1 catalytic subunit (PP1c) (PF3D7_1414400) operates in combination with various regulatory proteins to specifically direct and control its phosphatase activity. However, there is little information about this phosphatase and its regulators in the human malaria parasite, *Plasmodium falciparum.* To address this knowledge gap, we conducted a comprehensive investigation into the structural and functional characteristics of a conserved *Plasmodium*-specific regulator called Gametocyte EXported Protein 15, GEXP15 (PF3D7_1031600). Through in silico analysis, we identified three significant regions of interest in GEXP15: an N-terminal region hous-ing a PP1-interacting RVxF motif, a conserved domain whose function is unknown, and a GYF-like domain that potentially facilitates specific protein–protein interactions. To further elucidate the role of GEXP15, we conducted in vitro interaction studies that demonstrated a direct interaction between GEXP15 and PP1 via the RVxF-binding motif. This interaction was found to enhance the phosphatase activity of PP1. Additionally, utilizing a transgenic GEXP15-tagged line and live microscopy, we observed high expression of GEXP15 in late asexual stages of the parasite, with localization predominantly in the nucleus. Immunoprecipitation assays followed by mass spectrometry analyses revealed the interaction of GEXP15 with ribosomal- and RNA-binding proteins. Furthermore, through pull-down analyses of recombinant functional domains of His-tagged GEXP15, we confirmed its binding to PfPP1 and to the ribosomal complex via the GYF domain. Collectively, our study sheds light on the PfGEXP15–PP1–ribosome interaction, which plays a cru-cial role in protein translation. These findings suggest that PfGEXP15 could serve as a potential target for the development of malaria drugs.

**Keywords**: Protein Phosphatase 1; *Plasmodium*; malaria; GEXP15; CD2BP2; GYF domain; ribosome biogenesis

# Acknowledgment

As a prelude to this thesis, I wish to extend my heartfelt gratitude to the individuals whose unwavering support has been the very essence of this journey, shaping it into what it is today. These remarkable souls, through their trust, patience, and friendship, have illuminated the path of my three years in the realm of Apicomplexan Parasites Biology Lab.

This journey, ending in the completion of this work, would not have been conceivable without the involvement and assistance of numerous individuals, whose names cannot all be listed.

First and foremost, I would like to express my deepest gratitude to my thesis supervisor, Dr. Jamal KHALIFE. His support has been an invaluable inspiration guiding me throughout this academic journey. From the very first moment I embarked on this research journey, Dr. Khalife has not only been a dedicated mentor but also a pillar of strength in a foreign land. His guidance, mentorship, and genuine care exceeded the academic field, making me feel like a part of a second family during my time abroad. I am profoundly thankful for his wisdom, patience, and unwavering belief in my abilities, which have been instrumental in shaping this thesis. I will forever cherish the lessons learned and the bond forged. I am truly fortunate to have had such an exceptional supervisor.

I must also express my sincere appreciation to the beloved members of the lab: Dr. Christine Pierrot, Dr. Mathieu Gissot, Dr. El Moukhtar Aliouat, Dr. Sabrina Marion, Emmanuel, Thomas, Caroline, and Veronique. I am grateful for all the unforgettable moments I shared with my lab friends, Sylia, Claudianne, Maanasa, Lola, Claire, Layal, Marcin, Justine, Camille, Florianne, Cecilia, Sarah, Romain, Tom, Aya, and Amir. To the esteemed jury and CSI members, Dr. Benoit Foligne, Dr. Marie-France Delaw, Dr. Philippe Grellier, Dr. Alejandro Cabezas-Cruz, Dr. Hasna Bou Haroun and Dr. Vasant Muralidharan who agreed to evaluate this work, my heartfelt thanks.

I extend gratitude to our project collaborators, Thomas Hollin, Amaury Farce, Sophie Salomé-Desnoulez and Ida Chiara Guerrera.

My sincere appreciation goes to Mr. Francois DelCroix and Ms. Marjorie Vanderhove for their support during the thesis completion with EDBSL. I am forever grateful for the scholarship

7

opportunity          provided          by          the          University          of          Lille.

Beyond the lab, my friends Maria, Christy, and all those who made my stay in Lille memorable, you were my second family away from home. Your presence during challenging times has been a source of strength. This will not be complete without expressing my gratitude and love to my best friends, Murielle, Reina, Remi, Rita, and Sharen, whose unwavering support surpassed the distance.          I'm          lucky          to          have          you. Above all else, I want to convey the immense depths of my gratitude to my ever-caring, loving, and unwavering family. It's a feeling that exceeds words, a sentiment too profound to be adequately                                                                                expressed. To my beloved parents, Maroun and Assia, who selflessly gave their all for us, their children, I find myself overwhelmed with emotions. Your dedication and tireless determination have always been the guiding stars of my life. I owe you a debt of gratitude for the education that fills me with pride. This thesis not only reflects my persistent efforts but also serves as a testament to the enduring values you have conveyed to me, shaping me into the person I've become today.

Finally, I would like to thank my better half: my beloved brother 'Youssef' and two sisters 'Carol & Jocelyne', my brothers-in-law, nieces, and nephews, whose constant support and love pushed me forward during tough times. Your words of encouragement were my steadfast anchor, and I want you to know that I would not have reached this far without your presence in my life.

To all of you, I dedicate this thesis.

# Table of Contents

## List of Figures

# List of Tables

# List of Abbreviations

**A**  Adenine

**ACT**  Artemisinin-based combination therapy

**aPK**  atypical kinase

**ARC3**  Artemisinin Resistance Confirmation, Characterization, and Containment

**ARDS** Acute respiratory distress syndrome

**ATG8**  Autophagy-related proteins 8

**ATG12**  Autophagy-related proteins 12

**ATP**  Adenosine triphosphate

**BC**  Before Christ

**BP**  Base pairs

**Ca**  Calcium

**CAMK**  Clmodulin/calcium-dependent kinase

**CDK1**  Cyclin-dependent kinase 1

**CDPK**  Calcium-dependent protein kinase

**CK1**  Casein kinase 1

**COVID-19**  Corona Virus Disease of 2019

**CRISPR**  Clustered Regularly Interspaced Short Palindromic Repeats

**DHFR**  Dihydrofolate reductase

**DHPS**  Dihydropteroate synthase

**DNA**  Deoxyribonucleic acid

**ePK**  eukaryotic protein kinase

**FAK kinase**  Focal adhesion kinase

**Fe**  Iron

**FIND**  Foundation for Innovative New Diagnostics

**FU**  Fluorouracil

**GDV1**  Gametocyte development 1

**GI**  Gastrointestinal

**GMEP**  Global Malaria Eradication Program

**GPI**  Glycosylphosphatidylinositol

**GTP**  Guanosine triphosphate

**HAT**  Histone acetyltransferases

**HDAC**  Histone deacetylase

**HDA2**  Histone deacetylase 2

**HKDMs**  Histone lysine demethylase

**HKMT**  Histone lysine methyltransferase

**HP1**  Heterochromatin Protein 1

**IC50**  Inhibitory Concentration 50

**IDC**  Intraerythrocytic developmental cycle

**IMC**  Inner membrane complex

**iRBC**  infected Red Blood Cell

**IRES**  Internal ribosome entry sequences

**IRS**  Indoor residual spraying

**ITN**  Insecticides treated nets

**Kb**  Kilobases

**KD**  Knockdown

**kDa**  kiloDaltons

**LDH**  Lactate Dehydrogenase

**LSM**  Larval source management

**LysoPC**  Lysophosphatidylcholine

**MAP**  Mitogen-activated protein

**MAPK**  Mitogen-activated protein kinase

**Mb**  Megabases

**MDA**  Mass Drug Administration

**Mg**  Magnesium

**Mn**  Manganese

**MnCl2**  Manganese Chloride

**mRNA**  messenger Ribonucleic acid

**MSP1** Merozoite surface protein 1

**ncRNA** noncoding RiboNucleic Acid

**NGS** Next-Generation Sequencing

**NEDD8** Neural precursor cell-Expressed Developmentally Down-regulated 8

**NLK** Nemo-like kinase

**NMT** N-myristoyltransferase

**PCR** Polymerase Chain Reaction

**PfBDP** *P. falciparum* bromodomain protein

**PfEMP1** *P. falciparum* Erythrocyte Membrane protein 1

**PfHRP2** *P. falciparum* histidine-rich protein II

**Pfmdr1** *P. falciparum* multidrug resistant gene 1

**PfSPZ** *P. falciparum* sporozoites

**PIKK** Phosphatidylinositol 3-kinase-related kinases

**PKA** Protein kinase A

**PKG** Protein kinase G

**PP** Protein phosphatase

**PP1c** Protein phosphatase type 1 catalytic subunit

**PPM** Metal-dependent protein phosphatases

**PPP** Phosphoprotein phosphatases

**PSP** Serine-Threonine Phosphatase

**PSTP** $Ca^{2+}$dependent protein serine/threonine phosphatase

**PTM** Post-translational modification

**PTP** Protein Tyrosine Phosphatase

**PvCSP** *P.vivax* Circumsporozoite protein

**PvDBP** *P. vivax* Duffy-binding protein

**PvSPZ** *P. vivax* sporozoites

**RBC** Red Blood Cell

**RDT** Rapid Diagnostic Test

**R&D** Research and Development

**RGC** Receptor guanylate cyclases

**RIO** Right open reading

**RIPK** Receptor interacting serine/threonine protein kinase

**SUMO** Small ubiquitin-related modifier

**TARE** Telomere-associated lncRNA

**T** Thymine

**TKL** Tyrosine kinase-like

**TKS** Tyrosine kinase substrates

**U** Uridine

**UB** Ubiquitin

**UBls** Ubiquitin-like modifiers

**UFM1** Ubiquitin-fold modifier 1

**uORF** upstream Open reading frames

**UPS** Ubiquitin proteasome system

**URM1** Ubiquitin-related modifier 1

**VSP** Vacuolar-protein-sorting family

**WHO** World Health Organization

**YAP** Yes-associated protein

**Zn** Zinc

# INTRODUCTION

# I.  Introduction

## A.  Malaria

### 1.  History of the discovery of the malaria parasites

Malaria, an ancient and persistent disease, has plagued humanity for centuries. The origin of malaria is believed to extend back 50,000 to 100,000 years, with the deadliest strain for humans (Joy et al., 2003). There are numerous ancient written records of malaria, including Chinese documents from 2700 BC, Mesopotamian clay tablets from 2000 BC, Egyptian papyri from 1570 BC, and Hindu scriptures from the sixth century BC (which mention deadly fevers presumably related to the disease) (F. E. Cox, 2010).

The presence of malaria has been detected in old mummies dating back approximately 4,000 years (Nerlich et al., 2008). Prominent personalities like Tutankhamun, Alexander the Great and Genghis Khan are considered to have succumbed to malaria, while others like Christopher Columbus or George Washington were carriers at some time in their lives (Hawass et al., 2010).

The term malaria was derived from "bad air" which comes from the Latin word "palus," meaning "marsh." (Cook et al., 2000). Giovanni Maria Lancisi, a physician and professor, was the first to assume that the illness was caused by some form of poison coming from marshes and was likely carried by mosquitoes. Later, Albert Freeman Africanus King (1841–1914), Jakob Henle (1841–1914) and others backed this suggestion (Cook & Webb, 2000).

However, scientific findings directly related to malaria came up in the 1880s. One notable concept put out by Italian scientist Corrado Tommasi-Crudeli and German microbiologist Theodor Albrecht Edwin Klebs, indicated that they found a bacterium named Bacillus malariae. They claimed to have obtained this bacterium from the waters of the Pontine Marshes, a region known for its high incidence of malaria. When scientists cultivated and injected this bacterium into rabbits, it induced feverish illnesses and enlarged spleens, mimicking the signs of malaria. This study gave insight into the probable origin of the disease (F. E. Cox, 2010).

In the middle of this context, Charles Louis Alphonse Laveran, a French army officer stationed in Algeria, defied existing assumptions and began on a journey to examine the presence of pigment in malaria-infected patients. Through his examinations of fresh unstained blood, Laveran identified several varieties of erythrocytic organisms, including crescents, static bodies

with pigment, moving parts with pigment, and entities with flagella-like features. Laveran called the parasitic protozoan he discovered "*Oscillaria malariae*." Despite submitting his results to the French Academy of Medical Sciences in 1880, Laveran struggled to convince major microbiologists and malariologists of his time. However, his efforts paid off, and by 1884, he succeeded in persuading prominent Italian malariologists and renowned microbiologists, including Louis Pasteur, Charles Edouard Chamberland, and Pierre Paul Émile Roux, that malaria was caused by a protozoan rather than a bacterium (Laveran, 1884). Laveran was awarded the Nobel Prize for Medicine in 1907

In 1897, Ronald Ross, during his research in India, announced an important finding that culicine mosquitoes were capable of transmitting the avian malaria parasite *Plasmodium relictum*. This discovery inspired him to propose the idea that mosquitoes may also transmit malaria parasites to humans. Subsequently, in 1899, Ross clearly demonstrated that anopheline mosquitoes were definitely the carriers of human malaria parasites. It is worth mentioning that previous to Ross's findings, Italian scientists also provided data supporting the same result. Ross's most groundbreaking discovery, often overlooked, was the revelation that a blood-sucking insect had the ability to not only acquire infectious organisms from an infected individual but also transmit them to an uninfected host at a later feeding (F. E. Cox, 2010). Ross was awarded the Nobel Prize in Medicine in 1902. (Institute of Medicine (US) Committee on the Economics of Antimalarial Drugs; Arrow KJ, Panosian C, Gelband H, editors. (National Academies Press (US),2004.)

The identification of blood stages came in 1947, approximately 50 years after the first observations, due to the efforts of Shortt and Garnham. Then, in 1962, Krotoski uncovered the last puzzle concerning the permanence of liver stages. The remarkable journey to comprehend the complicated life cycle of malaria parasites was made possible by scientists who skillfully used knowledge gained by studying malaria in non-human animals, such as birds and primates, to the study of human malaria. This underscores the relevance of comparative studies in the research of human diseases (F. E. Cox, 2010).

## 2.    Epidemiology

Given its tremendous impact on morbidity and death, malaria poses a serious threat to the global public health. It is one of the main causes of sickness and mortality, especially in poor countries. The greatest burden of this disease falls on those most vulnerable, particularly children aged

under 5 years who have not yet developed antibodies to malaria and pregnant women whose immune systems are weakened during pregnancy.

The most recent World Malaria Report indicates that in 2021 compared to 2020, there was a slight increase in malaria cases and a minor decrease in malaria deaths. An estimated 247 million cases of malaria were recorded in 2021, which is a little higher from the 245 million cases reported in 2020. Compared to the 625,000 deaths recorded in 2020, the expected number of malaria deaths in 2021 was 619,000 (Figure 1).
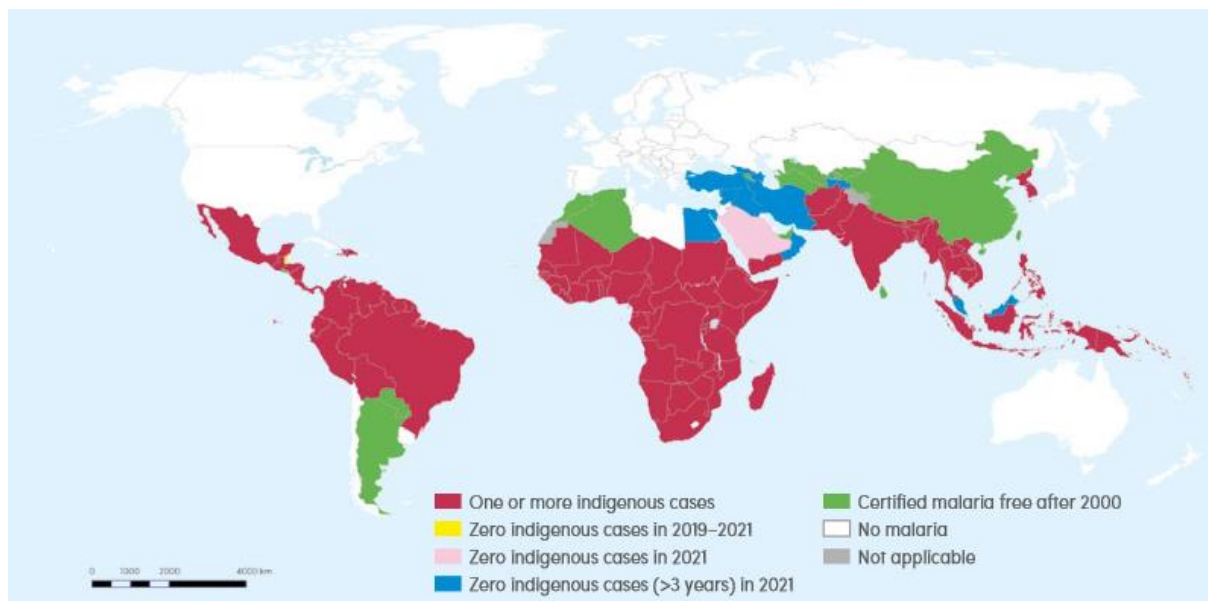


**Figure 1 Countries with indigenous cases in 2000 and their status by 2021**. Countries with zero indigenous cases for at least 3 consecutive years are considered to have eliminated malaria. In 2021, the Islamic Republic of Iran and Malaysia reported zero indigenous cases for the fourth consecutive year; also, Belize and Cabo Verde reported zero indigenous cases for the third time. China and El Salvador were certified malaria free in 2021, following 4 years of zero malaria cases. (Source: WHO database).

Malaria faced a huge setback due to the COVID-19 epidemic. During the pandemic's two peak years (2020–2021), the impact of COVID-19 resulted in an additional 13 million cases of malaria and 63,000 malaria-related deaths. Most deaths from malaria in the area occurred in children under the age of five (about 80% of all malaria deaths) (World Malaria Report, 2022).

Tropical and subtropical regions are mostly impacted by malaria worldwide. Approximately 95% of all malaria cases and 96% of deaths related to malaria occur in the WHO African Region, where the disease is still disproportionately prevalent. The significant incidence is caused by many factors, including:

1. Mosquito species: The Anopheles gambiae is a very effective mosquito vector that contributes to the disease's strong transmission.

2. Parasite species: *Plasmodium falciparum*, the main malaria parasite in the area, is more likely to cause severe malaria and fatalities.

3. Local climate factors: The local weather is generally favorable to year-round malaria transmission in vulnerable areas.

4. Resources limitations: The implementation of efficient malaria control strategies is hampered by a lack of resources and socioeconomic instability, aggravating the disease's burden (CDC, 2023.).

Malaria is acknowledged as having been successfully eradicated in nations where there have been no indigenous cases for at least three consecutive years. The latest report shows that, in 2020, the Islamic Republic of Iran and Malaysia reported no indigenous cases for the third year in a row, while Belize and Cabo Verde did the same for the second year. Additionally, in 2021, China and El Salvador received official certification as malaria-free countries after going four years without any malaria cases being reported. These achievements show how far these nations have come in successfully containing and eliminating malaria within their own borders.

## 3.    Social and financial impact of malaria

Malaria presents significant costs for individuals and governments. People have to cover expenses like prescribed medicines for treatment, medical care, travel expenses, missed days from work and school, preventive measures, and funeral costs in case someone dies from malaria. Governments are responsible for paying for the maintenance of medical facilities, the purchase of drugs, public health initiatives, reduced worker productivity, and compromised economic opportunities. Over $12 billion in direct expenses are spent each year. Beyond the direct costs of malaria, the disease has a greater impact on economic growth (World Malaria Report, 2022.).

## 4.    Symptoms

A malaria infection can cause a wide variety of symptoms, from minor to serious and even fatal issues. The disease can be categorized as uncomplicated or severe, with the potential for a full recovery if diagnosed and treated quickly and accurately.

## 4.1. Uncomplicated malaria

The classical sign of a malaria attack, although rarely observed, typically lasts for a duration of 6-10 hours. It consists of three distinct stages: the cold stage, which is characterized by shivering and a feeling of coldness; the hot stage, which is reported by fever, headaches, vomiting, and possibly seizures in young children; and finally, the sweating stage, which includes sweating, a return to normal body temperature, and a sense of fatigue (www.cdc.gov). Although they are rarely seen, these classic attacks happen every second day when "tertian" parasites like *P. falciparum*, *P. vivax*, and *P. ovale* are present, and every third day when "quartan" parasites like *P. malariae* are present or even daily when "quotidian" parasites like *P.knowlesi* are involved (for knowlesi Singh 2013). These attacks are triggered by the rupture of the infected red blood cells and the release of new parasites into the bloodstream. The synchronous nature of this cycle leads to the recurring pattern of malaria attacks, depending on the specie and its cell cycle duration (CDC, 2023).

However, more frequently, patients with malaria present with a combination of symptoms that include fever, chills, sweats, headaches, nausea and vomiting, body aches, fatigue, and other non-specific symptoms. These signs may be wrongly attributed to the flu, the common cold, or other common infections in areas where malaria cases are uncommon, particularly if malaria is not suspected. In contrast, people living in locations where malaria is common frequently recognize similar symptoms as being symptomatic of malaria and may choose to self-treat without getting an official diagnosis, relying on "presumptive treatment" methods.

Physical examinations can bring up certain symptoms like high body temperatures, sweating, weakness, an enlarged spleen, moderate jaundice, liver enlargement, and an accelerated breathing rate. The diagnosis of malaria can be supported by these clinical symptoms.

## 4.2. Severe/ Complicated malaria

Severe malaria is defined by the presence of serious organ failures or abnormalities in the patient's blood or metabolism, which complicate the infection. Included in this is cerebral malaria, that displays symptoms such as strange behavior, altered consciousness, convulsions, coma, or other neurological problems. Hemolysis, which results in severe anemia, causes red blood cells to be destroyed. Another effect of hemolysis is hemoglobinuria, which is the presence of hemoglobin in the urine. Even when the parasite counts have dropped as a result of treatment, acute respiratory distress syndrome (ARDS), an inflammatory reaction in the lungs

that impairs oxygen exchange, can take place. Acute kidney damage, hyper parasitemia (when more than 5% of red blood cells are infected by malaria parasites), abnormal blood coagulation, low blood pressure brought on by cardiovascular collapse, abnormal blood clotting, abnormal blood glucose levels, and metabolic acidosis are additional complications. As a medical emergency, the occurrence of severe malaria necessitates a quick and urgent medical treatment.

## 5. Diagnosis

Accurate and timely diagnosis of malaria plays a crucial role in ensuring effective treatment for affected individuals and containing the transmission of the disease within the community. This diagnosis is often supported by the previously discussed clinical symptoms.

### 5.1. Microscopy

It involves the morphological analysis of stained blood smears, remains the established standard for diagnosing malaria (Figure 2). Giemsa, Wright, or Wright-Giemsa stains are commonly used, with Giemsa being the preferred option due to its ability to reveal distinctive morphological features. Thick smears are employed for detecting the presence of parasites, while thin smears assist in identifying the specific malaria species. Furthermore, both thick and

thin smears can be utilized for quantifying the parasite load.
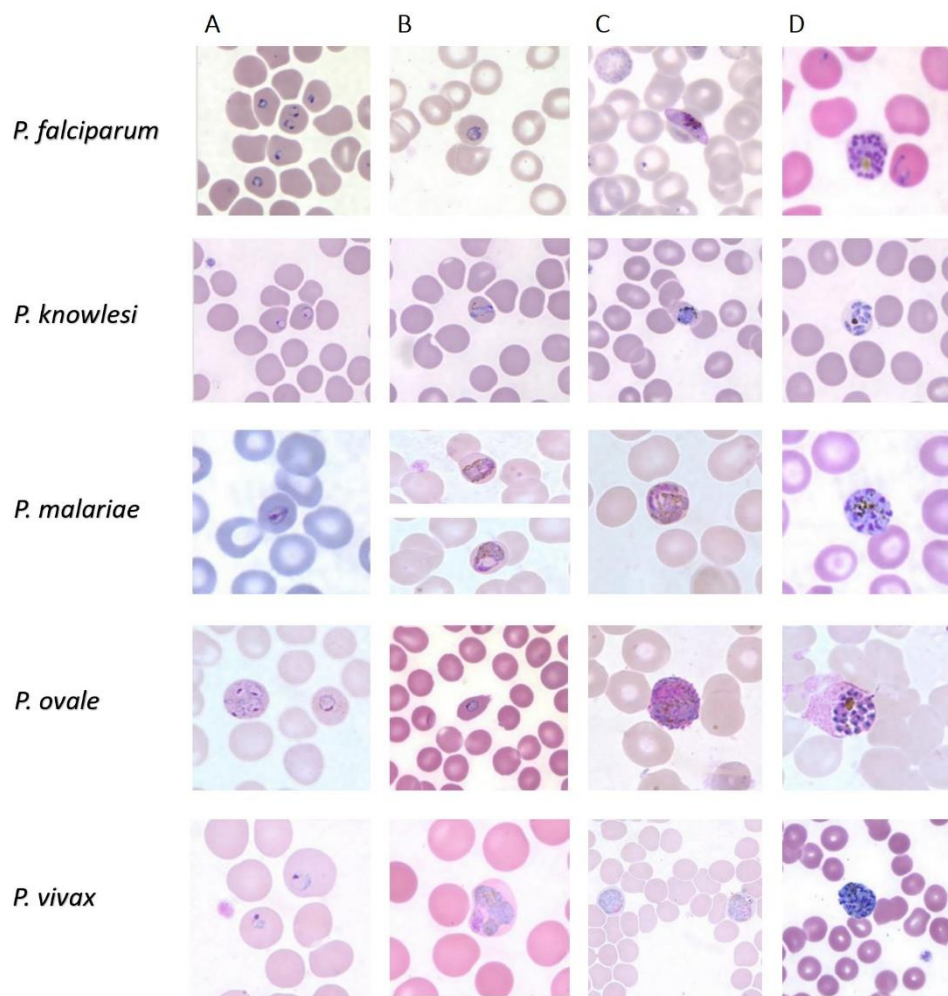


**Figure 2 Typical thin smear.** Microscope images of different parasite species and blood stages.However, there are instances where microscopists face challenges in distinguishing between species due to overlapping morphologic characteristics. Confirmatory molecular diagnostic tests are employed to determine the Plasmodium species accurately. (CDC, 2023)

**5.2. Polymerase Chain Reaction (PCR)**

It has the capability to detect parasites even when the level of parasitemia is below the detectable limit of traditional blood film examination. This molecular method provides a highly sensitive and specific approach for species identification, especially in cases where morphological differentiation is challenging.

**5.3. Antigen-based rapid diagnostic tests**

They correspond to test strips with a nitrocellulose membrane with capture antibodies and antibodies against target antigens (Baptista et al., 2022). The WHO, along with the Foundation for Innovative New Diagnostics (FIND) and other participants in malaria elimination, have

evaluated over 200 rapid diagnostic tests (RDTs) based on antigens. They were produced by more than 30 different manufacturers (WHO, 2022). The operational detection thresholds for these tests have been established at a low parasite density of 200 parasites/µl and a higher density of 2000-5000 parasites/µl. RDTs primarily detect the presence of *P. falciparum* histidine-rich protein II (PfHRP2), as well as *Plasmodium* lactate dehydrogenase and aldolase (WHO, 2022). It's important to note that while these tests can identify *P.falciparum*, they lack species-specific capability to detect all five malaria species and cannot provide information on different developmental stages (Zimmerman & Howes, 2015).

### 5.4. Lab-on-a-Chip and microdevices for Hemozoin-based malaria diagnosis

Based on the studies by Hole et al. (Hole & Pulijala, 2021) and Pisciotta et al. (Pisciotta et al., 2017), it has been found that $10^{10}$ parasites generate 3–4 µmol of hemozoin, which equates to approximately 0.4512 pg of hemozoin per parasite. Considering this information, and that hemozoin content rises as the disease progresses, whereas it is absent in individuals without infection, hemozoin serves as a significant biomarker for detecting and monitoring infections (Hänscheid et al., 2008). The Lab-on-a-chip and microdevices for Hemozoin-based malaria diagnosis are compact, portable devices that combine multiple laboratory techniques to enable simultaneous screening of different characteristics. Typically, these devices are linked with microfluidic systems equipped with reservoirs, enhancing the concentration of cells for more precise and sensitive detection (Baptista et al., 2022) .

## 6.    Treatment and Vaccines

Before discussing the topic of treatment and vaccines, it's crucial to consider the role of the preventive treatment, chemoprophylaxis, which involves the use of specific medications to prevent the development and the spread of malaria.

### 6.1.  Chemoprophylaxis

It is primarily recommended for travelers visiting malaria-endemic regions, categorized into different groups based on specific criteria. The selection of appropriate drugs for chemoprophylaxis depends on factors such as the travel destination, duration of potential mosquito exposure, patterns of parasite resistance, transmission levels and seasonality, as well as the age and pregnancy status of the individual. In endemic countries, chemoprophylaxis may also be recommended for local young children and pregnant women, taking into account the endemicity level and transmission seasonality(CDC, 2023).

In order to determine the appropriate treatment for malaria, four main factors should be considered:

1. *Plasmodium* species causing the infection: Determining the precise *Plasmodium* species that is causing the infection is important for numerous reasons. While *P. vivax*, *P. ovale*, and *P. malariae* are less likely to cause severe disease, *P. falciparum* and *P. knowlesi* infections can quickly progress to severe illness or even death. Furthermore, *P. vivax* and *P. ovale* infections need to be treated to eliminate hypnozoites, which remain dormant in the liver and can lead to relapses. Different geographic regions may exhibit different drug resistance patterns for *P. falciparum* and *P. vivax*, which emphasizes the significance of species identification.

2. Clinical condition of the patient: Malaria diagnoses are typically divided into two categories: uncomplicated or severe malaria. Oral antimalarials are an effective treatment for uncomplicated malaria. However, patients with severe symptoms or a parasitemia of less than 5% need to receive aggressive treatment with intravenous antimalarial therapy.

3. Drug susceptibility of the parasites: Understanding the geographic area where the infection was acquired provides insight on the possible drug resistance in the infecting parasite. This can help the clinician to choose the best medicine or drug combination for treatment. The CDC (https://www.cdc.gov/parasites/malaria/) malaria webpage provides useful details on malaria risk and parasite resistance. If malaria is suspected but not yet confirmed, or if species identification is not possible, urgent antimalarial treatment that is effective against chloroquine-resistant *P. falciparum* must be started, and once confirmatory results are available, the treatment can be changed.

4. Previous usage of antimalarials: It's crucial to take into account whether the person was taking medication for malaria chemoprophylaxis. If malaria still happens despite chemoprophylaxis, the prophylactic medication or medication combination should not be included in the treatment plan, unless there are no other available options.

**6.2. Treatment for uncomplicated malaria:**

Treatment options for *P. falciparum*-related uncomplicated malaria differ according to the presence or absence of chloroquine resistance in the region of infection. Here are the recommended treatment approaches:

### 6.2.1. *P. falciparum* Acquired in Areas with Chloroquine Resistance:

- Artemether-lumefantrine (Coartem®) and atovaquone-proguanil (MalaroneTM) are preferred options if easily available.

- Quinine sulfate plus doxycycline, tetracycline, or clindamycin is another option for treatment. Due to more available efficacy data, quinine sulfate combined with doxycycline or tetracycline is preferred.

- Mefloquine is an alternative option when other treatments are ineffective, however it has a rare but possible risk of serious neuropsychiatric side effects.

It is not required to switch regimens once therapy has begun and been tolerated, even if a preferable regimen becomes available. In order to evaluate clinical response and parasite density, hospitalization is advised, with consideration for outpatient completion of treatment once the patient's condition has improved.

### 6.2.2. *P. falciparum* Acquired in Areas Without Chloroquine Resistance:

- Patients can be treated with the recommended doses of oral chloroquine or hydroxychloroquine.

- Chloroquine-sensitive *P. falciparum* infections can be treated with any of the regimens indicated for chloroquine-resistant malaria.

- Hospitalization is required to closely monitor the clinical response and parasite density until improvement occurs, followed by potential outpatient completion of treatment.

For pregnant women with uncomplicated malaria acquired in areas with chloroquine-resistant *P. falciparum*, treatment options include artemether-lumefantrine, mefloquine, or a combination of quinine sulfate and clindamycin. While clindamycin treatment lasts for seven days regardless of where the illness occurred, quinine treatment lasts for seven days for infections in Southeast Asia and three days for infections elsewhere.

Malaria infection during pregnancy poses significant concerns, including maternal and perinatal morbidity and mortality. Miscarriage, early delivery, low birth weight, congenital infection, and perinatal death are just a few of the issues that might results from it. Prompt and adequate treatment is essential for pregnant women, and specific antimalarial alternatives should be chosen depending on whether or not chloroquine resistance is present.

## 6.2. Treatment for complicated malaria:

To avoid deadly results, severe malaria needs to be treated very rapidly. In order to treat severe malaria, intravenous (IV) artesunate is the recommended treatment regardless of the infecting species. In cases where IV artesunate is not immediately available, interim treatment with a potential oral antimalarial medication can be taken into consideration while purchasing IV artesunate from a commercial source. Alternative administration methods should be explored for patients unable to tolerate oral medications.

Due to its quick onset of action, artemether-lumefantrine (Coartem®) is the preferred oral option for interim treatment. Atovaquone-proguanil (MalaroneTM), quinine, and mefloquine are additional oral alternatives. Since clindamycin and tetracyclines (e.g., doxycycline) are slow-acting antimalarials and ineffective when administered alone for severe malaria, they are not suitable for interim treatment.

Upon arrival of IV artesunate, oral medication should be stopped, and parenteral treatment should be started. The recommended dose of IV artesunate is 2.4 mg/kg at 0, 12, and 24 hours. Until a negative result is obtained, routine blood smears should be done.

After finishing the initial course of IV artesunate, if the parasite density is less than 1% and the patient can tolerate oral treatment, a full treatment course with a follow-up regimen should be given. For a maximum of seven days, IV artesunate can be continued if the patient is still unable to tolerate oral drugs.

Infants, children, and pregnant women can all be treated by IV artesunate. Despite the risk, IV artesunate treatment is beneficial and should not be withheld, especially for pregnant women facing life-threatening severe malaria. The only contraindication to IV artesunate is a known allergy to artemisinins.

Although IV artesunate is usually well-tolerated, there have been a few reports of cases of delayed post-artemisinin hemolytic anemia. Hemoglobin concentration, reticulocyte count, haptoglobin, lactate dehydrogenase (LDH), and total bilirubin must all be regularly monitored for up to four weeks following the start of treatment. Depending on the severity of hemolysis and anemia symptoms, a blood transfusion may be necessary.

In the following table (Table 1), I have compiled a list of candidate molecules that are presently in the early stages of development for the treatment of clinical malaria.

**Table 1 Candidate molecules in the early development for the treatment of clinical malaria**

| Molecule | Parasite | Phase | Dose | | Activity | Resistance |
|---|---|---|---|---|---|---|
| **MMV533** | *P. falciparum* *P. vivax* | Completed Phase 1 | Predicted human dose | low | Fast-killing | No cross-resistance |
| **INE963** | *P. falciparum* *P. vivax* | Phase 1 | - | | Fast-killing | No cross-resistance |
| **GSK701** | *P. falciparum* | Phase 1 | Predicted human dose | low | fast-killing | - |
| **MMV183** | - | Preclinical development | Predicted human dose | low | Fast-killing | No pre-existing resistance |
| **GSK484** | - | Preclinical development | Predicted human dose | low | Fast-killing | No resistant parasite identified |
| **IWY357** | - | Preclinical development | Predicted human dose | low | Fast killing | No ability to select resistant mutants in vitro |
| **MMV609** | - | Preclinical development. | Predicted human dose | low | Fast-killing | - |

## 7. Vaccines

Based on the recommendations of two global advisory bodies within the World Health Organization (WHO), it is advised the use of the RTS, S/AS01 malaria vaccine for the prevention of *P. falciparum* malaria in children residing in regions with moderate to high malaria transmission, as defined by WHO. The vaccine should be administered in a schedule of four doses starting from 5 months of age to reduce the incidence and burden of malaria.

The recommendation is based on key findings from the malaria vaccine pilots conducted in Ghana, Kenya, and Malawi, under the leadership of their respective Ministries of Health. The pilots spanned two years and provided valuable data and insights, leading to the following findings:

1) Feasibility and Health Impact:
   - The introduction of the vaccine is feasible and improves health outcomes, with good and equitable coverage achieved through routine immunization systems, even in the context of the COVID-19 pandemic.
   - The vaccine helps to reach previously unreached populations, increasing equity in access to malaria prevention.
   - Data from the pilot program showed that a significant proportion of children who were not using bed nets benefited from the RTS, S vaccine.
2) Safety and Uptake:

- The vaccine has demonstrated a strong safety profile, with over 2.3 million doses administered in the three African countries.

- Introducing the vaccine did not negatively impact the use of bed nets, uptake of other childhood vaccinations, or health-seeking behavior for febrile illness. These essential malaria prevention and treatment measures continued to be implemented alongside the vaccine.

3) Real-life Impact:

- The vaccine has shown a significant reduction (30%) in severe cases of malaria, even in areas where insecticide-treated bed nets are widely used, and access to diagnosis and treatment is good.

4) Cost-effectiveness:

- Modelling estimates indicate that the vaccine is highly cost-effective in regions with moderate to high malaria transmission.

Based on these findings, the WHO recommends the use of the RTS, S/AS01 malaria vaccine as an integral component of comprehensive malaria control strategies in eligible regions, contributing to the reduction of malaria-related morbidity and mortality in children.

A table summarizing the malaria vaccine candidates currently in active development will be presented below (Table 2).

**Table 2 Malaria vaccine candidates (in active development)**

| Life cycle stage | Parasite | R&D phase | Name | Description |
|---|---|---|---|---|
| Pre-erythrocytic stage | *P. falciparum* | WHO recommended and prequalified | RTS,S/AS01 | Circumsporozoite protein |
| | | Phase 3 | R21/MatrixM | Circumsporozoite protein |
| | | Phase 2 | *Pf*SPZ Vaccine | Whole sporozoite |
| | | | *Pf*SPZ-CVac | *Pf*SPZ challenge under chemoprophylaxis |
| | | Phase 1 | VLPM01 | Virus-like particle |
| | | | rCSP/AP10-602 | Circumsporozoite protein |
| | | | *Pf*GAP3-KO | Genetically attenuated whole sporozoite |
| | | | FMP013 & FMP014 | Self-assembling nanoparticles |
| | | | *Pf*SPZ-GA1 | Genetically attenuated whole sporozoite |
| | | | DNA-ChAd63 *Pf*CSP | Heterologous prime-boost |
| | | Phase 2 | *Pv*CSP | Circumsporozoite protein |

| | | | | |
|---|---|---|---|---|
| | *P. vivax* | | *Pv*SPZ | Whole sporozoite |
| Blood stage | *P. falciparum* | Phase 2 | Rh5 | Reticulocyte binding protein |
| | | Phase 1 | BK-SE36 | *Pf*SERA5 antigen |
| | *P. vivax* | Phase 2 | *Pv*DBP | Duffy-binding protein |
| | | | *Pf*7G8 | Chemically attenuated whole parasite |
| | | | DNA-ChAd63 *Pf*CSP *Pf*AMA1 ME-TRAP | Heterologous prime-boost |
| Sexual stage | *P. falciparum* | Phase 2 | *Pf*s230D1M-EPA/AS01B | Pre-fertilization |
| | | | *Pf*s25M-EPA/AS01B | Post-fertilization |
| | | Phase 1 | *Pf*s25-IMX313/MatrixM | Post-fertilization |
| In Pregnancy | | Phase 1 | PRIMVAC | |
| | | | PAMVAC | |

# 8. Prevention

When it comes to combating malaria, prevention plays a pivotal role in reducing its impact and protecting vulnerable populations. In addition to chemoprophylaxis, vector control is a crucial component of malaria prevention strategies, focusing on the management and reduction of mosquito populations that transmit the disease.

In the fight against malaria, various strategies are used to prevent mosquito bites:

Measures include the use of mosquito bed nets, preferably treated with insecticides (ITN), indoor residual spraying (IRS), and larval source management (LSM).

- Insecticide-treated mosquito nets

ITNs consist of long-lasting insecticidal nets that keep their insecticidal capacity for up to 3 years, as well as conventionally treated nets with an insecticide lifespan of around 12 months. National malaria control programs have widely adopted the distribution of ITNs, aiming for universal coverage through mass distribution campaigns conducted at regular intervals (Tizifa et al., 2018).

- Indoor residual spraying

IRS was a main strategy in the Global Malaria Eradication Campaign, leading to the elimination of malaria in many countries and significantly reducing its burden in others.

Typically, IRS targets areas with low or seasonal transmission, but concerns have been raised about its long-term sustainability, particularly with its expansion into high transmission areas (www.who.int).

- Larval source management

LSM involves controlling potential mosquito breeding sites, primarily aquatic habitats, to prevent the development of mosquito larvae. Despite being one of the oldest tools in malaria control, LSM has been largely forgotten and overlooked in Africa (Fillinger & Lindsay, 2011). However, it has recently gained attention due to its dual benefits of reducing the population of mosquitoes that enter houses and those that bite outdoors (Tizifa et al., 2018).

- Genetically modified mosquitoes

The genetic modification of Anopheles mosquitoes has long been a subject of discussion, aiming to render them unable of reproducing to reduce or eliminate mosquito population or by making them genetically resistant to *Plasmodium*. Initially considered unachievable, recent advancements, such as the development of the CRISPR/Cas9 gene editing technique, offer the potential to turn this concept into a reality.

The modification consisted of a mutation in a gene known as "doublesex," which female mosquitoes need for normal development. The mutation deforms their mouths, making them incapable to bite and spread the parasite. It also deforms their reproductive organs, making them unable to lay eggs.

In addition, the male mosquitoes were engineered with a sequence of DNA known as a "gene drive" that can rapidly transmit a deadly mutation that wipes out populations of the insects (CDC).

However, several safety and ethical challenges need to be addressed to prove that the approach works and the mosquitoes would be safe to release into the wild (Greenwood, 2017).

- Mass drug administration

Another approach for malaria prevention is the Mass drug administration (MDA), which refers to the administration of a curative dose of a drug to the entire population within a specific area, regardless of whether individuals have been tested positive for malaria or have symptoms (Poirot et al., 2013) (CDC). MDA, when combined with other malaria control measures, has demonstrated success in effectively combatting the disease (Tizifa et al., 2018). As an example, the implementation of Mass Drug Administration (MDA) involving the use of sulphadoxine pyrimethamine in combination with Indoor Residual Spraying (IRS) yielded significant success in malaria control as demonstrated by the Garki Project conducted in Northern Nigeria in 1969 (Molineaux et al., 1980). Another effective strategy was the administration of a combination of primaquine and chloroquine to approximately 70% of Nicaragua's population, resulting in the prevention of around 9200 malaria cases (Garfield & Vermund, 1983).

## 9.    Resistance

In the years 1948-1950, cases of *P. falciparum* resistance to proguanil and pyrimethamine were reported. However, significant resistance to chloroquine or amodiaquine had not been reported before the initiation of the Global Malaria Eradication Program (GMEP) in 1955        (Covel, 1953). Around two years after the launch of GMEP, in 1957, resistance to chloroquine was first suspected in eastern Thailand due to delayed clinical response of P. falciparum to chloroquine (Thimasarn et al., 1995). Further studies in eastern Thailand revealed falciparum parasites resistant to all commonly used drugs except quinine (YOUNG et al., 1963). The widespread use of chloroquine contributed to the reduction of malaria mortality and morbidity, but it also facilitated the spread of resistance (WHO). By 1964, chloroquine resistance had been reported in Brazil, Cambodia, Colombia, Guyana, Malaysia, Thailand, and Vietnam (MOORE & LANIER, 1961).

In 1972, Chinese researchers made a significant discovery in the fight against malaria by identifying the antimalarial activity of artemisinin. This breakthrough was based on their study of medicinal plants mentioned in ancient texts (Barry & Potter, 2018). From the beginning, the advantages and disadvantages of artemisinin and its derivatives, such as artesunate, were known. These drugs were well tolerated, acted quickly, and rapidly reduced the parasite count in the bloodstream. However, they had a relatively short duration of effective concentration in the plasma after administration, leading to high rates of recrudescence with short oral treatment courses. To prevent the recurrence of parasitemia, a seven-day treatment course was necessary when using artemisinin or its derivatives as monotherapy(White, 2008). The development of

artemisinin-based combination therapies (ACTs) addressed this challenge by combining an artemisinin derivative with a partner drug that had a longer half-life. The rapid action of artemisinin derivatives was complemented by the partner drug, which helped prevent recrudescence even after a shorter three-day treatment (Jiang et al., 1982).

It was believed that the rapid elimination of artemisinins from the body would potentially delay or prevent the development of resistance. However, starting from 2003, data began to appear indicating prolonged clearance times after treatment with artesunate plus mefloquine for three days or artesunate monotherapy for seven days in the areas around the Cambodia-Thailand border (Noedl et al., 2008). In response to this emerging concern, the Artemisinin Resistance Confirmation, Characterization, and Containment (ARC3) project was funded by the Bill & Melinda Gates Foundation and coordinated by the World Health Organization (WHO). This project supported treatment efficacy trials and aimed to address the challenge of artemisinin resistance.

Various tools can be utilized to assess antimalarial drug resistance. In the case of certain drugs, specific genetic alterations linked to diminished drug efficacy have been identified. For instance, particular mutations in the Kelch13 gene of *P. falciparum* (PfKelch13) are associated with delayed parasite clearance following artemisinin-based treatments. Therefore, surveillance of these mutations can provide insights into the prevalence of artemisinin partial resistance, characterized by delayed clearance. Monitoring resistance to sulfadoxine-pyrimethamine (SP), a partner drug in artemisinin-based combination therapy (ACT) and a chemoprevention drug, involves detecting mutations in the dihydrofolate reductase (dhfr) and dihydropteroate synthase (dhps) genes of *P. falciparum*. Resistance to mefloquine is correlated with an increase in the copy numbers of the Pfmdr1 gene, while resistance to piperaquine is associated with amplified copy numbers of Pfplasmepsin 2/3 and mutations in the *P. falciparum* chloroquine resistance transporter (PfCRT). It is important to note that certain mutations have been validated solely as markers of resistance in parasite strains from specific regions. (WHO)
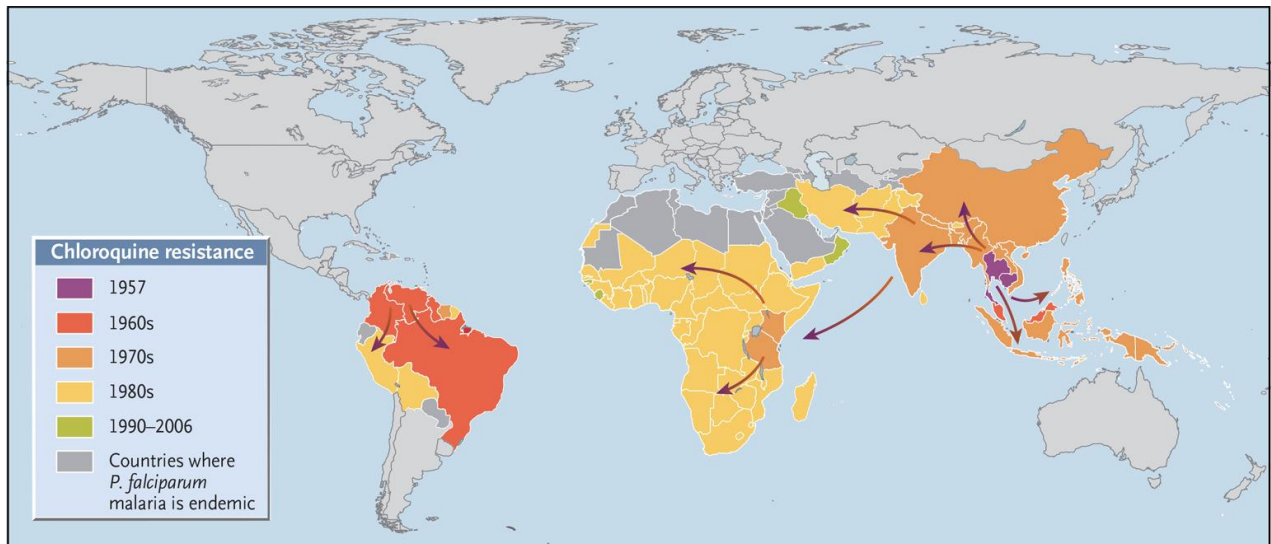
**Figure 3 History of Chloroquine-Resistant *P. falciparum* Malaria**. The New England Journal of Medicine(Packard, 2014)

# B. *Plasmodium falciparum*: Biology of the parasite

## 1. *Plasmodium*: Apicomplexan parasite

Apicomplexans, a group of single-celled intracellular parasites (Adl et al., 2007; CAVALIER-SMITH, 1993)that form a major clade of the subphylum Alveolata, including *Plasmodium*, *Cryptosporidium*, and *Toxoplasma*, cause significant global health burdens, leading to malaria-related deaths, infant diarrheal fatalities, and serious complications in pregnancy and immunocompromised individuals (WHO). *Cryptosporidium* infections rank as the second leading cause of the approximately 800,000 infant deaths associated with diarrheal diseases (Checkley et al., 2015; Kotloff et al., 2013) . On the other hand, *Toxoplasma*, affecting around 30% of the global population, is the primary cause of infectious retinitis in children and poses life-threatening risks during pregnancy and for individuals with compromised immune systems(Garza-Leon & Arellanes Garcia, 2012; Torgerson & Mastroiacovo, 2013) (Schlüter et al., 2014)

Other species impact agriculture, causing losses in the poultry and cattle industries. Treatment options are limited, and drug-resistant strains are emerging, necessitating the development of new therapeutics.

Apicomplexan parasites are found in diverse environments, spanning from marine to terrestrial habitats, and they show variability in their host preferences. They have intricate life cycles,

characterized by multiple hosts and developmental stages. These stages encompass sporogony (invasive stage with one round of asexual reproduction), merogony (invasive stage with multiple rounds of asexual reproduction), and gametogony (sexual reproduction). These stages can occur within the same organism and tissue (monoxenic lifestyle) or in different organisms and tissues (heteroxenic lifestyle) (Swapna & Parkinson, 2017).

Apicomplexans, a group of parasitic organisms, can be categorized into three major clades based on their evolutionary relationships and host preferences: Aconoidasida, Coccidia, and a third lineage comprising *Gregarina* and *Cryptosporidium* species (Barta & Thompson, 2006; Wasmuth et al., 2009).

The Aconoidasida clade includes Haemosporida (*Plasmodium*) and Piroplasmida (*Babesia* and *Theileria*). These parasites have heteroxenous life cycles, alternating between an arthropod vector, where sexual reproduction occurs, and a vertebrate host, supporting asexual propagation, typically in the circulatory system. In contrast, *Cryptosporidium* species are confined to the gastrointestinal (GI) tract of animals, while *Coccidia* encompass members that are either fully or partially restricted to the GI tract.

Although each lineage possesses distinct life cycle strategies, every species specializes in terms of host range and the specific tissues they infect (Cowper et al., 2012). For example, *T. gondii* is believed to exploit all warm-blooded animals as intermediate hosts, while *S. hominis* relies on bovines. Similarly, among ~200 *Plasmodium* species infecting erythrocytes, they exhibit specialized adaptations; *P. vivax* targets smaller or newer reticulocytes, whereas *P. falciparum* can infect all reticulocytes (Malleret et al., 2015; White, 2008).

Apicomplexans share distinct ultrastructural features and organelles that play crucial roles in their life cycle. One of these is the inner membrane complex (IMC), a specialized endomembrane system located directly beneath the plasma membrane in all alveolates. Comprising flattened sacs called alveoli, the IMC provides structural support, facilitates replication, motility, and invasion (Gubbels & Duraisingh, 2012; Harding & Meissner, 2014).

At the apical end of the parasite, unique secretory organelles are found, including bar-shaped micronemes, club-shaped rhoptries (comprising rhoptry neck and bulb regions), and dense granules. These organelles play crucial roles in processes like motility, invasion, and host modulation (Kemp et al., 2013). Dense granules have been identified in *Coccidia* and *Cryptosporidium* (BONNIN et al., 1995). Although dense granule-like structures are also found

in *Theileria* (Shaw et al., 1991), *Babesia* (Gohil et al., 2010), and *Plasmodium* (CULVENOR & CREWTHER, 1990), their specific functions in these species remain unclear (Mercier et al., 2005).

Another distinctive feature of apicomplexans is the apicoplast, a four-membraned organelle hosting vital metabolic pathways essential for parasite survival (Lim and McFadden, 2010, Notably, this organelle is absent in *Cryptosporidium* and *Gregarina*. These unique organelles and structures contribute to the remarkable adaptability and complexity of apicomplexans during their life cycle.

The year 2002 marked a significant milestone with the sequencing of the first apicomplexan genome, specifically that of *P. falciparum* (Gardner et al., 2002a). Since then, the field has witnessed remarkable advancements in genomic and transcriptomic research, thanks to the emergence of next-generation sequencing (NGS) technologies (Goodwin et al., 2016)These powerful tools have enabled researchers to assemble increasingly comprehensive datasets, providing deeper insights into the genetic makeup and gene expression patterns of apicomplexans.

## 2. *Plasmodium falciparum*: Genome and Proteome

### 2.1. Genome

The nuclear genome of *P. falciparum* 3D7 consists of approximately 22.8 megabases (Mb) spread across 14 chromosomes, with sizes ranging from around 0.643 to 3.29 Mb. The overall (A + T) composition stands at 80.6%, rising to approximately 90% within introns and intergenic regions. Around 5,300 protein-encoding genes were identified. This suggests an average gene density of 1 gene per 4,338 base pairs (bp) in *P. falciparum* (Gardner et al., 2002a).

In 54% of *P. falciparum* genes, introns were predicted. Excluding introns, *P. falciparum* genes had a mean length of 2.3 kb, notably larger than average gene lengths ranging from 1.3 to 1.6 kb in other organisms. Moreover, *P. falciparum* genes displayed a percentage of 15.5% of genes longer than 4 kb. Many of these longer genes encode uncharacterized proteins, possibly cytosolic, as they lack recognizable signal peptides. Notably, no transposable elements or retrotransposons were identified (Gardner et al., 2002a).

## 2.2. Proteome

The proteome analysis revealed that out of the 5,268 predicted proteins, approximately 60% (3,208 hypothetical proteins) lacked adequate similarity to proteins in other organisms, making it challenging to assign specific functions to them. This indicates that nearly two-thirds of the proteins are unique to *P. falciparum*, a much higher proportion compared to other eukaryotes. This distinctiveness could be attributed to the greater evolutionary divergence between *Plasmodium* and other sequenced eukaryotes, compounded by reduced sequence similarity due to the genome's high (A + T) content. Furthermore, an additional 257 proteins (5%) displayed significant similarity to hypothetical proteins found in other organisms (Gardner et al., 2002a).

Among the predicted proteins, 31% (1,631) contained one or more transmembrane domains, suggesting possible membrane-associated functions. Additionally, 17.3% (911) of the proteins possessed potential signal peptides or signal anchors, potentially indicating their involvement in secretion or membrane targeting (Gardner et al., 2002a).

## 3. *Plasmodium falciparum*: Life cycle

Malaria parasites exhibit a complex life cycle characterized by multiple rounds of asexual replication occurring in different stages and tissues within both the intermediate vertebrate host and the definitive insect host. In the vertebrate host, sexual stages known as gametocytes are exclusively formed in blood cells, while their subsequent gametogenesis and meiosis require transmission to the insect host. Throughout most *Plasmodium* species, asexual replication in circulating blood cells of the vertebrate host results in the highest cell numbers, with only a small fraction of these asexual parasites undergoing differentiation into sexual stages.

In recent years, there has been a renewed focus on the study of sexual stages and transmission, leading to a better understanding of the pathways that trigger their formation and their unique cellular characteristics. Furthermore, a series of studies have revealed that parasite replication and sexual differentiation also occur in the hematopoietic niche of the vertebrate host, introducing an unexpected and novel aspect to the malaria parasite life cycle (Venugopal et al., 2020).

The malaria parasite, *Plasmodium*, follows a largely conserved life cycle across different lineages that infect mammals (Figure 4). When a mosquito carrying the parasite takes a blood meal from a vertebrate host, it injects sporozoites into the skin. These motile sporozoites enter the bloodstream, allowing them to reach the liver and evade host immunity or drainage through

the lymphatic system(Amino et al., 2006; Tavares et al., 2013). Upon reaching the liver sinusoids, the sporozoites cross the sinusoidal barrier and enter hepatocytes, where they establish a parasitophorous vacuole and undergo the first round of asexual replication (Mota et al., 2001). Within 2 to several days, depending on the species, a multinucleated exo-erythrocytic schizont containing thousands of daughters merozoites forms. Some *Plasmodium* species, like *P. vivax* and *P. ovale*, can form a non-replicating hypnozoite instead of a schizont, leading to a period of latency and possible relapses (Sturm et al., 2006).

After egress from the hepatocyte, merozoites cluster in membrane-bound vesicles called merosomes and are released back into the bloodstream via the liver sinusoids (Sturm et al., 2006). The merozoites then invade red blood cells (RBCs), initiating a second asexual schizogony. This replication cycle lasts 24 to 72 hours (varies between species) and produces up to 32 merozoites. Through repeated rounds of invasion and growth, the parasite establishes acute and eventually chronic infections. Some species, like *P. vivax*, are restricted to infecting reticulocytes, which make up only a small fraction of circulating RBCs, limiting total parasitemia. In contrast, species like *P. falciparum* are not restricted and can infect a high proportion of RBCs, leading to a high parasite burden, which is associated with the severe disease caused by *P. falciparum* infections (Venugopal et al., 2020).

The sexual cycle in malaria parasites begins when a small fraction of asexual parasites commits to producing sexual progeny known as gametocytes. These mature gametocytes can circulate in the human blood for several days, increasing their chances of transmission to mosquitoes. Within minutes of entering the mosquito midgut, both male and female gametocytes use proteases to exit the red blood cells (RBCs) and transform into eight microgametes and one macrogamete, respectively. These gametes then fuse to form a zygote. The zygote undergoes further development, becoming a motile ookinete that crosses the midgut wall's epithelial layer and forms an oocyst (Sologub et al., 2011).

Within the oocyst, the parasites undergo the third cycle of asexual replication, generating thousands of sporozoites. These sporozoites are released into the mosquito's hemolymph. Some of the sporozoites migrate to the mosquito's salivary glands. When the mosquito takes another blood meal and injects its saliva into a new vertebrate host, the sporozoites are transmitted, starting the cycle again (Venugopal et al., 2020).

Gametocytogenesis, the process of forming gametocytes in malaria parasites, is regulated by a complex interplay of genetic, epigenetic, and environmental factors. Studies have revealed that

the ap2-g locus plays a crucial role as a transcriptional activator of sexual commitment in both *P. falciparum* and *P. berghei* (Kafsack et al., 2014). This locus is silenced in asexual parasites through the action of heterochromatin protein 1 (HP1) (Brancucci et al., 2014)and histone deacetylase 2 (HDA2) (Coleman et al., 2014). Recently, it was found that the perinuclear protein gametocyte development 1 (GDV1) (Eksi et al., 2012) interacts with HP1, leading to derepression of the ap2-g locus and subsequent sexual commitment in a subset of schizonts (Filarsky et al., 2018).

Environmental factors also influence the rate of sexual commitment(Buchholz et al., 2011). For instance, physiological levels of the human serum phospholipid lysophosphatidylcholine (LysoPC) can repress sexual commitment in vitro, as it serves as an environmental signal for nutrient availability required for parasite replication (Brancucci et al., 2018).

Gametocyte development can take different lengths of time, ranging from 1 to 12 days, depending on the species. In *P. falciparum*, the longest-known gametocyte development and spans five morphologically distinct phases (Hawking et al., 1971). Throughout gametocyte development in *P. falciparum*, a continuous sheath of microtubules assembles, attached to an array of alveolar sacs forming the inner membrane complex (IMC). The IMC is also present in sporozoites and ookinetes and is crucial for cellular motility and passage across barriers (Kannan et al., 2022).

Notably, *P. falciparum* gametocytes display unique features absent in asexual blood-stage parasites, including the continuous IMC assembly and alterations to the cytoskeleton of the infected red blood cell (iRBC), leading to increased rigidity (M. Dearnley et al., 2016; M. K. Dearnley et al., 2012).
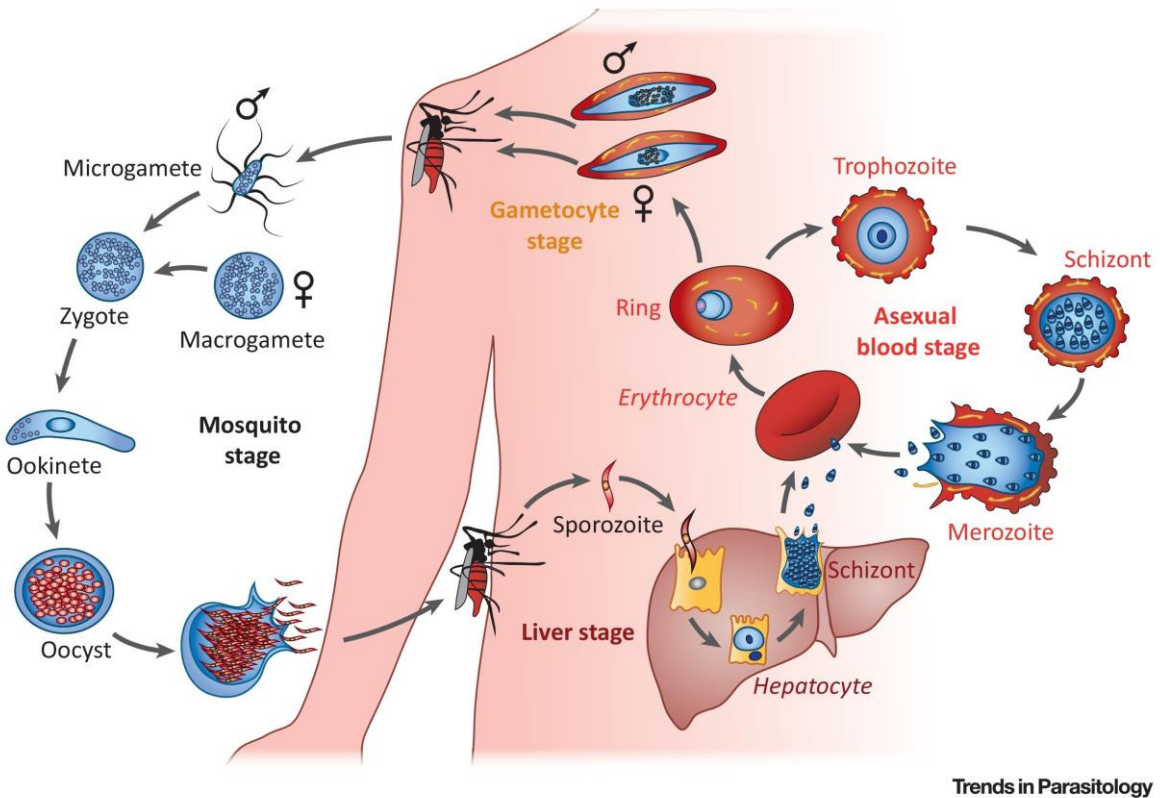
**Figure 4 : The life cycle of *Plasmodium falciparum*** (Maier et al., 2019).

# 4. Regulation of *P. falciparum* life cycle

During the life cycle of *P. falciparum*, various stages occur, including sporozoites, merozoites, rings, trophozoites, schizonts and gametocytes at different stages. This succession requires precise and finely tuned regulation, which can vary depending on the environment. Several regulatory mechanisms known in eukaryotes are also described to varying degrees in *Plasmodium spp*. The expression of a protein can be controlled upstream, during, and downstream of its translation.

## 4.1.Transcriptional modifications

- Transcription factors

Key transcription factors are pivotal in promoting or inhibiting gene transcription. Equipped with DNA-binding domains, they recognize specific DNA motifs like enhancers or promoter regions, recruiting chromatin modifying and remodeling complexes. Interestingly, *P.falciparum* has a relatively low number of specific transcription factors compared to its total number of genes, indicating a unique feature among eukaryotes (Templeton & Moorhead, 2004). The discovery of the ApiAP2 transcription factor family, specific to apicomplexan

44

parasites and analogous to Apetala-2 in plants, significantly advanced our understanding of gene regulation in *Plasmodium* (Balaji et al., 2005; Campbell et al., 2010). These ApiAP2 factors have drawn significant attention because they manage to tightly control the expression of over 5,500 coding genes throughout the parasite's life cycle.

Studies have shown that these ApiAP2 factors function as master regulators, transcribing hundreds of genes at specific stages of the parasite's life cycle. For instance, AP2-G and AP2-G2 are involved in gametocytes (Sinha et al., 2014; Yuda et al., 2015), AP2-O in ookinetes (Yuda et al., 2009), AP2-SP in sporozoites (Yuda et al., 2010), and AP2-L in liver stages (Iwanaga et al., 2012). Knock-out screenings in rodent *Plasmodium* have confirmed the essentiality of these factors during specific stages of parasite development (Modrzynska et al., 2017; Zhang et al., 2017).In summary, *Plasmodium* parasites have evolved distinct features to cope with their relatively fewer transcription factors.

- Epigenetic Regulation and Histone Modifications

Histone PTMs are tightly regulated by a diverse group of histone modifiers known as writers and erasers. Writers, like histone acetyltransferases (HATs) and histone lysine methyltransferases (HKMTs), deposit histone marks (Cui et al., 2008), while erasers, including histone deacetylases (HDACs) and histone lysine demethylases (HKDMs), remove these marks (Chaal et al., 2010; Cui et al., 2008). Interestingly, these histone modifiers themselves undergo PTMs, potentially influencing their activity during the parasite life cycle (Lasonder et al., 2016; Solyakov et al., 2011). Inhibition of HDACs or HATs in *P. falciparum* leads to gene expression dysregulation (Chaal et al., 2010; Cui et al., 2008), making these histone modifiers attractive targets for therapeutic interventions against malaria (Coetzee, 2020).

Apart from histone modifiers, epigenetic marks are recognized and interpreted by reader proteins, facilitating the recruitment of specific protein complexes that participate in various biological functions. Recent studies in *P. falciparum* identified readers, including Heterochromatin Protein 1 (HP1) associated with H3K9me3 and implicated in heterochromatin formation (Hoeijmakers et al., 2019; Pérez-Toledo et al., 2009), bromodomain proteins PfBDP1 and PfBDP2 enriched on acetylated H2B.Z, and PfGCN5-PfADA2, members of the transcriptional coactivator complex, associated with H3K4me2/me3 (Cheon et al., 2020).

Additionally, noncoding RNAs (ncRNAs) are emerging as important epigenetic regulators in many eukaryotes, including protozoan parasites. In *P. falciparum*, thousands of ncRNAs have been identified, with some belonging to the telomere-associated lncRNA (TARE) family involved in telomere maintenance and the regulation of virulence genes. These ncRNAs contribute to the complexity of epigenetic regulation in malaria parasites (Sierra-Miranda et al., 2017).

- Regulation of Virulence Genes in Plasmodium falciparum

One fascinating aspect of the parasite is its ability to evade the host's immune system, and to achieve this, *P. falciparum* employs clonally variant gene families, including var, rifin, stevor, and Pfmc-2TM, most of which are located in the subtelomeric regions. Among these, the var gene family, comprising approximately 60 genes that encode the PfEMP1 antigen, is extensively studied. PfEMP1 plays a crucial role in cytoadherence and sequestration of infected red blood cells. A remarkable feature is that only one var gene is expressed at a time, and its product is exported to the surface of the infected red blood cell, limiting the exposure of PfEMP1 variants to the host's immune system. This mutually exclusive expression necessitates precise regulation to repress all var genes while actively transcribing and translating only one var gene (Hollin & Le Roch, 2020).

During asexual blood stages, inactive var genes are enriched with H2A, as well as repressive marks like H3K9me3 and HP1 (Ukaegbu et al., 2014). These genes are found at the periphery of the nucleus, forming repressive clusters (Bunnik et al., 2018).Conversely, the active var gene is located at a perinuclear position, facilitating transcription, and exhibits high levels of H3K9ac and H3K4me3 marks, along with the histone variants H2A.Z/H2B.Z.

## 4.2.Post-transcriptional modifications

Post-transcriptional modifications are critical processes that occur during the transformation of the mRNA from its initial immature state to its mature form and involve extensive modifications, where each element and regulatory sequence present contributes to determining the ultimate destiny of the transcript. Elements like the mRNA 5' cap and poly(A) tail act as strong triggers for initiating translation, whereas other features such as internal ribosome entry sequences (IRES), upstream open reading frames (uORF), and complex RNA structures like hairpins exert their influence on translation in various ways (Gebauer & Hentze, 2004).

A variety of intricate post-transcriptional mechanisms are employed in *P. falciparum* to finely tune its gene expression, thereby influencing its life cycle, virulence, and adaptation strategies. One such mechanism is RNA splicing, which involves the removal of non-coding introns and the joining of exons to create mature mRNA. This process is particularly noteworthy in *P. falciparum* due to widespread alternative splicing that generates diverse transcripts and protein isoforms, contributing significantly to the parasite's adaptability and virulence (López-Barragán et al., 2011). Additionally, RNA editing, an exclusive phenomenon in *P. falciparum*, rectifies specific nucleotide sequences within its fragmented mitochondrial genome by inserting or deleting uridine (U) residues, thus ensuring the production of functional mRNAs (Sharma et al., 2009).

Post-transcriptional regulation further encompasses RNA modifications like m6A (N6-methyladenosine) and pseudouridylation, pivotal in shaping RNA stability, translation efficiency, and subcellular localization. In *P. falciparum*, the presence of m6A RNA modifications suggests their involvement in governing gene expression during various parasite life cycle stages, offering a potential avenue for intricate regulatory processes (Jha et al., 2021). Equally crucial is RNA degradation, orchestrated by PfRNases in *P. falciparum,* which significantly influences both gene expression control and growth rate dynamics (Morais et al., 2021).

Furthermore, the selective transport and localized translation of specific mRNAs are orchestrated by RNA-binding proteins like PfAlba1 in *P. falciparum.* This mechanism, vital for parasite development and pathogenesis, ensures that certain mRNAs are transported to distinct subcellular compartments for context-specific translation (Mair et al., 2006). Unraveling the complexities of these post-transcriptional modifications not only provides insight into the underlying biology of *P. falciparum* but also holds promise for the development of innovative therapeutic approaches.

### 4.3.Post translational modifications

**In the upcoming section, I will provide a concise overview of the various types of post-translational modifications. It is important to note that my thesis will primarily focus on**

**the dephosphorylation process, which will be thoroughly explored in the following chapters.**

Post-translational modifications (PTMs) encompass a broad range of biochemical changes in proteins, involving the addition or removal of chemical groups mediated by specific enzymes. These modifications contribute to the molecular complexity and diversity of the proteome in various cells and microorganisms(Kupferschmid et al., 2017). Reversible in nature, these induced modifications are implicated in protein activity, subcellular localization, protein-protein interactions, and other potential functions (Yakubu et al., 2018).

Numerous PTMs, such as acetylation, phosphorylation, lipidation, palmitoylation, ubiquitylation, and glycosylation, are involved in regulating various cellular processes. They play a crucial role in cell biology, pathogenicity, metabolic pathways, and the survival of pathogens including apicomplexan parasites like *Plasmodium* (Doerig et al., 2015; Manzano-Román & Fuentes, 2020).

In the case of *P. falciparum*, PTMs are widespread in proteins across different developmental stages and exert critical control over the virulence factors implicated in host-parasite interactions and pathogenesis (Rashidi et al., 2021).

Furthermore, it is important to explore some of the various PTMs occurring in *P. falciparum.*

### 4.3.1. Glycosylation

P. falciparum relies heavily on glucose as a vital energy source. To support the synthesis of various glycosylation precursors, the parasite enhances the permeability of the red blood cell (RBC) membrane to hexose molecules (Olszewski & Llinás, 2011). Among the glycoconjugates present in *P. falciparum*, glycosylphosphatidylinositol (GPI) anchors are the primary ones, and they participate in crucial glycosylation processes during the parasite's intracellular stages. These GPI anchors are attached to pathogen-associated molecular patterns and important surface proteins, including merozoite surface protein 1 (MSP1), which significantly contribute to the pathogenicity of *P. falciparum* (Cova et al., 2015; Gazzinelli et al., 2014).

### 4.3.2. Ubiquitylation

Protozoan parasites like *Plasmodium* possess ubiquitin (UB) and ubiquitin-like modifiers (Ubls), which include small ubiquitin-related modifier (SUMO), neural precursor cell-expressed developmentally down-regulated 8 (NEDD8), autophagy-related proteins 8 and 12 (ATG8 and ATG12), ubiquitin-related modifier 1 (URM1), and ubiquitin-fold modifier 1 (UFM1) (Hamilton et al., 2014; Karpiyevich & Artavanis-Tsakonas, 2020). These modifiers are expressed in all morphological stages of the erythrocytic cycle of *P. falciparum*.

The asexual intraerythrocytic developmental cycle (IDC) of *P. falciparum* heavily relies on protein degradation processes. Interestingly, more than half of the parasite's proteome appears to contain potential targets for ubiquitylation, particularly proteins expressed during the trophozoite stage. Thus, inhibition of the ubiquitin proteasome system (UPS), a significant intracellular proteolytic pathway, has been shown to reduce parasite infection. Moreover, ubiquitylation likely regulates essential processes such as DNA repair, replication, vesicular transport, catabolic events, and stress responses during *P. falciparum* infection and the IDC (Rashidi et al., 2021).

### 4.3.3. Protein lipidation

Protein lipidation is a crucial process in which lipids and lipid-related metabolites are covalently attached to proteins, thereby regulating numerous essential biological functions (B. Chen et al., 2018). Proteins that undergo lipidation exhibit shared functional regulation regarding associations with membrane proteins, albeit with variations in predictability and regulatory roles depending on the specific lipid involved (Resh, 2012).

Acylation, the general term used, refers to the addition of lipids like myristic or palmitic acid to protein N-termini or side chains. Two primary types of protein lipidation exist. First, palmitoylation entails the attachment of palmitic acid to a cysteine side chain through a thioester linkage. Second, N-myristoylation, catalyzed by an acyl transferase called N-myristoyltransferase (NMT), involves the addition of myristic acid to a specific set of protein substrates(Doerig et al., 2015).

### 4.3.4. Acetylation

Lysine enzymatic acetylation is a ubiquitous post-translational modification (PTM) observed in various organisms, including *P. falciparum* (Cobbold et al., 2016). More than 230 cytoplasmic and nuclear proteins have been identified as important targets of acetylation during

the intraerythrocytic development of *P. falciparum*. These proteins include the 14, 20S proteasome beta subunit, 6-phosphofructokinase, acetyl-CoA synthetase, actin I, elongation factor 1 and 2 (alpha and beta), and enolase (Miao et al., 2013). These findings highlight the widespread occurrence and potential regulatory significance of lysine acetylation in *P. falciparum.*

### 4.3.5. Epigenetic modifications

The discovery of epigenetic regulators, chromatin proteins, and epigenomic marks has provided valuable insights into the significant roles of epigenetic mechanisms in parasites (Duraisingh & Skillman, 2018). Epigenetic modifications, such as methylation and acetylation, are PTMs that play crucial roles in modulating chromatin structure. Dysregulation of these modifications can lead to abnormal gene expression or gene silencing. In malaria parasites, histone modifications have been implicated in their pathogenicity, highlighting the importance of identifying and understanding these PTMs. By identifying such epigenetic modifications, it may be possible to uncover potential epigenetic biomarkers and drug targets for the treatment of malaria (Saraf et al., 2016; Serrano-Durán et al., 2022).

## 5. Phosphorylation and dephosphorylation
### 5.1. General introduction

Protein phosphorylation is a prevalent post-translational modification (PTM) mechanism in cells, serving as a key regulator of protein function and playing critical roles in diverse cellular processes including cell proliferation (Figure 5) (Cohen, 2000; Hunter & Pawson, 2012). It involves the addition of phosphate groups to specific amino acids, namely serine (84.4%), threonine (13.2%), and tyrosine (2.4%), with percentages similar to those observed in humans or mice, catalyzed by specific enzymes (Lasonder, Green, et al., 2012; Pease et al., 2013; Solyakov et al., 2011). In the context of *P. falciparum*, three phosphoproteomes have allowed the detection of 8,463 phosphorylation sites on 1,673 proteins (Treeck et al., 2011), 1,177 sites on 650 proteins (Solyakov et al., 2011), and 2,541 sites on 919 proteins(Lasonder, Treeck, et al., 2012), and they are associated with essential cellular activities (Solyakov et al., 2011). The flexible, dynamic and yet tight regulation achieved by reversible phosphorylation control part of the complexity observed in the *Plasmodium* life cycle.
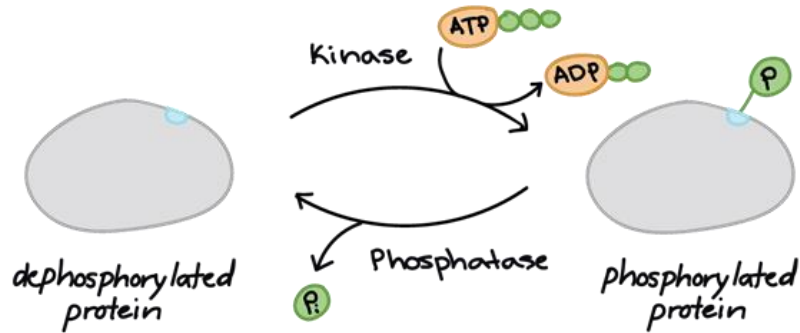
**Figure 5: A scheme representing phosphorylation/dephosphorylation phenomena**

## 5.2. Kinases

### 5.2.1. Introduction of kinases

Protein kinases act as molecular switches in signaling pathways governing cell division, metabolism, transcription, differentiation, and apoptosis. Their specific roles throughout the cell have become evident, with their dysregulation being linked to diverse disease development(Cipak, 2022).  At their core, these enzymes facilitate the transfer of γ-phosphate from ATP (or GTP) to protein substrates(Arendse et al., 2021).

There are two main types of protein kinases. The first type consists of proteins that phosphorylate tyrosine residues, while the second type is specific to modifications at serine and/or threonine residues. The majority of kinases share a similar mode of operation and a common structure, involving a β-sheet that binds to ATP and a predominant α-helix that associates with the peptide substrate in the N-lobe and C-lobe, respectively. Upon binding, the enzymes undergo a series of conformational changes associated with the rapid transfer of the phosphate group and the release of the modified product (Figure 6) (Brautigan & Brautigan, 2013).
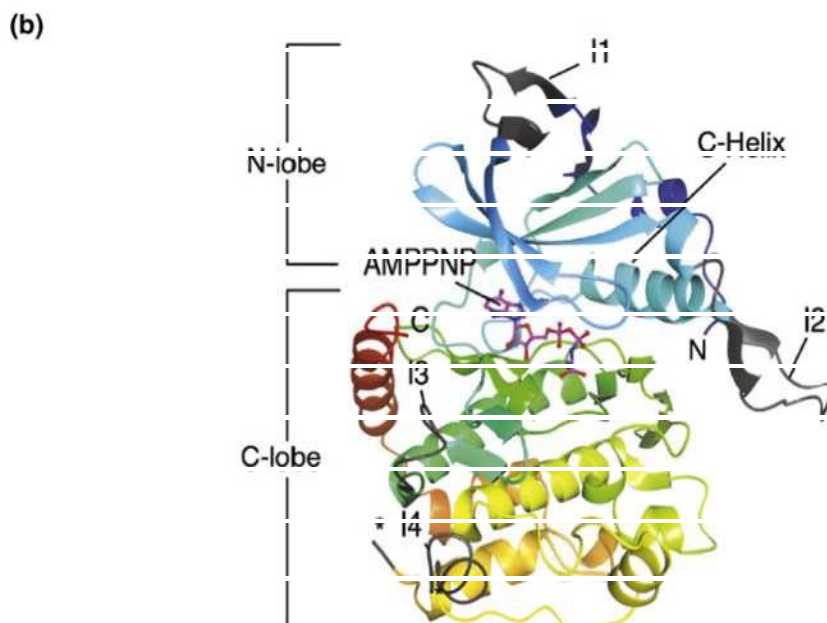
**Figure 6 The common structure of kinases**. *(Brautigan & Brautigan, 2013)*

### 5.2.2. Functions of kinases

In a recent review, DeRoo et al. investigate the pathologic implications of RIPK1 and RIPK3 kinases in cardiovascular disease, showing the efficacy of inhibitors targeting these kinases for cardiovascular disease prevention and treatment (Deroo et al., 2020). Another review focuses on casein kinase 1 (CK1) enzymes, discussing their substrates and therapeutic potential through inhibition (Janovská et al., 2020). In addition, CK1α and CK2 protein kinases show an important role in oncogenic and stress-related signaling in hematological cancers(Spinello et al., 2021). Daams and Massoumi explore Nemo-like kinase (NLK), an atypical proline-directed serine/threonine mitogen-activated protein (MAP) kinase, presenting its role in organ development and function, such as the lung, heart and skeleton using NLK-deficient mice (Daams & Massoumi, 2020). Additionally, recent studies investigate the diverse nature of tyrosine kinase substrates (TKS) scaffold proteins, to explore their structure, regulation, and involvement in various cellular processes, including migration, invasion, differentiation, and adipose tissue and bone homeostasis (Kudlik et al., 2020). Moreover, the synergistic effect of protein kinase CK2 inhibitors with 5-fluorouracil (5-FU) were examined in triple-negative breast cancer cells, suggesting FAK kinase as a potential target (Wińska et al., 2022). All these recent reviews and studies show the importance of the protein kinases as drug targets in various diseases.

### 5.2.3. *Plasmodium* kinome

The *Plasmodium* kinome accounts for approximately 1.7% of coding genes within *P. falciparum*(Miranda-Saavedra et al., 2012; Ward et al., 2004). While many of these kinases can be categorized into established eukaryotic protein kinase (ePK) groups such as AGC (named after protein kinase A, G, and C families, containing cyclic nucleotide and calcium/phospholipid-dependent kinases), CAMK (calmodulin/calcium-dependent kinase), CK1 (casein or cell kinase 1), CMGC (named after CDK, MAPK, GSK3, and CLK families), STE (homologues of yeast STE7, STE11, and STE20 genes, including kinases in MAPK pathways but not MAPKs), TKL (tyrosine kinase-like serine/threonine kinase), and others, or atypical kinase (aPK) groups like PIKK (phosphatidylinositol 3-kinase-related kinases) and RIO (right open reading frame).

The *Plasmodium* kinome exhibits substantial genetic divergence from both other eukaryotic organisms and its human host (Miranda-Saavedra et al., 2012; J. Zhang et al., 2001). Numerous *Plasmodium* kinases lack clear human orthologues, and even in instances where orthologues are present, significant structural disparities and distinctive features are noticeable. These variations encompass considerable insertions within kinase domains as well as marked differences in regulatory regions. Such divergences imply that regulatory mechanisms and functions of these kinases may substantially differ from those of their human counterparts.

The updated kinome of the human malaria parasite *P. falciparum* comprises approximately 89 PKs, with 65 ePKs, 19 FIKKs and 5 aPKsm, many of which are not related to established families of higher eukaryotes (Miranda-Saavedra et al., 2012).

Key distinctions setting the *Plasmodium* kinome apart from the human kinome encompass:

(1) the absence of tyrosine kinases (TK), the most extensive kinase group in humans, and structurally related receptor guanylate cyclases (RGCs);

(2) absence of readily identifiable MAPKK homologues, despite the existence of two MAPKs; (3) inclusion of the CAMK group, featuring a 7-member calcium-dependent protein kinase (CDPK) family also found in plants and other protists, yet devoid of mammalian counterparts;

(4) presence of FIKKs, an ePK-related family unique to apicomplexan parasites (Miranda-Saavedra et al., 2012; Ward et al., 2004).

The kinome remains generally conserved among *Plasmodium* species, although variations in kinase group counts suggest potential divergent roles and redundancy. The considerable expansion of the FIKK family in *P. falciparum* to 19 members, in contrast to other *Plasmodium* species maintaining only one, contributes significantly to this differentiation. All 18 distinct FIKKs display export signal sequences and are believed to influence virulence by modulating host factors (Kats et al., 2014; Nunes-Xavier et al., 2010).

A recent quantitative phosphoproteomics study by Davies et al. (Davies et al., 2020) exposes unique phosphorylation patterns associated with *P. falciparum* FIKK kinases, including FIKK-driven phosphorylation of parasite virulence factors and host erythrocyte proteins.

Figure 7 depicts the number of kinases in each family per organism as a percentage of their kinome.
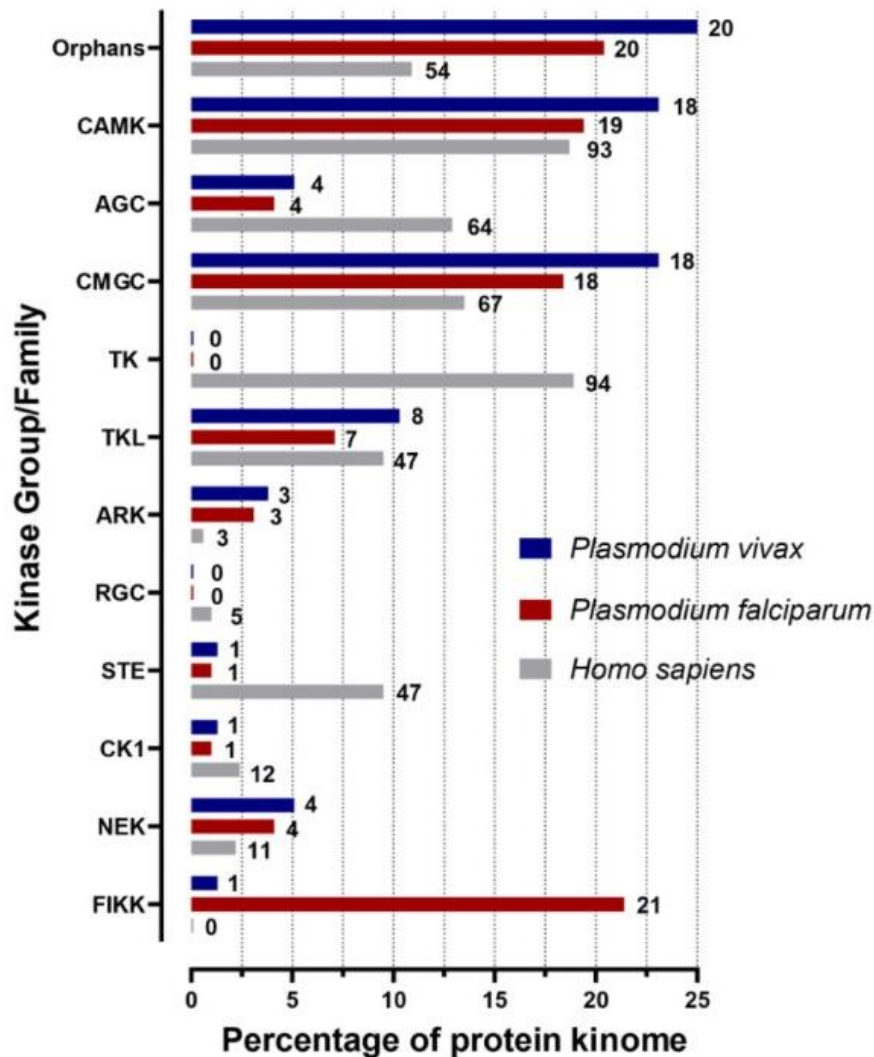
**Figure 7 Visualisation of the protein kinase family membership across *Homo sapiens, Plasmodium falciparum, Plasmodium vivax*.** The nine typical protein kinase families along with the Aurora kinase family (ARK) and the Apicomplexan-specific family of FIKK were included here. The remaining unassigned kinases are denoted as Orphans. Each group/family is represented as a percentage of the total protein kinome for each organism. Note atypical protein kinases are not included in this analysis. The number next to each bar indicates the number of kinases which belong to each of the respective families for each organism. Blue = *Plasmodium vivax*, Red = *Plasmodium falciparum* and Grey = *Homo sapiens* (Adderley & Doerig, 2022)

A comprehensive reverse genetics study aimed at disrupting the entire kinome gene set has highlighted the significance of these proteins during the asexual development of the pathogen. This work reveals that out of the 65 ePKs present in this organism, at least half are essential for maintaining its viability. However, these findings suggest the existence of functional redundancies for slightly less than half of these proteins. Therefore, the reality appears to be far from the simplistic notion that one kinase corresponds to one substrate(Solyakov et al., 2011).

**Table 3 Putative kinome of *Plasmodium falciparum*.** The name and family of the kinases alongside the references.

| Name | | Kinase Group/Family | Reference |
|---|---|---|---|
| PfTKL2 | | Tyrosine kinase-like | (Solyakov L. 2011) |
| PfTKL4 | | Tyrosine kinase-like | (Solyakov L. 2011) |
| PfeiK1 | | eIF2α kinase | (Fennell C. 2009) |
| PfeiK2 | | eIF2α kinase | (Schneider AG & Mercereau- Puijalon O. 2005) |
| Pfnek-3 | | NimA | (Solyakov L. 2011) |
| Pfnek-2 | | NimA | (Reininger L.. 2009) |
| Pfnek-4 | | NimA | (Solyakov L. 2011) |
| MAL13P1.196 | | CMGC/CDK | (Solyakov L. 2011) |
| Pfcrk-5 | | CMGC/CDK | (Solyakov L. 2011) |
| Pfmap-2 | | CMGC/GSK3 | (Dorin-Semblat D. 2007) |
| PfPK1 | | CMGC/MAPK | (Solyakov L. 2011) |
| PfCDPK7 | | CDPK | (Solyakov L.2011) |
| PfCDPK4 | | CDPK | (kato N. 2008) |
| PF14_0227 | | CamK | (Solyakov L. 2011) |
| Pf11-0239 | | CamK | (Solyakov L. 2011) |
| PfPKRP | | CamK | (Solyakov L. 2011) |
| PFB0665w | | CamK | (Solyakov L. 2011) |
| MAL7P1.18 | | CamK | (Solyakov L. 2011) |
| Pf11_0060 | | CamK | (Solyakov L. 2011) |
| PfPK8 | | Orpheline | (Solyakov L. 2011) |
| PfI1280c | | Orpheline | (Solyakov L. 2011) |
| Pf14_0392 | | Orpheline | (Solyakov L. 2011) |
| MAL7P1.78 | | Orpheline | (Solyakov L. 2011) |
| Pf14_0476 | | Orpheline | (Solyakov L. 2011) |
| PfPK7 | | Orpheline | (Dorin-Semblat D. 2008) |
| PfL2280w | | Orpheline | (Solyakov L. 2011) |
| PfCK1 | | Caseine Kinase 1 | (Solyakov L. 2011) |
| PfTKL3 | | Tyrosine kinase-like | (Abdi A. 2010) |
| PfTKL1 | | Tyrosine kinase-like | (Solyakov L. 2011) |
| PfK4 | | eIF2α kinase | (Solyakov L. 2011) |
| Pfnek-1 | | NimA | (Dorin-Semblat D. 2011) |
| Pfcrk-4 | | CMGC/CDK | (Solyakov L. 2011) |

| | | |
|---|---|---|
| **PfK6** | CMGC/CDK | (Solyakov L. 2011) |
| **Pfcrk-3** | CMGC/CDK | (Halbert J. 2010) |
| **PfPK5** | CMGC/CDK | (Solyakov L. 2011) |
| **Pfmrk** | CMGC/CDK | (Solyakov L. 2011) |
| **Pfcrk-1** | CMGC/CDK | (Solyakov L. 2011) |
| **Pfmap-2** | CMGC/CDK | (Dorin-Semblat D. 2007) |
| **PfCK2** | CMGC/CK2 | (Holland Z. 2009) |
| **MAL13P1.84** | CMGC/GSK3 | (Solyakov L. 2011) |
| **PfGSK3** | CMGC/GSK3 | (Solyakov L. 2011) |
| **PfCLK3** | CMGC/CDK-like | (Solyakov L. 2011) |
| **PfCLK1** | CMGC/CDK-like | (Agarwal S. 2011) |
| **PfCLK4** | CMGC/CDK-like | (Solyakov L. 2011) |
| **PfCLK2** | CMGC/CDK-like | (Agarwal S. 2011) |
| **PfPK2** | CamK | (Solyakov L. 2011) |
| **PfCDPK1** | CDPK | (kato N. 2008) |
| **PfCDPK5** | CDPK | (Dvorin JD. 2010) |
| **PfCDPK2** | CDPK | (Solyakov L. 2011) |
| **PfCDPK3** | CDPK | (Solyakov L. 2011) |
| **PfARK1** | Aurora | (Reininger L.. 2011) |
| **PfARK2** | Aurora | (Solyakov L. 2011) |
| **PfARK3** | Aurora | (Solyakov L. 2011) |
| **Pf11-0464** | AGC-related | (Solyakov L. 2011) |
| **Pf11-0227** | AGC-related | (Solyakov L. 2011) |
| **PfPKG** | AGC | (Taylor HM. 2010) |
| **PfPKB** | AGC | (Solyakov L. 2011) |
| **PfPKA** | AGC | (Solyakov L. 2011) |
| **PfEST** | Orpheline | (Solyakov L. 2011) |
| **Pf11_0488** | Orpheline | (Solyakov L. 2011) |
| **PfKIN** | Orpheline | (Solyakov L. 2011) |
| **PfPK9** | Orpheline | (Solyakov L. 2011) |

**Table 4. Putative kinome of *P. falciparum*.** A summarizing table of the kinase families, numbers and functions.

| Groups | | | Number | | Functions described in *Eukaryotes* and *Plasmodium* |
|---|---|---|---|---|---|
| ePKs (65 to 71) | CK1 | | 1 | | Proliferation and differentiation |
| | TKL | | 3 to 5 | | |
| | CMGC | CDK | 9 | | Proliferation, differentition and RNA splicing |
| | | MAPK | 2 | | |
| | | GSK3 | 3 | | |
| | | CLK | 4 | | |
| | CamK | | 12 to 13 | | Calcium dependent signalization |
| | AGC | | 5 | | Signalization |
| | Aurora | | 3 | | Cellular division |
| | Nima | | 4 | | Cellular division |
| | eIF2α | | 3 | | Translational regulation |
| | Orpheline | | 14 to 19 | | |
| aPK | RIO | | 2 | | RNA metabolism |
| | ABC1 | | 2 | | Oxidative stress response |
| FIKK | | | 20 to 21 | | Remodeling of host cell and protein trafficking |

### 5.2.3. Kinases as drug targets

Kinases are highly regarded as attractive drug targets in the context of cancer and other diseases due to several key factors:

1. The ATP binding site, a shared characteristic among all kinases, offers a promising chance for drug development. The strategies for designing potent ATP-competitive kinase inhibitors are well-established (Solyakov et al., 2011).

2. Essentiality is a critical aspect for drug discovery, requiring that kinase inhibition leads to parasite death. Ensuring the kinase's indispensability for parasite survival forms the basis for effective drug design (Cabrera et al., 2018).

3. The pursuit of selectivity over human kinases is imperative to diminish potential toxicity. Although slight differences exist between the ATP binding sites of various kinases in both *Plasmodium* and humans, beginning with compounds displaying minimal activity against human kinases is optimal. The utilization of structure-based approaches aids in the

development of selective inhibitors targeting the parasite enzyme rather than its human counterpart (Knight & Shokat, 2005; Miller et al., 2019).

4. A thorough understanding of how the target kinase behaves and responds to inhibition at different stages of the parasite life cycle is important. The best condition is when the kinase is necessary during various stages of the life cycle. If a kinase that plays a vital role in the liver, asexual blood, gametocyte, and mosquito stages can be targeted, it opens the possibility of developing antimalarial medications that can prevent the disease, treat it, and also block its transmission (Ward et al., 2004).

5. The challenge of combating resistance is significant for antimalarials, whether in the field of general anti-infectives or specific malaria treatments. Crucially, any new antimalarial should demonstrate no significant cross-resistance with existing antimalarials (Ding et al., 2012).

### 5.2.4. Promising *Plasmodium* kinase targets

Numerous *Plasmodium* kinases exhibit promise and are under investigation. This update highlights three chemically validated kinases essential for various stages of the *Plasmodium* life cycle and significant for malaria drug discovery.

- PI4KIIIβ: Initially identified as a potential antimalarial target in 2013, PI4KIIIβ has emerged as a valuable candidate. It was established as the primary target for certain imidazopyrazine/pyridine compounds that exhibited potent antiplasmodium activity across different life cycle stages. Genetic essentiality and target identification were confirmed through in vitro resistant selections and engineered parasite lines. Notably, the aminopyridine MMV390048, an ATP-competitive inhibitor, is now in Phase II clinical trials. Its efficacy extends to various life cycle stages and aligns with multiple therapeutic goals (TCP1, TCP4, and TCP5). PI4KIIIβ inhibitors face moderate resistance development, prompting exploration of new chemotypes. Human PI4KIIIβ structures offer insights into optimizing *Plasmodium* PI4KIIIβ inhibitors for potency and selectivity (Fienberg et al., 2020; Krishnan et al., 2020) (Brunschwig et al., 2018).
- PKG: *Plasmodium* PKG, distinct from mammalian PKGs, is a serine/threonine protein kinase essential across parasite life cycle stages. Effective inhibitors have demonstrated prophylactic liver-stage, blood-stage, and transmission-blocking antiplasmodium

activity. Lead compounds, such as ML10 and MMV030084, have displayed promising profiles. PKG inhibition remains challenging due to human kinase off-target selectivity concerns. Mechanisms of allosteric inhibition are understood, but allosteric PKG inhibitors with potent antiplasmodium activity are yet to be identified. PKG inhibitors exhibit slow in vitro killing but possess characteristics beneficial for generating multistage antimalarials with limited resistance potential (Franz et al., 2018; Koussis et al., 2020).

- CLK3: *Plasmodium* CLK3 stands out as a prospective multistage antimalarial target (Alam et al., 2019). Genetic essentiality in asexual blood-stage development and conservation across *Plasmodium* species underscore its potential (Bushell et al., 2017a). TCMDC-135051, a CLK3 inhibitor, has demonstrated liver-stage prophylactic, asexual blood-stage antiplasmodium activity, and transmission reduction. In vitro resistance selections and chemogenetics approaches provided further evidence for CLK3 as a vital target. This kinase's role in mRNA splicing contributes to its significance, and initial optimization efforts have commenced (Mahindra et al., 2020).

These chemically validated kinases show promise for malaria drug discovery, underscoring the importance of identifying essential targets with multiple-stage activity and potential for limited resistance (Adderley & Doerig, 2022).

## 5.3. Phosphatases

### 5.3.1. Introduction of phosphatases

Phosphatases play a crucial role in removing phosphate groups from biomolecules, acting as essential counterparts to kinases in maintaining the delicate balance of physiological phosphorylation states. Dysregulation of this balance can contribute to the onset and progression of various diseases, underscoring the significance of kinases and phosphatases as potential targets for drug development (H. Zhang et al., 2023).

Phosphatases exhibit diverse biochemical mechanisms. They vary in terms of their structure, active sites, and hydrolysis mechanisms, among other factors. Protein phosphatases can be classified into two major families: Serine-Threonine Phosphatases (PSPs) and Tyrosine Phosphatases (PTP) (Shi, 2009; Virshup & Shenolikar, 2009).

### 5.3.2. Serine/threonine phosphatases

Serine/Threonine Phosphatases, that we will be focused on, are enzymes responsible for the dephosphorylation of phosphorylated serine (pSer) or threonine (pThr) residues. They are categorized into at least three distinct families, which include serine/threonine-specific phosphoprotein phosphatases (PPPs), metal-dependent protein phosphatases (PPMs), and aspartate-based protein phosphatases (DxDxTs)(Brautigan & Brautigan, 2013). The most significant among them is the PhosphoProtein Phosphatases (PPP), which exhibit one of the highest levels of conservation observed in enzymes across species (approximately 80%). PPPs play pivotal roles in numerous essential cellular signaling pathways associated with processes like cell division and growth. Remarkably, over 90% of serine/threonine dephosphorylation events rely on PPPs (Brauer et al., 2021). PPP sequences have some distinctions that allow classification into different subtypes. Within the human genome, there are seven different subtypes including phosphatase type 1 (PP1), type 2A (PP2A), PP3 (PP2B or calcineurine), PP4, PP5, PP6, and PP7 (Shi, 2009). These proteins typically function as multimeric holoenzymes consisting of a highly conserved catalytic center from a structural and mechanistic perspective and regulatory subunits, allowing them to dephosphorylate a variety of substrates. They differ in terms of their outer solvent-exposed loops, which vary the shape and surface charge, modulating ligand affinity (Egloff et al., 1995; Goldberg et al., 1995). Among these, PP1 and PP2A stand out as the two most abundant protein phosphatases found in cells.

### 5.3.3. Functions of phosphatases

Protein phosphatases are integral to a wide array of biological processes and hold significant importance in the functioning of organisms. The figure 8 below provides a concise overview of some of the extensively studied biological roles of protein phosphatases in animal development (Zhang et al., 2023).
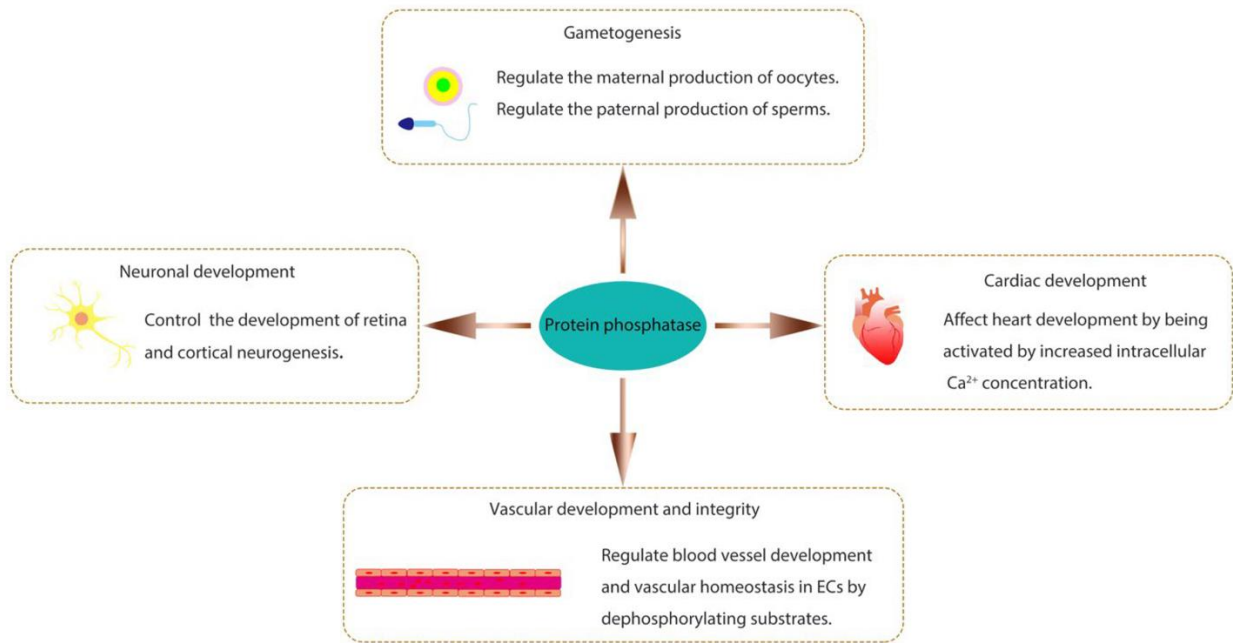
**Figure 8. Various biological functions of protein phosphatase** (Zhang et al., 2023).

Protein phosphatases play a crucial role in gametogenesis, regulating the production of oocytes and sperms. In Xenopus oocytes, PP2A, along with its regulatory subunit, control meiotic division and M-phase entry by counteracting the actions of protein kinase A (PKA) (Lemonnier et al., 2021). PP6 has also been implicated in gametogenesis. PP6 regulates meiotic recombination and fertility (Lei et al., 2020). In addition to the previous phosphatases, PP4 is crucial for normal sperm production, where its deletion in mouse germ cells leads to defects in sperm tail structure, reduced sperm count, and poor sperm motility, ultimately causing male infertility (Han et al., 2021). These findings highlight the indispensable roles of protein phosphatases in the complex processes of gametogenesis.

Protein phosphatases play significant roles in cardiac development. Calcineurin (PP2B), a $Ca^{2+}$-dependent protein serine/threonine phosphatase (PSTP), is crucial for cardiomyocytes. In zebrafish, the PP2A regulatory subunit PPP2R3A is essential for normal myocardium formation and cardiac contractile function (Song et al., 2018). Another phosphatase, Pez, a member of protein tyrosine phosphatases (PTP), is transiently expressed in the zebrafish embryo heart (Wyatt et al., 2007). Knocking down Pez leads to heart looping defects and the absence of functional atrio-ventricular (A-V) valves. These findings demonstrate the crucial involvement of protein phosphatases in cardiac development.

In the vascular system, PP2A, specifically its regulatory subunit PP2A-Bα, is essential for vascular lumen integrity in zebrafish by controlling the activity of histone deacetylase 7 (HDAC7), a vital regulator of vascular stability (Martin et al., 2013). Additionally, PP2A regulates angiogenesis by modulating the activity of Yes-associated protein (YAP), a key player in the Hippo signaling pathway, promoting endothelial cell functions like proliferation, migration, and sprouting in mice (X. Jiang et al., 2021).

In neuronal development, receptor-type phosphatases such as PTPα, PTPγ, PTPδ, and PTPσ, contribute to various facets of neural development in both vertebrates and invertebrates. They regulate processes like neurogenesis, axon growth and guidance, synapse formation, and plasticity (Tomita et al., 2020).

Overall, protein phosphatases are integral to a wide range of developmental processes, underscoring their significance in biology.

### 5.3.4. *Plasmodium* Phosphatome

Previous in silico experiments have characterized several *Plasmodium* phosphatases (Andreeva et al., 2001; Philip et al., 2012) and defined the *Plasmodium* phosphatome (Pandey et al., 2014; Wilkes & Doerig, 2008) which has led to the identification of sixty-seven protein phosphatases (Table 5 and 6) (Pandey et al., 2014). The protein phosphatases in *P. falciparum* can be classified into four main families: phosphoprotein phosphatases, protein phosphatases 2C, protein tyrosine phosphatases, and haloacid dehalogenases. The first two families fall under the category of metallophosphatases. The remaining enzymes are grouped into the diverse group, which includes members from the Histidine phosphatases, PAP2_like, and Exonuclease-endonucleases phosphatases families, among others. Out of the 67 putative phosphatases, 44 are expressed in both asexual and gametocyte stages, while 3 seem to be exclusive to schizonts and 4 to gametocytes.

**Table 5. *Plasmodium* Phosphatome**. The different phosphatases groups with their numbers and caracteristics.

| Groups | Number | Caracteristics |
|--------|--------|----------------|
|        |        |                |

| | | |
|---|---|---|
| Phosphoprotein phosphatases | **18** | **Dependent on metal ions (Mn2+, Ca2+ ...)** |
| Protein phosphatases 2C | **11** | **Dependent on metal ions (Mn2+, Mg2+ )** |
| Protein Tyrosine phosphatases | **4** | **Low molecular weight phosphatases.** |
| Haloacid Dehalogenase | **10** | **Catalytic reaction based on 1 aspartate** |
| Diverses | **24** | |

**Table 6.** *P. falciparum* **proteins with conserved phosphatase related superfamily domains** (accession numbers as per http://www.plasmoDB.org , version 9.2 and superfamily according to NCBI CDD search)

| ID | Description | Length |
|---|---|---|
| MPP (Metallophosphatase) superfamily | | |
| **PF3D7_0314400** | serine/threonine protein phosphatase, putative | 308 |
| **PF3D7_0802800** | serine/threonine protein phosphatase, putative | 604 |
| **PF3D7_0918000** | glideosome-associated protein 50, secreted acid phosphatase (GAP50) | 396 |
| **PF3D7_0925400** | protein phosphatase-beta | 466 |
| **PF3D7_0927700** | serine/threonine protein phosphatase, putative | 312 |
| **PF3D7_1018200** | serine/threonine protein phosphatase, putative | 2166 |
| **PF3D7_1206000** | protein phosphatase, putative | 304 |
| **PF3D7_1355500** | serine/threonine protein phosphatase (PP5) | 658 |
| **PF3D7_1403900** | phosphatase, putative | 298 |

| | | |
|---|---|---|
| **PF3D7_1406700** | phosphatase, putative | 194 |
| **PF3D7_1414400** | serine/threonine protein phosphatase (PP1) | 304 |
| **PF3D7_1423300** | serine/threonine protein phosphatase (PP7) | 959 |
| **PF3D7_1464600** | phosphatase, putative | 1442 |
| **PF3D7_1466100** | protein serine/threonine phosphatase | 889 |
| **PF3D7_1469200** | protein phosphatase, putative | 358 |
| **PF3D7_0107800** | DNA repair exonuclease Mre11, putative | 1233 |
| **PF3D7_0912400** | conserved Plasmodium protein, unknown function | 446 |
| **PF3D7_1340600** | RNA lariat debranching enzyme, putative (DBR1) | 575 |
| HP (Histidine phosphatases) superfamily | | |
| **PF3D7_1430300** | acid phosphatase, putative | 2657 |
| **PF3D7_0208400** | conserved Plasmodium protein, unknown function | 2010 |
| **PF3D7_0310300** | phosphoglycerate mutase, putative | 1165 |
| **PF3D7_0413500** | phosphoglucomutase-2 (PGM2) | 295 |
| **PF3D7_1120100** | phosphoglycerate mutase, putative (PGM1) | 250 |
| HAD_like (Haloacid Dehalogenase) superfamily | | |
| **PF3D7_0515900** | protein phosphatase, putative | 328 |
| **PF3D7_0726900** | protein phosphatase, putative | 519 |
| **PF3D7_1012700** | protein phosphatase, putative | 1438 |
| **PF3D7_1226100** | hydrolase/phosphatase, putative | 316 |
| **PF3D7_1355700** | protein phosphatase, putative | 1288 |
| **PF3D7_1363200** | bifunctional polynucleotide phosphatase/kinase (PNKP) | 462 |
| **PF3D7_0715000** | 4-nitrophenylphosphatase (PNPase) | 322 |
| **PF3D7_0817400** | conserved Plasmodium protein, unknown function | 739 |
| **PF3D7_1118400** | haloacid dehalogenase-like hydrolase, putative | 306 |
| **PF3D7_0303200** | HAD superfamily protein, putative | 1162 |
| PAP2_like (2-phosphatidic acid phosphatases) superfamily | | |
| **PF3D7_0625000.1** | phosphatidic acid phosphatase (PAP) | 439 |
| **PF3D7_0625000.2** | phosphatidic acid phosphatase | 461 |
| **PF3D7_0805600** | apicoplast phosphatidic acid phosphatase, putative | 308 |
| PP2Cc (Protein phosphatases 2c domain) superfamily | | |
| **PF3D7_1138500** | protein phosphatase 2c | 924 |
| **PF3D7_0410300** | protein phosphatase, putative | 906 |

| | | |
|---|---|---|
| **PF3D7_0520100** | protein phosphatase, putative | 706 |
| **PF3D7_0810300** | protein phosphatase, putative | 550 |
| **PF3D7_0810500** | protein phosphatase, putative | 303 |
| **PF3D7_1009600** | protein phosphatase, putative | 488 |
| **PF3D7_1135100** | protein phosphatase, putative | 689 |
| **PF3D7_1249300** | protein phosphatase, putative | 1027 |
| **PF3D7_1309200** | protein phosphatase 2c-like protein, putative | 827 |
| **PF3D7_1455000** | protein phosphatase, putative | 410 |
| **PF3D7_1208900** | conserved Plasmodium protein, unknown function | 1442 |
| EEP (Exonuclease-endonuclease Phosphatases) superfamily | | |
| **PF3D7_0319200** | endonuclease/exonuclease/phosphatase family protein, putative | 906 |
| **PF3D7_0705500** | inositol-phosphate phosphatase, putative | 2814 |
| **PF3D7_1111600** | endonuclease/exonuclease/phosphatase family protein, putative | 744 |
| **PF3D7_0107200** | carbon catabolite repressor protein 4, putative | 337 |
| **PF3D7_0305600** | AP endonuclease (DNA-[apurinic or apyrimidinic site] lyase), putative | 617 |
| **PF3D7_1238600** | sphingomyelin phosphodiesterase, putative | 393 |
| **PF3D7_1363500** | DNase I-like protein, putative | 836 |
| **PF3D7_1430600** | exodeoxyribonuclease III, putative | 876 |
| Syja_N (SacL homology domain) superfamily | | |
| **PF3D7_0705500** | inositol-phosphate phosphatase, putative | 2814 |
| **PF3D7_0802500** | inositol phosphatase, putative | 1419 |
| **PF3D7_1354200** | inositol-polyphosphate 5-phosphatase, putative | 803 |
| PTPLA (Protein tyrosine phosphatase-like protein) superfamily | | |
| **PF3D7_1331600** | protein tyrosine phosphatase, putative | 228 |
| RHOD (Rhodanese Homology Domain) superfamily | | |
| **PF3D7_1305500** | protein phosphatase, putative | 771 |
| **PF3D7_1206400** | rhodanese like protein, putative | 346 |
| CYTH-like_Pase (Triphosphate Tunnel Metaloenzyme Phosphatases) superfamily (Apicomplexan) | | |
| **PF3D7_0322100** | RNA triphosphatase (Prt1) | 591 |

| | | |
|---|---|---|
| PTH2_family (Peptidyl-tRNA hydrolase, type 2) superfamily | | |
| **PF3D7_0610500** | conserved protein, unknown function | 123 |
| PTPc (Protein Tyrosine phosphatase) superfamily | | |
| **PF3D7_0309000** | dual specificity phosphatase (YVH1) | 575 |
| **PF3D7_1113100** | protein tyrosine phosphatase (PRL) | 218 |
| **PF3D7_1127000** | protein phosphatase, putative | 287 |
| **PF3D7_1455100** | protein phosphatase, putative | 171 |
| Nucleoside Phosphatase superfamily | | |
| **PF3D7_1431800** | apyrase, putative | 874 |
| **PF3D7_1322000** | adenosine-diphosphatase, putative | 565 |

Among the parasite's protein phosphatases, 33 do not have human orthologs, including 6 that are specific to *Plasmodium* (Pandey et al., 2014). The pronounced divergence observed in the phosphatome of malaria parasites across major eukaryotic phyla suggests the potential of parasite-specific phosphatases as promising targets for antimalarial drug discovery.

Furthermore, in *P. berghei*, half of the protein phosphatases appear to be essential for the parasite's survival during the erythrocytic cycle, with six playing crucial roles in mosquito stages (Guttery et al., 2014). Among those essential during the asexual cycle, several are phosphoprotein phosphatases, including PP1c and PP2A.

Through genome-wide saturation mutagenesis in *P. falciparum*, the role of each gene in the asexual development of *Plasmodium* was evaluated. It was found that over 50% of phosphatases in *P. falciparum* are likely essential for the survival of these parasites within blood cells, underscoring the crucial importance of these enzymes (Figure 9) (Zhang et al., 2018).
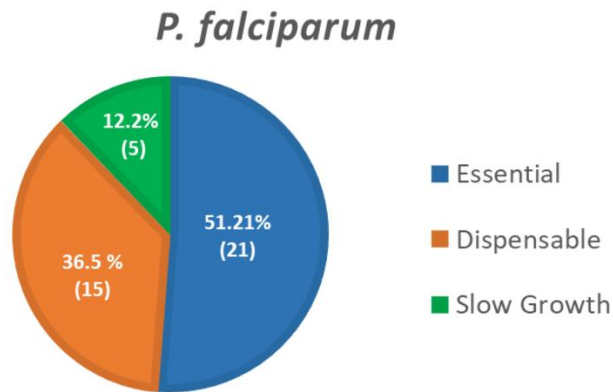
**Figure 9. Pie chart of the protein phosphatases' essentiality in *P. falciparum*** for the parasite blood stage development as determined in the genome-wide saturation mutagenesis (Zhang et al., 2018).

### 5.3.5. Phosphatases as drug targets

Recent research efforts have made significant strides in elucidating the functions and impact of phosphatase signaling in both normal development and pathological conditions (Figure 10).
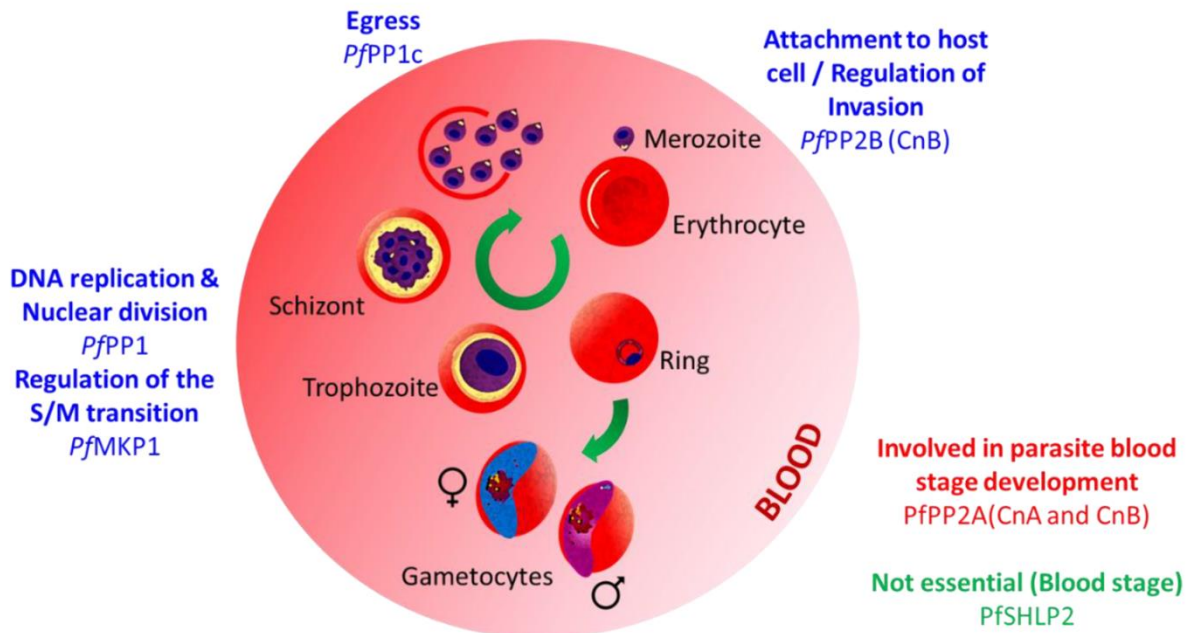


**Figure 10 Schematic illustration of *P. falciparum* development in red blood cell** showing the protein phosphatases with known stage specific function (Fréville et al., 2022).

The first noteworthy development emerged in 2016 when Chen et al. identified a small molecule called SHP099, capable of binding to and selectively inhibiting the activity of the

protein tyrosine phosphatase SHP2 (Chen et al., 2016). SHP2 was the first oncogenic phosphatase associated with multiple cancer types. SHP099 has exhibited potent inhibitory effects on the growth of human cancer cells in vitro and on xenograft tumors in a mouse model when administered orally. Ongoing clinical trials are currently underway to validate SH099 as a potential drug for the treatment of human diseases.

The second significant advancement stemmed from a study in which a specific inhibitor of a regulator of PP1 (PPP1R15B) was shown to effectively control translation, improve proteostasis, and mitigate deficiencies related to Huntington's disease in a mouse model (Krzyzosiak et al., 2018).

These successful strategies in the field of phosphatase research have played a pivotal role in the establishment, as of 2021, of the first research and development company, Anavo Therapeutics, with the explicit mission of developing drug candidates targeting phosphatases. This endeavor aims to expedite research in the field and offer additional avenues for the treatment of human diseases (https://www.anavotx.com/).

Within the identified phosphatases, our laboratory's primary focus is on the Protein Phosphatase Type 1 in *Plasmodium falciparum*. This thesis revolves around the study of PP1c, its mechanism of action, regulators, and biological functions.

## C. The case of Protein Phosphatase type 1 PP1

Protein Phosphatase 1 (PP1) holoenzyme, a ubiquitous serine/threonine phosphatase, plays a pivotal role in the regulation of cell signaling in eukaryotes. This holoenzyme consists of 1) a catalytic subunit and 2) regulatory subunits that govern its substrate specificity and cellular localization as well as its phosphatase activity (Heroes et al., 2013). Through the dephosphorylation of target proteins, the PP1 holoenzyme modulates critical cellular functions, including cell cycle progression, signal transduction, and gene expression (Brautigan & Shenolikar, 2018; Ceulemans & Bollen, 2004). Additionally, the binding of various regulatory subunits confers versatility to PP1 in response to environmental triggers and intracellular signaling pathways (Heroes et al., 2013). Understanding the complex regulatory mechanisms and the diverse functions of PP1 holoenzyme is essential for unraveling its significance in maintaining cellular homeostasis and responding to physiological challenges.

# 1. PP1 catalytic subunit: PP1c

In the field of protein phosphatases, Protein Phosphatase type 1 (PP1) holds a prominent position. This widely distributed enzyme, with a molecular weight spanning 35 to 38 kDa, specializes in the dephosphorylation of phosphoserine/threonine residues where biochemical evidence suggests it being responsible for the dephosphorylation of over 50% of phosphoserine/threonine residues in eukaryotic cells (Ferreira et al., 2019). It is classified within the phosphoprotein phosphatase (PPP) family of the eukaryotic protein phosphatome (M. J. Chen et al., 2017).

In contrast to the simplicity seen in some organisms like Saccharomyces cerevisiae, where a single gene (Glc7) governs PP1 expression, multiple genes encode various isoforms of PP1c in most eukaryotes (DOMBRÁDI et al., 1990; Farkas et al., 2007). These isoforms exhibit a high degree of conservation (Andreassen et al., 1998; Da Cruz E Silva et al., 1995).

This conservation is attributed to its critical role as a scaffold interacting with a myriad of partner proteins, where even subtle mutations can lead to significant alterations in its interactome and, consequently, impact its functionality (Heroes et al., 2013). This flexibility of PP1 is reflected in its involvement in a wide array of fundamental cellular processes (Camlin et al., 2023).

The catalytic subunit of PP1c demonstrates robust enzymatic activity on its own (Lad et al., 2003). However, to ensure precise regulation and prevent cellular toxicity, this activity necessitates control through a second subunit.

## 1.1. PP1c in mammals

PP1c exists in multiple isoforms, which are encoded by different genes and exhibit tissue-specific expression patterns and subcellular localization.

In mammals, PP1c is encoded by 3 genes: pp1ca (PP1α), ppp1cb (PP1β/δ), and ppp1cc (PP1γ). These genes can give rise to up to 7 isoforms, but 4 of them are considered predominant: PP1α, PP1β/δ, and PP1γ1, and γ2 (Korrodi-Gregório et al., 2014).

The distinct subcellular localization and association with regulatory subunits allow PP1c isoforms to target specific substrates and participate in diverse cellular functions.

The first three isoforms (PP1α, PP1β/δ, and PP1γ1) have ubiquitous expression, while PP1cγ2 is overexpressed in the testes and sperm (Goswami et al., 2019; Korrodi-Gregório et al., 2014; Peti et al., 2013). These different PP1c isoforms share a highly conserved catalytic domain of approximately 280 amino acids, presenting a similarity of more than 90%. They all possess the signature motif of serine/threonine phosphatases, the sequence LRGNHE (BARTON et al., 1994), which is conserved across all PP1c isoforms. Variations are mainly observed in the non-catalytic N- and C-terminal regions (Figure 11).
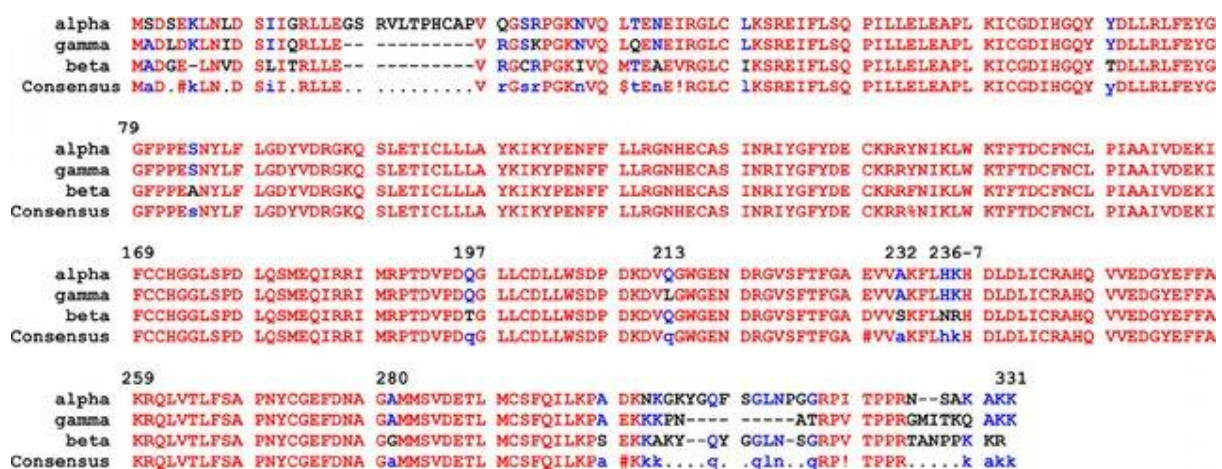


**Figure 11 Alignment of human PP1 isoforms.** A sequence alignment of the three isoforms of human PP1c was generated using the Network Protein Sequence Analysis: Multalin Alignment. Sequence similarity is indicated in red, and semiconserved or nonconserved residues in blue or black, respectively. (Scotto-Lavino, 2010)

PP1 exerts significant control over cellular processes (Bushell et al., 2017b; M. Zhang et al., 2018b). Its functions are multifaceted and include orchestrating key events in cell division, such as mitotic progression and chromosome segregation, by dephosphorylating critical substrates, including mitotic kinases like cyclin-dependent kinase 1 (CDK1) (Bollen et al., 2010; Heroes et al., 2013; Nilsson, 2019), as well as regulators of chromosome segregation (Hattersley et al., 2016; Zeeshan et al., 2021). It is important to point out that the PP1 activity per se is tightly regulated throughout mitosis, initially inhibited by the CDK1/cyclin B complex and Inhibitor 1 (Wu et al., 2009). However, during mitotic exit, a cascade of events, including cyclin B degradation and CDK1 dephosphorylation by CDC14, leads to PP1 reactivation through auto dephosphorylation, ending in the completion of mitotic exit (Grallert et al., 2015; Mochida & Hunt, 2012).

Furthermore, PP1 serves as a dominant contributor to total cellular phosphatase activity (Paul et al., 2020). Its role extends beyond mitosis, as PP1 functions as a master regulator, promoting energy-efficient processes such as nutrient utilization and glycogen storage in response to varying nutrient availability. Additionally, PP1 contributes to the relaxation of actomyosin fibers, reinstates basal protein synthesis patterns, and facilitates the recycling of essential transcription and splicing factors (Ceulemans & Bollen, 2004). During cellular stress, PP1 helps restore protein phosphorylation homeostasis by dephosphorylating target protein that were hyperphosphorylated during stress conditions; however, it can also induce apoptosis when cells are irreparably damaged. Furthermore, PP1 modulates ion pumps, transporters, and channels in various tissues, impacting neuronal excitation. Finally, PP1 plays a pivotal role in guiding cells out of mitosis and maintaining them in the G1 or G2 phases of the cell cycle (Ceulemans & Bollen, 2004; Zeeshan et al., 2021).

## 1.2. PP1c in Yeast

The first discovery of PP1c in *S. cerevisiae* was the result of a mutant analysis within the glycogen metabolic pathway (Cannon et al., 1994). The GLC7 mutant, harboring a mutation in the gene encoding PP1c, has been shown to display a deficiency in glycogen accumulation. This was mainly due to the, glycogen synthase which remains phosphorylated and inactive. In yeast, further studies showed that GLC7 plays a pivotal role in governing various cellular processes, encompassing glycogen and protein synthesis, actin cytoskeleton organization, gene expression, and cell division (Gibbons et al., 2007). Similar to its functions in higher eukaryotes, Glc7p also oversees several essential physiological events in yeast, such as sporulation (Ramaswamy et al., 1998) and the orchestration of transcriptional responses (De Wever et al., 2005).

An experiment involving the complementation of GLC7 with the human isoform PP1γ was conducted due to the significant identity shared (approximately 86%) between yeast PP1c and HsPP1c (Bhattacharyya et al., 2002). Yeast strains exhibited optimal growth rates when complemented with HsPP1α, while HsPP1β showed superior glycogen accumulation. This outcome is attributed to the stronger interaction between HsPP1β and Gac1p, a regulator of GLC7 involved in yeast glycogen metabolism. However, mutants complemented with any of the human PP1c isoforms: PP1β, PP1γ1, or PP1γ2, did not undergo yeast sporulation (Gibbons et al., 2007). These observations collectively underscore the high degree of PP1c conservation throughout eukaryotic evolution, with minor adaptations specific to each organism.

### 1.3. PP1c in Apicomplexa

Each of the four apicomplexan parasites: *Cryptosporidium parvum, Toxoplasma gondii, Plasmodium falciparum* and *Babesia bovis* encodes a single PP1 catalytic subunit, characterized by similar protein sequence lengths and a striking degree of identity to their human homologs. These four PP1 variants are denoted as CpPP1 (cgd7_2670), TgPP1 (TGME49_310700), PfPP1 (PF3D7_1414400), and BbPP1 (BBOV_III006130).

In the case of *T. gondii*, the detection of PP1 activity was initially inferred through indirect experiments demonstrating that the exposure to PPP Phosphatase inhibitors significantly impairs the parasite's invasiveness, suggesting a crucial role for this phosphatase in host cell invasion (Delorme et al., 2002). Subsequent genome sequencing efforts led to the identification of the *T. gondii* PP1 encoding gene. TgPP1 has been subsequently characterized and shown to exhibit phosphatase activity, notably showing an enhancement in activity in the presence of MnCl2, while its activity was effectively inhibited by the addition of okadaic acid in a dose-dependent manner (Daher et al., 2007). Further, transient transfection experiments, involving the introduction of its coding sequence fused with a cMyc epitope tag, confirmed its presence as expected in both the cytoplasm and nucleus (Daher et al., 2007).

### 1.4. PP1c in *Plasmodium*

The Protein Phosphatase 1 catalytic subunit of *Plasmodium falciparum* (PfPP1c) was first identified in 2002 on chromosome 14 (Bhattacharyya et al., 2002) and is known to be the smallest PP1c among known organisms (Kumar et al., 2002). Its gene, PF3D7_1414400, is 1560 base pairs long and contains 4 introns (PlasmoDB 2023). PfPP1c codes for a 304-amino acid protein with a molecular weight of 35 kDa. The phosphatase shares 87% and 83% homology with human and *S. cerevisiae*, respectively, and retains the signature motif LRGNHE of serine/threonine phosphatases (Bhattacharyya et al., 2002). The major differences between PfPP1c and other organisms lie in the N- and C-terminal regions. PfPP1c is expressed at all stages present in humans, including gametocytes (Figure 12) (Kumar et al., 2002).
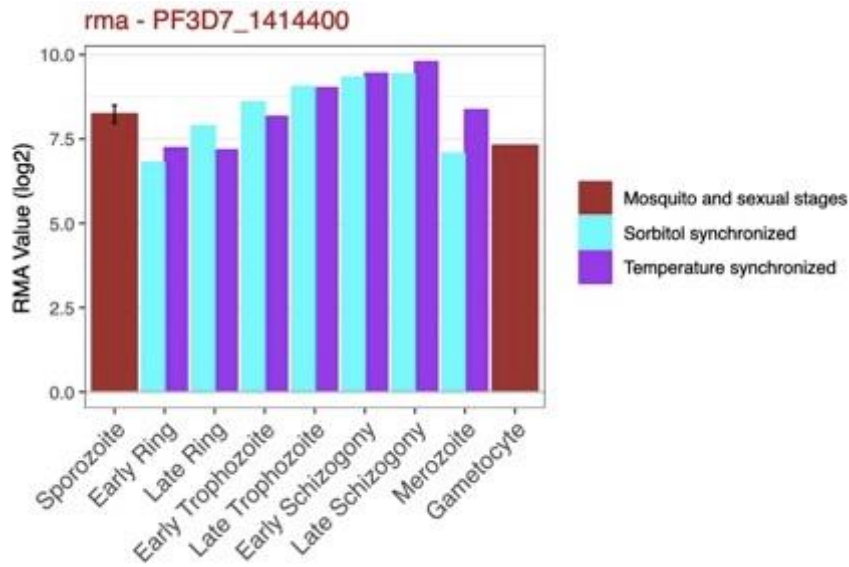
**Figure 12 Expression of PfPP1c at the different stages** (Le Roch et al., 2003).

In *P. berghei*, the ortholog PbPP1c has only two introns at the genomic level but shares 99% identity, with only a variation in the last three amino acids. PbPP1c transcription in the rodent parasite appears to be significant during the erythrocytic and gametogenesis stages, suggesting a strong activity during these stages (M. Zhang et al., 2016).

### 1.4.1. PP1c sequence analysis:

PfPP1 (accession number in PlasmoDB: PF3D7_1414400), shares a remarkable similarity of approximately 80% with sequences found in human, yeast, rabbit, rat, and plants (Bhattacharyya et al., 2002). PfPP1, existing as a single isoform located on chromosome 14, was cloned and characterized independently by two research teams (Bhattacharyya et al., 2002; Kumar et al., 2002). Its sequence spans 304 amino acids and bears the distinctive LRGNHE signature of Ser/Thr phosphatases (amino acids 119 to 124), along with two potential phosphorylation sites for protein kinase C and five for casein kinase II (Figure 13). Sequence comparisons between PfPP1 and its counterparts in rabbit, chicken, human, rat, *Toxoplasma gondii*, and yeast reveal perfect similarity within the catalytic domain (amino acids 10 to 300) and also at the binding sites for microcystin and okadaic acid (β12-β13 loop, amino acids 270 to 280) (Bhattacharyya et al., 2002). PfPP1 stands out as the smallest type 1 phosphatase identified to date. Interestingly, unlike its mammalian counterparts, it lacks a proline-rich C-terminal sequence (Kumar et al., 2002).

The coding sequence of PfPP1 is divided into five exons, with the first two being the largest and containing the majority of the catalytic core of the phosphatase (Kumar et al., 2002). The catalytic core, highly conserved across all members of the PP1 family, roughly corresponds to residues 5–260 of PfPP1. Within this region lie all the signature motifs and conserved residues crucial for the fundamental steps of catalysis, including substrate binding, metal ion coordination, and interaction with the phosphate group (Ansai et al., 1996).

However, an intriguing difference emerges in *Plasmodium* PP1c, as it lacks an 18-amino acid segment at the C-terminus, which contains the dynamic phosphorylation site threonine residue (Thr320). This phosphorylation is of utmost importance in regulating mammalian PP1c, especially in the context of cell mitosis entry (Kwon et al., 1997). This mode of phosphoregulation of PP1c appears to be absent in *Plasmodium.*

```
Plasmodium   --MALEIDIDNVISKLIEVRGTRPGKNVNLTENEIKILCLSSREIFLNQPILLELEAPIK  58
Human        MSDSEKLNLDSIIGRLLEVQGSRPGKNVQLTENEIRGLCLKSREIFLSQPILLELEAPLK  60
             *::*.:* :*:.**:*:******:*****.; ***.****** .**********:*

Plasmodium   ICGDIHGQFYDLLRLFEYGGFPPDANYLFLGDYVDRGKQSLETICLLLAYKIKYPENFFL  118
Human        ICGDIHGQYYDLLRLFEYGGFPPESNYLFLGDYVDRGKQSLETICLLLAYKIKYPENFFL  120
             ********:.***********:.:.*****************************

Plasmodium   LRGNHECASINRIYGFYDECKRRYSVKLWKTFIDCFNCLPVAAIIDEKIFCMHGGLSPEL  178
Human        LRGNHECASINRIYGFYDECKRRYNIKLWKTFTDCFNCLPIAAIVDEKIFCCHGGLSPDL  180
             ***********************.:.****** ******:***:****** ******:*

Plasmodium   NNMEQIRKITRPTDVPDNGLLCDLLWSDPEKEINGWGENDRGVSFTFGQDVVHNFLRKHE  238
Human        QSMEQIRRIMRPTDVPDQGLLCDLLWSDPDKDVQGWGENDRGVSFTFGAEVVAKFLHKHD  240
             ..****:* *******:.**********:*: ************** :** :**:**:

                               β12      loop        β13
Plasmodium   LDLICRAHQVVEDGYEFFAKRQLVTLFSAPNYCGEFDNAGAMMSVDETIMCSFQILKPVE  298
Human        LDLICRAHQVVEDGYEFFAKRQLVTLFSAPNYCGEFDNAGAMMSVDETIMCSFQILKPAD  300
             *********************************************************::

Plasmodium   KKK-----AAN-------------------------  304
Human        KNKGKYGQFSGLNPGGRPITPPR--NSAKAKK----  330
             *.*
```

**Figure 13 PfPP1 sequence comparison.** The predicted sequences of *Plasmodium* PP1 (this study) and human PP1 alpha (P08129) catalytic subunits were aligned using the CLUSTALW program at the European Bioinformatics Institute (EMBL) server, and later refined by visual inspection. The amino acid residue numbers are shown on the right. Residues are marked as: non-conservative replacement (.); conservative replacement (:), and identical (*). Residues important in I-2 interaction are highlighted in gray: E52, E54; D164, E165, and K166. (Kumar et al., 2002)

## 1.4.2.  PP1c structural analysis

PfPP1c displays 80% identity (with an 88% similarity) with HsPP1c and maintains its predicted secondary and overall tertiary structures with remarkable closeness with 9 α helices and 11 β-strands, strategically positioning the active site at the protein's core. (Figure 14). At the structural level, the catalytic domain assumes an ellipsoidal shape, excluding only the N- and C-terminal regions. Similar to HsPP1c, the catalytic site of PfPP1c is situated on the protein's surface (Egloff et al., 1995, 1997), at the junction of three grooves, creating a Y-shaped configuration, encompassing hydrophobic, acidic, or C-terminal characteristics.
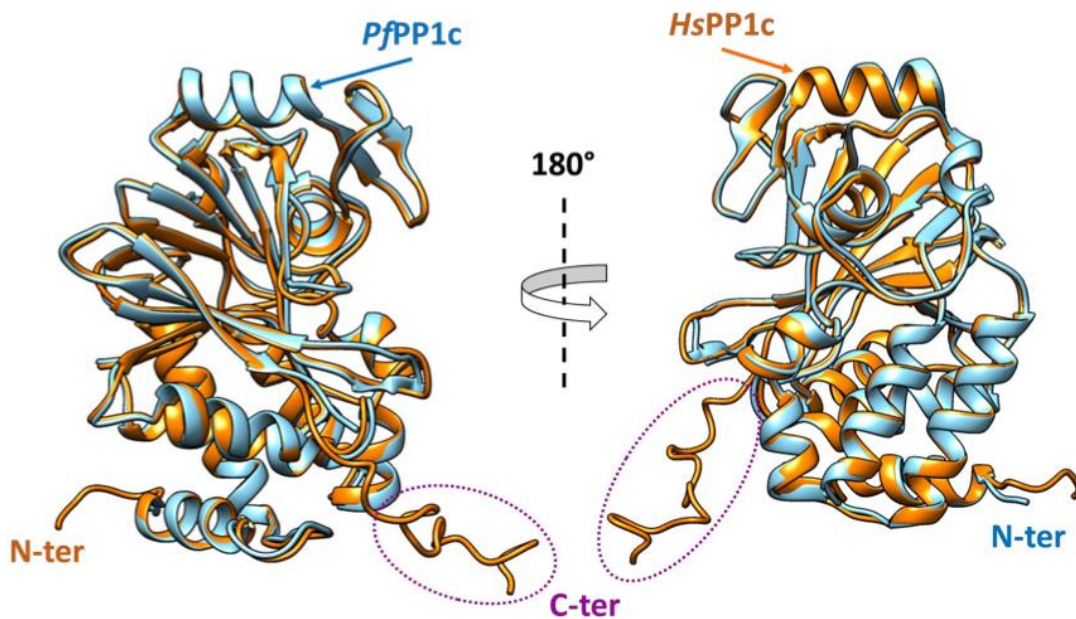


**Figure 14. 3D structure of PfPP1c and HsPP1c** (Khalife, 2021)

Specifically, within the β2-αB-β3-αC-β4 sheets and helices, two crucial metal ions bind to facilitate enzymatic catalysis (Egloff et al., 1995; Goldberg et al., 1995). While $Fe^{2+}$ or $Zn^{2+}$ ions are presumed to be necessary, $Mn^{2+}$ ions are typically utilized for recombinant bacterial production (Heroes et al., 2015). These ions activate a water molecule, initiating a nucleophilic attack on the phosphoryl group and forming a bond with the negatively charged oxygen atom. These metals contribute to PP1c's specificity towards various substrates, and chaperones are believed to be involved in ion loading at the catalytic site (Heroes et al., 2015).

This structural arrangement enables PP1c to perform its enzymatic function by exposing an accessible active site while offering the opportunity for interactions with its diverse regulatory subunits. Interestingly, the initial inhibitors identified for PP1c are natural toxins such as okadaic

acid, microcystin-LR, calyculin A, or tautomycin, among others (Lajarín-Cuesta et al., 2016). While these toxins lack specificity for PP1c, they effectively target metallophosphatases with nanomolar-range $IC_{50}$ values. The binding of okadaic acid and microcystin-LR to PP1c occurs via the hydrophobic groove, the active site, and β12 and β13 sheets, thus obstructing access to the active site (Ceulemans & Bollen, 2004; Goldberg et al., 1995).

Remarkably, there have been 15 holoenzyme crystals of PP1 to date. As predicted by the resolution of the Gmpeptide: PP1 complex, the conformation of this phosphatase remains unchanged and invariant upon binding to its regulators. Multiple binding sites for toxins and other protein partners appear to be pre-formed within the phosphatase. This concept suggests that the observed subtle changes involve specific secondary structures of the phosphatase, including the β12-β13 loops, which are implicated in the binding of inhibitory toxins (Connor et al., 2001), as well as αA'-β2, β11-β12, α1 helix, and β14 sheet, located at the C-terminus of the catalytic domain (Peti et al., 2013).

### 1.4.3. PP1c functional analysis

Apicomplexan PP1 enzymes participate in a wide array of processes, including glycogen metabolism, protein sorting, and export (Yang & Boddey, 2017).

The fundamental role of PfPP1c in dephosphorylation processes was initially inferred through the use of phosphatase inhibitors, such as okadaic acid, calyculin, and microcystin (Bhattacharyya et al., 2002). Subsequent reverse genetic screens have strongly indicated the indispensability of PP1c for the completion of the parasite Intraerythrocytic Development Cycle (IDC) in both *P. falciparum and P. berghei* (Bushell et al., 2017b; Guttery et al., 2014; )(Zhang et al., 2018)

The employment of two inducible knockdown (KD) strategies confirmed the critical role of PfPP1c in precisely regulating asexual development in the parasite (Paul et al., 2020). PfPP1c KD in early-stage parasites significantly hampered DNA replication, leading to the formation of multinucleate schizonts with fewer nuclei and delayed IDC progression. At various blood stages, the absence of PfPP1c resulted in egress blockage, as exonemes failed to release the protease PfSUB1, which orchestrates early egress stages and the rupture of the parasitophorous vacuole membrane (Collins et al., 2017; Paul et al., 2020). This impairment of microneme discharge further hindered the transition from egress to invasion (Paul et al., 2020). A phosphoproteomic approach was employed to identify potential proteins undergoing

(de)phosphorylation in a PfPP1c-dependent manner in KD parasites. The analysis uncovered hyperphosphorylation of Ser-29 PfHistone 3, analogous to the human ortholog Ser-28, which is a PP1-targeted site for mitotic exit and metaphase (De Castro et al., 2017). Additionally, a range of potential substrates including chromatin factors, AP2 transcription factors, and vacuolar-protein-sorting family (VSP) members were identified. The analysis highlighted intriguing candidates like GCα (guanylyl cyclase alpha). PfGCα is a well-known effector crucial for cGMP production and PfPKG stimulation, a key component of egress essential for PfSUB1 discharge from exonemes (Carucci et al., 2000; Taylor et al., 2010). A chemical-genetics assay demonstrated PfPP1c's pivotal role in regulating this protein and its egress-related functions. It also unveiled the involvement of host serum phospholipid PtdC (phosphatidylcholine) through PfPP1c-mediated dephosphorylation of a phospholipid transporter domain located at the N-terminus of GCα. In summary, PfPP1c serves as a central regulator of egress, ensuring the timely and proper propagation of the parasite in the blood by balancing environmental signals and intracellular pathways (A. S. Paul et al., 2020).

An additional conditional KD study carried out in *P. berghei* revealed that PbPP1c, despite its expression, is not essential from sporozoite formation to the release of hepatic merozoites. However, it appeared to be critical for establishing blood infection after PP1cKD sporozoite injection into mice (Zhang et al., 2016).

New findings revealed that PP1 exhibits constitutive expression and co-localizes with the kinetochore protein NDC80 throughout various phases of *Plasmodium*'s asexual and sexual development (Zeeshan et al., 2021). These findings suggest a potential involvement in atypical chromosome segregation processes. In this study conducted by Zeeshan et al. (2021) presenting a conditional PP1 gene knockdown, it was proposed that PP1 plays a pivotal role in mitotic division during male gametogony. Additionally, it may have a role in regulating cell polarity during meiosis, particularly in the transformation from zygote to ookinete (Zeeshan et al., 2021).The observed pattern of PP1-GFP accumulation at the kinetochore, starting at the initiation of nuclear division and declining upon completion, illustrates similar behavior seen in other eukaryotes. In these organisms, PP1 activity increases in the G2 phase, decreases during prophase and metaphase, and then rises again during anaphase (Nasa et al., 2018). This behavior implies a role for PP1 in overseeing the swift initiation and conclusion of mitosis during male gametogony. Further inspection of PP1 gene knockdown consequences revealed a significant reduction in male gamete formation, specifically during male gametogony (Zeeshan et al., 2021). Ultrastructural analysis unveiled fewer nuclear poles and basal bodies linked to

axonemes, alongside the absence of chromosome condensation in male gametocytes of these transgenic parasites. These findings point to PP1's involvement in processes related to chromosome segregation and gamete formation, notably flagella formation.

Recent observations in *Toxoplasma* propose that the apical PP1 holoenzyme serves context-specific, $Ca^{2+}$ responsive roles crucial for the parasitic lifestyle (Park et al., 2019; Philip et al., 2012). TgPP1 promotes the motility of the *Toxoplasma* parasite in response to $Ca^{2+}$ during host-cell egress (Herneisen et al., 2022). Indeed, parasites subject to conditional PP1 depletion exhibited diminished invasion capacity and a delay in host cell lysis in response to zaprinast, a phosphodiesterase inhibitor (Herneisen et al., 2022).

Observations indicate that PP1 activity enhances $Ca^{2+}$ entry, a process previously associated with increased parasite motility (Pace et al., 2014; Vella et al., 2021).

TgPP1 exerts significant regulatory control over multiple critical pathways involved in the generation of daughter cells. These pathways encompass various aspects, including organelle division, segregation processes, and the proper assembly of the inner membrane complex (IMC) within these offspring (Khelifa et al., 2023). Upon depletion of TgPP1, a notable consequence was the breakdown of the IMC structure, accompanied by the hyperphosphorylation of multiple IMC proteins. This observation implies that this protein may govern the assembly and stability of the IMC network (Khelifa et al., 2023).Furthermore, the presence of distinct nuclear and organelle segregation abnormalities following TgPP1 depletion suggests that this phosphatase likely targets elements that play crucial roles in orchestrating cell division within the parasite. An intriguing discovery was the formation of amylopectin granules in tachyzoites subsequent to TgPP1 depletion. This finding implies that TgPP1 plays a role in regulating the steady-state levels of amylopectin during the proliferation of tachyzoites (Khelifa et al., 2023). Notably, recent research has also implicated another phosphatase, TgPP2A, in this pathway. TgPP2A appears to contribute to the regulation of amylopectin metabolism by dephosphorylating TgCDPK2 at a specific site (S679), underscoring the pivotal role of TgCDPK2 in the accumulation of amylopectin (Wang et al., 2022).

In summary, despite the conservation of PP1 in *T. gondii* and *Plasmodium,* a significant functional disparity exists between these two parasites. This divergence highlights the remarkable adaptability of PP1c, which can be attributed to its remarkable ability to interact with a wide range of distinct and specific regulators.

## 2. PP1 and protein partners

As mentioned above, PP1c exhibits diverse functions, and our understanding of how it operates is gradually improving. Indeed, it becomes clear that PP1c needs regulator subunits to fine tune, direct and control the phosphatase activity of PP1c.

These regulatory subunits introduce an element of specificity in phosphatase actions, resulting in the formation of various multimeric holoenzymes that dictate its spatiotemporal functions. The spectrum of PP1 regulators can be categorized into primary and secondary regulators (Ceulemans et al., 2002), based on their origin as PP1 regulators or their subsequent acquisition of PP1-binding functionality during evolution. Primary regulators (e.g., inhibitor-2, NIPP1, and Sds22) typically harbor PP1-binding sites across all eukaryotic lineages where they are present. Conversely, secondary regulators (e.g., AKAP149, Nek2, Bcl2) exhibit functional domains shared with homologs lacking PP1-binding sites, suggesting that these sites emerged in proteins originally serving different functions, subsequently acquiring the PP1 interaction trait during evolution (Ceulemans & Bollen, 2004). Certain PP1 interactors seem to have emerged relatively late in specific eukaryotic lineages. This is indicated by the absence of homologs in other lineages. For instance, PKA-activated inhibitors are unique to vertebrates, while certain regulators in Drosophila (Bifocal, Klp38B) or fungal (Reg1/2, Gip1) regulators do not have apparent counterparts in vertebrates. The categorization of PP1's protein partners can also depend on their function (Bollen, 2001). These partners can be broadly classified into three categories based on their roles and interactions with PP1:

    a.  **Regulators. (e.g., inhibitor-1, DARPP-32, inhibitor-2)**
PP1 regulators are proteins that interact with the catalytic subunit of PP1 and modulate its activity, subcellular localization, and substrate specificity. These regulators can either activate or inhibit PP1, providing a level of control over its function. Regulators often contain specific docking motifs that enable their interaction with PP1. Examples include MYPT1 (Myosin Phosphatase Targeting Subunit 1) for regulating myosin light chain dephosphorylation and hence its smooth muscle contraction, NIPP1 (Nuclear Inhibitor of PP1) for nuclear PP1 targeting and I2 (Inhibitor 2) for cardiac function.

    b.  **Substrates:**
These are proteins that are direct targets of PP1's catalytic activity, and their phosphorylation status is regulated by PP1-mediated dephosphorylation. PP1 dephosphorylates specific

serine/threonine residues on these substrate proteins, modulating their functions and activities. Examples of PP1 substrates include key regulatory proteins involved in cell cycle progression, glycogen metabolism, transcriptional regulation, and various signaling pathways. (Aurora kinases, Nek2).

This classification's limitations lie in the fact that many interactor functions remain enigmatic, and certain interactors—like Reg1—assume dual roles as both substrate and regulator.

Which gives us a third class,

### c. Dual Function Proteins:

Some proteins can act both as substrates and regulators of PP1. These proteins are substrates for PP1-mediated dephosphorylation, but they can also function as regulatory subunits, influencing PP1 activity or targeting. These dual function proteins create complex regulatory networks that contribute to the precise control of PP1-mediated dephosphorylation. An example of such a dual function protein is the inhibitor-2 ($I_2$) subunit, which can be a substrate for PP1 and also inhibit its activity under certain conditions.

The interactions between PP1 and its interacting proteins are highly dynamic and context-dependent, enabling precise regulation of various cellular processes and signaling pathways, through reversible protein phosphorylation.

## 2.1. Known PP1 regulators

More than 200 genes encoding PIPs have been identified, and it is believed that there are potentially hundreds more yet to be uncovered (Bollen et al., 2010). Out of the 189 biochemically validated PIPs listed in the study by Heroes et al. (2013), Ferreira et al (2019) have identified genetically modified mouse models for 104 unique PIPs, accounting for approximately 55% of the known PIPs.

They later categorized PIPs into two functional groups: inhibitory PIPs (iPIPs) and guiding PIPs (gPIPs). iPIPs function by obstructing the dephosphorylation of substrates, effectively occupying the active site of PP1. Consequently, the removal of an iPIP in mice results in an increase in the dephosphorylation of physiological substrates associated with the PP1: iPIP holoenzyme. Conversely, gPIPs are defined as PIPs that direct PP1 toward specific subsets of substrates within a cell. Deleting a gPIP in mice leads to heightened phosphorylation levels of in vivo substrates targeted by the PP1: gPIP complex. They have examined genetically modified

mouse models for 7 iPIPs and 10 gPIPs, which are detailed in the following Table 7 and Table 8, respectively.

**Table 7. Mouse models of PP1 inhibitory PIPs** (Ferreira et al., 2019).

| Protein *gene* | Alterations in PP1/substrate[§] | Phenotype |
|---|---|---|
| **Inhibitor 1** *Ppp1r1a* | PLN-pS16 RYR2-pS2813 ↓ | ↓ No obvious phenotype, some neuro-logical and heart alterations |
| | PP1 level ↑ | Cardiac hypertrophy and mild cardiac dysfunction |
| | PP1 activity PLN-pS16/T17 ↑ | ↓, Enhanced cardiac function in long term and protection against pressure-overload-induced hypertrophy |
| | PLN-pS16 RYR2-pS2813 ↑ | ↑, Improved cardiac contractility in young mice, but lethal after catecholaminergic stress and with aging |
| | PP1 activity ↑, PLN-pS16/T17 ↓ RYR2-pS2813 ↑ | Impaired heart function and increased arrhythmias |
| | PP1 activity ↓, CREB1-pS133 ↑ CAMK2A-pT286 ↑ GLUR1-pS849 ↑ | Improved learning and enhanced memory, facilitated potentiation, impaired recovery from ischemia |
| **DARPP32** *Ppp1r1b* | *pGLUN1 ↓ | Diminished responses to dopamine, psy-chotomimetic and antipsychotic drugs |
| | *CREB1-pS133 *GSK3β-pS9 *H3-pS10 #pERK2 #H3-pS10/acK14 #GLUR1-pS849 #pRPS6 ↓ | ↓ Impaired response to psychotomimetic ↓ (dopaminergic agonists, serotonergic and ↓ glutamatergic antagonist) ↓ ↓ ↓ |
| | #pERK1/2 #H3-pS10/acK14 ↓ #GLUR1-pS849 #pRPS6 ↓ | ↓ Decreased motor behavior, abolished ↓ dyskinetic behavior in response to ↓ Parkinson's disease drug L-DOPA |

| Protein gene | Alterations in PP1/substrate[§] | | Phenotype |
|---|---|---|---|
| | [#]phosphorylation of ERK1/2, H3, GLUR1, RPS6: not altered | | Increased motor behavior, reduced cataleptic response to antipsychotic drug |
| **Inhibitor 2** *Ppp1r2* | Ho: PP1α-pT320 He: CREB1-pS133↑ He: PP1 activity ↓ | ↑ | Ho: embryonic lethal He: viable, no overt phenotype; increased memory formation |
| | PP1 level PP1 activity PLN-pS16 ↑ | ↑ ↓ | Enhanced cardiac contractility, but deleterious under conditions of pressure overload |
| | Normalized PP1 activity | | Normalized heart morphology and heart function |
| **CPI-17** *Ppp1r14a* | [**]MYPT1-pT852 [**]MYPT1-pT694 [**]MYL2-pS19 ↓ | ↓ ↓ | Decreased main blood pressure |
| | [**]MYPT1-pT852 [**]MYL2-pS19 ↓ | ↓ | Decreased main blood pressure |
| **KEPI** *Ppp1r14c* | [##]PP1 activity ↑ in thalamus | | Decreased response to morphine after chronic morphine injections, increased SARS coronavirus pathogenesis |
| **GBPI-1** *Ppp1r14d* | nd | | Abnormal heart morphology |
| **HSP20** *Hspb6* | PP1 activity PNL pS16/T17 ↑ | ↓ | Improved cardiac function and recovery reduced infarction, improved angiogenesis in diabetic hearts |

**Table 8 Mouse models of guiding PIPs.** (Ferreira, 2019)

| Protein/gene | Alterations in PP1/substrate[§] | Phenotype |
|---|---|---|
| | PP1 level/activity ↓ <br> GS-pS641/645 ↑ GP-pS15 ↑ | Decreased glycogen content; prediabetic phenotype in 129/Ola derived background but no obvious phenotype in C57BL/6, 129s2/sV and 129/SvJ background |
| **GM (R$_{GL}$)** *Ppp1r3a* | PP1 level ↑ | Increased muscle glycogen content, abolished GS activation in response to exercise |
| | GS activity ↓ <br> GP activity ↑ | Decreased muscle glycogen content |
| **GL** *Ppp1r3b* | GS level ↓ <br> GS-pS641 ↑ | Reduced hepatic glycogen content, impaired whole body glucose homeostasis |
| | GS-pS641/645 ↓ <br> GP-pS15 ↑ | Improved glucose tolerance |
| | Pan-pThr ↑ | Early embryonic lethality |
| **NIPP*1*** *Ppp1r8* | Nuclear PP1 activity ↓ <br> H3-pS10 ↑ | Improved memory performance, enhanced long-term potentiation and alteration in gene transcription |
| **Neurabin I** *Ppp1r9a* | PP1 levels ↓ <br> GluR1-pS849 ↓ <br> [§]GluR1-pS849 ↑ | Abnormal psychostimulant response and dopamine signaling transduction, reduced anxiety- and depression-related behaviors in young adult mice, impaired contextual fear memory |

| Protein/ gene | Alterations in PP1/substrate[§] | | Phenotype |
|---|---|---|---|
| **Spinophilin** *Ppp1r9b* | PP1 levels GluR1-pS849 [$]GluR1-pS849 ↑ | ↓ ↓ | Abnormal psychostimulant response and dopamine signaling transduction, reduced brain size, reduced anxiety- and depression-related behaviors in middle-aged mice and associative learning ability |
| | nd | | Embryonic lethality |
| **MYPT1** *Ppp1r12a* | [%]PP1β level [%]CPI-17-pT38 [%]pMYL2 ↑ | ↓ ↓ | Altered contractile responses in intestinal and vascular smooth muscle, hypertension |
| | PP1β level [%]CPI-17-pT38 ↓ | ↓ | Moderate alteration in bladder contractile responses |
| **MYPT2** *Ppp1r12b* | PP1β level PP1 activity pMYL2 ↓ | ↑ ↑ | Left ventricular heart enlargements with heart dysfunctions |
| **GADD34** *Ppp1r15a* | *eIF2α-pS52 ↑ | | No overt phenotype, reduced hepatocarcinogenesis in chemical-induced tumorigenesis |
| | [#]eIF2α-pS52 ↑ | | Hypersplenism, erythrocyte abnormalities, resembling mild thalassemia syndromes |
| | (*) eIF2α-pS52 ↑ | | No overt phenotype |
| | (*) eIF2α-pS52 ↑ | | Perinatal lethality, impaired erythropoiesis |
| **CReP** *Ppp1r15b* | nd | | Early embryonic lethality |
| | Unphosphory-latable eIF2α[S52A] | | Rescue of the early embryonic lethality by the eIF2α[S52A]mutation |
| **PHACTR4** *Phactr4* | PP1 activity PP1-pT320 Rb-pS601↑ Rb-pS800/804 ↑ | ↓ ↑ | Lethality at birth; neuronal tube, eye and gastrointestinal defects in embryos; resembles human Hirschsprung disease |

| Protein/ gene | Alterations in PP1/substrate[§] | Phenotype |
|---|---|---|
| nd | | Rescue of the *Phactr4[R650P/R650P]*phenotype by loss of E2f1 |

## 2.2. PP1 interaction motifs

In order to fulfill diverse functions of PP1c, an array of regulators binds to the catalytic subunit to finely control its phosphatase activity, substrate specificity, or localization. This assembly of the holoenzyme encompasses a broad spectrum of interaction (docking) motifs. On average, these motifs span 4 to 8 amino acids, potentially affording PP1c up to 30 non-overlapping interaction sites, despite commonalities shared among most partners (Table 9) (Bollen et al., 2010)

**Table 9 Table representing the different binding motifs to PP1**, the regulator possessing them alongside their function. (Heroes et al., 2013)

| NAME OF THE MOTIF | EXAMPLE OF A REGULATOR HAVING IT | FUNCTION |
|---|---|---|
| RVXF | Inhibitor 1, 2 and 3 | PP1 fixation |
| SILK | Inhibitor 2 | PP1 fixation |
| MYPHONE | Mypt 1 | Substrate selection |
| SPIDOC | Spinophiline | Substrate selection |
| IDOHA | Inhibitor 2 | Inhibition |
| RNYF | iASPP | ? |
| BISTRIP | SDS22 | ? |
| ANKCAP | Mypt1 | Substrate selection |

Regulators engage with PP1c through one or several interaction motifs, primarily identified as RVxF, SILK, φφ, Fxx[RK]x[RK], or MyPhoNE motifs (Heroes et al., 2013). The RVxF motif, that we will focus on, is recognized as the major binding motif with the phosphatase, discovered in around 70% to 90% of partners (Bollen et al., 2010; Peti et al., 2013).

In 1997, the Barford team unveiled, for the first time, the structure of PP1 bound to a peptide named "RVxF," derived from the Gm protein (a subunit facilitating the localization of the phosphatase at glycogenic particles) (Egloff et al., 1995). Subsequent findings highlighted that over 90% of PP1 regulators harbored an identifiable "RVxF" motif (Bollen et al., 2010). This

observation marked an initial elucidation of the mechanisms governing the attachment of the phosphatase's various regulatory subunits.

The "RVxF" motif predominantly adheres to the consensus sequence [K/R] [K/R] [V/I] [x] [F/W], where x represents any residue except phenylalanine, isoleucine, methionine, tyrosine, asparagine, or proline (Hendrickx et al., 2009; Meiselbach et al., 2006; Wakula et al., 2003). PP1 structure reveals that at the phosphatase site, the binding site is situated 20 Å from the active site, comprising two deep hydrophobic pockets fashioned by invariant or highly conserved residues. Within these pockets, amino acids composing the "RVxF" motif lie (Figure 15). A negatively charged region accommodates the basic residues frequently found upstream of the motif.
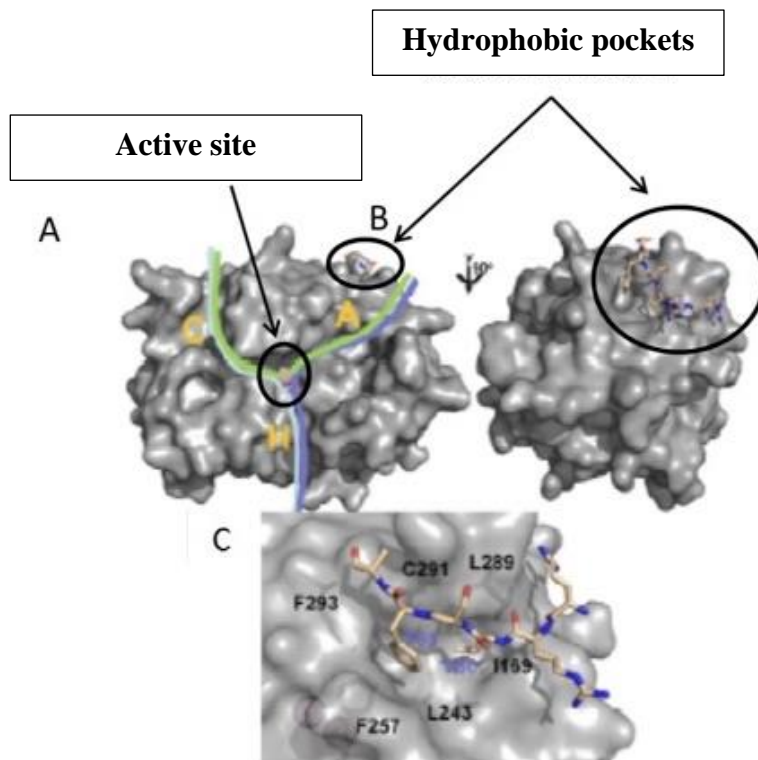


**Figure 15**. **PP1 structure showing the active site and hydrophobic pockets positions**.(Egloff, 1997; Peti, 2012)

Despite the pivotal role the motif plays in PP1c's interaction with most regulators, additional binding sites exist that not only stabilize complexes but also modulate the phosphatase's activity and/or specificity. These motifs adhere to distinct rules, collectively referred to as the "PP1

binding code." None of the interaction motifs can bind to any phosphatase other than PP1c, even with PP2A or PP2B, whose structures bear considerable similarity to PP1c (Heroes et al., 2013; Verbinnen et al., 2017). These motifs are also highly conserved across eukaryotes, and their degeneration promotes the flexibility of interactions.

Most of these binding domains span 4 to 8 residues, with an average length of 400 Å (Bollen et al., 2010). These interaction motifs, often compact, reside within disordered regions prone to numerous mutations. This conformation could present an evolutionary advantage in case of favorable functional mutations (Heroes et al., 2013).

Despite the possibility of simultaneous interaction with multiple partners, PP1c is considered a platform that predominantly interacts with numerous partners, although typically at distinct time points or localizations (Bollen et al., 2010). Competitive dynamics also occur among regulatory subunits competing to create a holoenzyme with PP1c. Cellular concentration and affinity arrange complex formation according to the cell's requirements (Heroes et al., 2013). Notably, partner protein concentration vastly exceeds that of the catalytic subunit to prevent the presence of single PP1c, which carries a risk of uncontrolled dephosphorylation-associated toxicity.

The conformation of PP1c appears to remain invariant (Peti et al., 2013). It was previously suggested that proteins regulated by various partners exhibit a low evolutionary rate which might elucidate the remarkable structural and functional conservation seen across all PP1 homologs (Manna et al., 2009). The attachment of a regulator via a motif doesn't alter PP1c's conformation, but rather facilitates binding through secondary motifs that modulate phosphatase activity (Bollen et al., 2010).

## 2.3. Regulation of PP1c in *Plasmodium*

Earlier investigations, rooted in comparative sequence analysis, unveiled that *P. falciparum* primarily expresses four well-conserved PfPP1c regulators similar to their mammalian counterparts: PfI2 (Inhibitor 2), PfI3 (Inhibitor 3), PfLRR1 (Leucine Rich repeat 1) and Pfeif2ß (eukaryotic initiation factor 2ß)(Fréville et al., 2012; Tellier et al., 2016) (Daher et al., 2006; Fréville et al., 2013)

### 2.3.1. Inhibitor 2:

Inhibitor 2 ($I_2$) was initially discovered in 1976 and characterized as a thermostable protein capable of inhibiting PP1 activity (HUANG & GLINSMANN, 1976). It stands as the oldest among the regulators of PP1. Homologs of $I_2$ are found in yeast (Glc8), *Caenorhabditis elegans*,

*Drosophila*, *Xenopus*, and across all mammals (Li et al., 2007; Tung et al., 1995). $I_2$ is predominantly unstructured in solution, except for an α-helix spanning residues 135 to 143 (Huang et al., 2000). This regulator appears to belong to a class of proteins that gain structure upon binding to their partner (Garner et al., 1999). The mammalian Inhibitor 2 contains three binding regions to the phosphatase, all of which have been remarkably conserved throughout evolution (Hurley et al., 2007).

Three major interaction regions have been identified on $I_2$, corresponding to the KGILK domain (SILK motif), KKSQKW domain (RVxF motif), and FEMKRKLHYNE domain in vertebrate I2 (Hurley et al., 2007).

The first, and smallest, binding domain encompasses residues 12 to 17 (KGILKN, SILK motif) and involves a mixture of hydrophobic interactions and hydrogen bonds. Various deletion and directed mutagenesis experiments have demonstrated the significance of this N-terminal domain in regulating phosphatase activity (Helps et al., 1998; H. Bin Huang et al., 1999). In fact, certain Inhibitor 2 proteins found in rats (I2β (Osawa et al., 1996)), Drosophila (Helps et al., 1998), and yeast (Glc8 (Tung et al., 1995)) that lack this sequence exhibit limited PP1 inhibition capacity.

The second domain consists of residues 44 to 56 (KSQKWDEMNILAT), facilitating interaction with the phosphatase at a hydrophobic groove previously recognized for accommodating subunits bearing the "RVxF" binding motif. This interaction mode is prevalent among the majority of phosphatase regulators. The RVxF motif is distinct as it involves a glutamine instead of the usual valine or isoleucine.

The last and longest domain, encompassing residues 130 to 169, forms an elongated α-helix interrupted at positions 149 and 153. The 130-146 segment docks along the hydrophobic groove of PP1, while amino acids 147-151 directly bind to the active site, obstructing its access to other substrates (Hurley et al., 2007).

Over the course of numerous years, the phosphorylation of inhibitor 2 bound to PP1 by the GSK3 kinase was extensively investigated due to its involvement in regulating the catalytic subunit PP1c (Ballou et al., 1985). Findings suggest that under different conditions, $I_2$ could function as either an inhibitor or an activator of the phosphatase. This dual nature drew parallels with the RCN family of calcineurin phosphatase regulators (Hilioti et al., 2004).

Inhibition of PP1c by $I_2$ occurs at three levels (Cannon, 2013). Firstly, by occupying a significant portion of PP1c, from the hydrophobic and acidic groove to its catalytic site, the enzyme's

activity is hindered, preventing interaction with various substrates (Hurley et al., 2007). Subsequently, PP1c can be inactivated by removing a metal ion (Bollen et al., 2010; Cannon, 2013). Finally, tyrosine 149 (Y149) in $I_2$ is positioned exactly within the PP1c's catalytic site, and through steric hindrance, prevents the second metal ion from binding. This leaves the phosphatase in an inactive state. Phosphorylation of $I_2$ at threonine 72 (T72) or 74 in humans and mice, respectively, restores phosphatase activity by facilitating the binding of the second ion (Cannon, 2013). This phosphorylation-induced activation doesn't result in a significant conformational change in $I_2$, but rather a subtle variation in the interaction between the two proteins (Lin et al., 2003).

In addition to its role in mediating metal ion binding and release, inhibitor 2 (I2) is implicated in chromosome segregation and mitosis. During *Drosophila* embryogenesis, inhibitor 2 (DmI2) is initially present in the cytoplasm but concentrates around condensed chromosomes during mitosis, a process crucial for proper chromosome distribution (W. Wang, Todd Stukenberg, et al., 2008). Remarkably, a significant reduction in DmI2 protein concentration leads to substantial embryonic lethality, likely arising from disrupted mitotic synchronization and incomplete anaphase due to abnormal chromosome segregation (W. Wang, Cronmiller, et al., 2008). The indispensability of $I_2$ might be tied to its involvement in the PP1c-Nek2 complex (Eto et al., 2002). Nek2 kinase partners with phosphatase via its RVxF motif (KVHF). The mutual complex formation could enable reciprocal phosphorylation and dephosphorylation, with $I_2$ potentially tipping the balance in favor of Nek2 at the right moment to promote chromosome separation (Eto et al., 2002).

Notably, $I_2$ appears to be extensively phosphorylated at its T72 near centrosomes during mitosis in humans (Leach et al., 2003; Li et al., 2007) and *Drosophila* (W. Wang, Cronmiller, et al., 2008), suggesting that this phosphorylation holds a pivotal role in the intricate balance of mitotic regulation.

In *Plasmodium*, The Inhibitor 2 protein (PfI2) exhibits a 28% identity with its human counterpart, HsI2 (Fréville et al., 2013). Notably, PfI2 is smaller than its human ortholog, featuring a truncation in the N-terminal region that results in the absence of the SILK motif. While the HYNE and RVxF motifs are conserved, the RVxF motif in PfI2 follows a more conventional sequence with isoleucine replacing glutamine (KKTISW). Through nuclear magnetic resonance (NMR) studies, the presence of an Fxx[RK]x[RK] motif was demonstrated (Fréville et al., 2014). PfI2 in the parasite interacts with PfPP1c, where the RVxF motif is the

primary, though not exclusive, contributor to this interaction (Fréville et al., 2014). Although the absence of viable parasites upon gene knockout suggests the essentiality of PfI$_2$ for parasite survival (Fréville et al., 2013), a more recent study, founded on saturation mutagenesis to identify essential *P. falciparum* genes, suggested that PfI$_2$ might not be essential during IDC. However, it's noteworthy that PfI$_2$ may play a role in blood stage development, as insertions in its gene were associated with a slow-growth phenotype (M. Zhang et al., 2018a), being linked to the regulation of mitosis, specifically in cytokinesis (Wang, et al., 2008).

### 2.3.2. Inhibitor 3:

Considerably less investigated than inhibitor 2, inhibitor type 3 (I3) (PPP1R11 or Ypi1 in yeast) was initially described in humans, where this small, thermostable, hydrophilic molecule of 126 amino acids was characterized for its inhibitory activity against the catalytic subunit of phosphatase 1 ( Zhang et al., 1998). Subsequent studies in yeast and plants revealed that their counterparts in *Saccharomyces cerevisiae* and *Arabidopsis thaliana* exhibited the same inhibitory activity (Takemiya et al., 2009).

Inhibitor 3 is a nuclear protein, localized within the nucleolus, centrosomes, and the cellular mitotic apparatus. Structurally, the protein's sequence exhibits clear organization. The human sequence features two groups of basic residues, "RKRK" (N-terminal portion) that facilitates nuclear localization, and "HRKGRRR" (C-terminal end) that guides the protein toward the nucleolus (H. S. Huang et al., 2005; C. Zhang et al., 2008).

It possesses two sites crucial for interaction with Protein Phosphatase 1. The first, "39KKVEW43," conforms to the "RVxF" motif where it engages with the phosphatase through it (KKVEW) (C. Zhang et al., 2008).A second region spanning amino acids 65 to 77 seems crucial for its inhibitory function. I3 possesses a Nuclear Localization Signal (NLS) and colocalizes with PP1α at centrosomes and PP1γ1 in the nucleolus (Huang et al., 2005). In vitro, I$_3$ interacts with both isoforms but not with PP1β, implying interaction and localization specificity. In vivo studies demonstrate the loss of its inhibitory activity following phosphorylation by kinases A, C, or casein 2 (Zhang et al., 1998).

Studies conducted in yeast revealed the essential role of inhibitor 3 in the organism's development. Inhibitor 3 is involved in a trimeric complex that includes Protein Phosphatase 1 and the Sds22 protein. The latter contains a succession of 11 Leucine Rich Repeat (LRR)

domains, enabling it to bind to the triangular α4/α5/α6 motif situated near the active site of the phosphatase (Ceulemans et al., 2002).

In this context, both $I_3$ and Sds22 can simultaneously attach to PP1, with Sds22 promoting the gradual conversion of the phosphatase into an inactive form (Lesage et al., 2007; Pedelini et al., 2007). The heterotrimer $I_3$-SDS22-PP1c likely drives the nuclear localization of the phosphatase. So, the conditional loss of either of these proteins results in altered nuclear localization of the phosphatase, halting cell growth during mitosis, and leading to the formation of aberrant mitotic networks (Pedelini et al., 2007; Peggie et al., 2002).

*Plasmodium falciparum's* Inhibitor 3 (PfI$_3$) shares a 31% identity with its human homolog, and its RVxF interaction motif (KVVRW) is conserved (Fréville et al., 2012) While this motif is indispensable for interaction with PfPP1c, it's possible that a secondary site could be involved, as seen in the case of the human counterpart. Surprisingly, PfI$_3$ cannot complement a Ypi1-deficient yeast strain, despite its interaction with GLC7. This suggests that some or all of Ypi1's functions may not be compensated for by PfI$_3$. Additionally, despite its sequence similarity to its yeast and human orthologs, it appears to play a distinct regulatory role on PfPP1c. An increase in PfPP1c activity in the presence of PfI$_3$ in vitro, rather than inhibition, further suggests that PfI$_3$ is not the exact ortholog of Ypi1 (Fréville et al., 2012).

Functionally, Inhibitor 3 play a role in a shared pathway regulating cell division, ensuring proper chromosome segregation (Pedelini et al., 2007). A recent study suggested that, in addition to PfI$_2$, PfI$_3$ also might not be essential during IDC. (Zhang et al., 2018).

Further investigations are required to confirm the importance of $I_2$ and $I_3$ through targeted inducible knockdown experiments (iKd). Notably, previous studies have demonstrated that synthetic peptides containing the RVXF motifs exhibit potent inhibitory effects on the in vitro growth of *P. falciparum*. However, it should be noted that the inhibitory potential of these derived peptides on other PP1-RVXF-dependent interactions cannot be ruled out.

Regarding PfI$_2$ and PfI$_3$, their primary amino acid sequences revealed the presence of RVxF consensus motifs. As anticipated, biochemical and mutational analyses underscored the significant contribution of this motif to PfPP1c binding. NMR spectroscopy elucidated the 3D structures of PfI$_2$ and PfI$_3$ in isolation and in the presence of PfPP1c, confirming interaction via the RVxF motif in solution. PfI$_2$, in particular, displayed a more intricate interaction pattern, involving an additional FxxR/KxR/K motif, also known as Fxx, previously associated with PP1c

binding in anti-apoptotic proteins and ion transporters. Notably, deviations were observed in the primary sequence of PfI$_2$ compared to its human ortholog, with the RVxF motif notably deviating from the consensus sequence. Furthermore, PfI$_2$ is approximately 30% shorter than its mammalian counterpart and lacks a SILK motif, known for its crucial role in PP1c binding and regulation in mammals (Hurley et al., 2007; Yang et al., 2015). These differences underscore a distinct mode of binding of PfI2 to PfPP1c compared to its human ortholog. It's important to highlight that the identity of the x residue in the RVxF motif could potentially influence interaction stability, as previously reported (Ragusa et al., 2010). Notably, this x residue does not exhibit conservation between the conserved *P. falciparum* PIPs and their human counterparts.

### 2.3.3. LRR1:

Leucine-rich repeat protein 1 (LRR1) is a significant and ancient PIP lacking the RVxF binding motif that is found in approximately 85% of PIPs. Instead, LRR1 relies on its leucine-rich repeat domains to establish a connection with PP1c (Ceulemans et al., 2002). LRR1 stands as an ortholog of human SDS22.

In the case of human Sds22, it was initially identified in yeast as a pivotal regulator of cell division, specifically implicated in the metaphase-to-anaphase progression (Ohkura & Yanagida, 1991). In the context of anaphase, SDS22 plays a crucial role in ensuring the stability of kinetochore-spindle attachment (Rodrigues et al., 2015). It is SDS22 that distinctly delineates the localization of PP1c at the kinetochore, thereby providing a mechanism for accurate chromosome segregation.

A recent crystallography investigation conducted by Heroes and colleagues unveiled that human SDS22 most probably engages with PP1c through a domain distinct from the binding sites utilized by previously identified interactors. This revelation sparked speculation that SDS22 might serve as the third interactor within various PP1 complexes, thereby exhibiting a range of functions (Grusche et al., 2009). Beyond its role in cell division, SDS22 has been implicated in diverse processes such as cell shape and polarity control (Grusche et al., 2009) maintenance of epithelium integrity, regulation of sperm motility (Cheng et al., 2009), and participation in plant immunity mechanisms. Consequently, SDS22 is attracting growing attention as a potential therapeutic target in cancer research (Paul et al., 2019).

*In Plasmodium*, PfLRR1 shares a 42% identity and an overall similarity of 61.5% with *S. pombe* Sds22, a similarity level comparable to the one observed between Sds22 of *S. pombe* and *S. cerevisiae* (Daher et al., 2006). Through sequence analysis, PfLRR1 emerges as a strong candidate for regulating PP1 function. One notable feature of PfLRR1 is the presence of several LRRs known for their involvement in protein-protein interactions, with an additional interaction facilitated by its C-terminal LRR cap motif (Pierrot et al., 2018). It's noteworthy that PfLRR1 encompasses 10 LRRs, about 86% of the entire protein. Each LRR unit, characteristic of Sds subfamily proteins, comprises a 20-to-24 residue motif (Kobe & Kajava, 2001). Structurally, the arrangement of LRR repeats forms a horseshoe shape with curved parallel β-strands lining the concave side, while helices flank its convex side (Kobe & Deisenhofer, 1995; Kobe & Kajava, 2001) LRR domains have been recognized for their involvement in diverse processes like bacterial pathogenesis and plant immune responses, driven by macromolecular interactions (Heroes et al., 2019).

Furthermore, PfLRR1 actively suppresses the activity of PP1c (Daher et al., 2006). Its inhibitory activity against the phosphatase has been demonstrated both in vitro and in *Xenopus*. Through genome-wide saturation mutagenesis, it has been established that the gene encoding LRR1 is non-mutable, suggesting its likely indispensability for the successful completion of the *P. falciparum* blood-stage cycle (Zhang et al., 2018). Intriguingly, a recent proteomic approach aiming to explore PfPP1c signaling events reported a significant accumulation of PfLRR1 and PfI2 in a *P. falciparum* strain in which PP1c was depleted (Paul et al., 2020)

In the case of PP1c-PfLRR1 binding, pepscan analysis pinpointed a single synthetic peptide derived from Leucine-Rich Repeats (LRRs) that participates in this binding. Surprisingly, the peptide corresponding to the C-terminal LRR cap domain, previously recognized for its role in protein stabilization and integrity, was also identified as directly interacting with PP1c. Notably, this differs from the binding pattern observed for its human ortholog, SDS22, which involves six LRR motifs without implicating the C-terminal LRR cap domain (Pierrot et al., 2018).

## 2.3.4. Eukaryotic initiation factor 2ß

Human eIF2β, a member of the eIF2 complex responsible for regulating protein synthesis, has been observed to associate with PP1, as demonstrated in both in vitro experiments and cell lysates (Wakula et al., 2006). Interestingly, this interaction places eIF2β in the regulator/substrate category, as its binding to PP1 activates the dephosphorylation of eIF2β while concurrently inhibiting PP1's activity towards other substrates (Wakula et al., 2006).

Structurally and functionally, eIF2β consists of three domains: the N-terminal domain, which interacts with eIF5 and eIF2B; the central domain responsible for eIF2γ binding, and the C-terminal domain that includes a region involved in mRNA binding (Thompson et al., 2000).

In *Plasmodium*, the most recently identified regulator is eIF2β (PfeIF2β) (Tellier et al., 2016). Despite being 33% smaller than its human counterpart, it interacts with PfPP1c through two interaction motifs. In addition to its binding to the phosphatase, PfeIF2β can form complexes with PfeIF2γ and PfeIF5. It is indispensable for parasite survival, and like in humans, the role of the PfeIF2β-PfPP1c complex remains unknown. The absence of identifiable GADD34 or CrEP homologs suggests that, during and after cellular stress, the regulation of eIF2α phosphorylation differs. Dephosphorylation is likely no longer mediated by PfPP1c but by UIS2 (Up-regulated in Infective Sporozoites 2), a phosphatase known to be overexpressed in sporozoites (Zhang et al., 2016).

PfeIF2β interacts with PfPP1c through two interaction motifs: the conserved Fxx[RK]x[RK] motif (FGEKKK) and an RVxF motif distinct from the human version (KVAW). Mutation of each motif individually does not prevent binding to the phosphatase in GST pull-down assays. However, simultaneous mutation of both sites inhibits interaction with PfPP1c, indicating that either motif is sufficient for in vitro interaction (Tellier et al., 2016).

### 2.3.5. PfPP1 specific partners

Next, employing yeast two-hybrid (Y2H) assays and in silico RVxF motif screenings, a total of 134 and 55 PfPIPs were identified, respectively (Hollin et al., 2016). Additionally, a recent proteomics investigation conducted in *P. berghei* schizonts unveiled the presence of 178 potential PIPs (Hollin et al., 2019a), among which 19 proteins have been experimentally confirmed to physically interact with PP1c. These confirmations were achieved using both Y2H assays and binding assays employing recombinant proteins in *P. falciparum* (Daher et al., 2006; Fréville et al., 2013; Hollin et al., 2016). Notably, 80 of these PIPs, accounting for 70% of the proteins with available data, appear to be indispensable for the completion of the *P. berghei* intraerythrocytic developmental cycle (IDC), as evidenced by the absence of viable knockout parasites (Bushell et al., 2017).

Comparative analysis has further revealed that 31.5% of the potential PbPIPs lack homologs in humans, rendering them promising drug targets. Within this context, two proteins initially identified as PfPIPs in Y2H screenings, and whose expression is restricted to *Plasmodium*, were

subjected to in-depth investigation. Through biochemical and reverse genetics approaches, it was determined that the first of these, designated RCC-PIP, exhibits binding and transport capabilities not only for PfPP1c but also for the kinase PfCDPK7 (Lenne et al., 2018). The second PIP, PfGEXP15, functions as a regulator that enhances PfPP1c activity (Hollin et al., 2019).

# II.  Objectives

Our initial work using the yeast two-hybrid (Y2H) system showed that a fragment of PfGEXP15 (PfGEXP15 $_{8-182}$) interacts with PfPP1 (Hollin et al., 2016).The first analysis of the derived amino acid sequence from this fragment revealed the presence of a well-known binding motif to PP1 corresponding to the consensus RVxF sequence. Further mutagenesis studies of this motif confirmed its involvement in the binding activity. PfGEXP15 encodes a protein of 904 amino acids for which up to 15 peptides were detected in schizonts by proteomic approaches, confirming its expression in blood stage parasites (PlasmoDb). Unfortunately, the elucidation of the biochemical activity of PfGEXP15 as full-length protein was hampered as all attempts to obtain the entire nucleotide sequence with the correct open reading frame failed. To decipher further the role of GEXP15, we searched its Homologs. These were found in different *Plasmodium* species, including *P. berghei* (PBANKA_0515400). The predicted protein of PbGEXP15 (656 aa) shares an overall identity of 41% with PfGEXP15. In particular, the putative consensus RVxF binding motif to PP1 present in the interacting region of PfGEXP15 is completely conserved in PbGEXP15 ($^{29}$KKKK**KVQF**$^{36}$). The work performed on PbGEXP15 confirmed that it is the functional homolog of PfGEXP15. Indeed, it has been shown that PbGEXP15 was able to bind exclusively through its first RVXF binding motif (postion:29-36) and to enhance the PP1c activity in vitro. Further, PbGEXP15 deficient parasites were shown to be unable to develop lethal infection in BALB/c mice or to establish experimental cerebral malaria in C57BL/6 mice (Hollin et al., 2019). Further, although deficient parasites produced gametocytes, they did not produce any oocysts/sporozoites indicating a high fitness cost in the mosquito, suggesting that PbGEXP15 affects both the asexual and sexual lifecycle of *P. berghei.*

Yet despite its crucial function(s), our understanding of its exact role(s) during *Plasmodium falciparum* life cycle is still unknown. In the present project, **my main objective is to examine the role of GEXP15 in the human malaria parasite *P. falciparum.*** To achieve this work, the thesis project is structured around two main goals:

1- Exploration of the GEXP15 functions by reverse genetics across *Plasmodium falciparum*'s developmental stages.

2- Analysis of PfGEXP15 sub-cellular localization and identification of the PfGEXP15's interactome, contributing to the understanding of *Plasmodium*'s signaling cascade

# RESULTS

# III. Results

## A.    In Silico Analysis

### 1.    *Plasmodium* GEXP15 protein sequence analysis

Earlier study suggested a potential relationship between GEXP15 and the human CD2BP2 (CD2 Cytoplasmic Tail Binding Protein 2) (Sorber et al., 2011). CD2BP2 is known to interact with splicing factors and PP1 through its GYF domain (Laggerbauer et al., 2005) and an RVxF motif (Albert et al., 2015), respectively. At the protein level, GEXP15 in *P. berghei* exhibited a relatively low identity to HsCD2BP2, while containing a GYF-like domain that did not precisely match the consensus sequence (GP[YF]xxxx[MV]xxWxxx[GN]YF) (Freund et al., 1999). Despite this difference, PbGEXP15 interactome analysis has indicated the presence of spliceosome protein complexes (Hollin et al., 2019).

To gain deeper insights into the structure and functional roles of GEXP15 in *P. falciparum* (PfGEXP15), we conducted an amino acid sequence analysis, aiming to identify both known motifs present in PfGEXP15 and potential novel signatures using latest updated software tools. An initial comparison of PfGEXP15's primary structure, consisting of 904 amino acids, with that of *Homo sapiens* (Hs) CD2BP2 (UniProt_O95400), which spans 341 amino acids, unveiled a sequence identity of 23%, with this identity being predominantly concentrated in two distinct regions, one situated centrally and the other located at the C-terminal end. (Figure 16).

```
GEXP15  MLNEEKLGEENDLDKFNNDVNEDIIKDDVNKSKEKKKKKVQFSNNNETIYYEKDESENSY  60    DSVGKKNLLQVRIRAKSSIQHGEENLNVVKKNDEVEKNDEVEKNDEVEKNDEVEKNDEVE  532
CD2BP2  ------------------------------------------------------------  0     ------------------------------------------------------------  139


GEXP15  FNFTLNNFNYFECFYNDIYGDHFNDQIIRNNQYNENNGDEEDGDDEEDGDDEEDGDDEDD  120   KNDEVEKNDEVEKNDEVEKNDEVERNDEVERNDMAERNDMSERNDMAERNDMAEKNNDDV  592
CD2BP2  ------------------------------------------------------------  0     ----------------------------------------D-SEEEDSLGQTSMS------A  154
                                                                              * **.:*  :..*:            .


GEXP15  DDEEDDDDEDGDDQNDKGENIENNINDEDNKSEEINHKNNNCNNNKNNNCSNNKNTILNG  180   KVPENNLIEAPMDKEHIMI--NNSEEESIGNNKKSEEQKNYNLYNDDDEKKNIVHNERLE  650
CD2BP2  ------------------------------------------------------------  0     QALLEGLLELLLPRETVAGALRRLGARGGGKGRKGPGQ--------------PSSPQRLD  200
                                                                              :. :.*:*  : :* :   .   .. ..*::.*. *               :**:


GEXP15  INNINNNDNNNNTTNLKKKKKKKKKKNIDHSIYNNEQVSKNMVSLKKSGNNKNNIDDLKS  240   ELENLKQ-MYQKITLD-YKTIERRF-NNLIDLTQK-L--TN--EYKNV-YF---LTKREF  698
CD2BP2  --------------------------------------MPKRKVTFQGVGDEE--------  15    RLSGLADQMVARGNLGVYQETRERLAMRLKGLGCQTLGPHNPTPPPSLDMFAEELAEEEL  260
                                          : *. :::*  *:::             .*..* : *  : .*. *:  ..*:  .*  .*  :  *    .:  *   *::.*:


GEXP15  GKKNCLLSNIFISHDENNNLKKKKKNVGNITNDNFKREKFHQS--FNEDP---SFEINNI  295   EAL-----CKKLEEYKENVDIHWQLKWMNGVDNNVYGPYNYYDIYNFITTGLVTVLNPIL  753
CD2BP2  --------------DEDEIIVPKKKLVDPVAGSGGPGSRFKGKHSLDSDEEEDDDDGGSS  61    ETPTPTQRGEAESRGDGLVDVMWEYKWENTGDAELYGPFTSAQMQTWVSEGYFPD--GVY  318
                      **:: :  *** *. ::...   .:*:  . ::.*    .  :. .         *:   :    : ...  **: *: ** *  * ::***:. :: .::: *  .   :


GEXP15  HTAILN---AEERTIHYSKDYFGYDIEPFNMKNELTQGYIDKDGNYIYNESDNDEVEEAW  352   LRRINNKNEVLENIWQMYDAVNYLIFVTNDNIKKKRKHDGLISKNKDQDSDNNEEDNENN  813
CD2BP2  KYDILASEDVEGQEAATLPSEGGVRITPFNLQEEMEEGHFDADGNYFLNRD--AQIRDSW  119   CRKLDPPGGQFYN----SKRIDFDLYT---------------------------------  341
                : **   .*  :    .   * * ***:::*: :*::* ****: *.. ::.::*         *::: . : *   . :: ::.


GEXP15  LKSVDEQDPLSTFSNNTLQAQKFQETQSKFHMTYDKLNNNILSINIFDALYSLSCLLIDE  412   KNTDVDGDGDDDDDDNDDENDNDDENDYDLLNKKKKKKKGLIQISKKKKKKKKEHYEENN  873
CD2BP2  LDNIDWVKIRERPPGQ-RQAS---------------------------------------  139   ------------------------------------------------------------  341
                *..:*  .    .:  **.


GEXP15  KETPIKAMIRYKNDLKVCKNYLNQYESKIDKINSLSINSNAEQKIQSTEEHEQNGETLQT  472   IFNDNNNNQGNSSNNEEHSDNEDYYDNGYEF  904
CD2BP2  ------------------------------------------------------------  139   ------------------------------  341
```

**Legend**
D : Aspartic acid
E : Glutamic acid
N : Asparagine

**Figure 16 The protein sequence alignment of PfGEXP15 and HsCD2BP2.** The alignment was performed using ClustalW. Colored amino acids represent low complexity regions. The identity and similarity are represented by * and : respectively.

The observed low identity might be attributed to the presence of multiple low-complexity regions (LCRs) in PfGEXP15. *P. falciparum* proteins are notably enriched in repetitive LCRs, with some estimates suggesting they constitute approximately 30% of the genome (Gardner et al., 2002b). A significant portion of these repetitive sequences consists of amino acid repeats, including asparagine (N), lysine (K), glutamic acid (E), and aspartic acid (D), and it has been suggested that these LCRs may not serve any specific function (Muralidharan & Goldberg, 2013). In a previous study involving PfRPN6, it was demonstrated that the deletion of a poly-asparagine tract had no discernible impact on protein stability, cellular localization, protein-protein interactions, or the progression of the IDC cycle (Muralidharan et al., 2011). Regarding PfGEXP15, it's noteworthy that these regions predominantly encompass the low-homology sequences, accounting for both the disparities in length and the reduced identity between the two proteins.

Furthermore, we extended the analysis of PfGEXP15 and its potential homologs in *P. berghei* (PBANKA_0515400) to counterparts in other species, including *Toxoplasma gondii* (Tg) (TGGT1_217010), *Saccharomyces cerevisiae* (Sc) (known as "LIN1" in yeast, NP_012026), and HsCD2BP2. Alignment of these five CD2BP2 protein sequences shows that the amino acid similarity is found throughout the entire length of the protein, with local concentration of identity in two main regions (Figure 17). The alignment presented in Figure 17 shows that the RVxF motif, known to bind to PP1(Hollin et al., 2016) is conserved except for yeast, suggesting its inability to bind to PP1. However, the GYF like domain is present in all of the aligned sequences. Interestingly, this alignment shed the light on a central unknown domain conserved across these species which will be interesting to discover its function.
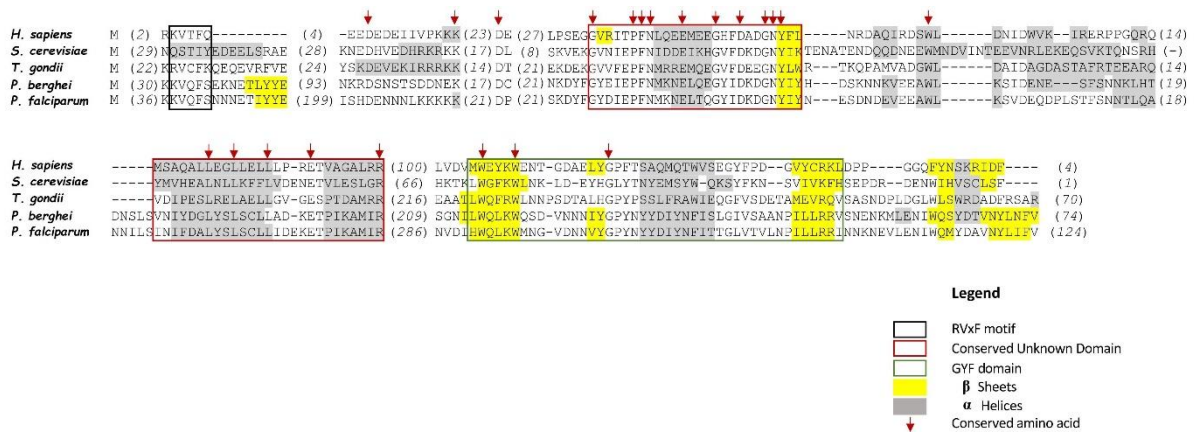
**Figure 17 Alignment of PfGEXP15 and its main counterparts.** CD2BP2 homologs amino acid sequences from *Homo sapiens*, *Saccharomyces cerevisiae*, *T. gondii*, *P. berghei* and *P. falciparum* were aligned using MAFFT alignment program. Relevant motifs among them are boxed. Alfa helices and Beta sheets are highlighted in gray and yellow, respectively. Red arrow indicates a conserved amino acid residue across the sequences.

In the initial step, a sequence alignment was performed, comparing the central region of PfGEXP15 (residues 315-425) with that of PbGEXP15 (residues 199-309), HsCD2BP2 (residues 84-194), TgCD2BP2 (residues 119-215), and ScLIN1 (residues 120-212). This analysis unveiled identities ranging from 25% to 37% and similarities spanning from 39% to 65% (Figure 18).
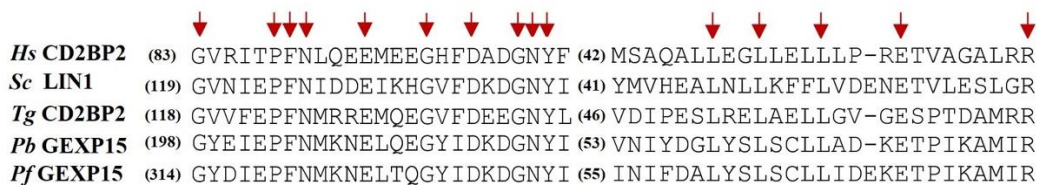


**Figure 18 In silico analysis of *Plasmodium* GEXP15 and CD2BP2 homologs.** Multiple protein sequence alignment of an unknown conserved domain (UD). Arrows show the conserved amino acid residues.

While there is no documented function associated with this uncharacterized domain (UD), it is worth highlighting the presence of conserved residues within this UD, including glycines (G315, G330, and G336) and leucines (L402, L405, and L408). The second conserved region encompasses the GYF motif of CD2BP2, which was identified in both Pb (residues 516-568)

103

and Pf (residues 713-765), referred to as GYF-like due to variations in its amino acid consensus sequence, and is also present in homologs from Sc and Tg (Figure 19).



```
Hs CD2BP2  (279)  VMWEYKWENT-GDAELY GPFTSAQMQTWVSEGYF PD
Sc LIN1    (281)  KLWGFKWLNK-LD-EYH GLYTNYEMSYW-QKSYF KN
Tg CD2BP2  (434)  TLWQFRWLNNPSDTALH GPYPSSLFRAWIEQGFV SD
Pb GEXP15  (515)  ILWQLKWQSD-VNNNIY GPYNYYDIYNFISLGIV SA
Pf GEXP15  (713)  IHWQLKWMNG-VDNNVY GPYNYYDIYNFITTGLV TV
```

```
Hs CD2BP2   GPFTSAQMQTWVSEGYF

            GP +      +     + + +  G

Pf GEXP15   GPYNYYD I YN F ITTGLV

Consensus   GP[YF]xxxx[MV]xxWxxx[GN]YF
```

**Figure 19 In silico analysis of *Plasmodium* GEXP15 and CD2BP2 homologs.** Multiple protein sequence alignment of GYF and GYF-like domain alignment with the consensus sequence. Red arrows show the conserved amino acid residues. Blue arrows show the conserved aa between human CD2BP2 and PfGEXP15.

The alignment revealed a 27% identity and a 52% similarity within the GYF motif between the two *Plasmodium* species. Notably, deviations from the canonical GYF consensus sequence were observed in *Plasmodium*. Specifically, amino acids phenylalanine (F), methionine (M), tryptophan (W), valine (V), and serine (S) were substituted with tyrosine (Y), isoleucine (I), phenylalanine (F), isoleucine (I), and threonine (T) in Pf, respectively. These substitutions in *Plasmodium* included amino acids with similar physicochemical properties (i.e., hydrophobic) to those in the human homolog. However, two glycines (G), a proline (P), and a tyrosine (Y) within this domain remained highly conserved. These observed variations in the amino acid consensus sequence may have implications for the functional role of GYF-like domains.

Upon further examination of PfGEXP15, a PP1 binding motif was identified in the protein's N-terminus, similar to PbGEXP15 and the human CD2BP2 (Figure 20).

```
Hs CD2BP2   M (1)  K  RKVTFQ
Sc LIN1     M (28) H  NQSTIY
Tg CD2BP2   M (21) A  KRVCFK
Pb GEXP15   M (29) K  KKVQFS
Pf GEXP15   M (35) K  KKVQFS

Consensus      [K/R][K/R][V/I][x][F/W]
```

**Figure 20**. *In silico* **analysis of *Plasmodium* GEXP15 and CD2BP2 homologs.** Multiple alignments of the conserved RVxF motif, represented above its consensus sequence.

The PP1 binding motif KKVQF, found in PfGEXP15 (residues 39-43), aligns with the canonical RVxF-motif, conforming to the consensus sequence [K/R][K/R][V/I][x][F/W] (Hendrickx et al., 2009; Wakula et al., 2003) (Figure 20). Although this motif is conserved in *Tg*, its absence in *Sc* implies either a distinct mechanism of interaction with PP1 in yeast or the possibility that it does not bind to PP1 at all, suggesting a lack of regulation by this phosphatase. Additionally, a second minimal PP1 binding RVxF-motif was located in the C-terminus of PfGEXP15 (KNVYF, residues 688-692), which corresponds to the less specific and minimal consensus sequence. Notably, the direct interaction of human CD2BP2 with PP1 is exclusively associated with the RVxF motif, also present in the N-terminal end (Albert et al., 2015). Similarly, in PbGEXP15, only the first RVxF-motif was capable of binding to and enhancing PP1 activity, indicating a shared PP1 binding mechanism between *Plasmodium* GEXP15 and CD2BP2 (Hollin et al., 2019).

To further validate the identified motifs and domains, MEME Suite tool was employed, which specializes in motif-based sequence analysisThrough this process, we successfully identified five conserved motifs shared between *H. sapiens*, *S. cerevisiae*, *P. berghei*, and *P. falciparum* and *T. gondii* (Figure 21).
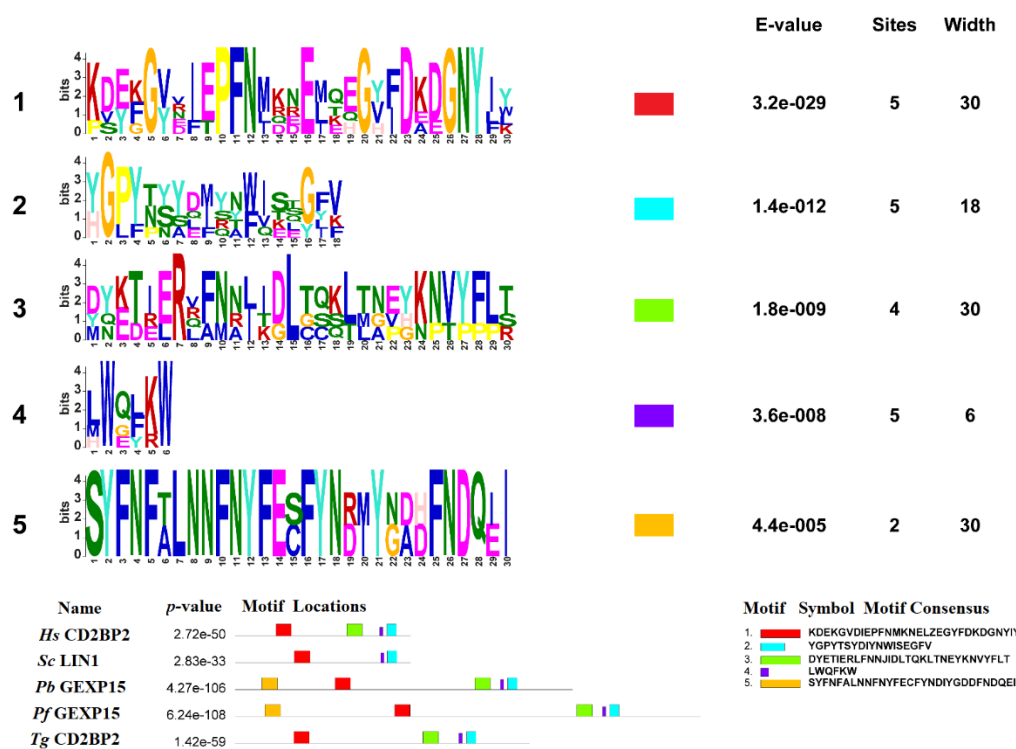
**Figure 21. MEME motif search of GEXP15 and CD2BP2 proteins.** MEME motif search of GEXP15 and CD2BP2 proteins. (A) The 5 most significant sequence logos identified by MEME are represented, as well as their respective E-value, number of sites and width. The height and size of the letters represent the amino acid frequency. (B) Distribution of these motifs across HsCD2BP2, ScLIN1, PbGEXP15, PfGEXP15 and TgCD2BP2. The color of each motif is indicated in part A. P-value and consensus sequence are also reported.

We have successfully verified the presence of the unknown domain (UD) (designated as motif 1), which contains conserved glycine residues, as well as the sequences PFN and GNY (Figure 21). In addition to these findings, two additional motifs were identified, one upstream (motif 4, residues 715-720) and the other downstream (motif 2, residues 729-746) of the GYF motif. These motifs displayed high variability, consistent with the degenerate consensus sequence, except for two tryptophans (W) and one glycine (G), which were well-conserved across species (motifs 2 and 4, Figure 21). Notably, motif 5 comprises highly conserved amino acids and was exclusively detected in PfGEXP15 and PbGEXP15, suggesting that this motif may serve a specific function in the parasite.

In Table 10, I have summarized our current knowledge regarding the structural and functional characteristics of *Plasmodium* GEXP15 and its counterparts. Collectively, these observations indicate that these proteins appear to belong to a group that shares functional homology to some extent.

**Table 10. Summary of *Plasmodium* GEXP15 and its counterparts** sequence analysis and function(s)

| | HUMAN CD2BP2 (O95400) | PBGEXP15 (PBANKA_05 15400) | PFGXP15 (PF3D7_10316 00) | *T. GONDII* (TGGT1_217010) | YEAST LIN1 (P38852) |
|---|---|---|---|---|---|
| **LENGTH (A.A)** | 341 | 656 | 904 (107Kda) | 570 | 340 |
| **PP1 RVXF BINDING MOTIF (NT)** | (R)KVTF | (K)KVQF | (K)KVQF | (K)RVCF | NON |
| **GYF MOTIF (CT)** | GYF | GYF like | GYF like | GYF like | GYF like |
| **OTHER CONSERVED MOTIFS(NT)** | Yes Unknown region conserved | Yes Unknown region conserved | Yes Unknown region conserved | Yes Unknown region conserved | Yes Unknown region conserved |
| **KNOWN INTERACTORS** | PP1/spliceosome factors(s) | PP1 spliceosome factor(s) | PP1 spliceosome factors | ? | Spliceosome factor(s) |
| **FUNCTION (S) REVERSE GENETICS** | Lymphocyte activation Splicing Embryogenesis | KO viable No lethality No oocytes | Non mutable (Piggy back) | Likely essential | Chromosome segragation DNA replication Splicing |

## 2. GEXP15 3D structure modeling

Next, the structure of PfGEXP15 was investigated. The prediction of its secondary structure with PSIPRED (http://bioinf.cs.ucl.ac.uk/psipred) shows that the protein has 29 α helices and 10 β sheets. No transmembrane domain was identified (Figure 22).
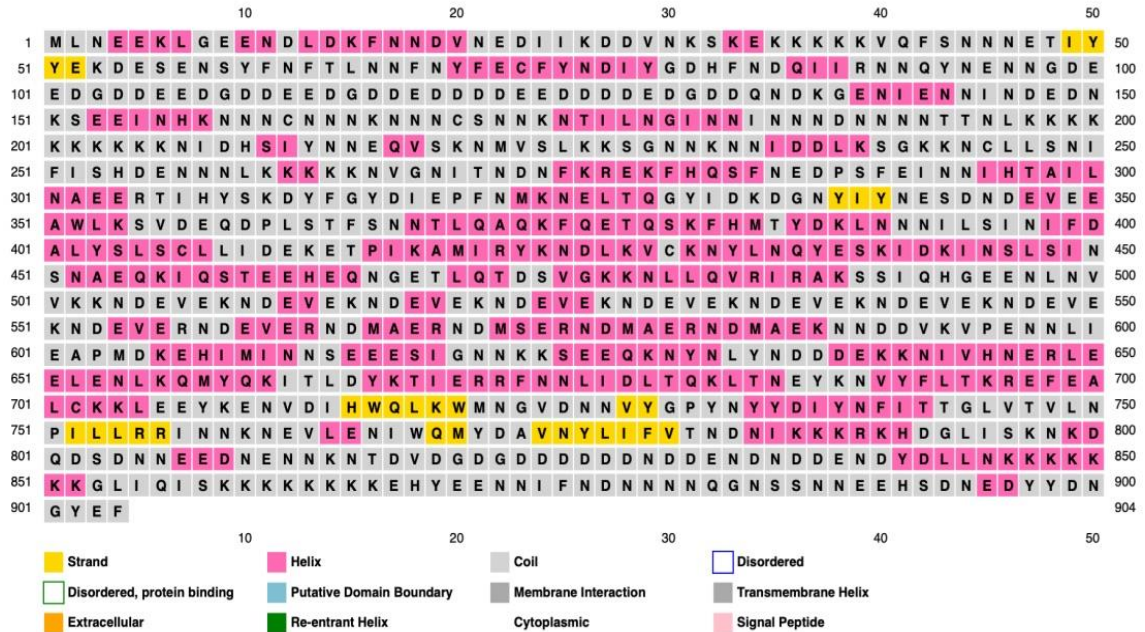


**Figure 22 GEXP15 structural analysis.** The secondary structure of PfGEXP15 predicted using PSIPRED.

The three-dimensional (3D) structures of PfGEXP15, PbGEXP15 and HsCD2BP2 were predicted using AlphaFold (Figure 23). The models generated for these three proteins showed well-defined and structured domains along with long unfolded regions, represented as unstructured straight chains of different lengths.
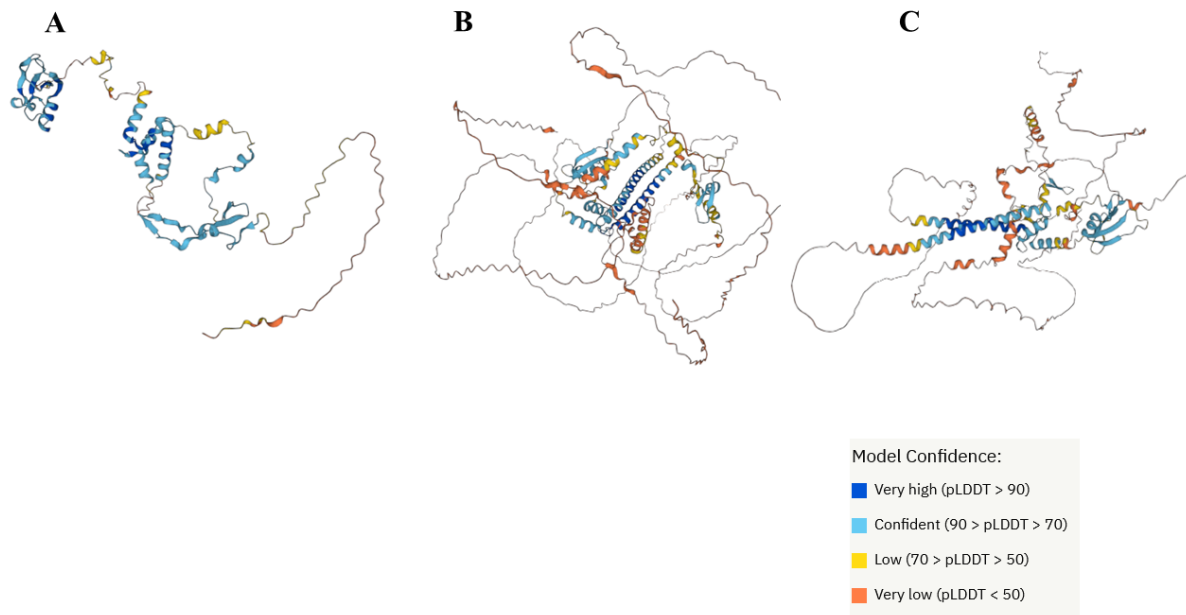
**Figure 23. The 3D structure prediction of HsCD2BP2, PfGEXP15 and PbGEXP15.** The models of HsCD2BP2 (A), PfGEXP15 (B) and PbGEXP15 (C) were generated by AlphaFold.

In order to enhance the accuracy of 3D predictions and minimize potential inaccuracies associated with unfolded regions, we opted to perform separate modeling for the UD and GYF-like domains, considering that domains represent fundamental structural units of proteins. When focusing on the UD, the presence of disordered regions posed a challenge for achieving a complete superposition between the two *Plasmodium* proteins. Nevertheless, both resulting 3D models shared a common structural arrangement, featuring six alpha helices accompanied by a short two-stranded beta-sheet. This arrangement closely resembled the I-TASSER (5.1) prediction, which also indicated a compact structure comprising six helices without beta sheets (Figure 24).
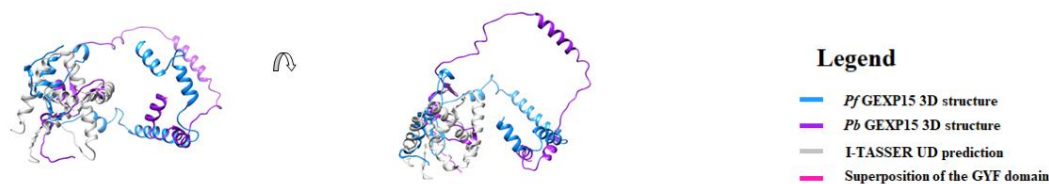
**Figure 24. 3D structure prediction of Pf and Pb GEXP15.** The predicted 3D structure of UD for PfGEXP15 and PbGEXP15 were retrieved from AlphaFold and are shown in blue and purple, respectively. The protein structure predictions are shown in grey. Both models were superimposed to the GYF motif NMR structure of human CD2BP2 (PDB entry: 1gyf) using MatchMaker tool from Chimera (version 1.14).

In contrast, when examining the GYF-like motif, we observed that both PfGEXP15 and PbGEXP15 possessed a similar domain organization but displayed distinct spatial architectures (Figure 25). These structural disparities align with existing NMR experimental data concerning the GYF-containing region of CD2BP2 (residues 280-338) (Kofler et al., 2005). Specifically, in PbGEXP15, we noted a right-angle orientation between the N-terminal helix and the beta-sheet, resulting in an almost linear alignment between these structural elements. This discrepancy is likely attributed to the relatively less structured C-terminal portion of the predicted GYF domain in PbGEXP15, which could have induced alterations in the orientation of the beta-sheet group during the optimization stages of the AlphaFold model construction process.
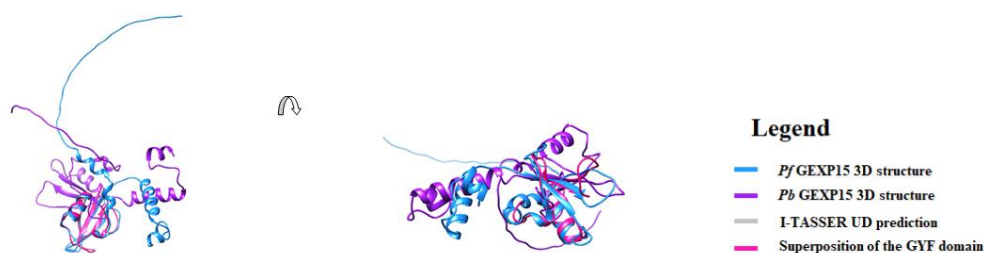


**Figure 25 3D structure prediction of Pf and Pb GEXP15.** The predicted 3D structure of GYF domains for PfGEXP15 and PbGEXP15 were retrieved from AlphaFold and are shown in blue and purple, respectively. The protein structure predictions are shown in grey. Both models were superimposed to

the GYF motif NMR structure of human CD2BP2 (PDB entry: 1gyf) using MatchMaker tool from Chimera (version 1.14).

No model was generated for the RVxF motif since it is often present in unstructured regions of PP1 regulators (Terrak et al., 2004). This inherent lack of a defined conformation within the RVxF motif plays a pivotal role in its interaction with PP1, constituting a phenomenon termed "structure upon binding." This unique ability of the RVxF motif to transform from an initially unstructured state into a well-defined conformation upon binding is a distinctive characteristic that underscores its functional significance in the regulation of PP1 activity (Ceulemans & Bollen, 2004).

## 3.    Evolutionary conservation of GEXP15 and CD2BP2

To investigate the evolution of the CD2BP2 protein and its homologs, 75 protein sequences were retrieved (Table in M&M) using HsCD2BP2 as a query.

We compared these sequences using BLASTP and considered sequences exhibiting > 30% overall identity with HsCD2BP2 and sharing the conserved UD domain and the GYF motif as CD2BP2 homologs. Proteins with an identity lower than 30% and with the UD domain and the GYF motif were considered CD2BP2-like proteins.

Results revealed the distribution of CD2BP2 homologs across Metazoan and CD2BP2-like proteins across 20 phyla, including dictyostelids, fungi, choanoflagellates, rhodophytes, chlorophytes, dinoflagellates, apicomplexan parasites, and oomycetes (Figure 26).

All CD2BP2 homologs showed the presence of RVxF motif and the GYF or GYF-like domains. However, CD2BP2-like proteins in Rhizaria, Plantae, and Amoebozoa lacked the RVxF motif, suggesting a potential absence of PP1 binding ability. We classified PfGEXP15 as a CD2BP2-like protein because it exhibited < 30% overall identity but contained a conserved RVxF motif, a UD, and a GYF-like domain.

**Figure 26 Distribution of CD2BP2 homologs and their domains in Eukaryotes.** The figure displays the distribution of CD2BP2 in the phylogenetic tree of life. Open and closed circles represent absence and presence of RVxF motif, unknown domain, GYF domain, CD2BP2 homologs and CD2BP2-like proteins, respectively. For fungi, *Saccharomyces* species were the main ones considered.

The conservation of these domains was tested in 75 CD2BP2 homologs represented across Metazoans (Figure 27) using the MEME Suite.
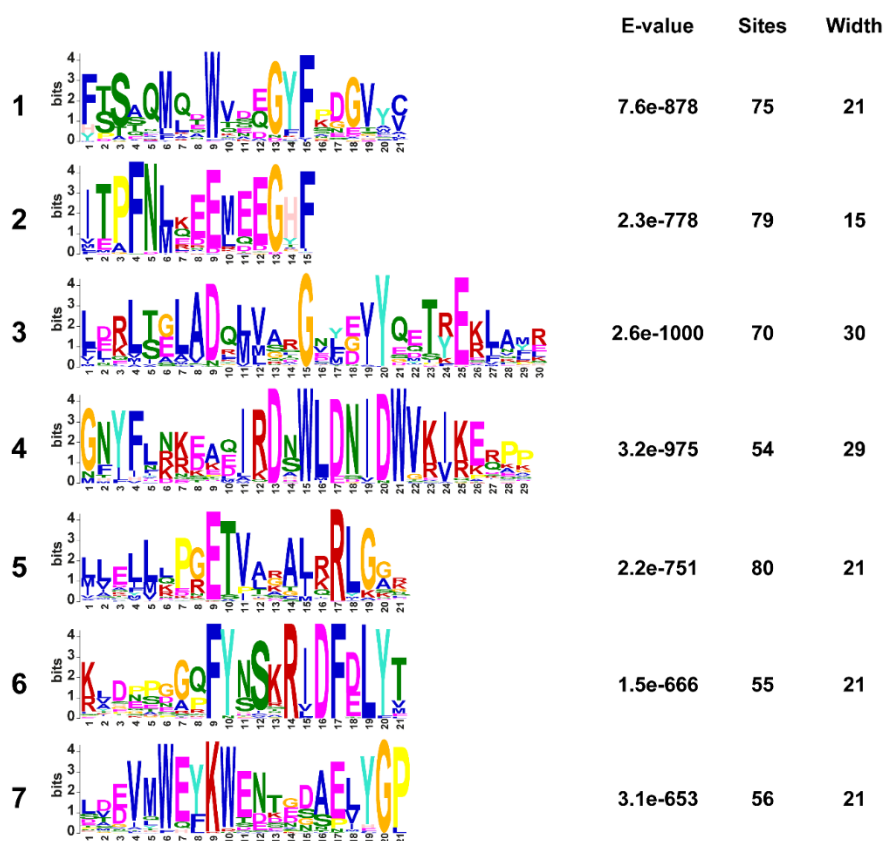
**Figure 27 MEME motif search of CD2BP2 homologs in eukaryotes.** The 7 most significant sequence logos identified by MEME are represented, as well as their respective E-value, number of sites and width across the protein sequences. The height and size of the letters represent the amino acid frequency.

The identified motifs present in the UD and the GYF portions are presented in Figure 27. The conservation of the PF and asparagine (N) sequence, as well as several G, aspartic (D), and glutamic acids (E) suggest that these residues may be critical for the function of the UD. In apicomplexan parasites, fungi, and oomycetes, motif 4 was not detectable indicating a variability of this domain for these species. For the GYF motif, the GPF and GYF residues were well-conserved, in accordance with the consensus sequence, but additional regions showed a high conservation such as WExKW, located upstream of the GYF domain (motif 7). Similarly, only one of the three motifs has been identified in Apicomplexa confirming the presence of a GYF-like domain. Considering the short length and the degeneracy of the RVxF motif, the lack of its detection by MEME is not surprising. Using an alternative approach, the FIMO tool, we directly searched for the RVxF motif using its consensus sequence (Not shown) (Grant et al., 2011).

An RVxF motif was detected in the majority of the species with the exception of the platyhelminths, chlorophytes and dinoflagellates tested. Although some species exhibited a second RVxF motif, the main one appeared to be consistently located in the N-terminal region. In mammals, amphibians and nematodes, the sequence KVTF is well conserved and positioned between amino acids 4 and 8.

Given the predominant presence of CD2BP2 homologs within the animal kingdom, our investigation was directed toward metazoan species. Subsequently, we depicted our findings within the metazoan phylogenetic tree, as illustrated in Figure 28.



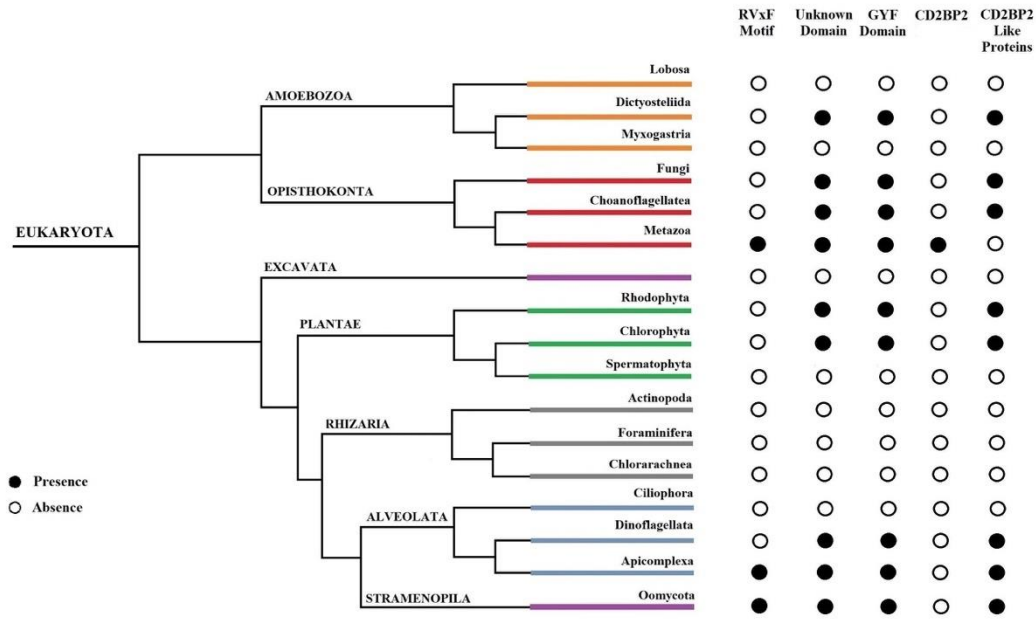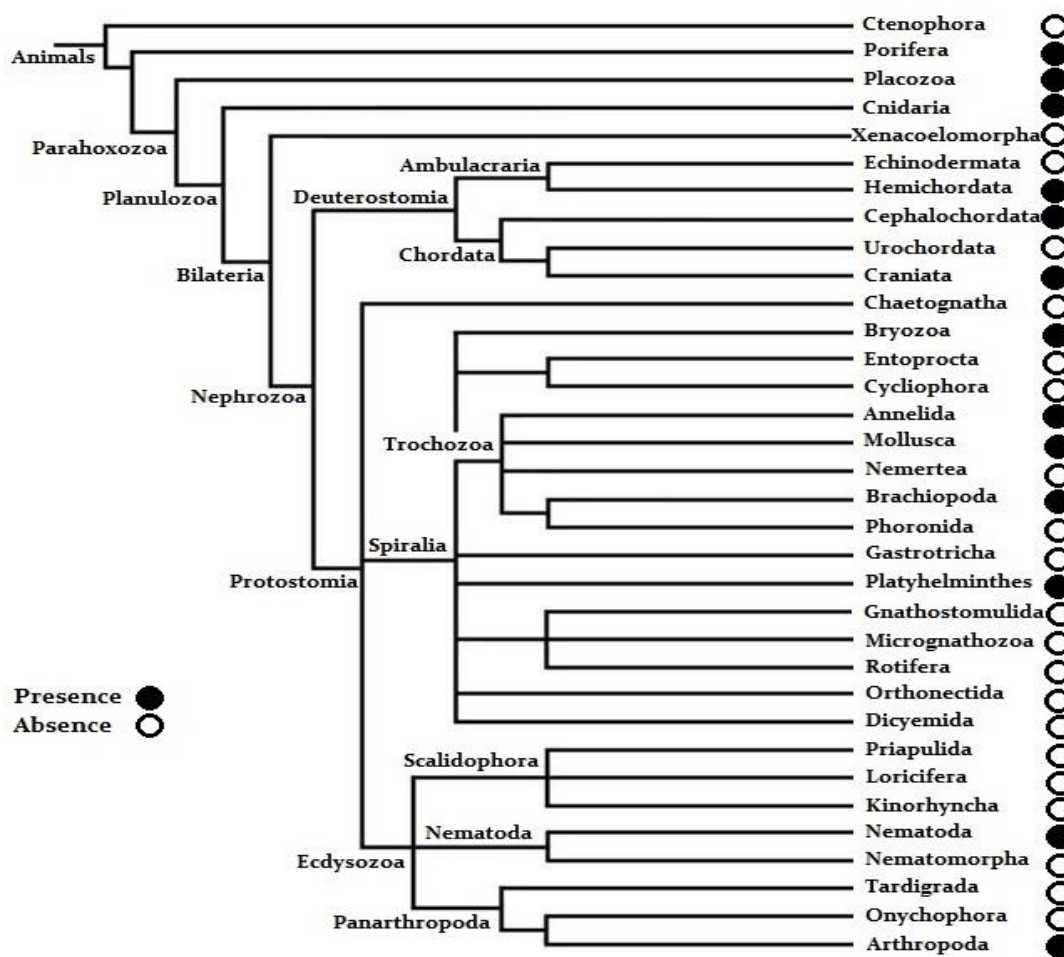**Figure 28 Distribution of CD2BP2 homologs in Metazoa**. The figure displays the distribution of CD2BP2 in the phylogenetic tree of metazoa. Open and closed circles represent absence and presence, respectively, of CD2BP2 homologs.

Having shown some conservation of GEXP15 and CD2BP2 at the protein level, our investigation was extended deeper into the genomic level to elucidate the evolutionary

connections between these organisms, shedding light on potential common ancestry. The examination of CD2BP2's exon-intron architecture revealed noticeable evolutionary patterns. We conducted a comparative analysis of CD2BP2 gene structures in various species, encompassing *Homo sapiens*, *Danio rerio*, *Sphaerodactylus townsendi*, *Xenopus laevis*, *Toxoplasma gondii*, *Caenorhabditis elegans*, *Drosophila melanogaster*, *Saccharomyces cerevisiae, Plasmodium falciparum*, and *Plasmodium berghei* (Figure 29).

Our analysis unveiled distinct groupings. The gene structures of CD2BP2 in *H. sapiens*, *D. rerio, S. townsendi, X. laevis*, and *T. gondii* exhibited similarity, marked by the presence of 7 exons, which shared comparable sizes. In contrast, the gene structures of *C. elegans*, *D. melanogaster, S. cerevisiae, P. falciparum,* and *P. berghei*, while resembling one another to some extent, diverged from the first group. This divergence may have arisen due to the loss of introns during the course of evolution. *C. elegans* and *D. melanogaster*, for instance, possessed 5 and 3 exons, respectively, while *S. cerevisiae*, *P. falciparum*, and *P. berghei* retained only one exon.

Furthermore, we observed a distinct pattern in exon sizes, with vertebrates displaying a progression from shorter to longer exons, with the exception of the sixth exon. Notably, the length of 157 nucleotides in the fourth exon remained conserved throughout evolution. Additionally, both *D. rerio* and *X. laevis* exhibited N-linked glycosylation sites in their third and fifth exons. Although the conservation of the number of exons, but the exon size pattern in *Toxoplasma gondii* is different, which was unexpected but could be explained by the divergent evolutionary pressures these parasites have encountered, shaping their unique genetic landscapes and strategies for survival and propagation within their respective hosts.
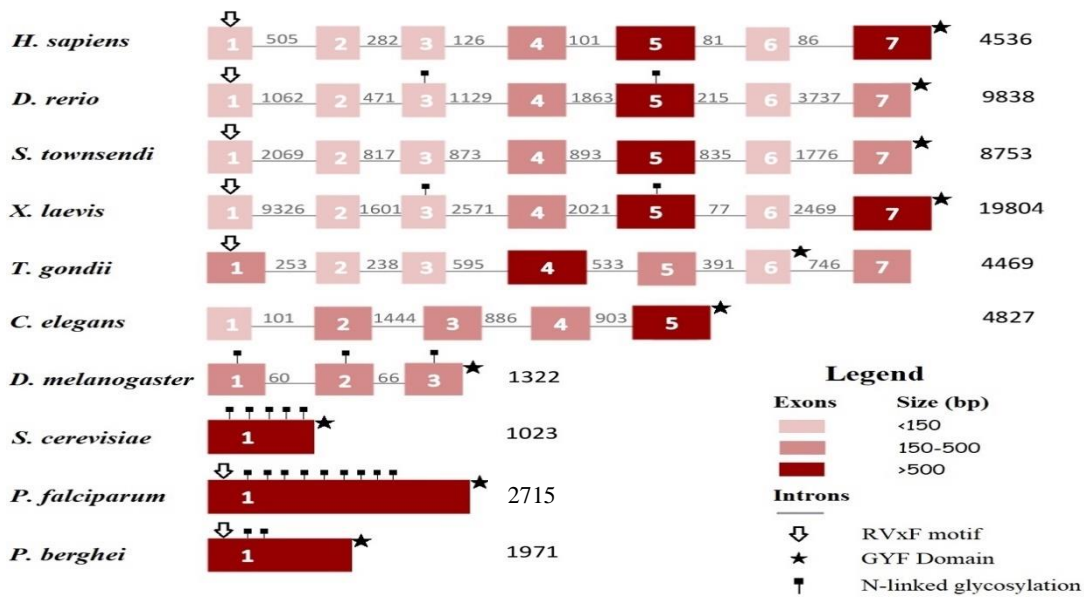
**Figure 29 Genomic organization of CD2BP2 homologs and like proteins across selected eukaryotic species.** The genomic organization of the coding regions of *Homo sapiens*, *Danio rerio, Sphaerodactylus townsendi, Xenopus laevis, Toxoplasma gondii, Caenorhabditis elegans, Drosophila melanogaster, Saccharomyces cerevisiae, Plasmodium falciparum* and *Plasmodium berghei* are shown. The sizes of introns are shown in base pairs above the lines. Black arrow and star indicate the presence of an RVxF motif and GYF like domain, respectively.

Our findings not only confirmed the similarities between these genes at the protein level but also expanded this observation to the genomic level, except for *S. cerevisiae* and *Plasmodium* genes. However, the genomic organization suggest that CD2BP2 homologs and related proteins may have clustered together during the course of evolution. This hypothesis can be further investigated through a comprehensive phylogenetic analysis.

## 4. Phylogenetic analysis of GEXP15

Next, we investigated the phylogenetic relationships among CD2BP2 homologs. To this aim, 66 CD2BP2 and CD2BP2-like proteins, as well as three *Plasmodium* GEXP15 sequences and six homologs from other Apicomplexa parasites were selected and a neighbor-joining phylogenetic tree was constructed.

The phylogenetic tree showed that the CD2BP2 amino acid sequences were grouped in two major clusters. Cluster I included sequences from both vertebrates and invertebrates and Cluster II contained sequences of Apicomplexa, Arthropods, Mollusca, Nematodes and Cnidarians (Figure 30). Within Cluster I, vertebrate CD2BP2 sequences (Cluster Ia) clustered separately

from invertebrate CD2BP2 sequences (Cluster Ib), suggesting that vertebrate and invertebrate CD2BP2 in Cluster I share a common ancestor and are orthologs. However, due to the lack of bootstrap support for Cluster I, the hypothesis of homology between vertebrate and invertebrate CD2BP2 is provisional. The extension of Arthropod CD2BP2 sequences across multiple clusters within Clusters Ib and II suggests the emergence of several CD2BP2 paralogs, probably due to gene duplications during the evolution of this lineage. The invertebrate-specific Cluster II contains the Apicomplexa CD2BP2-like sequences, which are clustered together with high bootstrap support (i.e., bootstrap 97), suggesting that they share a common ancestor. This result strongly suggests that the CD2BP2 homologs and CD2BP2-like proteins identified in Apicomplexa share a common evolutionary ancestor. However, subsequent independent evolution throughout eukaryotic organisms has resulted in divergent evolutionary paths for these proteins.
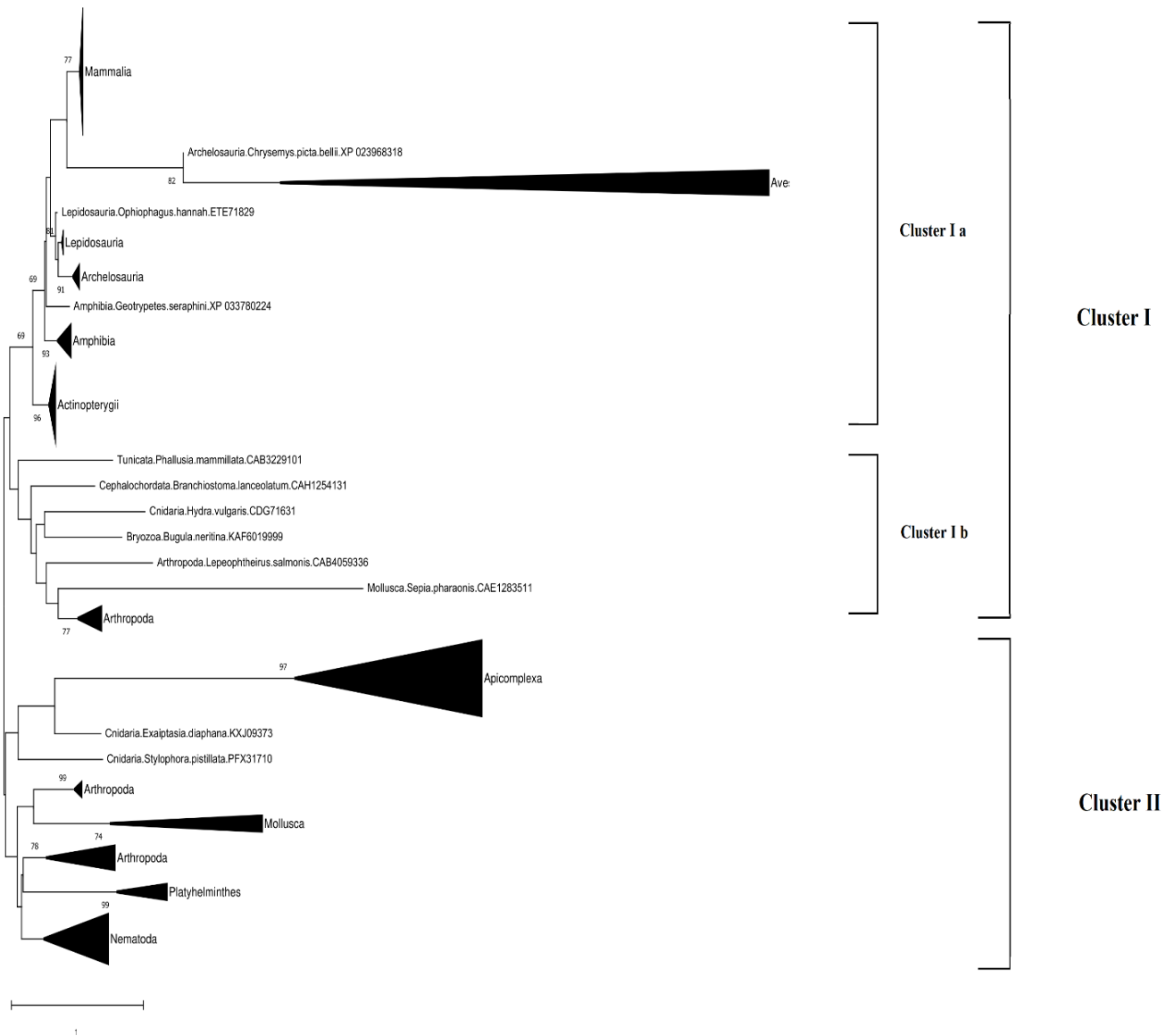
**Figure 30. Phylogenetic tree of CD2BP2 and GEXP15 proteins.** The evolutionary history was inferred using the Neighbor-Joining method (Saitou & Nei, 1987*)*.The optimal tree is shown. The percentage of replicate trees in which the associated taxa clustered together in the bootstrap test (500 replicates) are shown next to the branches (Felsenstein, 1985).The tree is drawn to scale, with branch lengths in the same units as those of the evolutionary distances used to infer the phylogenetic tree. The evolutionary distances were computed using the JTT matrix-based method (Jones et al., 1992)and are in the units of the number of amino acid substitutions per site. The rate variation among sites was modeled with a gamma distribution (shape parameter = 1). This analysis involved 66 amino acid sequences. All positions with less than 95% site coverage were eliminated, i.e., fewer than 5% alignment gaps, missing data, and ambiguous bases were allowed at any position (partial deletion option). There was a total of 213 positions in the final dataset. Evolutionary analyses were conducted in MEGA 11 (Tamura et al., 2021).

# B.    Binding and activation of PfPP1 by PfGEXP15

In a previous study conducted in the team, three clones carrying PfGEXP15 with the RVxF motif were identified through a Y2H screening, employing PfPP1c as the bait molecule (Hollin et al., 2016). In this study, the plasmid containing a fragment encompassing the initial RVxF motif of PfGEXP15 (residues 8-182) was utilized to assess and confirm its ability to bind to PP1c. It was observed that only diploid cells expressing both PfGEXP15 RVxF and PfPP1c demonstrated growth on selective media. In contrast, no yeast growth was observed when different control plasmids were employed, underscoring a specific interaction between PfGEXP15 and PfPP1c (Figure 31).
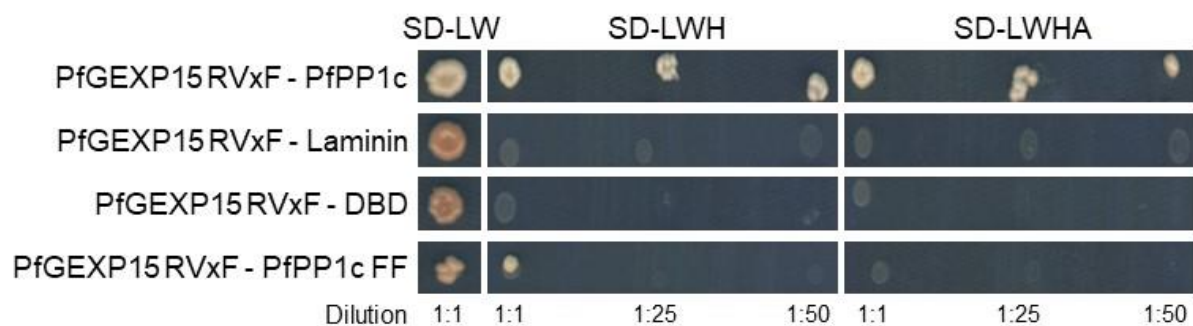


**Figure 31 Interaction of PfGEXP15 with PfPP1c and its regulatory effect on the phosphatase activity.** Yeast two-hybrid assay. pGADT7-PfGEXP15 RVxF was mated with pGBKT7-PfPP1c (lane 1), pGBKT7-Laminin (lane 2), pGBKT7-DBD (lane 3) and pGBKT7-PfPP1c F255A F256A (FF) (lane 4). Yeast diploids were plated on SD-LW, SD-LWH and SD-LWHA selective media and interactions were identified by growth of undiluted and diluted (1:25 and 1:50) cultures.

The interaction between PfGEXP15 and PfPP1c was dependent on the presence of the RVxF motif, as mutations within this binding region of PP1c (involving residues F255A and F256A) prevented yeast growth, even under stringent selection conditions.

To further support the direct nature of this interaction, a GST pull-down assay was conducted using the His-PfGEXP15 RVxF recombinant protein. Immunoblot analysis clearly demonstrated that PfGEXP15 bound to GST-PfPP1c but not to the control protein (Figure 32). Interestingly, it was noteworthy that even the dimerized form of PfGEXP15, which can occur during production and purification in E. coli, retained its ability to bind PfPP1c, likely due to the exposure of RVxF motif in this dimeric state, facilitating its binding to PP1 (Figure 32).
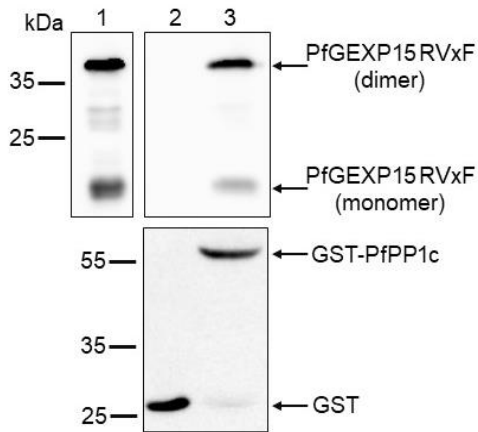
*Figure 32  I*nteraction of PfGEXP15 with PfPP1c and its regulatory effect on the phosphatase **activity**. GST Pull-down assay. Lane 1 shows the input of 6-His PfGEXP15 RVxF (500 ng) and in lanes 2 and 3 the eluted proteins (2 ug) after incubation with GST alone or GST-PfPP1c, respectively. Immunoblots are revealed with mAb anti-His (upper panel) and anti-GST (lower panel).

Two additional PfGEXP15 fragments encompassing the UD and GYF domain were generated and examined for their capacity to interact with PP1. It was determined that neither of these PfGEXP15 fragments exhibited any binding to GST-PfPP1c (Figure 33), confirming the predominant role of the RVxF motif in the interaction between PfGEXP15 and PfPP1c and consistent with previous findings involving PbGEXP15 (Hollin et al., 2019).
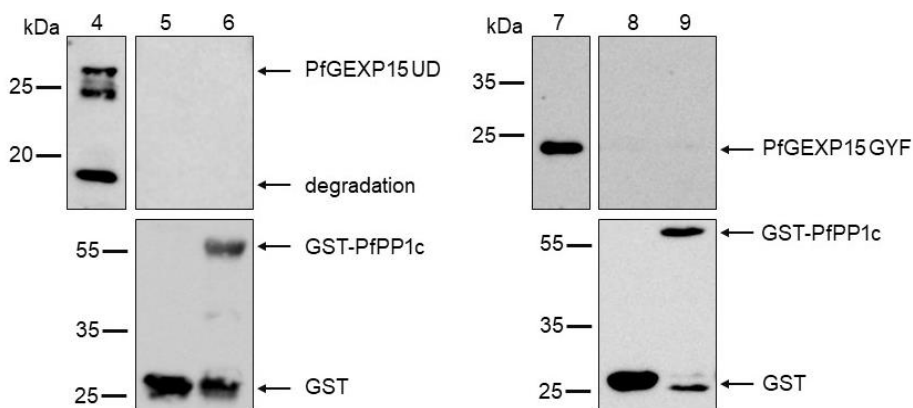


**Figure 33  Interaction of PfGEXP15 with PfPP1c and its regulatory effect on the phosphatase activity.** GST Pull-down assay.The recombinant proteins 6-His PfGEXP15 UD and 6-His PfGEXP15 GYF are loaded in the same conditions in lanes 4-5-6 and 7-8-9, respectively. Immunoblots are revealed with mAb anti-His (upper panel) and anti-GST (lower panel).

The detection of free GST is not unusual in GST pull down experiments. This can be caused by intracellular cleavage of the fusion protein or a proteolytic cleavage during protein extraction,

which can result in the binding of this free GST to beads. Furthermore, a translational pausing during protein expression in *E. coli* can be suspected as well (Tsalkova et al., 1999). However, the use of GST alone (lanes 2, Figure 32) (lane 5, Figure 33) and (lane 8, Figure 33) confirmed that this free GST cannot bind to the different recombinant proteins and the detection of these fragments was only due to GST-PP1.

We conducted further investigations to assess whether the binding of PfGEXP15 could regulate the phosphatase activity of PP1. The addition of PfGEXP15 RVxF led to a significant concentration-dependent enhancement of p-Nitrophenyl Phosphate (pNPP) dephosphorylation by PfPP1c, reaching a level similar to that observed with PbGEXP15 (Figure 34). Conversely, PfGEXP15 UD and PfGEXP15 GYF did not exhibit a dose-dependent increase in PP1c activity, with only PfGEXP15 GYF at a concentration of 200 pmol/well demonstrating aslight but significant enhancement of PP1c activity.
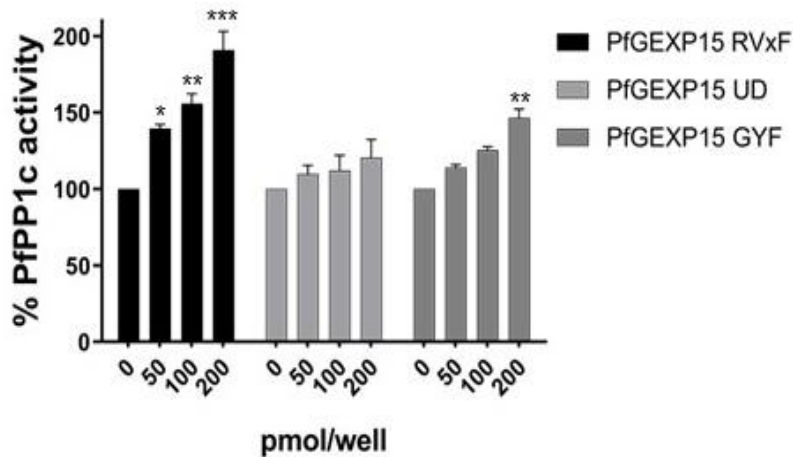


**Figure 34  Interaction of PfGEXP15 with PfPP1c and its regulatory effect on the phosphatase activity.** pNPP-phosphatase assay. The recombinant proteins 6-His PfGEXP15 RVxF, 6-His PfGEXP15 UD and 6-His PfGEXP15 GYF were incubated at different concentrations with PfPP1c for 30 min at 37˚C before the addition of para-nitrophenyl phosphate (pNPP). The linear formation of the dephosphorylated product, para-nitrophenol, was measured by optical density after 1h at 37˚C. Results are reported as mean ± SD of the percent relative activity (n=2 in duplicate). Significance was determined by Kruskal-Wallis with Dunn's post-hoc test: * $p<0.05$, ** $p<0.01$, *** $p<0.001$.

Altogether, these data showed that PfGEXP15 interacts directly and specifically with PfPP1c, mainly via its RVxF motif, and this binding enhances the phosphatase activity *in vitro*.

# C. Conditional mutants, expression and localization of PfGEXP15

## 1. Generation of inducible knock down (iKd) GEXP15 parasites utilizing the DDD system in *P. falciparum*:

Previous results by Zhang et al. using genome-wide saturation mutagenesis suggested that PfGEXP15 could play essential function(s) in asexual stages of Pf, as no viable parasites were detected (Zhang et al., 2018). To further investigate the role of PfGEXP15, we generated transgenic Pf parasites using an all-inclusive construction PfGEXP15-GFP-DDD-HA (Figure 35), based on the pGDB plasmid generated by Vasant et al. (Muralidharan et al., 2011), which is an all-inclusive system combining a DHFR Destabilization Domain, stabilized by a folate analog trimethoprim (TMP), that could allow protein level modulation. In addition, we are able to follow up the protein localization through live fluorescence microscopy and to probe for our protein in western blot as it contains GFP and HA tags. The plasmid also contains a blasticidin (BSD) resistance cassette that allows us to select for plasmid integration.
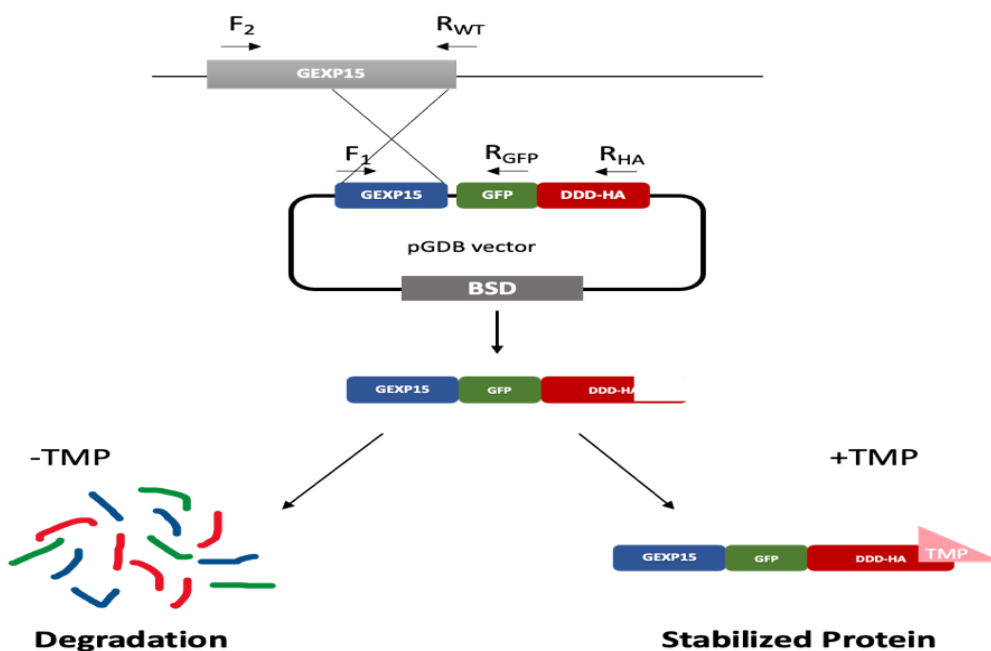


**Figure 35  Outline of the pGDB construct scheme**. The GEXP15 is tagged with DDD+GFP+HA, allowing protein knockdown, live fluorescence microscopy, and affinity purification of associated proteins.

To generate PfGEXP15 ikd parasites, PM1KO strain was used, where the Plasmepsin 1 is replaced by the human dihydrofolate reductase (hDHFR) expression cassette providing resistance to Trimethoprim (TMP). PM1KO parasites were cultured, synchronized then transfected with the pGDB-GEXP15 plasmid. Drug selection and cycling were performed using 5µM TMP (Sigma) and 2.5µg/ml Blasticidin (Sigma).

Three independent transfections were performed.

Two days following the transfection process, blasticidin was introduced into the culture. During this period, the culture appeared devoid of any visible live parasites, due to the killing effect of the BSD. After approximately three weeks, live parasites began to re-emerge, and when the parasitemia reached around 2%, we ceased the blasticidin treatment, applying a selective pressure on cells (Figure 36). Subsequently, the culture exhibited exponential growth for the following three weeks, during which we refrained from adding the drug. Following this growth phase, we reintroduced blasticidin. This enriches the culture for transfected cells and confirms successful transfection. Thus at this stage, the parasites that continued to thrive in the presence of the drug were identified as the positive clones we were seeking to select.
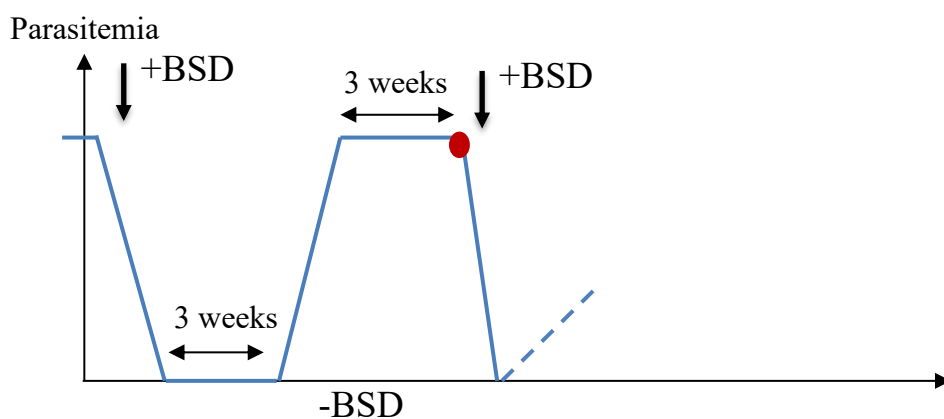


**Figure 36 A scheme representing BSD cycles after transfection**.

Correct integration of the transfected plasmid at the PfGEXP15 locus was checked by integration-specific PCR in the cloned population, using a primer at the 5' end of the GEXP15 and a reverse primer in the GFP sequence. The wild type parasites were used as a control. The positions of primers used for genotyping are indicated in Figure 37, with P1/P2 and P1/ P3 to detect the transgenic and WT genes respectively.
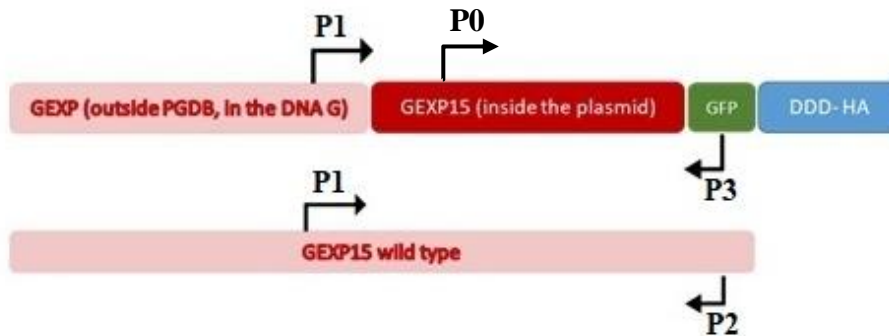
**Figure 37 Schematic representation of the pGDB construct.** The primers used to check plasmid presence and integration are represented. The GEXP15 is tagged with DDD, GFP and HA tags.

Genotyping was performed in parallel on total DNA from parental and transfected parasites extracted from late trophozoites /schizonts pellets using the KAPA Express Extract Kit (KAPA Biosystem). Analysis of the integrated gene by PCR, restriction digestion and gene sequencing has confirmed the in frame insert of our GEXP15-HA-GFP-tagged gene. The PCR was repeated every 15 days, to check the integration's stability.

As we can see in the Figure 38 below, the PCR results showed a positive signal in the PM1KO parasites with $F_{P1}R_{P2}$ (1.4kb), which was expected since the primers belong to the wild type gene; Hence, they were negative for the plasmid presence and integration. However, transgenic parasites showed 3 positive bands for the wild type gene as well as the plasmid presence and integration.

|  | PM1KO | PM1KO | PM1KO | T$_1$ | T$_1$ | T$_1$ |
|---|---|---|---|---|---|---|
|  | F$_{P1}$R$_{P2}$ | F$_{P0}$R$_{P3}$ | F$_{P1}$R$_{P3}$ | F$_{P1}$R$_{P2}$ | F$_{P0}$R$_{P3}$ | F$_{P1}$R$_{P3}$ |

| A | GEXP15 WT | Plasmid presence | Plasmid integration | GEXP15 WT | Plasmid presence | Plasmid integration |
|---|---|---|---|---|---|---|
|  | + | - | - | + | + | + |
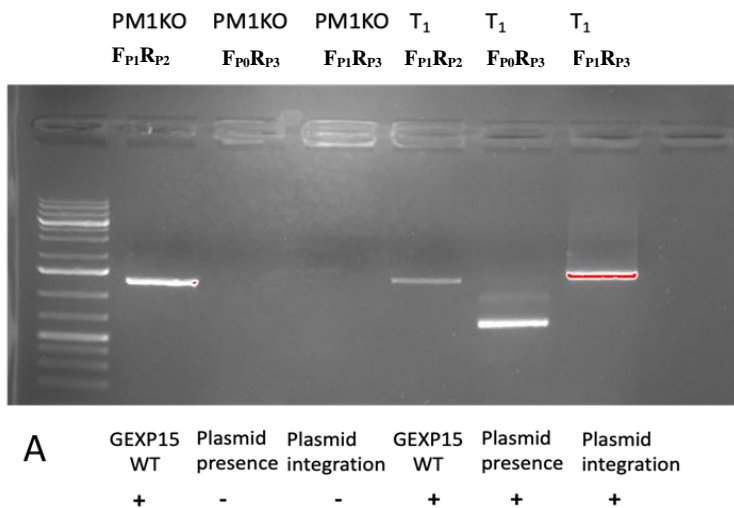
**Figure 38 Diagnostic PCR analysis of ikd GEXP15 transfected PM1KO cultures**; lanes 1 to 3 correspond to DNA extracted from wild type PM1KO parasites and lanes 4 to 6 to DNA extracted from transfected parasites. Lanes 1 and 4 represent the detection of the wild type locus; lanes 2 and 5 represent the detection of the plasmid construct; lanes 3 and 6 correspond to the integration of the plasmid. B) Lanes 1 to 2 correspond to DNA extracted from transfected parasites. Lane 1 corresponds to the transgenic parasites. Lane 2 represents the detection of the wild type locus.

The expression of PfGEXP15-GFP-DDD-HA was also explored using western blot of parasite extracts probed with anti HA antibody in order to check the expression of the fusion protein at the expected size (~135 kDa). In this context, immunoblots were carried out on total protein extracts from trophozoites and schizonts of transfected parasites, purified from infected red blood cells. In parallel, protein extracts from wild type PM1KO parasites were used as control (expected size of the WT PfGEXP15 protein is ~ 106 Kda)

A representative Western blot shown in Figure 39 reveals a band that migrates at ~ 135 kDa. The presence of two additional bands was observed after long exposure (between 135 and 180 Kda). Anti-actin antibody was used as loading control. No bands detected against PM1KO parasites, since the wild type protein (106 kDa) doesn't contain any HA tag.
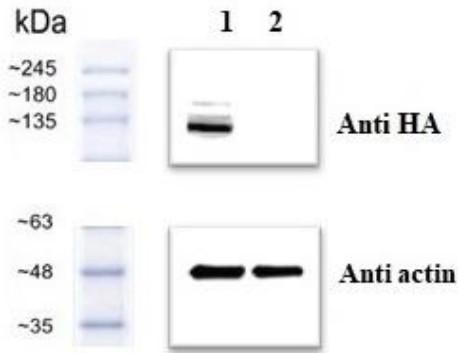
**Figure 39 Western Blot analysis representing the soluble protein extract from transgenic PfGEXP15** in lane 1 and WT parasites as negative control in lane 2. They were revealed with mAb anti-HA rabbit. In the lower panel, anti-actin was used as a positive loading control. 40 million parasites were used.

The presence of these double bands could potentially be attributed to various factors such as protein degradation during the extraction and preparation processes, potential processing within the parasite leading to the loss of its N-terminal region (since the detected HA tag is located in the C-terminal portion of the protein), or the occurrence of post-translational modifications.

Next, we took advantage of the generated transgenic clones to detect the expression of PfGEXP15 during the asexual cycle. First, we confirmed the correct integration of the transfected plasmid at the PfGEXP15 locus by performing integration-specific PCR on the cloned population (Figure 40).
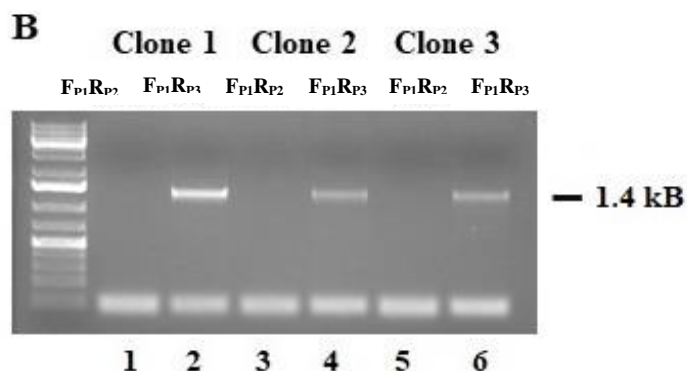


**Figure 40 Diagnostic PCR analysis of tagged GEXP15 clones**. Lanes 1-6 correspond to gDNA extracted from transfected parasites. Lanes 1, 3 and 5 represent the detection of the wild-type (WT) locus; lanes 2, 4 and 6 correspond to the integration of the construct.

Then, western blot analysis revealed PfGEXP15 expression mainly in the trophozoite and schizont stages (Figure 41), with the highest expression in the latter. This observation is in agreement with RNA-seq analysis, showing a peak transcript expression in late trophozoites and early schizonts (Toenhake et al., 2018).
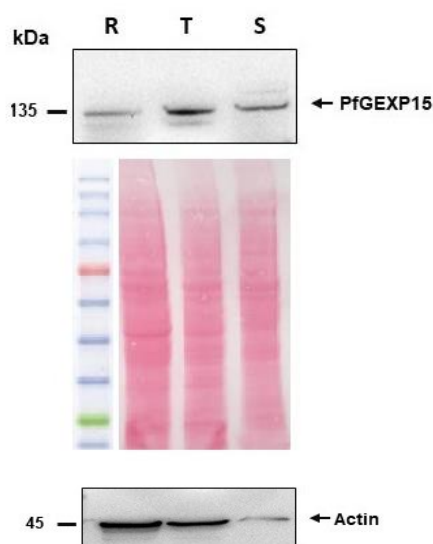


**Figure 41 Western Blot analysis representing the soluble protein extract from transgenic iKd PfGEXP15 of ring (R), trophozoite (T) and schizont (S) stages**. In the lower panel, total protein detected by Ponceau Red staining and anti-actin were used as a positive loading control.

As the pGDB-PfGEXP15 constructs contains the GFP at its Ct side, it is expected that the correct recombination should lead to GFP+ parasites. Hence, the presence of GFP-tagged PfGEXP15 was examined using live fluorescence microscopy (Bicel platform, Lille) in the presence of TMP required for protein stabilization.

Results depicted in Figure 42 showed that PfGEXP15 was mainly localized in the nucleus of late trophozoite and schizont stages, with foci overlapping DNA staining. This is supported by proteomic studies indicating the detection of PfGEXP15 in nuclear extracts of schizonts (Oehring et al., 2012). In the case of Pb, however, GEXP15 was clearly detected also in the parasite cytosol (Hollin et al., 2019), suggesting species-specific function(s) of GEXP15.

The examination of ring stages did not show detectable signal or it was at the limit of detection. This, once again, proves that GEXP15 protein is highly expressed later in the intraerythrocytic lifecycle. It could be assumed that the function(s) of GEXP15 should take place mainly during the growth/development of late parasite stages.
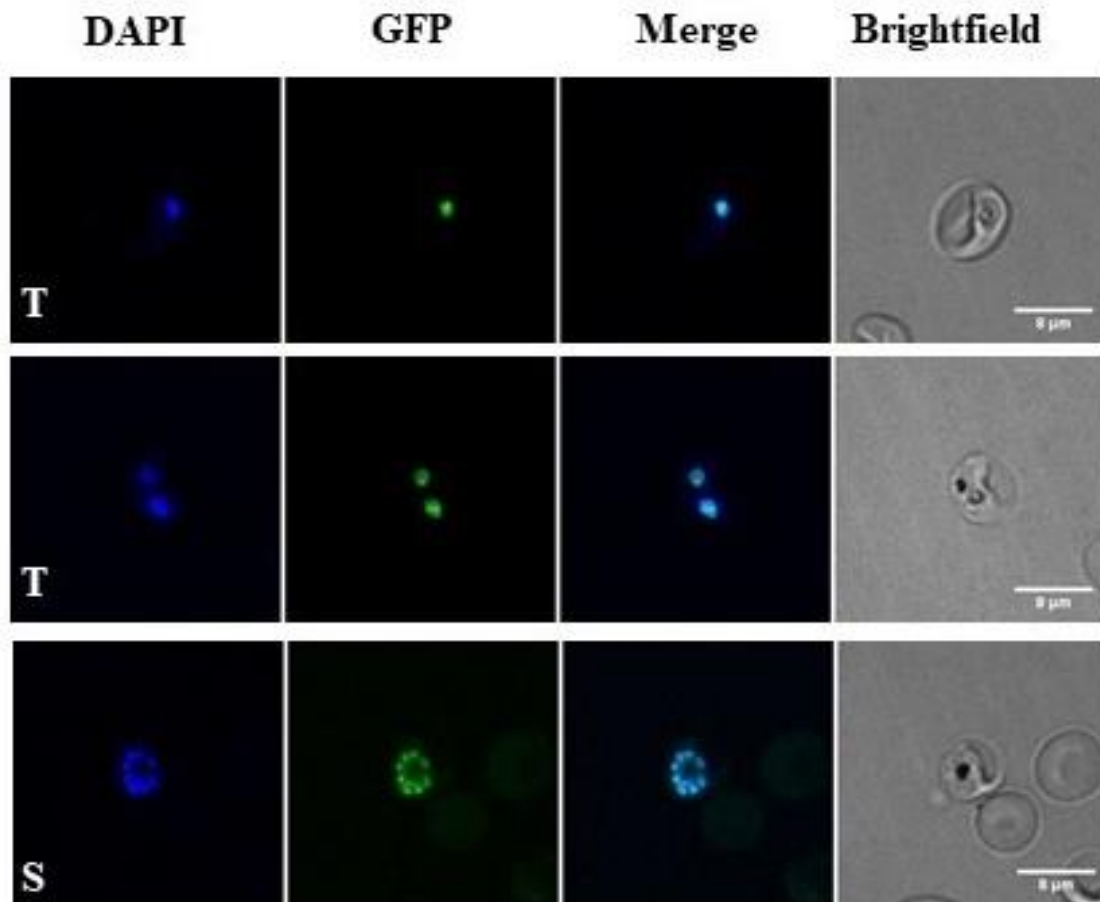
**Figure 42 Localization of PfGEXP15-GFP-DDD-HA**. Confocal laser scanning microscopy showing GFP expressing parasites in transfected cultures. Parasite's nuclei were stained with DAPI and transgenic parasites are expressing PfGEXP15-GFP-DDD-HA. Merged images showed protein colocalization.

## 2. Effect of TMP on PfGEXP15 parasite growth and PfGEXP15 protein stabilization.

The essentiality of GEXP15 in the blood stages was suggested by a previous study using a piggyBac transposon inserted randomly in *P. falciparum* genome (Zhang, 2018) in which they did not obtain viable parasites with a disrupted PfGEXP15 gene despite the presence of 35 potential insertion sites.

From the resistant mutants we generated, it is anticipated that the presence of TMP (5µM) stabilizes the PfGEXP15-GFP-DDD-HA protein by blocking its degradation. PfGEXP15-GFP-

DDD-HA clones were cultured in the absence of TMP and parasitemia levels were followed using stained thin blood smears. In this experiment, the initial parasitemia at day 0 was 0.5 or 1% and their growth was monitored over several days.

Evaluation of parasite growth over several days with at least three replication cycles shows, unexpectedly, that after TMP removal PfGEXP15 protein remains stable over time with no effect on parasite growth (Figure 43).

Further, no difference in the growth characteristics of the parasites in the presence and absence of TMP as all intraerythrocytic blood stage parasites (rings, trophozoites and schizonts) are still detectable throughout the different time points.
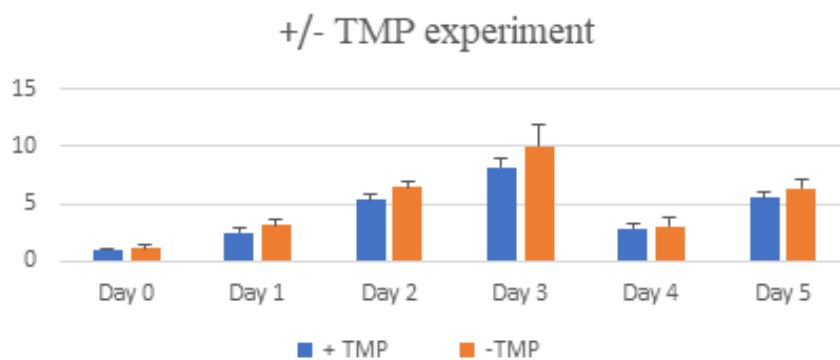


**Figure 43 Parasitemia of iKd PfGEXP15 line was measured with and without TMP cultures**. The results are shown as the mean parasitemia ± SD. (n=4).

The lack of any growth defect of parasites in the absence of TMP (delay or parasite death) led us to check the presence of protein levels by live fluorescence microscopy. As shown in Figure 44, at day12 after removal of TMP we did not observe significant degradation of the PfGEXP15-GFP-DDD-HA protein with no influence on PfGEXP15 localization.
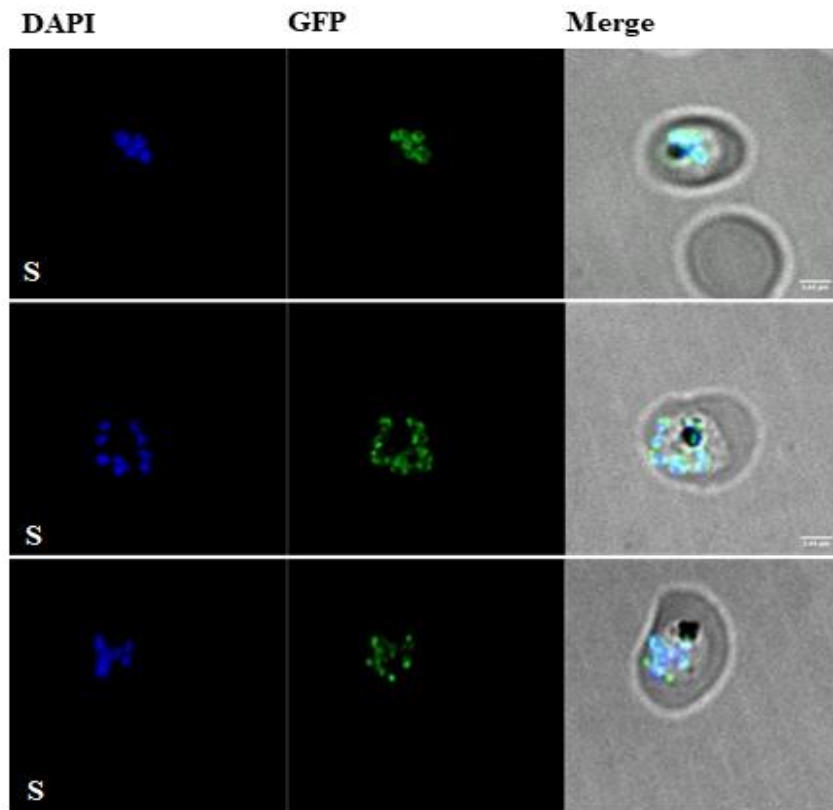
**Figure 44 . Confocal laser scanning microscopy showing GFP expressing parasites in transfected cultures without TMP.** Parasite's nuclei were stained with DAPI and transgenic parasites are expressing PfGEXP15-GFP-DDD-HA. Merged images showed the protein colocalization.

Western blot examination of parasite lysates confirmed that PfGEXP15 protein levels remained stable over time (Figure 45).

**Figure 45 Western Blot analysis representing the total protein extract from transgenic iKd PfGEXP15 with TMP in lane 1 and without TMP in lane 2**. They were revealed with mAb anti-HA. In the lower panel, anti-actin was used as a positive loading control. 40 million parasites were used in each lane.

The persistence of PfGEXP15, regardless of the presence of TMP, indicates that this method is not suitable for its degradation and these unexpected data are in line with previous studies of protein chaperones (Cobb et al., 2017).

To rule out any potential technical concerns, Dr. Muralidharan provided us with control strains, specifically the RPN6 strain for the DDD system. The outcome of the same experiment using rpn6Δ parasites generated with the same construct (Muralidharan, 2011) involving the removal of TMP, as depicted in Figure 46, clearly indicate that this system functions effectively with another gene, thereby confirming that the issue does not stem from a technical problem and supporting the validity of our methodology. Notably, after just two cycles, the parasitemia in the -TMP condition was almost negligible.
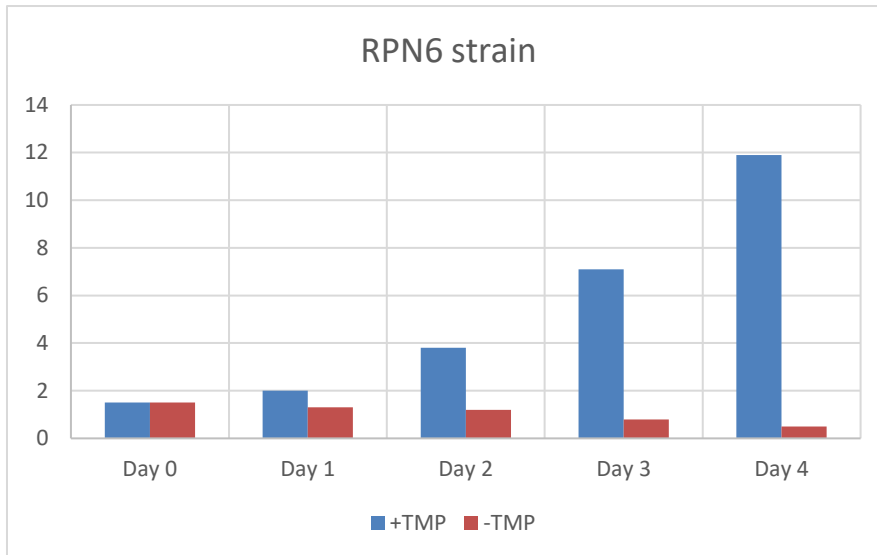
**Figure 46 Parasitemia of rpn6Δ line was measured with and without TMP cultures.** The results are shown as the mean parasitemia ± SD. (n=3).

# D. Identification of PfGEXP15 interacting proteins.

In order to gain deeper insights into the biological roles of GEXP15 in the asexual stages of Pf, it was imperative to enhance our comprehension of PfGEXP15 complexes. To explore the potential interactome of GEXP15, we performed an immunoprecipitation (IP) of PfGEXP15-HA-GFP using anti-GFP nanobodies. This was carried out after extracting sufficient quantities of soluble proteins from late trophozoite and schizont stages of *P. falciparum* tagged lines, as well as from the parental strain, serving as a control. Subsequently, the immunoprecipitated proteins were subjected to mass spectrometry analysis (IP/MS). The IP/MS analysis, conducted on three independent biological replicates, resulted in the identification of 1200 Pf proteins that were recovered from the beads (Supplementary Table 1). To refine the results, we ensured that proteins were identified in a minimum of two out of three biological replicates, while also considering a significance threshold ($p < 0.05$) and the difference (log 2 FC) compared to the control parental strain. In total, 16 proteins were recognized, with the majority being associated with either the ribosomal complex (7 proteins) or RNA binding (3 proteins) (Figure 47). Subsequent STRING analysis of this interactome confirmed the enrichment of processes related to ribosome biogenesis and translation (Figure 47).

It is noteworthy that, using this method, PfPP1 did not meet the predefined cutoff criteria (Figure 47). This observation may be attributed to the potential instability of the PfGEXP15-

PP1 complex at the selected time point and/or the relatively weak or transient nature of their association. In this approach, we prioritized the detection of the most abundant and stable protein complexes.
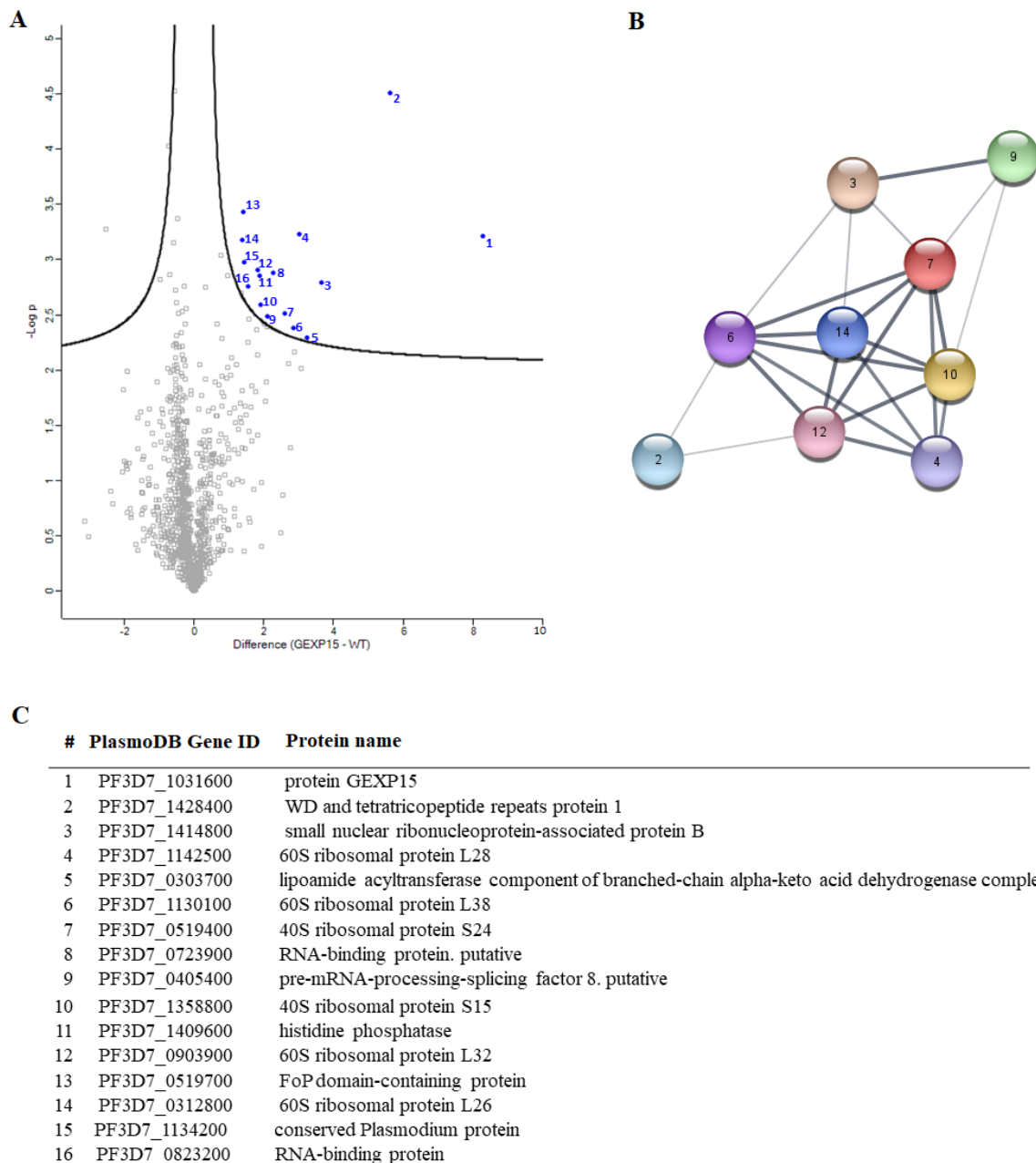


**Figure 47 PfGEXP15 interactome analysis**. (A) Volcano plot representation of PfGEXP15 immunoprecipitation. (B) STRING network visualization of PfGEXP15-interacting proteins using Cytoscape software. (C) List of PfGEXP15 interacting partners. Proteins were ranked according to their student's t-test difference PfGEXP15–WT in the schizont stage.

In contrast, in *P. berghei,* PbGEXP15 emerged as one of the top 10 PP1-interacting proteins during both schizont and gametocyte stages (De Witte et al., 2022). Furthermore, the reciprocal immunoprecipitation/mass spectrometry (IP/MS) approach conducted by Hollin et al (Hollin,

2019) identified PbPP1 following PbGEXP15 immunoprecipitation. These findings strongly support the likelihood of this interaction between GEXP15 and PP1.

Following this, we aimed to employ an additional approach to investigate deeper into the protein profile and determine the precise regions of GEXP15 involved in these interactions. To accomplish this, pulldown experiments were conducted using recombinant proteins encompassing distinct protein domains. His-tagged proteins incorporating: 1) the RVxF motif, 2) the unknown conserved domain (UD), and 3) the GYF domain were synthesized and linked to nickel agarose beads (Figure 48). As a negative control, a tetR bacterial protein was employed.
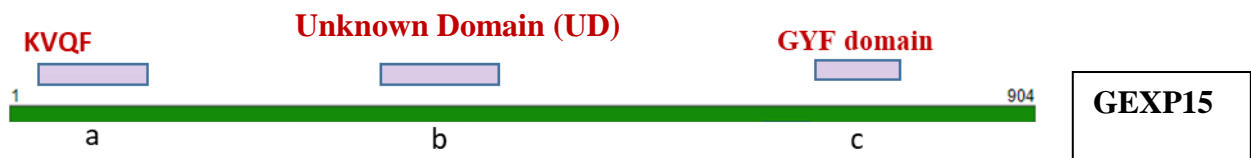


**Figure 48 Outline representing the different binding motifs/domains of GEXP15**

For the pulldown experiments, soluble proteins were extracted as described in materials and methods from three independent biological replicates and incubated with the different recombinant proteins bound to beads. Prior to pull-down experiments, the presence of the tagged fragments adsorbed to the beads was checked by immunoblot (Figure 49).
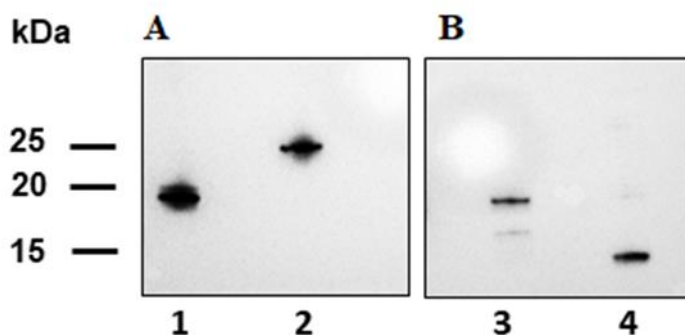


**Figure 49 Western blot analysis representing A)** the RVxF motif (lane 1), the tetR protein (lane 2) **B)** the UD (lane 1) and the GYF domain (lane 2), recombinant proteins eluted from nickel beads and detected using anti-His antibodies. The figure was set up from the same western blot at different exposures.

The eluted proteins were subjected to direct MS analysis to determine the partners associated with GEXP15. A total of 312 interacting proteins were identified through the various domains (Supplementary Table 2). PF3D7_1444100 was consistently detected across all GEXP15

domains and thus excluded from the analysis, along with PF3D7_1206200, which was common between the RVxF and GYF fragments. Principal component analysis (PCA) of the different protein domains displayed distinct clusters, particularly evident in the GYF pull-down, suggesting it harbors a highly specific and distinct group of interactants differing from those associated with RVxF and UD (Figure 50).
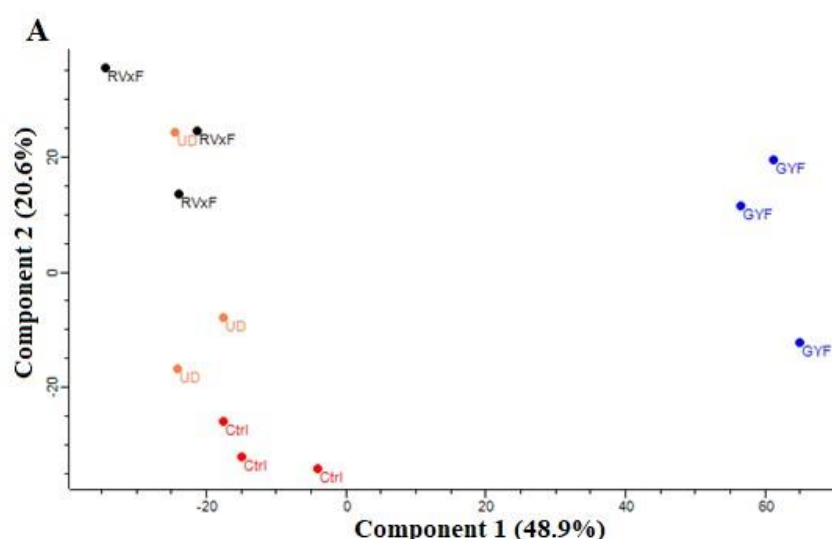


**Figure 50 PCA analysis of the outcome of the pull-downs of PfGEXP15** RVxF (black), UD (orange) and GYF (blue) in three different replicates. The control samples (Ctrl) are indicated in red.

Following the filtration of proteins based on their p-value ($p<0.05$) and difference (log 2 FC), it was determined that RVxF, UD, and GYF-containing proteins were significantly enriched with 9, 2, and 80 proteins, respectively. As expected, PP1 was identified as the primary interactor of the RVxF-containing protein, validating the reliability of this approach (Figure 51). Although STRING analysis of the other 8 potential partners did not reveal any significant enrichment, they were found to be associated with DNA/RNA/ATP binding and translation initiation activity (Table 11, Figure 51).

**Table 11  Identified proteins after RVxF containing protein pulldown in *P. falciparum* extracts.** The table shows the protein name and accession number of the specific proteins pulled down with RVxF containing frangment in at least two experiments with peptides ≥ 2 and with peptides and spectra ≥ 2 fold compared with the control strain.

| NAME | ACCESSION NUMBER |
|---|---|
| **GEXP15** | PF3D7_1031600 |
| **60S RIBOSOMAL PROTEIN L39** | PF3D7_0611700 |
| **PF3D7_1313100** | PF3D7_1313100 |

| | |
|---|---|
| **PSEUDOURIDYLATE SYNTHASE** | PF3D7_0914000 |
| **ABC TRANSPORTER I FAMILY MEMBER 1** | PF3D7_0319700 |
| **DYNEIN HEAVY CHAIN** | PF3D7_0729900 |
| **EUKARYOTIC TRANSLATION INITIATION FACTOR 3 SUBUNIT C** | PF3D7_1206200 |
| **PP1** | PF3D7_1414400 |
| **26S PROTEASOME REGULATORY SUBUNIT RPN3** | PF3D7_1338100 |
| **PEPTIDASE FAMILY C50** | PF3D7_0809600 |
| **PF3D7_0716300** | PF3D7_0716300 |
| **PF3D7_1444100** | PF3D7_1444100 |
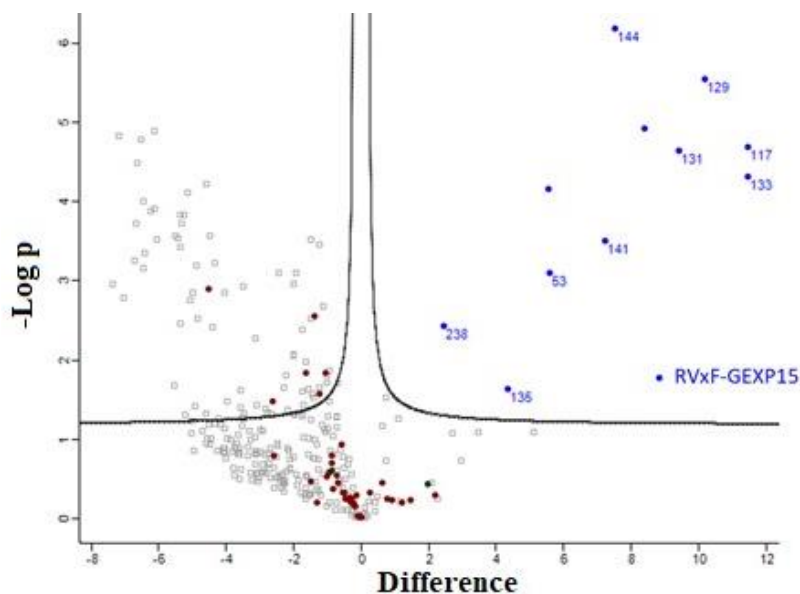


**Figure 51  Volcano plot representation of the outcome of the RVxF pulldown**. The proteins significantly co-purified are indicated in blue. Purple and green dots represent proteins detected with GYF and UD pulldowns. Gray dots represent proteins detected with no statistical significance.

Subsequently, the pulldown experiment targeting the UD revealed only 2 distinct proteins (Table 12, Figure 52). One of them, the erythrocyte membrane-associated antigen, is membrane-associated and was excluded from further analysis, as GEXP15 is a nuclear protein. Thus, exportin-7 emerged as the sole specific protein associated with the UD-containing protein. This protein is conserved across eukaryotes and is involved in facilitating the export of proteins from the nucleus to the cytoplasm. While a similar function may exist in *Plasmodium* for the transport of GEXP15, additional investigations are required to confirm this hypothesis.

**Table 12 Identified proteins after UD containing protein pulldown in *P. falciparum* extracts.** The table shows the protein name and accession number of the specific proteins pulled down with UD containing fragment in at least two experiments with peptides ≥ 2 and with peptides and spectra ≥ 2 fold compared with the control strain.

| NAME | ACCESSION NUMBER |
|---|---|
| **EXPORTIN-7** | PF3D7_0910100 |
| **PF3D7_1444100** | PF3D7_1444100 |
| **ERYTHROCYTE MEMBRANE-ASSOCIATED ANTIGEN** | PF3D7_0703500 |
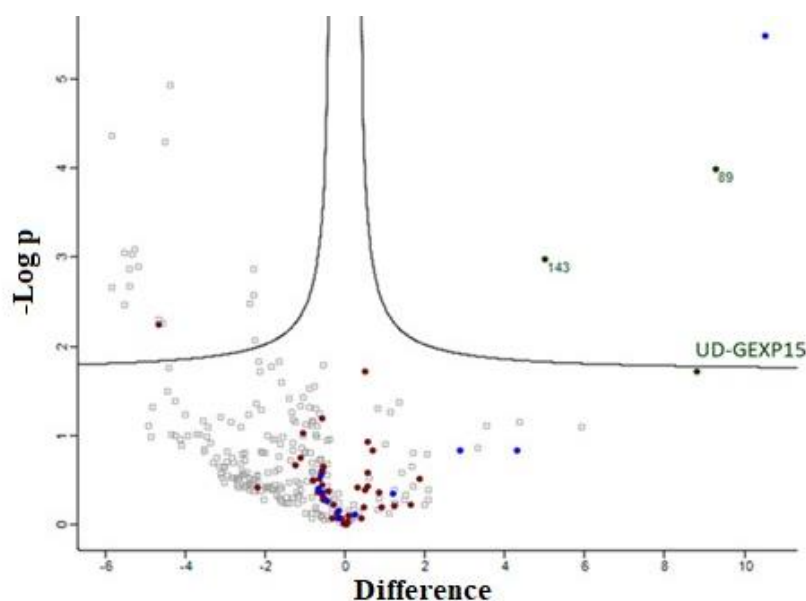


**Figure 52 Volcano plot representation of the outcome of the UD pulldown.** The proteins significantly co-purified are indicated in green. Purple and blue dots represent proteins detected with GYF and RVxF pulldowns. Gray dots represent proteins detected with no statistical significance.

For the GYF domain, 36% of the significant proteins (29/80) were found to be ribosomal subunits or ribosome-associated proteins, suggesting that this domain co-precipitated large part of the 60S and 40S ribosomal complexes (Table13, Figure 53).

**Table 13 Identified proteins after GYF containing protein pulldown in *P. falciparum* extracts.**The table shows the protein name and accession number of the specific proteins pulled down with GYF containing frangment in at least two experiments with peptides ≥ 2 and with peptides and spectra ≥ 2 fold compared with the control strain.

| NAME | ACCESSION NUMBER |
|---|---|
| **PF3D7_1308700** | PF3D7_1308700 |
| **EARLY TRANSCRIBED MEMBRANE PROTEIN 2** | PF3D7_0202500 |
| **DYNAMIN-LIKE PROTEIN** | PF3D7_1218500 |

| | |
|---|---|
| **60S RIBOSOMAL PROTEIN L34** | PF3D7_0710600 |
| **PF3D7_1319900** | PF3D7_1319900 |
| **MEMBRANE ASSOCIATED HISTIDINE-RICH PROTEIN 1** | PF3D7_1370300 |
| **60S RIBOSOMAL PROTEIN L13** | PF3D7_1004000 |
| **RECEPTOR FOR ACTIVATED C KINASE** | PF3D7_0826700 |
| **GEXP15** | PF3D7_1031600 |
| **60S RIBOSOMAL PROTEIN L37AE** | PF3D7_0210100 |
| **60S RIBOSOMAL PROTEIN L30E** | PF3D7_1019400 |
| **60S RIBOSOMAL PROTEIN L37** | PF3D7_0706400 |
| **60S RIBOSOMAL PROTEIN L31** | PF3D7_0503800 |
| **DNA-DIRECTED RNA POLYMERASE II SUBUNIT RPB2** | PF3D7_0215700 |
| **EARLY TRANSCRIBED MEMBRANE PROTEIN 14.1** | PF3D7_1401400 |
| **60S RIBOSOMAL PROTEIN L14** | PF3D7_1431700 |
| **60S RIBOSOMAL PROTEIN L10** | PF3D7_1414300 |
| **60S RIBOSOMAL PROTEIN L15** | PF3D7_0415900 |
| **40S RIBOSOMAL PROTEIN S9** | PF3D7_0520000 |
| **60S RIBOSOMAL PROTEIN L26** | PF3D7_0312800 |
| **40S RIBOSOMAL PROTEIN S8E** | PF3D7_1408600 |
| **EUKARYOTIC TRANSLATION INITIATION FACTOR 3 SUBUNIT A** | PF3D7_1212700 |
| **60S RIBOSOMAL PROTEIN L27A** | PF3D7_0618300 |
| **PLASMODIUM EXPORTED PROTEIN** | PF3D7_1353100 |
| **PROTEIN TRANSPORT PROTEIN SEC61 SUBUNIT ALPHA** | PF3D7_1346100 |
| **60S RIBOSOMAL PROTEIN L4** | PF3D7_0507100 |
| **UBIQUITIN SPECIFIC PROTEASE** | PF3D7_0904600 |
| **40S RIBOSOMAL PROTEIN S16** | PF3D7_0813900 |
| **RNA-BINDING PROTEIN** | PF3D7_1330800 |
| **CHLOROQUINE RESISTANCE TRANSPORTER** | PF3D7_0709000 |
| **MEMBRANE ASSOCIATED HISTIDINE-RICH PROTEIN 2** | PF3D7_1353200 |
| **CALCIUM-TRANSPORTING ATPASE** | PF3D7_0106300 |
| **60S RIBOSOMAL PROTEIN L2** | PF3D7_0516900 |
| **40S RIBOSOMAL PROTEIN S23** | PF3D7_0306900 |
| **NUCLEOLAR PROTEIN 56** | PF3D7_1118500 |
| **60S RIBOSOMAL PROTEIN L24** | PF3D7_1309100 |
| **RAS-RELATED PROTEIN RAB-1B** | PF3D7_0512600 |
| **METHIONINE-TRNA LIGASE** | PF3D7_1034900 |
| **60S RIBOSOMAL PROTEIN L3** | PF3D7_1027800 |
| **PF3D7_1237700** | PF3D7_1237700 |
| **PF3D7_1447700** | PF3D7_1447700 |
| **PF3D7_0305300** | PF3D7_0305300 |
| **KNOB-ASSOCIATED HISTIDINE-RICH PROTEIN** | PF3D7_0202000 |
| **GLUTAMATE-TRNA LIGASE** | PF3D7_1349200 |
| **TUDOR STAPHYLOCOCCAL NUCLEASE** | PF3D7_1136300 |
| **AUTOPHAGY-RELATED PROTEIN 18** | PF3D7_1012900 |
| **60S RIBOSOMAL PROTEIN L21** | PF3D7_1426000 |

| | |
|---|---|
| **60S RIBOSOMAL PROTEIN L44** | PF3D7_0304400 |
| **40S RIBOSOMAL PROTEIN S15** | PF3D7_1358800 |
| **RIBONUCLEOSIDE-DIPHOSPHATE REDUCTASE SMALL CHAIN** | PF3D7_1405600 |
| **SUCCINATE-COA LIGASE [ADP-FORMING] SUBUNIT ALPHA** | PF3D7_1108500 |
| **RHOPTRY NECK PROTEIN 2** | PF3D7_1452000 |
| **V-TYPE H(+)-TRANSLOCATING PYROPHOSPHATASE** | PF3D7_1456800 |
| **PLASMODIUM EXPORTED PROTEIN** | PF3D7_0702500 |
| **RAS-RELATED PROTEIN RAB-2** | PF3D7_1231100 |
| **DNAJ PROTEIN** | PF3D7_0823800 |
| **AMINO ACID TRANSPORTER AAT1** | PF3D7_0629500 |
| **HIGH MOBILITY GROUP PROTEIN B2** | PF3D7_0817900 |
| **RNA-BINDING PROTEIN** | PF3D7_1110400 |
| **SPERMIDINE SYNTHASE** | PF3D7_1129000 |
| **MSP7-LIKE PROTEIN** | PF3D7_1334500 |
| **HIGH MOLECULAR WEIGHT RHOPTRY PROTEIN 2** | PF3D7_0929400 |
| **60S RIBOSOMAL PROTEIN L32** | PF3D7_0903900 |
| **L-LACTATE DEHYDROGENASE** | PF3D7_1324900 |
| **60S RIBOSOMAL PROTEIN L5** | PF3D7_1424100 |
| **HEAT SHOCK PROTEIN 101** | PF3D7_1116800 |
| **40S RIBOSOMAL PROTEIN S25** | PF3D7_1421200 |
| **40S RIBOSOMAL PROTEIN S3** | PF3D7_1465900 |
| **PF3D7_1306200** | PF3D7_1306200 |
| **TRANSLOCATION PROTEIN SEC63** | PF3D7_1318800 |
| **DYNEIN LIGHT CHAIN 1** | PF3D7_1213600 |
| **PHOSPHOENOLPYRUVATE CARBOXYKINASE** | PF3D7_1342800 |
| **HISTONE H2B** | PF3D7_1105100 |
| **ACYL-COA SYNTHETASE** | PF3D7_0731600 |
| **PF3D7_1444100** | PF3D7_1444100 |
| **PF3D7_1036900** | PF3D7_1036900 |
| **HISTONE H2A** | PF3D7_0617800 |
| **UBIQUITIN-60S RIBOSOMAL PROTEIN L40** | PF3D7_1365900 |
| **ENDOPLASMIN** | PF3D7_1222300 |
| **ALPHA TUBULIN 1** | PF3D7_0903700 |
| **ELONGATION FACTOR 2** | PF3D7_1451100 |
| **MULTIDRUG RESISTANCE PROTEIN 1** | PF3D7_0523000 |
| **EUKARYOTIC TRANSLATION INITIATION FACTOR 3 SUBUNIT C** | PF3D7_1206200 |
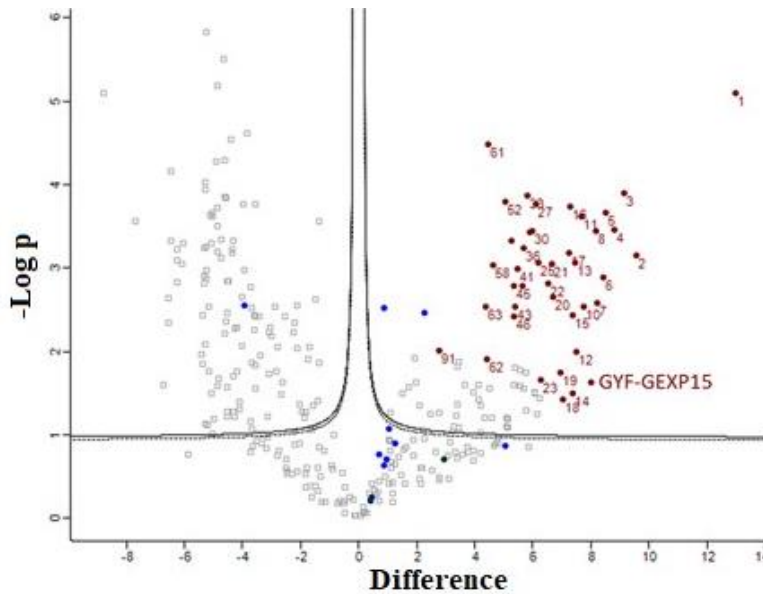
**Figure 53 Volcano plot representation of the outcome of the GYF pulldown**. The proteins significantly co-purified are indicated in purple. Blue and green dots represent proteins detected with RVxF and UD pulldowns. Gray dots represent proteins detected with no statistical significance.

STRING analysis confirmed this observation with the enrichment of structural constituents of ribosomes (FDR= $1.73e^{-17}$) as well as rRNA binding. 19 biological processes were also enriched, including translation (FDR= $1.33e^{-13}$) and biosynthetic processes (Figure 54).
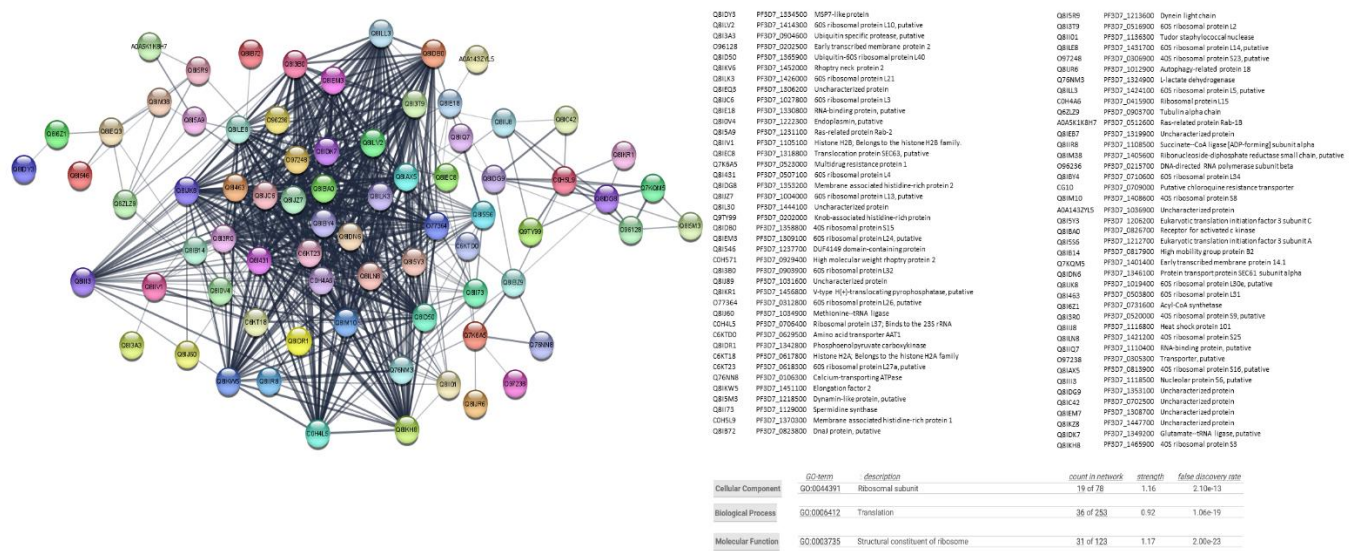


**Figure 54 GYF-domain containing protein pulldown analysis. A.** STRING network visualization of GYF-interacting proteins using Cytoscape software **B.** List of GYF interacting partners, as well as the processes they may be involved.

140

By comparing the results of the two approaches, three common proteins were shared between the GYF pulldown and the global PfGEXP15 IP: the 60S ribosomal proteins L26, L32 and the 40S ribosomal protein S15. However, other partners can be taken into account since they share similar functions such as small ribonucleoproteins and RNA-binding proteins. These data revealed that the most dominant network involving GEXP15 corresponds to the 40S and 60S ribosomal proteins. These two approaches suggest that RVxF is mainly involved in PP1 interaction and the GYF motif plays a role in the recognition of ribosomal machinery, unlike UD, which does not appear to be a protein-protein interactions.

# Discussion
# &
# Perspectives

# IV. Discussion & Perspectives

Based on the previous data obtained during the establishment of the interactome of PfPP1c (Hollin et al., 2016), Gametocyte Exported Protein 15 (GEXP15) was classified among the top candidate partners of the phosphatase. Therefore, characterizing this protein was the main objective of this thesis.

GEXP15 in *Plasmodium*, exhibits remarkable structural and functional resemblances to CD2 Binding Protein 2 (CD2BP2) in humans, despite variations in their overall protein sequences and lengths. These similarities are particularly evident when examining their respective structural characteristics, which will be discussed in detail later. Although GEXP15 and CD2BP2 may serve distinct roles in their respective organisms, they both play roles in cellular regulation, potentially influencing crucial processes such as mitosis, meiosis, and protein dephosphorylation (Ceulemans & Bollen, 2004; Hollin et al., 2016; Kofler et al., 2005).

The protein CD2 Binding Protein 2 (CD2BP2) was originally characterized as an interacting partner of two conserved proline-rich motifs within the cytoplasmic domain of the T cell adhesion molecule CD2 (Nishizawa et al., 1998). While there has been some debate regarding its potential scaffolding role at the T cell membrane (Freund et al., 2002; Heinze et al., 2007), a more comprehensive understanding of CD2BP2's function has emerged. Specifically, it was observed that its GYF domain (comprising amino acids 280 to 341) primarily localizes to the spliceosome. In various cell lines, CD2BP2 predominantly resides within the cell nucleus. Further investigation, under more physiologically relevant conditions, revealed that the aromatic 'ratchet' region of the GYF fold interacts with proline-rich sequence (PRS) hubs present in multiple small nuclear ribonucleoprotein (snRNP) particles and associated molecules. Additionally, the highly charged 'back-side' of the GYF domain facilitates a specific interaction with U5-15K in the U5 snRNP. In vitro experiments demonstrated that the isolated GYF domain can inhibit splicing, with assembly being interrupted at the early spliceosome stage. Notably, the N-terminal portion of CD2BP2 interacts with the U5 snRNP protein Prp6, supporting the notion that CD2BP2 plays a role in U5 snRNP formation or disassembly (Laggerbauer et al., 2005). Recent studies have also detected CD2BP2 in the tri-snRNP and the precatalytic B complex, although it appears to dissociate upon B complex activation and complex C formation (Schmidt et al., 2014).

The importance of CD2BP2 extends to embryonic development, as its absence results in growth delay, vascularization defects, and premature death at embryonic day 10.5 (Albert et al., 2015). Further studies involving bone marrow-derived macrophages have indicated that CD2BP2 plays a role in the alternative splicing of mRNA transcripts from diverse sources (Albert et al., 2015). At the molecular level, it has been revealed that the phosphatase PP1 is recruited to the spliceosome through the N-terminus of CD2BP2 (Albert et al., 2015).

The discovery of these structural and functional resemblances between GEXP15 and CD2BP2 opens up captivating possibilities for understanding the regulatory mechanisms involving Protein Phosphatase 1 (PP1) in both *Plasmodium* and humans.

In this work, we provided a better understanding of the structure and evolution of GEXP15 and its homologs in various organisms. A closer examination of these proteins highlighted three regions of particular interest. First, an RVxF motif was detected by manual inspection in the N-terminal region of PfGEXP15, PbGEXP15, TgCD2BP2, and HsCD2BP2. Using the FIMO tool, we confirmed the presence of this motif in various phyla including Apicomplexa, Metazoa, and Nematoda. This motif is known to be implicated in PP1 interaction in eukaryotes and our previous work conducted in *Plasmodium* had already established the capacity of PbGEXP15 as well as other regulators to modulate the activity of PP1 (Fréville et al., 2014; Hollin et al., 2019). In this previous study, using Yeast Two-Hybrid (Y2H) screening with PfPP1c (*Plasmodium falciparum* PP1 catalytic subunit) as bait, PbGEXP15 was identified as a candidate binding partner (Hollin et al., 2016). Importantly, the study also demonstrated that the RVxF motif within PbGEXP15 played a pivotal role in mediating this interaction. The addition of PbGEXP15 to PP1 increased its dephosphorylation activity in a concentration-dependent manner, indicating that PbGEXP15 acts as a regulator of PP1 activity (Hollin et al., 2016).

In our study, we conducted a series of experiments to shed light on PfGEXP15's interaction with PP1 and its role in modulating PP1 activity. Through Y2H and GST pull-down assays, we validated that PfGEXP15 binds to PP1, with this interaction being RVxF-specific, supported by the inability of the PP1 mutant and other GEXP15 regions to engage in this interaction. Furthermore, we demonstrated the ability of PfGEXP15 to regulate the dephosphorylation activity of PP1 through its N-terminal region containing the RVxF-binding motif. These findings confirmed the preponderant role of the RVxF motif in the interaction and regulation of PP1 by GEXP15.

Notably, these results resonate with previous findings related to CD2BP2. CD2BP2, similar to PfGEXP15, has been shown to bind PP1 through its N-terminal RVxF motif (Albert et al., 2015). Of particular significance is the involvement of this interaction in regulating the alternative splicing of mRNA transcripts derived from diverse origins (Albert et al., 2015). This underscores the critical role of the CD2BP2-PP1 interaction in regulating RNA processing and modulating gene expression. It's worth noting that CD2BP2's interaction with PP1 is not confined to the spliceosome but extends to associations with the tri-snRNP and the precatalytic B complex, as previously reported by Schmidt et al. (2014). Intriguingly, it appears to dissociate upon B complex activation and complex C formation, indicating a dynamic interplay between CD2BP2 and PP1 during these cellular processes.

Second, a conserved domain with an unknown function was identified through the in silico comparative study conducted on the different species as well as with the MEME analysis. Although our pull-down and interactome analyses showed that this domain is unlikely to be involved as a platform for protein interactions, the conservation of critical residues across distant species suggests that this UD region may play a crucial unknown role. From the MS analysis of the pull-down performed with this domain, we found only the exportin 7 (PF3D7_0910100) as a potential binder, which was detected in the nuclear fraction of Pf, suggesting its potential role in PfGEXP15 nuclear trafficking (Oehring et al., 2012). In this context, it should be noted that a previous study reported that exportin 5 is required in nuclear export of 60S ribosome subunits in human cells (Kutay et al., 2010). Further studies will be necessary for *Plasmodium* to elucidate the contribution of this domain to GEXP15 function.

Finally, our in-silico study highlighted the presence of a GYF-like domain in GEXP15. The GYF domain is present in a diverse array of proteins, known to interact with proline-rich peptides, including those found in RNA-binding proteins, cytoskeletal proteins, and transcription factors (Kofler et al., 2009). Notably, the function of the GYF domain can be modulated by subtle changes in its amino acid sequence, making it a flexible region for regulating protein–protein interactions in a context-dependent manner (Kofler et al., 2009). This observation may explain why among the sequences of CB2BP2 and GEXP15 analyzed in this study, only the metazoan proteins had a GYF domain matching the currently described consensus sequence. However, despite the observed differences, the MEME analysis and 3D modeling confirmed some degree of conservation of the GYF-like domains identified in the other species, which may confer adaptation to mediate distinct protein–protein interactions.

It is noteworthy that while two proteins sharing similar overall structural architectures and conserved functional residues may exhibit disparate functions (Bartlett et al., 2005), structural information and the in-silico analysis remain invaluable for function prediction in several ways (Punta & Ofran, 2008). First, it is important to point out that proteins with similar structures can reveal their shared evolutionary lineage or functional convergence, even if they do not have significant sequence similarity. This can be seen in examples such as lipocalins and viral RNA-dependent polymerases, where common constraints have shaped their structures despite differences in their sequences (Valdés et al., 2016). Second, structural motifs often serve as indicators of binding sites, where residues forming functional signatures tend to cluster in the 3D structure, creating binding sites for various molecules, such as the well-known helix-turn-helix motif found in DNA-binding proteins (Aravind et al., 2005). Third, residues with similar functions in different proteins frequently possess analogous physicochemical characteristics; for instance, residues involved in DNA binding share common structural and physicochemical features in DNA-binding proteins, aiding in the prediction of functional residues (Corona & Guo, 2016; Ludlow et al., 2015) Additionally, knowledge of subcellular localization helps to narrow down a protein's potential functions, and this can be predicted through homology and motif analysis (Zhou & Skolnick, 2010). Lastly, structural analysis can unveil insights that are experimentally elusive; for instance, all-atom molecular dynamics simulations derived from 3D models revealed how a single amino acid mutation repels a water molecule crucial for coordinating the position of a metal ion cofactor (Eyer et al., 2017). These multifaceted contributions of structural information underscore its significance in advancing our understanding of protein function.

To further investigate the functional role of GEXP15, we attempted to conditionally knock down PfGEXP15 using a degradation domain since the protein was previously suggested as essential for the development of blood-stage parasites (Zhang, 2018). Notably, despite the successful integration of the degradation domain, confirmed by genotyping and immunoblotting, phenotypic analysis was not possible as the protein remained stable, suggesting that GEXP15 may be intricately involved in a resilient molecular complex, which could account for its remarkable stability and resistance to degradation. Indeed, a previous study proposed that proteins shielded from proteasomal for degradation could be a challenge for knockdown experiments (Russo et al., 2010).

Several plausible explanations can be suggested. Firstly, it's conceivable that GEXP15 has undergone mutations that fortify its resistance to degradation. These mutations might alter the

recognition sites essential for ubiquitin-proteasome interactions or perturb the protein's structural conformation. Alternatively, there might exist counteracting pathways that actively stabilize the protein, potentially involving chaperone proteins that counterbalance the degradation signal. Furthermore, it's worth noting that post-translational modifications can exert a considerable influence on protein stability.

In light of these challenges, other systems can be considered. For instance, the Cre-LoxP system, which can be used to excise the gene of interest (Kudyba et al., 2021). However, potential disadvantages associated with the incorporation of artificial LoxP sites may lead to an altered gene expression with off-target effects that could increase the complexity of the study. Another system that might be considered is the *TetR*-DOZI aptamer module which can effectively repress translation. Nevertheless, concerns about the loss and instability of aptamers after the recombination in the parasites can compromise knockdown efficiency (Kudyba et al., 2021). Yet, a redesigned version with improved stable aptamers can be used for further investigations (Rajaram et al., 2020).

To deepen our understanding of GEXP15 functions, and taking into account the difficulities posed by studying *P. falciparum*, we turned our attention to exploring its functional homolog in *T. gondii*. As previously mentioned, *T. gondii's* homolog of GEXP15, designated TGGT1_217010, possesses the RVxF motif and exhibits the two conserved domains, UD and GYF. This protein has been described as essential, primarily localized within the nucleus, and suggested to be a component of the U5 snRNP complex (toxodb). To facilitate our investigation, the Auxin degron system was employed, a genetic tool that involves introducing a recognition sequence into the gene of interest. Consequently, the gene expresses a protein fused to this recognition sequence, which, in the presence of auxin, is targeted and degraded by the proteasome through recognition by the TIR1 protein. This approach also allowed us to incorporate an HA tag for easy monitoring of the protein. Despite numerous attempts, we encountered challenges in obtaining viable parasites with this construct. Consequently, one of the perspectives appears to be creating a new construct at the N-terminal of the protein which may hold the key to generating transgenic parasites and enabling us to advance our research in this direction.

Subsequently, we employed the GFP and HA tagging of GEXP15 to investigate its expression and monitor its intracellular localization during various stages within erythrocytes. First, immunoblot analysis revealed an unusual pattern of protein migration, characterized by the

presence of a double band at the expected molecular weight. This abnormal migration pattern could potentially arise from the identification of phosphorylation sites on PfGEXP15, encompassing six serine residues and one tyrosine residue during the schizont stage (PlasmoDB 2023). However, even though it is plausible that additional phosphorylation sites may be present on the protein during the same or different stages, these alone may not entirely explain the observed size difference. The discrepancy in size could be attributed to various post-translational modifications. Nevertheless, the most plausible hypothesis, without excluding the previous ones, pertains to the interaction with SDS, whose binding can significantly fluctuate depending on the protein's conformation, thereby influencing the migration behavior of GEXP15 (Rath et al., 2009).

Second, confocal microscopy results in our study demonstrated high expression of GEXP15 in late asexual stages of the parasite's life cycle, consistent with earlier transcriptomics data (PlasmoDB). Notably, GEXP15 was primarily localized within the parasite nucleus. This localization pattern differs from that of PbGEXP15, which has been shown to be present in both the nucleus and cytoplasm (Hollin et al., 2019a). Interestingly, the nuclear localization of GEXP15 in *P. falciparum* mirrors the subcellular distribution of human CD2BP2 (Heinze et al., 2007). To validate whether this difference in GEXP15 localization is species-specific, further investigations employing techniques such as electron microscopy or subcellular fractionation are warranted.

The diversity in protein localization within the *Plasmodium* genus presents a captivating facet of parasite biology. For instance, PfEMP1, a key virulence factor in *P. falciparum*, is known for its export to the surface of infected red blood cells, where it plays pivotal roles in cytoadherence, immune evasion, and disease severity (Smith et al., 2013). However, when examining other *Plasmodium* species like *P. knowlesi*, a related protein termed "NEMP1" (Non-falciparum Erythrocyte Membrane Protein 1) has been identified. In contrast to PfEMP1 in *P. falciparum*, NEMP1 in P. knowlesi does not undergo export to the infected red blood cell surface. Instead, it localizes within the parasite's membrane-bound structures (Grüring et al., 2014). This divergence in subcellular localization underscores the distinct strategies employed by different *Plasmodium* species to interact with their respective host environments, highlighting the remarkable adaptability and diversity exhibited by these parasites in fine-tuning the functions of crucial proteins to suit their specific host niches.

To gain a deeper understanding of the function of PfGEXP15, we profiled the GEXP15 interactome. A first approach based on immunoprecipitation experiments of endogenous tagged PfGEXP15-DDD-GFP-HA present in protein extracts by MS was applied to identify binding partners. This allowed the identification of 10 proteins related to one main functional group corresponding to the ribosomal complex and RNA-binding proteins.

Intriguingly, while PfPP1 was not detected in the PfGEXP15 immunoprecipitation/mass spectrometry (IP/MS) assay, compelling evidence supporting the likelihood of their interaction through the RVxF motif has emerged through a series of complementary approaches. These include yeast two-hybrid (Y2H) assays, GST pull-down experiments, and additional pull-down experiments (using RVxF containing fragments) conducted in this study, thus reaffirming previous research findings (De Witte et al., 2022; Hollin et al., 2016). The significance of these findings is underscored by similar observations in *P. berghei* parasites. In *P. berghei*, PbGEXP15 consistently emerged as one of the top PP1-interacting proteins during both schizont and gametocyte stages (De Witte et al., 2022). Furthermore, a reciprocal IP/MS analysis provided substantial support for the PfGEXP15-PP1 interaction, identifying PbPP1 after PbGEXP15 immunoprecipitation (Hollin et al., 2019). These collective findings suggest that while PfPP1 might not have been captured in the PfGEXP15 IP/MS analysis, the PfGEXP15-PP1 complex could be characterized by its potential instability or transient nature at the specific time point under investigation, shedding light on the dynamic intricacies of this protein-protein interaction within the Plasmodium lifecycle. Such insights into the multifaceted interactions between PfGEXP15 and PP1 contribute to a more comprehensive understanding of their regulatory roles (De Witte et al., 2022; Hollin et al., 2016, 2019).

A complementary approach involving pull-down experiments, utilizing recombinant GYF-domain bound to beads and soluble protein extracts, yielded noteworthy results by identifying 29 proteins associated with ribosomal subunits and ribosomal-associated proteins. Notably, three of these proteins overlapped with the ribosomal proteins identified in the IP-MS experiments. The disparity in partner identification between the IP and pull-down methods is unsurprising, given their inherent differences in studying protein interactomes. It is well-established that the quantity of immunoprecipitated tagged protein, which can differ from that engaged in pull-down experiments, significantly influences the accuracy of mass spectrometry (MS) identification.

These results, taken together, suggest that PfGEXP15 is indeed a ribosome-associated protein. Of particular interest is the revelation that the GYF-domain-containing protein of PfGEXP15 interacts with ribosomal complex proteins, in contrast to the GYF domain of its human counterpart, CD2BP2, which is known to bind spliceosomal proteins (Kofler et al., 2009). This unexpected finding underscores the notion that GYF-containing proteins may exhibit diverse interactomes based on several factors, including subcellular localization, the presence and availability of species-specific interaction partners, and potentially subtle differences in amino acid sequences within or surrounding the GYF domain itself. Notably, this concept is further supported by the divergence in binding partners observed between Pf and Pb GEXP15, as demonstrated by IP experiments. In the case of Pb, these partners belong to spliceosomal and proteasomal core complexes, which could be attributed, at least in part, to variations in the subcellular localization of GEXP15 between the two parasites.

The IP/MS we already performed with conserved regulators of PP1 in *P. berghei* (LRR1, Inhibitor 2, GEXP15) and published (Open Biology 2022, IJMS 2022 and PloS Path 2019) did not show significant detection of ribosomal protein complexes. This excludes technical issues and/or non-specific binding of ribosome proteins, considering their high concentration in soluble protein extracts.

The pull down/MS experiments were designed to include also an unrelated protein as a control. This control protein was produced under the same conditions and used alongside other recombinant Pf proteins in the presence of the same protein extracts in 3 independent biological replicates. This design allowed us to discard non-specific proteins detected under experimental conditions. In addition, the detection of specific protein complexes is further supported when the patterns of partners of the 3 selected recombinant proteins derived from PfGEXP15 were compared (PCA data). Further statistical analysis showed clearly that only the GYF-containing protein was able to pull down ribosomal protein complex.

A closer examination of the identified proteins in the PfGEXP15 interactome showed the presence of the ribosomal RNA processing 1 homolog b (PF3D7_1414800). It is a crucial player in ribosome biogenesis and maturation. Interestingly, an earlier study using quantitative affinity purification followed by mass spectrometry demonstrated that human RRP1B was the most abundant partner of PP1 (Srivastava et al., 2022), modulating its activity, particularly in the context of rRNA processing and ribosome assembly. Moreover, it has been reported that nucleolar complexes contain both RRP1B and PP1 as components of pre-ribosomal subunit

processing complexes (Chamousset et al., 2010). The potential involvement of PfGEXP15 in this RRP1B-PP1 complex could therefore be envisaged. Altogether, these findings are consistent with the fact that reversible phosphorylation events via PfPP1 likely contribute to fine-tuning ribosomal biogenesis.

A striking analogy can be drawn between PfGEXP15 and PfPuf3, both proteins displaying intriguing localization patterns within the nucleus and nucleolus during the asexual stages of *P. falciparum*. Similarly, the association of PfPuf3 with various 60S ribosomal proteins suggests a possible convergence in their roles pertaining to ribosome assembly, mirroring the situation observed with PfGEXP15 (Liang et al., 2018). This implies that both PfPuf3 and PfGEXP15 may contribute significantly to the intricate process of 60S ribosomal subunit biogenesis. An additional noteworthy point is the synchronized temporal expression pattern of PfPuf3 and PfGEXP15, with both proteins peaking during the early trophozoite stage. This synchronized timing aligns with the heightened phase of protein synthesis observed during trophozoite growth, further underlining the potential involvement of both PfPuf3 and PfGEXP15 in facilitating this critical cellular process (Liang et al., 2018).

Although direct evidence regarding the impact of PfGEXP15 on intraerythrocytic parasite development remains elusive due to unsuccessful knockdown attempts via protein degradation, our findings present compelling arguments for the essentiality of PfGEXP15 in *Plasmodium* biology. Firstly, PfGEXP15 has demonstrated its ability to (1) bind and regulate PfPP1c activity, which is vital for Plasmodium survival, through its N-terminal domain, and (2) interact with the ribosomal protein complex through its C-terminal region, a process crucial for protein translation. These dual roles strongly underscore PfGEXP15's importance.

What adds an intriguing layer to this complexity is the functional disparity between human CD2BP2 and PfGEXP15, particularly in their specific binding partners mediated by the GYF domain-containing protein. Understanding the precise nature of these interactions is crucial, as it could potentially be harnessed for malaria drug development.

Notably, we have previously demonstrated the feasibility of disrupting PP1's interactions with its regulators through the RVxF-binding motif using peptides, effectively inhibiting Pf growth in vitro (Fréville et al., 2013). Building on this proof of concept and our validation of PfGEXP15's interactions with PP1 and the ribosomal complex, new opportunities arise for identifying small inhibitors capable of disrupting this interaction network, offering new avenues

for anti-malarial drug development. Such targeted interventions may hold the key to combatting this devastating disease more effectively (Fréville et al., 2013).

In summary, our study incorporated several analyses that were not previously conducted in *P. berghei* (Pb), including in-depth in silico motif analysis, phylogenetic evolutionary analysis, and the development of a 3D model. Notably, the primary commonality between PbGEXP15 and PfGEXP15 lies in their binding to PP1c via the RVXF binding motif, which regulates phosphatase activity. Nevertheless, substantial functional disparities exist between PbGEXP15 and PfGEXP15, primarily linked to their distinct subcellular localizations and interactomes. Whereas PbGEXP15 was found to exist in both nuclear and cytoplasmic compartments, PfGEXP15 exclusively resides in the nucleus. Furthermore, their respective interactomes demonstrate significant dissimilarity, with PbGEXP15 associating with spliceosome and proteosome complexes, as previously reported in PLOS Pathogens, while PfGEXP15 predominantly interacts with ribosomal proteins. This disparity strongly suggests that these proteins have specific functions, in part explained by their distinct localizations, emphasizing the need for caution when extrapolating protein functions and essentiality from *P. berghei* to *P. falciparum*. This complexity is further underscored by a review conducted by Oberstaller et al. (Oberstaller et al., 2021), comparing gene essentiality between *P. berghei* and *P. falciparum*, revealing significant differences among orthologous genes in terms of mutability and dispensability in the two species. Thus, it becomes evident that extrapolating protein functions, even among homologs, is a nuanced process that demands careful consideration of contextual differences.

In summary, this research, although still in its early stages, has expanded and deepened our understanding of PP1 regulation via GEXP15 in *Plasmodium*. PP1 is a protein that plays a crucial role in the parasite's physiology. We have also discovered several mechanisms that contribute to our understanding of how PfGEXP15 could function mainly by its capacity to interact with ribosomes. Importantly, from *P. falciparum* studies, it can be deduced that PfGEXP15 demonstrates differences in both its localization and function when compared to its counterpart in *P. berghei*. These differences may be evident in its interactions with other protein partners, like ribosomes, indicating its involvement in a distinct pathway from that previously described in *P. berghei*. Additionally, it is tempting to suggest that the presence of PP1 in PfGEXP15-ribosome complex may contribute to the control of phosphorylation status of ribosomal proteins necessary for ribosome biogenesis and/or of PfGEXP15.

A promising perspective involves the investigation of alternative inducible knockdown systems. In response to this challenge, we have developed a novel plasmid construct designed to enable the generation of transgenic parasites, wherein the targeted gene can be selectively degraded at the RNA level. This innovative system controls the PfDOZI-10x aptamer system, a ligand-regulatable approach that orchestrates the interaction of a protein module with synthetic RNA aptamers to exert precise control over the translation of the target gene (Rajaram et al., 2020). Notably, this strategy employs a vector system in which the aptamer is purposely engineered to be stable and prone to degradation in the absence of anhydrotetracycline (atc). This pKD-based construction additionally facilitates the generation of GEXP15-HA tagged genes, simplifying the tracking of transfected parasites and streamlining the cloning process. This promising avenue holds the potential to shed new light on the regulation of PfGEXP15 and its functional implications in the parasite's life cycle.

In the context of this thesis, another valuable perspective emerges when considering reciprocal experiments involving ribosomal protein candidates as individual baits in IP experiments. These reciprocal experiments would shed light on the specific interactions between these ribosomal proteins and PfGEXP15. However, it is essential to acknowledge a potential limitation in the immunoprecipitation of ribosomal proteins, stemming from the relatively low expression levels of PfGEXP15 in comparison to the ribosomal proteins themselves. Therefore, it becomes imperative to explore alternative approaches to address this question comprehensively. The production of recombinant proteins for subsequent interaction experiments, such as GST pull-down assays or Biacore analyses, presents an attractive avenue. Additionally, the utilization of a Y2H (Yeast Two-Hybrid) approach holds promise in providing valuable insights.

These diverse experiments have the potential to conclusively address the question of whether PfGEXP15 can directly bind to ribosomal proteins. The results of these investigations could provide a solid foundation for future studies, creating exciting opportunities for additional research and exploration to develop innovative therapeutic strategies against malaria and effective antimalarial molecules, bringing us closer to the goal of reducing the global burden of this deadly disease

# Materials and Methods

# V. Materials and Methods

## Plasmids

Plasmids pGDB and pKD were a kind gift from Vasant Muralidharan (University of Georgia, Athens, USA). The integration plasmid, pGEXP15GDB, was synthetized by introducing a 984 bp fragment from the 3′ end of the GEXP15 ORF (without the stop codon) into pGDB between the XhoI/AvrII (New England Biolabs) (Figure 55). As our gene is highly rich in A and T, hampering to obtain reliable DNA sequence by PCR, the sequence inserted in pGDB was synthetized and sequenced by Gene Script. PetDuet-1 was purchased from Novagen. pGADT7/pGBKT7 were purchased by Clontech.

<div style="border:1px solid black; padding:10px;">

ctcgag
GATATGGCAGAAAGAAATGATATGGCAGAAAAAAATAACGATGATGTAAAAGTCCCAGAAAATAATTTGATAGAGGCCCC
CATGGACAAAGAACATATAATGATAAACAATTCAGAAGAGGAATCAATAGGTAATAATAAAAAATCAGAGGAGCAGAAG
AATTACAATCTGTATAATGATGATGATGAAAAAAAAAAATATTGTACATAATGAGAGGTTAGAAGAATTAGAGAACTTAAA
ACAAATGTATCAAAAGATTACTCTTGATTATAAAACTATAGAAAGACGGTTCAATAACCTAATAGATTTAACACAAAAGTT
AACAAATGAATATAAAAATGTGTACTTTTTAACAAAACGCGAATTCGAAGCATTATGTAAGAAACTTGAAGAATATAAAG
AAAACGTAGACATACATTGGCAACTGAAATGGATGAATGGTGTTGATAATAATGTATATGGTCCTTATAATTATTATGATA
TATATAATTTTATAACAACTGGATTGGTAACCGTTCTAAATCCTATACTTCTAAGAAGAATAAATAATAAAAATGAAGTATT
AGAAAATATATGGCAAATGTATGATGCTGTTAATTATTTAATATTTGTTACTAATGATAATATTAAAAAGAAGAGAAAGCA
TGATGGTCTAATTAGTAAAAACAAGGACCAAGATTCTGATAACAATGAAGAAGATAATGAAAATAATAAAAACACTGATG
TTGATGGTGATGGTGATGATGATGATGATGATAACGATGACGAGAATGATAACGATGACGAGAATGATTATGATTTACTCA
ATAAAAAAAAAAAAAAAGAAAAAAGGATTAATACAAATATCAAAAAAAAAAAAAAAAAAAAAAAAAAAAAAAGAACATTATGAAG
AAAATAATATTTTTAATGATAATAATAATAATCAAGGCAATTCTTCGAACAATGAAGAACATAGTGATAATGAGGACTATT
ATGATAATGGATATGAATTTcctagg

</div>

**Figure 55 The gene sequence of PfGEXP15 inserted in the pGDB vector** between XhoI and AvrII.

## 1.    In Silico analysis
### 1.1. MEME and FIMO analysis

MEME Suite v5.5.1 (https://meme-suite.org/meme/tools/meme) was used on the full-length sequence of GEXP15 and CD2BP2 proteins to identify conserved motifs. Maximum 5 motifs were searched for Pf, Pb, Tg, Sc and human sequences with maximum width of 30 and default parameters. For the 84 CD2BP2 proteins identified, a maximum of 7 motifs were searched with the same settings. FIMO v5.5.1 (https://meme-suite.org/meme/doc/fimo.html) was used to scan the RVxF motif among the 84 sequences using the consensus sequence [RK][RK][VI]X[FW] and default parameters.

### 1.2. 3D Modeling

The modeling of PfGEXP15 (PF3D7_1031600), HsCD2BP2 (NP_006101) and PbGEXP15 (PBANKA_0515400) were generated by Alphafold (https://alphafold.ebi.ac.uk/). I-TASSER software (https://zhanggroup.org/I-TASSER/) was used for the modelling of the two domains: UD (145 a.a.) and GYF (100 a.a.) domains.

## 1.3. Phylogeny analysis

The amino acid sequences of 66 identified CD2BP2 proteins were retrieved from NCBI database (https://www.ncbi.nlm.nih.gov/) as well as three *Plasmodium* GEXP15 sequences and six homologs from Apicomplexa parasites, using HsCD2BP2 as a query. The species and accession numbers of each sequence is provided in the table x below. Multiple sequence alignment of these full-length sequences was performed by Clustal Omega (https://www.ebi.ac.uk/Tools/msa/clustalo/). Then, Neighbor-Joining method and JTT matrix-based model, implemented in MEGA X software, were used to build a phylogenetic tree from the sequence alignment. A gamma distribution equals to one with partial deletion was used. Reliability of internal branches was assessed using the bootstrapping method (500 bootstrap replicates).

**Table 14 The accession numbers** of 66 CD2BP2 and CD2BP2-like proteins, including representatives from model organisms, as well as three *Plasmodium* GEXP15 sequences and six homologs from other Apicomplexa parasites

| Species | Accession number |
|---|---|
| *Cardiosporidium.cionae* | KAF8821205 |
| *Cyclospora.cayetanensis* | XP_026194271 |
| *Plasmodium.yoelii* | UEK52836 |
| *Plasmodium.berghei* | PBANKA_0515400 |
| *Plasmodium.falciparum* | PF3D7_1031600 |
| *Toxoplasma.gondii* | TGGT1_217010 |
| *Cyclospora.cayetanensis* | cyc_06759 |
| *Besnoitia.besnoiti* | XP_029217581 |
| *Neospora.caninum* | BN1204_059300 |
| *Homo.sapiens* | NP_006101 |
| *Marmota monax* | KAI6062690 |
| *Gulo.Gulo.luscus* | KAI5764196 |
| *Phodopus.roborovskii* | CAH6793141 |
| *Rattus.norvegicus* | AAI68174 |
| *Bos.taurus* | AAI34721 |
| *Mus.musculus* | NP_001272835 |
| *Ursus.arctos* | XP_026371573 |

| | |
|---|---|
| *Macaca.mulatta* | NP_001247625 |
| *Pongo.abelii* | NP_001125729 |
| *Leopardus.geoffroyi* | XP_045317687 |
| *Camelus.bactrianus* | XP_045364336 |
| *Macaca.fascicularis* | XP_015297600 |
| *Echinops.telfairi* | XP_045141822 |
| *Danio.rerio* | AAI64209 |
| *Oreochromis.niloticus* | AII77160 |
| *Epinephelus.fuscoguttatus* | XP_049418079 |
| *Lemur.catta* | XP_045399310 |
| *Astyanax.mexicanus* | XP_007235412 |
| *Megalobrama.amblycephala* | XP_048062072 |
| *Micropterus.dolomieu* | XP_045898802 |
| *Silurus.meridionalis* | XP_046721412 |
| *Thunnus.albacares* | XP_044186462 |
| *Solea.senegalensis* | XP_043906410 |
| *Branchiostoma.lanceolatum* | CAH1254131 |
| *Phallusia.mammillata* | CAB3229101 |
| *Xenopus.laevis* | AAI08871 |
| *Bufo.gargarizans* | XP_044128962 |
| *Bufo.bufo* | XP_040296865 |
| *Rana.temporaria* | XP_040211759 |
| *Geotrypetes.seraphini* | XP_033780224 |
| *Sphaerodactylus.townsendi* | XP_048373985 |
| *Ophiophagus.hannah* | ETE71829 |
| *Sceloporus.undulatus* | XP_042327608 |
| *Zootoca.vivipara* | XP_034992191 |
| *Mauremys.mutica* | .XP_044872259 |
| *Dermochelys.coriacea* | XP_043372004 |
| *Chrysemys.picta.bellii* | XP_023968318 |
| *Chelydra.serpentina* | KAG6922158 |
| *Gallus.gallus* | XP_040512770 |
| *Strigops.habroptila* | XP_030330587 |
| *Camarhynchus.parvulus* | XP_030826421 |
| *Lepeophtheirus.salmonis* | CAB4059336 |
| *Drosophila.melanogaster* | NP_609404 |
| *Trichonephila.clavipes* | PRD24727 |
| *Nephila.pilipes* | GFU22065 |
| *Blomia.tropicalis* | KAI2804787 |
| *Dermatophagoides.farinae* | KAH9497637 |
| *Tyrophagus.putrescentiae* | KAH9389852 |
| *Homalodisca.vitripennis* | KAG8302665 |

| | |
|---|---|
| *Chionoecetes.opilio* | KAG0714872 |
| *Trichinella.britovi* | KRY47133 |
| *Trichinella.spiralis* | KRY41686 |
| *Trichinella.patagoniensis* | KRY10239 |
| *Trichinella.murrelli* | KRX45991 |
| *Caenorhabditis.elegans* | NP_499455 |
| *Toxocara.canis* | KHN80241 |
| *Paragonimus.westermani* | KAA3672431 |
| *Schistosoma.bovis* | RTG81184 |
| *Mytilus.edulis* | CAG2230311 |
| *Sepia.pharaonis* | CAE1283511 |
| *Mytilus.coruscus* | CAC5421461 |
| *Stylophora.pistillata* | PFX31710 |
| *Exaiptasia.diaphana* | KXJ09373 |
| *Hydra.vulgaris* | CDG71631 |
| *Bugula.neritina* | KAF6019999 |

## 2.     Cell culture

### 2.1 *Plasmodium falciparum* culture

Pf3D7 strain was grown according to Trager and Jensen in RPMI 1640 medium with 10% human $AB^+$ serum, in the presence of $O^+$ erythrocytes (Trager & Jensen, 1976).Cultures were maintained at 37°C in a humidified atmosphere (5% $CO_2$, 5% $O_2$, and 90% $N_2$). Parasites were synchronized by successive rounds of 5% sorbitol treatment as described previously (Fréville et al., 2012; Vernes et al., 1984).

## 3.     Molecular biology

### 3.1. Generation of transgenic *P. falciparum* line

To generate transgenic parasite line, first we prepared 10 µl of dissolved plasmid (pGDB or pKD) (10 µg/µl) in sterile TE, followed by the addition of 290 µl of cytomix buffer (120 mM KCl; 0.15 mM CaCl2; 2 mM EDTA; 5 mM MgCl2; 10 mM K2HPO4/KH2PO4 pH 7.6; 25 mM Hepes, pH 7.6). Next, we centrifuged the equivalent of 100 µl of infected red blood cells (RBCs) with media, removed the supernatant, and prepared a culture flask with 3 ml of RPMI supplemented with 240 µl of 50% RBCs and the stabilizing drug (TMP/aTC). It's important to note that fresh blood is recommended. The plasmid/cytomix mixture (300 µl) was added to the 100 µl of RBCs and gently mixed by pipetting to avoid bubble formation. The mixture was then transferred to an electroporation tube (Biorad 0.2 cm gap or equivalent).

In parallel, the electroporation device was turned on with specific settings, including user and *Plasmodium* parameters. After setting the voltage to 310 V, capacity to 950 µF, electrodes gap to 2.0 mm, and the number of pulses to 1, the electroporation was initiated with the metal side on the metal. Resistance was checked ($\Omega$) before starting, and the process was completed within a time frame of 7 to 13 ms. Then, 1 ml of RPMI was added to the electroporation tube, and its contents were transferred to a prepared flask of culture medium. The tube was then rinsed again with 1 ml of RPMI, which was also added to the flask. The flask was gently swirled, and the parasites were maintained at 37°C in a humidified atmosphere.

Between 5 to 8 hours post-transfection, the supernatant was removed, and fresh media was added. For drug selection with Blasticidin (2.5 µg/ml), this was typically introduced around 48 hours post-transfection, to allow the resistance gene to be expressed, typically when the parasites reached the trophozoite stage. Incubation was continued at 37°C. Media, along with the drug, was changed daily for 5 to 6 consecutive days. Smears were prepared on days 3 and 5 to monitor parasite status. On Day 7, a smear was examined to ensure the absence of viable parasites. To maintain the culture, 100 µl of fresh 50% RBCs were added weekly.

Blasticidin was retained in the culture until the parasites reappeared, which usually occurred after about 3 weeks. At this point, the drug could be temporarily removed for around three additional weeks, during which the parasitemia would increase exponentially. After 3 weeks, Blasticidin was reintroduced to eliminate non-resistant parasites, with the expectation that the resistant ones had successfully integrated the plasmid. It's important to note that TMP/aTC should be present at all times, except when attempting to degrade the protein and study the phenotype. Integrant clones were isolated by limiting dilution.

### 3.2. Genomic parasite DNA extraction

Genomic DNA (gDNA) extraction was performed on both transgenic and parental parasite strains using the Promega Wizard genomic DNA purification kit. Initially, Nuclei Lysis solution was added to the parasite pellet, which was then carefully resuspended. Subsequently, RNase was added into the solution, followed by an incubation period at 37°C for 15-30 minutes. Next, protein precipitation solution was introduced at room temperature, and the mixture underwent a brief vortexing step, after which it was allowed to incubate on ice for 5 minutes. The mixture was then subjected to centrifugation at 14,000 rpm for 4 minutes at 4°C. The resulting supernatant was carefully transferred to a new Eppendorf tube, where isopropanol was added to facilitate DNA precipitation. After mixing, the solution was once again subjected to

centrifugation at 14,000 rpm for 30 minutes at 4°C. The supernatant was then discarded, and the remaining DNA pellet was washed with 70% ethanol. Following this, the mixture was centrifuged at 14,000 rpm for an additional 30 minutes at 4°C. The ethanol was subsequently removed, and the DNA pellet was allowed to fully air-dry at room temperature. Finally, the genomic DNA was reconstituted in 40 µl of Milli Q water, allowed to dissolve completely, and its concentration was measured using a nanodrop spectrophotometer (GE Healthcare). The extracted DNA samples were stored at -20°C for future use.

### 3.3. Cloning by limiting dilution

Prior to cloning, the culture is subjected to agitation to ensure the presence of only a single parasite per infected red blood cell (RBC), thereby ensuring clonality. A standard culture originating from a flask, typically containing 600µl of blood with parasitemia ranging from 1 to 8%, is diluted to a 1/40 ratio. This diluted culture is then employed for quantifying the RBCs per milliliter using a counting chamber (e.g., Thomas, Neubauer, etc.). For instance, if the 1/40 dilution yields a concentration of 18 million cells/ml, equivalent to 18000 cells/µl, the preparation of a 96-well plate for 150 wells is undertaken. Each well consists of 200 µl of medium and 5 µl of blood (hematocrit 2.5%), along with the addition of 0.3 parasites per well, totaling 45 parasites for 150 wells. If the parasitemia of the original culture is 6.4%, equating to 64 parasites per 1000 cells, adjustments are made in the dilution process to achieve 1152 parasites/µl in the 1/40 dilution. Subsequently, a 1/100 dilution of the 1/40 dilution is performed to attain 11.5 parasites/µl, and 3.9 µl of this dilution is withdrawn to obtain the required 45 parasites.

The resulting mixture consists of 750 µl of blood (5µl of blood per well, for 150 wells), 29.25 ml of medium (195 µl of medium per well, for 150 wells), and 3.9 µl from the 1/100 dilution (of the 1/40 dilution). This mixture is aliquoted at 200 µl per well. After incubation for one week, the medium is refreshed twice within the week, and 0.5 µl of fresh blood is added to each well once.

The screening of the plate is conducted between Day 15 and Day 17. This involves the removal of 100 µl of medium from each well, resuspension of the remaining 100 µl, and the creation of small 1 µl droplets from each well, which are allowed to dry before being subjected to Giemsa staining. In total, the contents of the 96 wells can be accommodated on 2 glass slides, ensuring that the drops are well-aligned to facilitate subsequent microscopic examination. It should be

noted that additional slides can be employed for convenience. Successful cloning is typically indicated by the presence of no more than approximately thirty positive wells.

## 4. Genotyping of *Pf* transfectants

### 4.1. Immunoblot assays

Parasites were suspended in 4X Laemmli loading buffer (240mM Tris-HCl pH 6.8; 8% SDS; 40% sucrose; 0.04% bromophenol blue and 400mM DTT) and total proteins were subjected to electrophoresis in a 10% polyacrylamide gel. By a standard western blot procedure, the proteins were transferred onto a nitrocellulose membrane (Amersham Protran 0.45μm NC). The membrane was blocked with 5% milk (non-fat milk powder dissolved in PBS) and probed with primary antibodies (rabbit anti-HA,1/1000) or (mouse anti-His, 1/2000) diluted in the blocking buffer. The primary antibodies were followed by respective species-specific secondary antibodies conjugated to HRP (Anti rabbit, 1/20000, Sigma) or (Anti mouse, 1/20000, Rockland). The antibody incubations were followed by thorough washing using PBS tween 0.4%. The membranes were visualized using Dura/ Fento Western blotting substrate.

### 4.2. PCR

The gDNA mentioned above is used for all the amplifications necessary for the construction of plasmids. All primers used for the PCRs are listed in Table 15. The PCRs were carried out using the enzyme Taq Advantage (Takara Bio) according to the manufacturer's recommendations and the following parameters:

Initial Denaturation 95°C                            5mins

Denaturation 95°C                                    30sec
Annealing Primer dependent ($\approx$ 50-65°C)  30sec      25-35 cycles
Elongation 72°C                                      60sec/Kb

Final elongation 72°C                                10mins
Storage 4°C                                          $\infty$

Agarose gel electrophoresis separates DNA fragments based on fragment sizes. It was performed to verify PCR amplifications and all subsequent DNA analysis steps. DNA fragments were purified using NucleoSpin Gel and PCR Cleanup kit (Machery Nagel)

after PCR amplification or restriction digestion. Throughout this study, the restriction enzymes used, and their respective buffer were supplied by Thermofisher.

**Table 15 Forward and Reverse primers used to genotype the plasmid's integration**

| Primer name | Orientation | Sequence 5' to 3' | Plasmid | Use |
|---|---|---|---|---|
| P0 | F | CTGGATTGGTAACCGTTCTAAATCC | PGDB | Genotyping |
| P1 | F | GGGCTAAATCATCAATCCAGCATGGAG | pGDB | Genotyping |
| P2 | R | GTACTTCCACGTGGTGAAGAG | pGDB | Genotyping |
| P3 | R | CCGTATGTTGCATCACCTTCACCCTC | pGDB | Genotyping |

**Table 16 Couples of forward and reverse primers used, with their products'expected sizes**.

| Primer P0 CTGGATTGGTAACCGTTCT AAATCC | Primer P3 CCGTATGTTGCATCACCTTCACCCTC | 0.75 kb Expected size | To check plasmid presence |
|---|---|---|---|
| Primer P1 GGGCTAAATCATCAATCCA GCATGGAG | Primer P3 CCGTATGTTGCATCACCTTCACCCTC | 1.4 kb expected size | To check integration |
| Primer P1 GGGCTAAATCATCAATCCA GCATGGAG | Primer P2 GTACTTCCACGTGGTGAAGAG | 1.3 kb expected size | To check wild type parasites for cloning |

# 5. Phenotyping of *Pf* transfectants
## 5.1. Fluorescence microscopy

Transgenic and parental parasites were washed then fixed with 4% paraformaldehyde and 0.0075% glutaraldehyde for 15 min at 4°C. After PBS washing, cells were settled on Poly-L-lysine coated coverslips. The coverslips were mounted in Mowiol with DAPI (1μg/ml) and multipoint-confocal imaging was performed with a spinning disk Live SR (stand Nikon Ti-2 combined with Live-SR module Gataca Systems), with a 63x PL APO 1.40 oil objective and a camera Prime95B. Under these acquisition conditions, the pixel size is 109 nm in X and Y. The delta Z is 500nm. Figures are produced using ImageJ/Fiji software (National Institute of Health (NIH)). The images were processed by filtration (radius1 median filter) and contract adjustment, then the fluorescence channels were projected by maximum intensity projection.

# 6. Interaction tests

## 6.1. Yeast two-hybrid assays

The Nt fragment of PfGEXP15 containing aa 8-182, cloned into the pGADT7 vector, was obtained from the *P. falciparum* cDNA library (Dualsystems Biotech) and purified following yeast two-hybrid screening (Hollin et al., 2016). Gal4-DBD-Laminin and Gal4-DBD-PfPP1c had been previously cloned (Fréville et al., 2013). PfPP1c F255A/F256A mutant was generated through site-directed mutagenesis using DNA polymerase (MP Biomedicals) with pGBKT7-PfPP1c as template. The resulting pGADT7 and pGBKT7 constructs were transformed into yeast strains Y2H Gold and Y187 (Clontech), respectively, and plated on Synthetic Defined agar lacking leucine (SD-L) or tryptophan (SD-W), respectively, followed by incubation at 30°C for 3-5 days. Various crosses were performed and spread on selective SD-LW medium. These diploids were then transferred to more stringent SD-LWH and SD-LWHA (L: Leucine, W: Tryptophane, H: Histidine, A: Adenine) media at different dilutions (1:1, 1:25, 1:50). Diploids were incubated for 4-6 days at 30°C. Empty vectors pGADT7 or pGBKT7 and pGBKT7-Laminin served as negative controls.

## 6.2. pNPP phosphatase assays

The effect of GEXP15 on PfPP1c activity was carried out using the p-nitrophenyl phosphate (pNPP) assay. Different amounts of PfGEXP15 RVxF-, UD- and GYF-containing proteins, described above, were preincubated with 40 pmol of PfPP1c for 30 min at 37°C. The enzymatic reaction was initiated by adding p-nitrophenyl phosphate (pNPP) substrate (Sigma-Aldrich) to the reaction mixture. After 1h of incubation, absorbance was measured at 405 nm (Thermo Scientific Multiskan FC). Two independent experiments were carried out in duplicate, and a Kruskal-Wallis test followed by a Dunn's multiple comparison test as a post hoc analysis was conducted using GraphPad Prism to compare phosphatase activity in the presence and absence of GEXP15.

# 7. Pulldown and interactome study

## 7.1. Recombinant protein production

The coding region of the three recombinant protein fragments were PCR amplified using genomic DNA with the following primers: 1) P4-P5 for the N terminal fragment (21-546 bp) containing the RVxF motif (Table 17); 2) P6-P7 for the central region (625-1242 bp) containing

the UD and 3) P8-P9 for the C terminal portion (1878-2445 bp) containing the GYF domain. They were cloned into pETDuet-1 (Novagen) using the In-Fusion HD Cloning system (Clontech).

For pulldown experiments, the RVxF-containing protein, described above, was used. As for the other two recombinant protein, shorter fragments were synthesized in order to retain the minimal functional domains based on sequence and structure analyses (UD:853-1266 bp; GYF:2053-2347 bp) and cloned into the pETDuet-1 vector (Novagen) in GeneScript. The expression of His6-motifs was carried out in One Shot® BL21 StarTM (DE3) Chemically Competent *E. coli* cells (Life Technologies), in the presence of 0.5 mM IPTG at 37 °C for 2 h or at 16 °C overnight. Bacterial cells were harvested in non-denaturing lysis buffer (20 mM Tris, 150 mM NaCl, 20 mM Imidazole, Triton 1%, Lysozyme 1mg/50ml, DNase I and protease inhibitor cocktail (Roche), pH 7.5), followed by sonication and ultracentrifugation. Sonication involves subjecting the lysate to high-frequency sound waves, effectively breaking down cell membranes, homogenizing the sample, and assisting in solubilizing proteins. Subsequently, ultracentrifugation uses high centrifugal forces to separate cellular debris, organelles, and large particles from the soluble protein fraction. This step allows for the removal of impurities and concentrates the protein of interest, which is usually found in the supernatant, enhancing the purity and yield of the recombinant protein.

**Table 17 The primers used to produce the recombinant protein.**

| P4 | F | CATCACCACAGCCAGGATCCAGGGGAGGAAAATGACTTGGATAAATTC | pETDuet-1 | Recombinant protein |
| P5 | R | CATTATGCGGCCGCAAGCTTGTTAATTCCATTCAATATGGTATTTTTAT | pETDuet-1 | Recombinant protein |
| P6 | F | CATCACCACAGCCAGGATCCGGACCATTCTATATATAATAACG | pETDuet-1 | PfGEXP15 central region, UD-containing fragment |
| P7 | R | CATTATGCGGCCGCAAGCTTCTCTTTTTCATCTATTAATAAAC | pETDuet-1 | |
| P8 | F | CATCACCACAGCCAGGATCCGGAGCAGAAGAATTACAATC | pETDuet-1 | PfGEXP15 C terminal region, GYF-containing fragment |
| P9 | R | CATTATGCGGCCGCAAGCTTGTTTTTATTATTTTCATTATCTTC | pETDuet-1 | |

Recombinant proteins were purified according to manufacturer's instructions by Ni2+-NTA agarose beads (QIAGEN).

Washing steps were performed with a buffer containing 20 mM Tris, 150 mM NaCl and 20 mM imidazole, pH 7.5.

For GST pull-down experiment, His-tagged proteins were eluted from beads with buffer containing 20 mM Tris, 500 mM NaCl and 600 mM Imidazole, pH 7.5 and then the imidazole was eliminated by dialysis. The purified recombinant proteins were analyzed by western-blot with anti-His antibody (1:2000 dilution) (Qiagen) followed by HRP-labeled anti-mouse IgG (1:50000 dilution) and quantified with Pierce™ BCA Protein Assay Kit (Life Technologies). GST-PfPP1c and PfPP1c were produced as previously described (Hollin et al., 2019).

GST or GST-PfPP1c coupled with Glutathione-Sepharose beads (Sigma-Aldrich) were saturated with 25 µg of BSA and incubated overnight at 4°C with 2 µg of PfGEXP15 RVxF, UD and GYF in binding buffer (20 mM Tris, 150 mM NaCl, 0.2 mM EDTA, 20 mM HEPES, 1 mM MnCl2, 1 mM DTT, 0.1% Triton X-100, 10% glycerol, protease inhibitor cocktail (Roche) and pH 7.5). After washes, proteins were analyzed by western-blot, as well as 500 ng of PfGEXP15 RVxF, UD and GYF used as inputs.

For the pulldown experiments, additional 3 washing steps with a buffer containing 20 mM Tris, 150 mM NaCl, 0.5% Triton X-100 and protease inhibitor cocktail (Roche), pH 7.5, were done before adding the soluble proteins of parasite extracts. The various recombinant proteins were analyzed by SDS-PAGE and stained with Coomassie Blue or subjected to Western blotting. In the case of Western blotting, the proteins were transferred to a nitrocellulose membrane, incubated with anti-His antibodies (dilution 1:2000) (Qiagen), followed by anti-mouse IgG HRP antibodies (dilution 1:50000). Detection was performed using chemiluminescence with SuperSignalTM West Dura Extended Duration Substrate (Life Technologies). The quantification of recombinant proteins was carried out using the PierceTM BCA Protein Assay (Life Technologies).

### 7.2. Pulldown assays

For the pulldown experiment, trophozoites/schizonts of parental wild-type parasites were suspended in 50 mM Tris, 0.5% Triton X-100, 150 mm NaCl and protease inhibitor cocktail (Roche), pH 7.5. After ten consecutive freezing-thawing cycles and sonication, soluble fractions were obtained after repeated centrifugations at 13000 rpm at 4°C.

The agarose nickel beads coated with the recombinant proteins were mixed overnight at 4°C with parasite soluble extracts in 20 mM Tris, 150 mM NaCl, 0.5% Triton X-100 and protease inhibitor cocktail (Roche), pH 7.5.

Beads were washed and elution was performed in Laemmli buffer. Then after 3 min at 95°C, samples were loaded on a 4–20% SDS-PAGE for western blot or mass spectrometry analyses. Western blots were carried out probed with anti-His mAb (1:1000, Invitrogen) followed by anti-mice IgG-HRP (1:20000, Sigma-Aldrich).

## 7.3. Sample preparations and Immunoprecipitation assays

In order to gain a better understanding of the biological roles of GEXP15 in the asexual stages of Pf, it was important to study the complexes formed by PfGEXP15.

Pf enriched trophozoites and schizonts cultures of PfGEXP15-GFP-DDD-HA or parental wildtype strain (control) were used for protein extracts as described above. Immunoprecipitation experiments were performed using 3 biological replicates of each strain. Each biological replicate contained 10 isolated pellets of trophozoites and schizonts, each purified from one culture flask of 75 cm$^2$. Soluble proteins extractions and immunoprecipitation assays were performed as previously described (Hollin et al., 2019). Purified parasites of each strain were suspended in 50 mM Tris, 0.5% Triton X-100, 150 mm NaCl and protease inhibitor cocktail (Roche), pH 7.5. on ice. After ten consecutive freezing-thawing cycles and sonication, soluble fractions were obtained after repeated centrifugations at 13000 rpm at 4°C, to eliminate cell debris. Around 10% of the lysate volume was kept for WB verification (boiled in 4X laemmeli buffer then kept at -20°C). These soluble fractions were incubated with pre-washed GFP-Trap magnetic agarose (ChromoTek, Germany) overnight at 4°C on a rotating wheel. The second day, beads were washed 10 times with washing buffer containing 20 mM Tris,150 mM NaCl, 0.5% Triton X-100, and protease inhibitor cocktail (Roche, Basel, Switzerland) at pH 7.5. Elution was performed in Laemmli buffer for 3 minutes at 100°C.

## 7.4. Sample preparation for Mass Spectrometry

S-Trap$^{TM}$ micro spin column (Protifi, Huntington, USA) digestion was performed on immunoprecipitation eluates and pulldown eluates according to manufacturer's instructions. Briefly, samples were supplemented with 20% SDS to a final concentration of 5%, reduced with 20 mM TCEP (Tris(2-carboxyethyl) phosphine hydrochloride) and alkylated with 50 mM CAA (chloroacetamide) for 5 min at 95ºC. Aqueous phosphoric acid was then added to a final concentration of 2.5% following by the addition of S-Trap binding buffer (90% aqueous methanol, 100mM TEAB, pH7.1). Mixtures were then loaded on S-Trap columns. Five washes were performed for thorough SDS elimination. Samples were digested with 2 µg of trypsin

(Promega, Madison, WI, USA) at 47°C for 2 h. After elution, peptides were vacuum dried and resuspended in 2% ACN, 0.1% formic acid in HPLC-grade water prior to MS analysis.

## 7.5. NanoLC-MS/MS Protein Identification and Quantification

The tryptic peptides were resuspended in 30 µL and an amount of 400 ng was injected on a nanoElute (Bruker Daltonics, Germany) HPLC (high-performance liquid chromatography) system coupled to a timsTOF Pro (Bruker Daltonics, Germany) mass spectrometer. HPLC separation (Solvent A: 0.1% formic acid in water; Solvent B: 0.1% formic acid in acetonitrile) was carried out at 250 nL/min using a packed emitter column (C18, 25 cm×75 µm 1.6 µm) (Ion Optics, Australia) using a 40 min gradient elution (2 to 11% solvent B during 19 min; 11 to 16% during 7 min; 16% to 25% during 4 min; 25% to 80% for 3min and finally 80% for 7 min to wash the column). Mass-spectrometric data were acquired using the parallel accumulation serial fragmentation (PASEF) acquisition method in DDA (Data Dependent Analysis) mode. The measurements were carried out over the m/z range from 100 to 1700 Th. The range of ion mobilities values from 0.7 to 1.1 V s/cm$^2$ (1/k0). The total cycle time was set to 1.2s and the number of PASEF MS/MS scans was set to 6.

Data analysis was performed using MaxQuant software version2.1.3.0 and searched with Andromeda search engine against the TrEMBL/Swiss-Prot *Plasmodium falciparum* 3D7 database downloaded from Uniprot on 10/10/2022 (5392 entries) and *E. coli* BL21-DE3 database downloaded from Uniprot on 10/10/2022 (4173 entries). To search parent mass and fragment ions, we set a mass deviation of 10 ppm for the main search and 40 ppm respectively. The minimum peptide length was set to 7 amino acids and strict specificity for trypsin cleavage was required, allowing up to 2 missed cleavage sites. Carbamidomethylation (Cys) was set as fixed modification, whereas oxidation (Met) and N-term acetylation (Prot N-term) were set as variable modifications. The false discovery rates (FDRs) at the peptide and protein levels were set to 1%. Scores were calculated in MaxQuant as described previously(Cox & Mann, 2008) The reverse and common contaminants hits were removed from MaxQuant output as well as the protein only identified by site. Proteins were quantified according to the MaxQuant label-free algorithm using LFQ intensities and protein quantification was obtained using at least 1 peptide per protein. Match between runs was allowed only with IP samples.

Statistical and bioinformatic analysis, including heatmaps, profile plots and clustering, were performed with Perseus software (version 1.6.15.0) freely available at www.perseus-framework.org (Tyanova et al., 2016).For statistical comparison, we set four groups, each

containing up to 3 biological replicates for the pulldown samples (Control, RVxF, UD, GYF). For the IP samples we set two groups with 3 biological replicates each (Control, GEXP15). We then filtered the data to keep only proteins with at least 3 and 2 valid values in at least one group for pulldown and IP experiments, respectively. Next, the data were imputed to fill missing data points by creating a Gaussian distribution of random numbers with a standard deviation of 33% relative to the standard deviation of the measured values and using 3 and 1.8 SD downshift of the mean to simulate the distribution of low signal values for pull-down and IP datasets, respectively. We then performed an ANOVA test (FDR<0.05, S0=1) for the pull-down samples and statistical t-test (FDR<0.05, S0=0.1) for IP samples. Hierarchical clustering of proteins that survived the test was performed in Perseus on logarithmised LFQ intensities after z-score normalization of the data using Euclidean distances.

# Bibliography

# Bibliography

Adderley, J., & Doerig, C. (2022). Comparative analysis of the kinomes of Plasmodium falciparum, Plasmodium vivax and their host Homo sapiens. *BMC Genomics*, *23*(1). https://doi.org/10.1186/S12864-022-08457-0

Adl, S. M., Leander, B. S., Simpson, A. G. B., Archibald, J. M., Anderson, O. R., Bass, D., Bowser, S. S., Brugerolle, G., Farmer, M. A., Karpov, S., Kolisko, M., Lane, C. E., Lodge, D. J., Mann, D. G., Meisterfeld, R., Mendoza, L., Moestrup, Ø., Mozley-Standridge, S. E., Smirnov, A. V., & Spiegel, F. (2007). Diversity, nomenclature, and taxonomy of protists. *Systematic Biology*, *56*(4), 684–689. https://doi.org/10.1080/10635150701494127

Alam, M. M., Sanchez-Azqueta, A., Janha, O., Flannery, E. L., Mahindra, A., Mapesa, K., Char, A. B., Sriranganadane, D., Brancucci, N. M. B., Antonova-Koch, Y., Crouch, K., Simwela, N. V., Millar, S. B., Akinwale, J., Mitcheson, D., Solyakov, L., Dudek, K., Jones, C., Zapatero, C., … Tobin, A. B. (2019). Validation of the protein kinase Pf CLK3 as a multistage cross-species malarial drug target. *Science (New York, N.Y.)*, *365*(6456). https://doi.org/10.1126/SCIENCE.AAU1682

Albert, G. I., Schell, C., Kirschner, K. M., Schäfer, S., Naumann, R., Müller, A., Kretz, O., Kuropka, B., Girbig, M., Hübner, N., Krause, E., Scholz, H., Huber, T. B., Knobeloch, K. P., & Freund, C. (2015). The GYF domain protein CD2BP2 is critical for embryogenesis and podocyte function. *J MOL CELL BIOL*, *7*(5), 402–414. https://doi.org/10.1093/JMCB/MJV039

Amino, R., Thiberge, S., Martin, B., Celli, S., Shorte, S., Frischknecht, F., & Ménard, R. (2006). Quantitative imaging of Plasmodium transmission from mosquito to mammal. *Nature Medicine*, *12*(2), 220–224. https://doi.org/10.1038/NM1350

Andreassen, P. R., Lacroix, F. B., Villa-Moruzzi, E., & Margolis, R. L. (1998). Differential Subcellular Localization of Protein Phosphatase-1 α, γ1, and δ Isoforms during Both Interphase and Mitosis in Mammalian Cells. *The Journal of Cell Biology*, *141*(5), 1207. https://doi.org/10.1083/JCB.141.5.1207

Andreeva, N. S., Rumsh, L. D., Shemjakin, M. M., & Ovchinnikov, Y. A. (2001). Analysis of crystal structures of aspartic proteinases: On the role of amino acid residues adjacent to the catalytic site of pepsin-like enzymes. *Protein Science*, *10*(12), 2439–2450. https://doi.org/10.1110/PS.25801

Ansai, T., Dupuy, L. C., & Barik, S. (1996). Interactions between a minimal protein serine/threonine phosphatase and its phosphopeptide substrate sequence. *The Journal of Biological Chemistry*, *271*(40), 24401–24407. https://doi.org/10.1074/JBC.271.40.24401

Aravind, L., Anantharaman, V., Balaji, S., Babu, M. M., & Iyer, L. M. (2005). The many faces of the helix-turn-helix domain: transcription regulation and beyond. *FEMS Microbiology Reviews*, *29*(2), 231–262. https://doi.org/10.1016/J.FEMSRE.2004.12.008

Arendse, L. B., Wyllie, S., Chibale, K., & Gilbert, I. H. (2021). Plasmodium Kinases as Potential Drug Targets for Malaria: Challenges and Opportunities. *ACS Infectious Diseases*, *7*(3), 518–534. https://doi.org/10.1021/ACSINFECDIS.0C00724

Balaji, S., Madan Babu, M., Iyer, L. M., & Aravind, L. (2005). Discovery of the principal specific transcription factors of Apicomplexa and their implication for the evolution of the AP2-integrase DNA binding domains. *Nucleic Acids Research*, *33*(13), 3994–4006. https://doi.org/10.1093/NAR/GKI709

Ballou, L. M., Villa-Moruzzi, E., & Fischer, E. H. (1985). Subunit structure and regulation of phosphorylase phosphatase. *Current Topics in Cellular Regulation*, *27*(C), 183–192. https://doi.org/10.1016/B978-0-12-152827-0.50022-0

Baptista, V., Peng, W. K., Minas, G., Veiga, M. I., & Catarino, S. O. (2022). Review of Microdevices for Hemozoin-Based Malaria Detection. *Biosensors*, *12*(2). https://doi.org/10.3390/BIOS12020110

Barry, P., & Potter, V. L. (2018). Professor Barry V.L. Potter: Winner of the 2018 Tu Youyou Award in Honor of the Co-Recipient of the 2015 Nobel Prize in Physiology or Medicine for Her Discoveries Concerning a Novel Therapy against Malaria. *Molecules 2018, Vol. 23, Page 1651*, *23*(7), 1651. https://doi.org/10.3390/MOLECULES23071651

Barta, J. R., & Thompson, R. C. A. (2006). What is Cryptosporidium? Reappraising its biology and phylogenetic affinities. *Trends in Parasitology*, *22*(10), 463–468. https://doi.org/10.1016/J.PT.2006.08.001

Bartlett, G. J., Todd, A. E., & Thornton, J. M. (2005). Inferring Protein Function from Structure. *Structural Bioinformatics*, 387–407. https://doi.org/10.1002/0471721204.CH19

BARTON, G. J., COHEN, P. T. W., & BARFORD, D. (1994). Conservation analysis and structure prediction of the protein serine/threonine phosphatases. Sequence similarity with diadenosine tetraphosphatase from Escherichia coli suggests homology to the protein phosphatases. *European Journal of Biochemistry*, *220*(1), 225–237. https://doi.org/10.1111/J.1432-1033.1994.TB18618.X

Bhattacharyya, M. K., Hong, Z., Kongkasuriyachai, D., & Kumar, N. (2002). Plasmodium falciparum protein phosphatase type 1 functionally complements a glc7 mutant in Saccharomyces cerevisiae. *International Journal for Parasitology*, *32*(6), 739–747. https://doi.org/10.1016/S0020-7519(02)00007-3

Bollen, M. (2001). Combinatorial control of protein phosphatase-1. *Trends in Biochemical Sciences*, *26*(7), 426–431. https://doi.org/10.1016/S0968-0004(01)01836-9

Bollen, M., Peti, W., Ragusa, M. J., & Beullens, M. (2010). The extended PP1 toolkit: designed to create specificity. *Trends in Biochemical Sciences*, *35*(8), 450–458. https://doi.org/10.1016/J.TIBS.2010.03.002

BONNIN, A., GUT, J., DUBREMETZ, J. F., NELSON, R. G., & CAMERLYNCK, P. (1995). Monoclonal antibodies identify a subset of dense granules in Cryptosporidium parvum zoites and gamonts. *The Journal of Eukaryotic Microbiology*, *42*(4), 395–401. https://doi.org/10.1111/J.1550-7408.1995.TB01601.X

Brancucci, N. M. B., Bertschi, N. L., Zhu, L., Niederwieser, I., Chin, W. H., Wampfler, R., Freymond, C., Rottmann, M., Felger, I., Bozdech, Z., & Voss, T. S. (2014). Heterochromatin protein 1 secures survival and transmission of malaria parasites. *Cell Host & Microbe*, *16*(2), 165–176. https://doi.org/10.1016/J.CHOM.2014.07.004

Brancucci, N. M. B., De Niz, M., Straub, T. J., Ravel, D., Sollelis, L., Birren, B. W., Voss, T. S., Neafsey, D. E., & Marti, M. (2018). Probing plasmodium falciparum sexual commitment at the single-cell level [version 4; referees: 2 approved]. *Wellcome Open Research*, *3*. https://doi.org/10.12688/WELLCOMEOPENRES.14645.4/DOI

Brauer, B. L., Wiredu, K., Mitchell, S., Moorhead, G. B., Gerber, S. A., & Kettenbach, A. N. (2021). Affinity-based profiling of endogenous phosphoprotein phosphatases by mass spectrometry. *Nature Protocols*, *16*(10), 4919–4943. https://doi.org/10.1038/S41596-021-00604-3

Brautigan, D. L., & Brautigan, D. L. (2013). Protein Ser/Thr phosphatases – the ugly ducklings of cell signalling. *The FEBS Journal*, *280*(2), 324–325. https://doi.org/10.1111/J.1742-4658.2012.08609.X

Brautigan, D. L., & Shenolikar, S. (2018). Protein Serine/Threonine Phosphatases: Keys to Unlocking Regulators and Substrates. *Annual Review of Biochemistry*, *87*, 921–964. https://doi.org/10.1146/ANNUREV-BIOCHEM-062917-012332

Brunschwig, C., Lawrence, N., Taylor, D., Abay, E., Njoroge, M., Basarab, G. S., Le Manach, C., Paquet, T., Gonzàlez Cabrera, D., Nchinda, A. T., de Kock, C., Wiesner, L., Denti, P., Waterson, D., Blasco, B., Leroy, D., Witty, M. J., Donini, C., Duffy, J., … Manach, L. C. (2018). *UCT943, a Next-Generation Plasmodium falciparum PI4K Inhibitor Preclinical Candidate for the Treatment of Malaria*. https://doi.org/10.1128/AAC.00012

Buchholz, K., Burke, T. A., Williamson, K. C., Wiegand, R. C., Wirth, D. F., & Marti, M. (2011). A High-Throughput Screen Targeting Malaria Transmission Stages Opens New Avenues for Drug Development. *The Journal of Infectious Diseases*, *203*(10), 1445. https://doi.org/10.1093/INFDIS/JIR037

Bunnik, E. M., Cook, K. B., Varoquaux, N., Batugedara, G., Prudhomme, J., Cort, A., Shi, L., Andolina, C., Ross, L. S., Brady, D., Fidock, D. A., Nosten, F., Tewari, R., Sinnis, P., Ay, F., Vert, J. P., Noble, W. S., & Le Roch, K. G. (2018). Changes in genome organization of parasite-specific gene families during the Plasmodium transmission

stages. *Nature Communications 2018 9:1*, *9*(1), 1–15. https://doi.org/10.1038/s41467-018-04295-5

Bushell, E., Gomes, A. R., Sanderson, T., Anar, B., Girling, G., Herd, C., Metcalf, T., Modrzynska, K., Schwach, F., Martin, R. E., Mather, M. W., McFadden, G. I., Parts, L., Rutledge, G. G., Vaidya, A. B., Wengelnik, K., Rayner, J. C., & Billker, O. (2017). Functional Profiling of a Plasmodium Genome Reveals an Abundance of Essential Genes. *Cell*, *170*(2), 260-272.e8. https://doi.org/10.1016/J.CELL.2017.06.030

Cabrera, D. G., Horatscheck, A., Wilson, C. R., Basarab, G., Eyermann, C. J., & Chibale, K. (2018). Plasmodial Kinase Inhibitors: License to Cure? *Journal of Medicinal Chemistry*, *61*(18), 8061. https://doi.org/10.1021/ACS.JMEDCHEM.8B00329

Camlin, N. J., Venkatachalam, I., & Evans, J. P. (2023). Oscillations in PP1 activity are essential for accurate progression through mammalian oocyte meiosis. *Cell Cycle (Georgetown, Tex.)*, *22*(13), 1614–1636. https://doi.org/10.1080/15384101.2023.2225924

Campbell, T. L., de Silva, E. K., Olszewski, K. L., Elemento, O., & Llinás, M. (2010). Identification and genome-wide prediction of DNA binding specificities for the ApiAP2 family of regulators from the malaria parasite. *PLoS Pathogens*, *6*(10). https://doi.org/10.1371/JOURNAL.PPAT.1001165

Cannon, J. F. (2013). How phosphorylation activates the protein phosphatase-1 • inhibitor-2 complex. *Biochimica et Biophysica Acta*, *1834*(1), 71–86. https://doi.org/10.1016/J.BBAPAP.2012.09.003

Cannon, J. F., Pringle, J. R., Fiechter, A., & Khalil, M. (1994). Characterization of glycogen-deficient glc mutants of Saccharomyces cerevisiae. *Genetics*, *136*(2), 485–503. https://doi.org/10.1093/GENETICS/136.2.485

Carucci, D. J., Witney, A. A., Muhia, D. K., Warhurst, D. C., Schaap, P., Meima, M., Li, J. L., Taylor, M. C., Kelly, J. M., & Baker, D. A. (2000). Guanylyl cyclase activity associated with putative bifunctional integral membrane proteins in Plasmodium falciparum. *The Journal of Biological Chemistry*, *275*(29), 22147–22156. https://doi.org/10.1074/JBC.M001021200

CAVALIER-SMITH, T. (1993). The Protozoan Phylum Opalozoa. *Journal of Eukaryotic Microbiology*, *40*(5), 609–615. https://doi.org/10.1111/J.1550-7408.1993.TB06117.X

*CDC - Parasites - Malaria*. (n.d.). Retrieved September 27, 2023, from https://www.cdc.gov/parasites/malaria/index.html

Ceulemans, H., & Bollen, M. (2004). Functional diversity of protein phosphatase-1, a cellular economizer and reset button. *Physiological Reviews*, *84*(1), 1–39. https://doi.org/10.1152/PHYSREV.00013.2003

Ceulemans, H., Stalmans, W., & Bollen, M. (2002). Regulator-driven functional diversification of protein phosphatase-1 in eukaryotic evolution. *BioEssays : News and Reviews in Molecular, Cellular and Developmental Biology*, *24*(4), 371–381. https://doi.org/10.1002/BIES.10069

Chaal, B. K., Gupta, A. P., Wastuwidyaningtyas, B. D., Luah, Y. H., & Bozdech, Z. (2010). Histone deacetylases play a major role in the transcriptional regulation of the Plasmodium falciparum life cycle. *PLoS Pathogens*, *6*(1). https://doi.org/10.1371/JOURNAL.PPAT.1000737

Chamousset, D., De Wever, V., Moorhead, G. B., Chen, Y., Boisvert, F. M., Lamond, A. I., & Trinkle-Mulcahy, L. (2010). RRP1B Targets PP1 to Mammalian Cell Nucleoli and Is Associated with Pre-60S Ribosomal Subunits. *Molecular Biology of the Cell*, *21*(23), 4212. https://doi.org/10.1091/MBC.E10-04-0287

Checkley, W., White, A. C., Jaganath, D., Arrowood, M. J., Chalmers, R. M., Chen, X. M., Fayer, R., Griffiths, J. K., Guerrant, R. L., Hedstrom, L., Huston, C. D., Kotloff, K. L., Kang, G., Mead, J. R., Miller, M., Petri, W. A., Priest, J. W., Roos, D. S., Striepen, B., … Houpt, E. R. (2015). A review of the global burden, novel diagnostics, therapeutics, and vaccine targets for cryptosporidium. *The Lancet. Infectious Diseases*, *15*(1), 85–94. https://doi.org/10.1016/S1473-3099(14)70772-8

*Chemotherapy of malaria / by Sir Gordon Covell*. (n.d.). Retrieved September 27, 2023, from https://iris.who.int/handle/10665/64247

Chen, B., Sun, Y., Niu, J., Jarugumilli, G. K., & Wu, X. (2018). Protein Lipidation in Cell Signaling and Diseases: Function, Regulation, and Therapeutic Opportunities. *Cell Chemical Biology*, *25*(7), 817–831. https://doi.org/10.1016/J.CHEMBIOL.2018.05.003

Cheng, L., Pilder, S., Nairn, A. C., Ramdas, S., & Vijayaraghavan, S. (2009). PP1γ2 and PPP1R11 Are Parts of a Multimeric Complex in Developing Testicular Germ Cells in which their Steady State Levels Are Reciprocally Related. *PLoS ONE*, *4*(3), 4861. https://doi.org/10.1371/JOURNAL.PONE.0004861

Chen, M. J., Dixon, J. E., & Manning, G. (2017). Genomics and evolution of protein phosphatases. *Science Signaling*, *10*(474). https://doi.org/10.1126/SCISIGNAL.AAG1796

Chen, Y. N. P., Lamarche, M. J., Chan, H. M., Fekkes, P., Garcia-Fortanet, J., Acker, M. G., Antonakos, B., Chen, C. H. T., Chen, Z., Cooke, V. G., Dobson, J. R., Deng, Z., Fei, F., Firestone, B., Fodor, M., Fridrich, C., Gao, H., Grunenfelder, D., Hao, H. X., … Fortin, P. D. (2016). Allosteric inhibition of SHP2 phosphatase inhibits cancers driven by receptor tyrosine kinases. *Nature*, *535*(7610), 148–152. https://doi.org/10.1038/NATURE18621

Cheon, Y., Kim, H., Park, K., Kim, M., & Lee, D. (2020). Dynamic modules of the coactivator SAGA in eukaryotic transcription. *Experimental & Molecular Medicine*, *52*(7), 991. https://doi.org/10.1038/S12276-020-0463-4

Cipak, L. (2022). Protein Kinases: Function, Substrates, and Implication in Diseases. *International Journal of Molecular Sciences*, *23*(7). https://doi.org/10.3390/IJMS23073560

Cobb, D. W., Florentin, A., Fierro, M. A., Krakowiak, M., Moore, J. M., & Muralidharan, V. (2017). The Exported Chaperone PfHsp70x Is Dispensable for the Plasmodium falciparum Intraerythrocytic Life Cycle. *MSphere*, *2*(5). https://doi.org/10.1128/MSPHERE.00363-17

Cobbold, S. A., Santos, J. M., Ochoa, A., Perlman, D. H., & Llinas, M. (2016). Proteome-wide analysis reveals widespread lysine acetylation of major protein complexes in the malaria parasite. *Scientific Reports*, *6*. https://doi.org/10.1038/SREP19722

Coetzee, M. (2020). Key to the females of Afrotropical Anopheles mosquitoes (Diptera: Culicidae). *Malaria Journal*, *19*(1), 1–20. https://doi.org/10.1186/S12936-020-3144-9/FIGURES/1

Cohen, P. (2000). The regulation of protein function by multisite phosphorylation--a 25 year update. *Trends in Biochemical Sciences*, *25*(12), 596–601. https://doi.org/10.1016/S0968-0004(00)01712-6

Coleman, B. I., Skillman, K. M., Jiang, R. H. Y., Childs, L. M., Altenhofen, L. M., Ganter, M., Leung, Y., Goldowitz, I., Kafsack, B. F. C., Marti, M., Llinás, M., Buckee, C. O., & Duraisingh, M. T. (2014). A Plasmodium falciparum Histone Deacetylase Regulates Antigenic Variation and Gametocyte Conversion. *Cell Host & Microbe*, *16*(2), 177. https://doi.org/10.1016/J.CHOM.2014.06.014

Collins, K. A., Snaith, R., Cottingham, M. G., Gilbert, S. C., & Hill, A. V. S. (2017). Enhancing protective immunity to malaria with a highly immunogenic virus-like particle vaccine. *Scientific Reports*, *7*. https://doi.org/10.1038/SREP46621

Connor, J. H., Weiser, D. C., Li, S., Hallenbeck, J. M., & Shenolikar, S. (2001). Growth arrest and DNA damage-inducible protein GADD34 assembles a novel signaling complex containing protein phosphatase 1 and inhibitor 1. *Molecular and Cellular Biology*, *21*(20), 6841–6850. https://doi.org/10.1128/MCB.21.20.6841-6850.2001

Cook, G. C., & Webb, A. J. (2000). Perceptions of malaria transmission before Ross' discovery in 1897. *Postgraduate Medical Journal*, *76*(901), 738–740. https://doi.org/10.1136/PMJ.76.901.738

Corona, R. I., & Guo, J. T. (2016). Statistical analysis of structural determinants for protein-DNA-binding specificity. *Proteins*, *84*(8), 1147–1161. https://doi.org/10.1002/PROT.25061

Cova, M., Rodrigues, J. A., Smith, T. K., & Izquierdo, L. (2015). Sugar activation and glycosylation in Plasmodium. *Malaria Journal*, *14*(1). https://doi.org/10.1186/S12936-015-0949-Z

Cowper, B., Matthews, S., & Tomley, F. (2012). The molecular basis for the distinct host and tissue tropisms of coccidian parasites. *Molecular and Biochemical Parasitology*, *186*(1), 1–10. https://doi.org/10.1016/J.MOLBIOPARA.2012.08.007

Cox, F. E. (2010). History of the discovery of the malaria parasites and their vectors. *Parasites & Vectors*, *3*(1). https://doi.org/10.1186/1756-3305-3-5

Cox, J., & Mann, M. (2008). MaxQuant enables high peptide identification rates, individualized p.p.b.-range mass accuracies and proteome-wide protein quantification. *Nature Biotechnology*, *26*(12), 1367–1372. https://doi.org/10.1038/NBT.1511

Cui, L., Fan, Q., Cui, L., & Miao, J. (2008). Histone lysine methyltransferases and demethylases in Plasmodium falciparum. *International Journal for Parasitology*, *38*(10), 1083. https://doi.org/10.1016/J.IJPARA.2008.01.002

CULVENOR, J. G., & CREWTHER, P. E. (1990). S-Antigen Localization in the Erythrocytic Stages of Plasmodium falciparum. *The Journal of Protozoology*, *37*(1), 59–65. https://doi.org/10.1111/J.1550-7408.1990.TB01117.X

Daams, R., & Massoumi, R. (2020). Nemo-Like Kinase in Development and Diseases: Insights from Mouse Studies. *International Journal of Molecular Sciences*, *21*(23), 1–8. https://doi.org/10.3390/IJMS21239203

Da Cruz E Silva, E. F., Fox, C. A., Ouimet, C. C., Gustafson, E., Watson, S. J., & Greengard, P. (1995). Differential expression of protein phosphatase 1 isoforms in mammalian brain. *The Journal of Neuroscience : The Official Journal of the Society for Neuroscience*, *15*(5 Pt 1), 3375–3389. https://doi.org/10.1523/JNEUROSCI.15-05-03375.1995

Daher, W., Browaeys, E., Pierrot, C., Jouin, H., Dive, D., Meurice, E., Dissous, C., Capron, M., Tomavo, S., Doerig, C., Cailliau, K., & Khalife, J. (2006). Regulation of protein phosphatase type 1 and cell cycle progression by PfLRR1, a novel leucine-rich repeat protein of the human malaria parasite Plasmodium falciparum. *Molecular Microbiology*, *60*(3), 578–590. https://doi.org/10.1111/J.1365-2958.2006.05119.X

Daher, W., Oria, G., Fauquenoy, S., Cailliau, K., Browaeys, E., Tomavo, S., & Khalife, J. (2007). A Toxoplasma gondii Leucine-Rich Repeat Protein Binds Phosphatase Type 1 Protein and Negatively Regulates Its Activity. *Eukaryotic Cell*, *6*(9), 1606. https://doi.org/10.1128/EC.00260-07

Davies, H., Belda, H., Broncel, M., Ye, X., Bisson, C., Introini, V., Dorin-Semblat, D., Semblat, J. P., Tibúrcio, M., Gamain, B., Kaforou, M., & Treeck, M. (2020). An exported kinase family mediates species-specific erythrocyte remodelling and virulence

in human malaria. *Nature Microbiology*, *5*(6), 848–863. https://doi.org/10.1038/S41564-020-0702-4

Dearnley, M., Chu, T., Zhang, Y., Looker, O., Huang, C., Klonis, N., Yeoman, J., Kenny, S., Arora, M., Osborne, J. M., Chandramohanadas, R., Zhang, S., Dixon, M. W. A., & Tilley, L. (2016). Reversible host cell remodeling underpins deformability changes in malaria parasite sexual blood stages. *Proceedings of the National Academy of Sciences of the United States of America*, *113*(17), 4800–4805. https://doi.org/10.1073/PNAS.1520194113/SUPPL_FILE/PNAS.1520194113.SM05.AVI

Dearnley, M. K., Yeoman, J. A., Hanssen, E., Kenny, S., Turnbull, L., Whitchurch, C. B., Tilley, L., & Dixon, M. W. A. (2012). Origin, composition, organization and function of the inner membrane complex of Plasmodium falciparum gametocytes. *Journal of Cell Science*, *125*(Pt 8), 2053–2063. https://doi.org/10.1242/JCS.099002

De Castro, I. J., Budzak, J., Di Giacinto, M. L., Ligammari, L., Gokhan, E., Spanos, C., Moralli, D., Richardson, C., De Las Heras, J. I., Salatino, S., Schirmer, E. C., Ullman, K. S., Bickmore, W. A., Green, C., Rappsilber, J., Lamble, S., Goldberg, M. W., Vinciotti, V., & Vagnarelli, P. (2017). Repo-Man/PP1 regulates heterochromatin formation in interphase. *Nature Communications 2017 8:1*, *8*(1), 1–16. https://doi.org/10.1038/ncomms14048

Delorme, V., Garcia, A., Cayla, X., & Tardieux, I. (2002). A role for Toxoplasma gondii type 1 ser/thr protein phosphatase in host cell invasion. *Microbes and Infection*, *4*(3), 271–278. https://doi.org/10.1016/S1286-4579(02)01538-1

Deroo, E., Zhou, T., & Liu, B. (2020). The Role of RIPK1 and RIPK3 in Cardiovascular Disease. *International Journal of Molecular Sciences*, *21*(21), 1–18. https://doi.org/10.3390/IJMS21218174

De Wever, V., Reiter, W., Ballarini, A., Ammerer, G., & Brocard, C. (2005). A dual role for PP1 in shaping the Msn2-dependent transcriptional response to glucose starvation. *The EMBO Journal*, *24*(23), 4115–4123. https://doi.org/10.1038/SJ.EMBOJ.7600871

De Witte, C., Aliouat, E. M., Chhuon, C., Guerrera, I. C., Pierrot, C., & Khalife, J. (2022). Mapping PP1c and Its Inhibitor 2 Interactomes Reveals Conserved and Specific Networks in Asexual and Sexual Stages of Plasmodium. *International Journal of Molecular Sciences*, *23*(3), 1069. https://doi.org/10.3390/IJMS23031069

Ding, X. C., Ubben, D., & Wells, T. N. (2012). A framework for assessing the risk of resistance for anti-malarials in development. *Malaria Journal*, *11*. https://doi.org/10.1186/1475-2875-11-292

Doerig, C., Rayner, J. C., Scherf, A., & Tobin, A. B. (2015). Post-translational protein modifications in malaria parasites. *Nature Reviews. Microbiology*, *13*(3), 160–172. https://doi.org/10.1038/NRMICRO3402

DOMBRÁDI, V., AXTON, J. M., BREWIS, N. D., DA CRUZ E SILVA, E. F., ALPHEY, L., & COHEN, P. T. W. (1990). Drosophila contains three genes that encode distinct isoforms of protein phosphatase 1. *European Journal of Biochemistry*, *194*(3), 739–745. https://doi.org/10.1111/J.1432-1033.1990.TB19464.X

Duraisingh, M. T., & Skillman, K. M. (2018). Epigenetic Variation and Regulation in Malaria Parasites. *Annual Review of Microbiology*, *72*, 355–375. https://doi.org/10.1146/ANNUREV-MICRO-090817-062722

Egloff, M. P., Cohen, P. T. W., Reinemer, P., & Barford, D. (1995). Crystal structure of the catalytic subunit of human protein phosphatase 1 and its complex with tungstate. *Journal of Molecular Biology*, *254*(5), 942–959. https://doi.org/10.1006/JMBI.1995.0667

Egloff, M. P., Johnson, D. F., Moorhead, G., Cohen, P. T. W., Cohen, P., & Barford, D. (1997). Structural basis for the recognition of regulatory subunits by the catalytic subunit of protein phosphatase 1. *The EMBO Journal*, *16*(8), 1876–1887. https://doi.org/10.1093/EMBOJ/16.8.1876

Eksi, S., Morahan, B. J., Haile, Y., Furuya, T., Jiang, H., Ali, O., Xu, H., Kiattibutr, K., Suri, A., Czesny, B., Adeyemo, A., Myers, T. G., Sattabongkot, J., Su, X. zhuan, & Williamson, K. C. (2012). Plasmodium falciparum Gametocyte Development 1 (Pfgdv1) and Gametocytogenesis Early Gene Identification and Commitment to Sexual Development. *PLoS Pathogens*, *8*(10). https://doi.org/10.1371/JOURNAL.PPAT.1002964

Eto, M., Elliott, E., Prickett, T. D., & Brautigan, D. L. (2002). Inhibitor-2 regulates protein phosphatase-1 complexed with NimA-related kinase to induce centrosome separation. *The Journal of Biological Chemistry*, *277*(46), 44013–44020. https://doi.org/10.1074/JBC.M208035200

Eyer, L., Kondo, H., Zouharova, D., Hirano, M., Valdés, J. J., Muto, M., Kastl, T., Kobayashi, S., Haviernik, J., Igarashi, M., Kariwa, H., Vaculovicova, M., Cerny, J., Kizek, R., Kröger, A., Lienenklaus, S., Dejmek, M., Nencka, R., Palus, M., … Ruzek, D. (2017). Escape of Tick-Borne Flavivirus from 2'- C-Methylated Nucleoside Antivirals Is Mediated by a Single Conservative Mutation in NS5 That Has a Dramatic Effect on Viral Fitness. *Journal of Virology*, *91*(21). https://doi.org/10.1128/JVI.01028-17

Farkas, I., Dombrádi, V., Miskei, M., Szabados, L., & Koncz, C. (2007). Arabidopsis PPP family of serine/threonine phosphatases. *Trends in Plant Science*, *12*(4), 169–176. https://doi.org/10.1016/J.TPLANTS.2007.03.003

Felsenstein, J. (1985). Confidence Limits on Phylogenies: An Approach Using the Bootstrap. *Evolution*, *39*(4), 783. https://doi.org/10.2307/2408678

Ferreira, M., Beullens, M., Bollen, M., & Van Eynde, A. (2019). Functions and therapeutic potential of protein phosphatase 1: Insights from mouse genetics. *Biochimica et*

*Biophysica Acta. Molecular Cell Research*, *1866*(1), 16–30.
https://doi.org/10.1016/J.BBAMCR.2018.07.019

Fienberg, S., Eyermann, C. J., Arendse, L. B., Basarab, G. S., McPhail, J. A., Burke, J. E., &
Chibale, K. (2020). Structural Basis for Inhibitor Potency and Selectivity of Plasmodium
falciparum Phosphatidylinositol 4-Kinase Inhibitors. *ACS Infectious Diseases*, *6*(11),
3048–3063. https://doi.org/10.1021/ACSINFECDIS.0C00566

Filarsky, M., Fraschka, S. A., Niederwieser, I., Brancucci, N. M. B., Carrington, E., Carrió,
E., Moes, S., Jenoe, P., Bártfai, R., & Voss, T. S. (2018). GDV1 induces sexual
commitment of malaria parasites by antagonizing HP1-dependent gene silencing.
*Science (New York, N.Y.)*, *359*(6381), 1259–1263.
https://doi.org/10.1126/SCIENCE.AAN6042

Fillinger, U., & Lindsay, S. W. (2011). Larval source management for malaria control in
Africa: myths and reality. *Malaria Journal*, *10*. https://doi.org/10.1186/1475-2875-10-
353

Franz, E., Knape, M. J., & Herberg, F. W. (2018). cGMP Binding Domain D Mediates a
Unique Activation Mechanism in Plasmodium falciparum PKG. *ACS Infectious
Diseases*, *4*(3), 415–423. https://doi.org/10.1021/ACSINFECDIS.7B00222

Freund, C., Dotsch, V., Nishizawa, K., Reinherz, E. L., & Wagner, G. (1999). The GYF
domain is a novel structural fold that is involved in lymphoid signaling through proline-
rich sequences. *Nature Structural Biology*, *6*(7), 656–660. https://doi.org/10.1038/10712

Freund, C., Kühne, R., Yang, H., Park, S., Reinherz, E. L., & Wagner, G. (2002). Dynamic
interaction of CD2 with the GYF and the SH3 domain of compartmentalized effector
molecules. *The EMBO Journal*, *21*(22), 5985. https://doi.org/10.1093/EMBOJ/CDF602

Fréville, A., Cailliau-Maggio, K., Pierrot, C., Tellier, G., Kalamou, H., Lafitte, S., Martoriati,
A., Pierce, R. J., Bodart, J. F., & Khalife, J. (2013). Plasmodium falciparum encodes a
conserved active inhibitor-2 for Protein Phosphatase type 1: perspectives for novel anti-
plasmodial therapy. *BMC Biology*, *11*. https://doi.org/10.1186/1741-7007-11-80

Fréville, A., Gnangnon, B., Khelifa, A. S., Gissot, M., Khalife, J., & Pierrot, C. (2022).
Deciphering the Role of Protein Phosphatases in Apicomplexa: The Future of Innovative
Therapeutics? *Microorganisms*, *10*(3).
https://doi.org/10.3390/MICROORGANISMS10030585

Fréville, A., Landrieu, I., García-Gimeno, M. A., Vicogne, J., Montbarbon, M., Bertin, B.,
Verger, A., Kalamou, H., Sanz, P., Werkmeister, E., Pierrot, C., & Khalife, J. (2012).
Plasmodium falciparum inhibitor-3 homolog increases protein phosphatase type 1
activity and is essential for parasitic survival. *The Journal of Biological Chemistry*,
*287*(2), 1306–1321. https://doi.org/10.1074/JBC.M111.276865

Fréville, A., Tellier, G., Vandomme, A., Pierrot, C., Vicogne, J., Cantrelle, F. X., Martoriati, A., Cailliau-Maggio, K., Khalife, J., & Landrieu, I. (2014). Identification of a Plasmodium falciparum inhibitor-2 motif involved in the binding and regulation activity of protein phosphatase type 1. *The FEBS Journal*, *281*(19), 4519–4534. https://doi.org/10.1111/FEBS.12960

Gardner, M. J., Hall, N., Fung, E., White, O., Berriman, M., Hyman, R. W., Carlton, J. M., Pain, A., Nelson, K. E., Bowman, S., Paulsen, I. T., James, K., Eisen, J. A., Rutherford, K., Salzberg, S. L., Craig, A., Kyes, S., Chan, M. S., Nene, V., … Barrell, B. (2002). Genome sequence of the human malaria parasite Plasmodium falciparum. *Nature*, *419*(6906), 498–511. https://doi.org/10.1038/NATURE01097

Garfield, R. M., & Vermund, S. H. (1983). Changes in malaria incidence after mass drug administration in Nicaragua. *Lancet (London, England)*, *2*(8348), 500–503. https://doi.org/10.1016/S0140-6736(83)90523-8

Garner, E., Romero, P., Dunker, A. K., Brown, C., & Obradovic, Z. (1999). Predicting Binding Regions within Disordered Proteins. *Genome Informatics*, *10*, 41–50. https://doi.org/10.11234/GI1990.10.41

Garza-Leon, M., & Arellanes Garcia, L. (2012). Ocular toxoplasmosis: clinical characteristics in pediatric patients. *Ocular Immunology and Inflammation*, *20*(2), 130–138. https://doi.org/10.3109/09273948.2012.656878

Gautam Srivastava, A., Bajaj, R., Senthil Kumar, G., Peti, W., Trinkle-Mulcahy, L., Srivastava, G., Gaudreau-Lapierre, A., Nicolas, H., Chamousset, D., Kreitler, D., & Page, R. (2022). *The ribosomal RNA processing 1B:protein phosphatase 1 holoenzyme reveals non-canonical PP1 interaction motifs*. https://doi.org/10.1016/j.celrep.2022.111726

Gazzinelli, R. T., Kalantari, P., Fitzgerald, K. A., & Golenbock, D. T. (2014). Innate sensing of malaria parasites. *Nature Reviews. Immunology*, *14*(11), 744–757. https://doi.org/10.1038/NRI3742

Gebauer, F., & Hentze, M. W. (2004). Molecular mechanisms of translational control. *Nature Reviews. Molecular Cell Biology*, *5*(10), 827–835. https://doi.org/10.1038/NRM1488

Gibbons, J. A., Kozubowski, L., Tatchell, K., & Shenolikar, S. (2007). Expression of human protein phosphatase-1 in Saccharomyces cerevisiae highlights the role of phosphatase isoforms in regulating eukaryotic functions. *The Journal of Biological Chemistry*, *282*(30), 21838–21847. https://doi.org/10.1074/JBC.M701272200

Gohil, S., Kats, L. M., Sturm, A., & Cooke, B. M. (2010). Recent insights into alteration of red blood cells by Babesia bovis: moovin' forward. *Trends in Parasitology*, *26*(12), 591–599. https://doi.org/10.1016/J.PT.2010.06.012

Goldberg, J., Huang, H. Bin, Kwon, Y. G., Greengard, P., Nairn, A. C., & Kuriyan, J. (1995). Three-dimensional structure of the catalytic subunit of protein serine/threonine phosphatase-1. *Nature*, *376*(6543), 745–753. https://doi.org/10.1038/376745A0

Goodwin, S., McPherson, J. D., & McCombie, W. R. (2016). Coming of age: ten years of next-generation sequencing technologies. *Nature Reviews. Genetics*, *17*(6), 333–351. https://doi.org/10.1038/NRG.2016.49

Goswami, S., Korrodi-Gregório, L., Sinha, N., Bhutada, S., Bhattacharjee, R., Kline, D., & Vijayaraghavan, S. (2019). Regulators of the protein phosphatase PP1γ2, PPP1R2, PPP1R7, and PPP1R11 are involved in epididymal sperm maturation. *Journal of Cellular Physiology*, *234*(3), 3105–3118. https://doi.org/10.1002/JCP.27130

Grallert, A., Boke, E., Hagting, A., Hodgson, B., Connolly, Y., Griffiths, J. R., Smith, D. L., Pines, J., & Hagan, I. M. (2015). A PP1-PP2A phosphatase relay controls mitotic progression. *Nature*, *517*(7532), 94–98. https://doi.org/10.1038/NATURE14019

Grant, C. E., Bailey, T. L., & Noble, W. S. (2011). FIMO: scanning for occurrences of a given motif. *Bioinformatics (Oxford, England)*, *27*(7), 1017–1018. https://doi.org/10.1093/BIOINFORMATICS/BTR064

Greenwood, B. (2017). Elimination of malaria: halfway there. *Transactions of the Royal Society of Tropical Medicine and Hygiene*, *111*(1), 1–2. https://doi.org/10.1093/TRSTMH/TRX012

Grüring, C., Moon, R. W., Lim, C., Holder, A. A., Blackman, M. J., & Duraisingh, M. T. (2014). Human red blood cell-adapted Plasmodium knowlesi parasites: a new model system for malaria research. *Cellular Microbiology*, *16*(5), 612. https://doi.org/10.1111/CMI.12275

Grusche, F. A., Hidalgo, C., Fletcher, G., Sung, H. H., Sahai, E., & Thompson, B. J. (2009). Sds22, a PP1 phosphatase regulatory subunit, regulates epithelial cell polarity and shape [Sds22 in epithelial morphology]. *BMC Developmental Biology*, *9*(1), 14. https://doi.org/10.1186/1471-213X-9-14

Gubbels, M. J., & Duraisingh, M. T. (2012). Evolution of apicomplexan secretory organelles. *International Journal for Parasitology*, *42*(12), 1071–1081. https://doi.org/10.1016/J.IJPARA.2012.09.009

Guttery, D. S., Poulin, B., Ramaprasad, A., Wall, R. J., Ferguson, D. J. P., Brady, D., Patzewitz, E. M., Whipple, S., Straschil, U., Wright, M. H., Mohamed, A. M. A. H., Radhakrishnan, A., Arold, S. T., Tate, E. W., Holder, A. A., Wickstead, B., Pain, A., & Tewari, R. (2014). Genome-wide Functional Analysis of Plasmodium Protein Phosphatases Reveals Key Regulators of Parasite Development and Differentiation. *Cell Host & Microbe*, *16*(1), 128. https://doi.org/10.1016/J.CHOM.2014.05.020

Hamilton, M. J., Lee, M., & Le Roch, K. G. (2014). The ubiquitin system: an essential component to unlocking the secrets of malaria parasite biology. *Molecular BioSystems*, *10*(4), 715–723. https://doi.org/10.1039/C3MB70506D

Han, E. J., Lee, H. N., Kim, M. K., Lyu, S. W., & Lee, W. S. (2021). Efficacy of intralipid administration to improve in vitro fertilization outcomes: A systematic review and meta-analysis. *Clinical and Experimental Reproductive Medicine*, *48*(3), 203–210. https://doi.org/10.5653/CERM.2020.04266

Hänscheid, T., Längin, M., Lell, B., Pötschke, M., Oyakhirome, S., Kremsner, P. G., & Grobusch, M. P. (2008). Full blood count and haemozoin-containing leukocytes in children with malaria: Diagnostic value and association with disease severity. *Malaria Journal*, *7*(1), 1–10. https://doi.org/10.1186/1475-2875-7-109/TABLES/5

Harding, C. R., & Meissner, M. (2014). The inner membrane complex through development of Toxoplasma gondii and Plasmodium. *Cellular Microbiology*, *16*(5), 632–641. https://doi.org/10.1111/CMI.12285

Hattersley, N., Cheerambathur, D., Moyle, M., Stefanutti, M., Richardson, A., Lee, K. Y., Dumont, J., Oegema, K., & Desai, A. (2016). A Nucleoporin Docks Protein Phosphatase 1 to Direct Meiotic Chromosome Segregation and Nuclear Assembly. *Developmental Cell*, *38*(5), 463–477. https://doi.org/10.1016/J.DEVCEL.2016.08.006

Hawass, Z., Gad, Y. Z., Ismail, S., Khairat, R., Fathalla, D., Hasan, N., Ahmed, A., Elleithy, H., Ball, M., Gaballah, F., Wasef, S., Fateen, M., Amer, H., Gostner, P., Selim, A., Zink, A., & Pusch, C. M. (2010). Ancestry and pathology in King Tutankhamun's family. *JAMA*, *303*(7), 638–647. https://doi.org/10.1001/JAMA.2010.121

Hawking, F., Wilson, M. E., & Gammage, K. (1971). Evidence for cyclic development and short-lived maturity in the gametocytes of Plasmodium falciparum. *Transactions of the Royal Society of Tropical Medicine and Hygiene*, *65*(5), 549–559. https://doi.org/10.1016/0035-9203(71)90036-8

Heinze, M., Kofler, M., & Freund, C. (2007). Investigating the functional role of CD2BP2 in T cells. *International Immunology*, *19*(11), 1313–1318. https://doi.org/10.1093/INTIMM/DXM100

Helps, N. R., Vergidou, C., Gaskell, T., & Cohen, P. T. w. (1998). Characterisation of a novel Drosophila melanogaster testis specific PP1 inhibitor related to mammalian inhibitor-2: identification of the site of interaction with PP1. *FEBS Letters*, *438*(1–2), 131–136. https://doi.org/10.1016/S0014-5793(98)01286-1

Hendrickx, A., Beullens, M., Ceulemans, H., Den Abt, T., Van Eynde, A., Nicolaescu, E., Lesage, B., & Bollen, M. (2009). Docking motif-guided mapping of the interactome of protein phosphatase-1. *Chemistry & Biology*, *16*(4), 365–371. https://doi.org/10.1016/J.CHEMBIOL.2009.02.012

Herneisen, A. L., Li, Z. H., Chan, A. W., Moreno, S. N. J., & Lourido, S. (2022). Temporal and thermal profiling of the Toxoplasma proteome implicates parasite Protein Phosphatase 1 in the regulation of Ca2+-responsive pathways. *ELife*, *11*. https://doi.org/10.7554/ELIFE.80336

Heroes, E., Lesage, B., Görnemann, J., Beullens, M., Van Meervelt, L., & Bollen, M. (2013). The PP1 binding code: a molecular-lego strategy that governs specificity. *The FEBS Journal*, *280*(2), 584–595. https://doi.org/10.1111/J.1742-4658.2012.08547.X

Heroes, E., Rip, J., Beullens, M., Van Meervelt, L., De Gendt, S., & Bollen, M. (2015). Metals in the active site of native protein phosphatase-1. *Journal of Inorganic Biochemistry*, *149*, 1–5. https://doi.org/10.1016/J.JINORGBIO.2015.03.012

Heroes, E., Van der Hoeven, G., Choy, M. S., Garcia, J. del P., Ferreira, M., Nys, M., Derua, R., Beullens, M., Ulens, C., Peti, W., Van Meervelt, L., Page, R., & Bollen, M. (2019). Structure-Guided Exploration of SDS22 Interactions with Protein Phosphatase PP1 and the Splicing Factor BCLAF1. *Structure (London, England : 1993)*, *27*(3), 507-518.e5. https://doi.org/10.1016/J.STR.2018.12.002

Hilioti, Z., Gallagher, D. A., Low-Nam, S. T., Ramaswamy, P., Gajer, P., Kingsbury, T. J., Birchwood, C. J., Levchenko, A., & Cunningham, K. W. (2004). GSK-3 kinases enhance calcineurin signaling by phosphorylation of RCNs. *Genes & Development*, *18*(1), 35. https://doi.org/10.1101/GAD.1159204

Hoeijmakers, W. A. M., Miao, J., Schmidt, S., Toenhake, C. G., Shrestha, S., Venhuizen, J., Henderson, R., Birnbaum, J., Ghidelli-Disse, S., Drewes, G., Cui, L., Stunnenberg, H. G., Spielmann, T., & Bártfai, R. (2019). Epigenetic reader complexes of the human malaria parasite, Plasmodium falciparum. *Nucleic Acids Research*, *47*(22), 11574–11588. https://doi.org/10.1093/NAR/GKZ1044

Hole, A. P., & Pulijala, V. (2021). An Inductive-Based Sensitive and Reusable Sensor for the Detection of Malaria. *IEEE Sensors Journal*, *21*(2), 1609–1615. https://doi.org/10.1109/JSEN.2020.3016657

Hollin, T., De Witte, C., Fréville, A., Guerrera, I. C., Chhuon, C., Saliou, J. M., Herbert, F., Pierrot, C., & Khalife, J. (2019). Essential role of GEXP15, a specific Protein Phosphatase type 1 partner, in Plasmodium berghei in asexual erythrocytic proliferation and transmission. *PLoS Pathogens*, *15*(7). https://doi.org/10.1371/JOURNAL.PPAT.1007973

Hollin, T., De Witte, C., Lenne, A., Pierrot, C., & Khalife, J. (2016). Analysis of the interactome of the Ser/Thr Protein Phosphatase type 1 in Plasmodium falciparum. *BMC Genomics*, *17*(1), 1–16. https://doi.org/10.1186/S12864-016-2571-Z/FIGURES/4

Hollin, T., & Le Roch, K. G. (2020). From Genes to Transcripts, a Tightly Regulated Journey in Plasmodium. *Frontiers in Cellular and Infection Microbiology*, *10*. https://doi.org/10.3389/FCIMB.2020.618454

Huang, H. Bin, Horiuchi, A., Watanabe, T., Shih, S. R., Tsay, H. J., Li, H. C., Greengard, P., & Nairn, A. C. (1999). Characterization of the inhibition of protein phosphatase-1 by DARPP-32 and inhibitor-2. *The Journal of Biological Chemistry*, *274*(12), 7870–7878. https://doi.org/10.1074/JBC.274.12.7870

HUANG, F. L., & GLINSMANN, W. H. (1976). Separation and characterization of two phosphorylase phosphatase inhibitors from rabbit skeletal muscle. *European Journal of Biochemistry*, *70*(2), 419–426. https://doi.org/10.1111/J.1432-1033.1976.TB11032.X

Huang, H. B., Chen, Y. C., Tsai, L. H., Wang, H. C., Lin, F. M., Horiuchi, A., Greengard, P., Nairn, A. C., Shiao, M. S., & Lin, T. H. (2000). Backbone 1H, 15N, and 13C resonance assignments of inhibitor-2 - A protein inhibitor of protein phosphatase-1 [6]. *Journal of Biomolecular NMR*, *17*(4), 359–360. https://doi.org/10.1023/A:1008355428294

Huang, H. S., Pozarowski, P., Gao, Y., Darzynkiewicz, Z., & Lee, E. Y. C. (2005). Protein phosphatase-1 inhibitor-3 is co-localized to the nucleoli and centrosomes with PP1gamma1 and PP1alpha, respectively. *Archives of Biochemistry and Biophysics*, *443*(1–2), 33–44. https://doi.org/10.1016/J.ABB.2005.08.021

Hunter, T., & Pawson, T. (2012). The evolution of protein phosphorylation. Preface. *Philosophical Transactions of the Royal Society of London. Series B, Biological Sciences*, *367*(1602), 2512. https://doi.org/10.1098/RSTB.2012.0374

Hurley, T. D., Yang, J., Zhang, L., Goodwin, K. D., Zou, Q., Cortese, M., Dunker, A. K., & DePaoli-Roach, A. A. (2007). Structural basis for regulation of protein phosphatase 1 by inhibitor-2. *The Journal of Biological Chemistry*, *282*(39), 28874–28883. https://doi.org/10.1074/JBC.M703472200

Iwanaga, S., Kaneko, I., Kato, T., & Yuda, M. (2012). Identification of an AP2-family Protein That Is Critical for Malaria Liver Stage Development. *PLOS ONE*, *7*(11), e47557. https://doi.org/10.1371/JOURNAL.PONE.0047557

Janovská, P., Normant, E., Miskin, H., & Bryja, V. (2020). Targeting Casein Kinase 1 (CK1) in Hematological Cancers. *International Journal of Molecular Sciences*, *21*(23), 1–19. https://doi.org/10.3390/IJMS21239026

Jha, P., Gahlawat, A., Bhattacharyya, S., Dey, S., Kumar, K. A., & Bhattacharyya, M. K. (2021). Bloom Helicase Along with Recombinase Rad51 Repairs the Mitochondrial Genome of the Malaria Parasite. *MSphere*, *6*(6). https://doi.org/10.1128/MSPHERE.00718-21

Jiang, J. B., Guo, X. B., Li, G. Q., Cheung Kong, Y., & Arnold, K. (1982). Antimalarial activity of mefloquine and qinghaosu. *Lancet (London, England)*, *2*(8293), 285–288. https://doi.org/10.1016/S0140-6736(82)90268-9

Jiang, X., Hu, J., Wu, Z., Cafarello, S. T., Di Matteo, M., Shen, Y., Dong, X., Adler, H., Mazzone, M., Ruiz de Almodovar, C., & Wang, X. (2021). Protein Phosphatase 2A

Mediates YAP Activation in Endothelial Cells Upon VEGF Stimulation and Matrix Stiffness. *Frontiers in Cell and Developmental Biology*, *9*. https://doi.org/10.3389/FCELL.2021.675562

Jones, D. T., Taylor, W. R., & Thornton, J. M. (1992). The rapid generation of mutation data matrices from protein sequences. *Computer Applications in the Biosciences : CABIOS*, *8*(3), 275–282. https://doi.org/10.1093/BIOINFORMATICS/8.3.275

Joy, D. A., Feng, X., Mu, J., Furuya, T., Chotivanich, K., Krettli, A. U., Ho, M., Wang, A., White, N. J., Suh, E., Beerli, P., & Su, X. zhuan. (2003). Early origin and recent expansion of Plasmodium falciparum. *Science (New York, N.Y.)*, *300*(5617), 318–321. https://doi.org/10.1126/SCIENCE.1081449

Kafsack, B. F. C., Rovira-Graells, N., Clark, T. G., Bancells, C., Crowley, V. M., Campino, S. G., Williams, A. E., Drought, L. G., Kwiatkowski, D. P., Baker, D. A., Cortés, A., & Llinás, M. (2014). A transcriptional switch underlies commitment to sexual development in malaria parasites. *Nature*, *507*(7491), 248–252. https://doi.org/10.1038/NATURE12920

Kannan, D., Kaur, A., Salunke, D. B., & Singh, S. (2022). Toll-Like Receptor-Based Adjuvants: A Gateway Toward Improved Malaria Vaccination. *Drug Development for Malaria: Novel Approaches for Prevention and Treatment*, 319–351. https://doi.org/10.1002/9783527830589.CH14

Karpiyevich, M., & Artavanis-Tsakonas, K. (2020). Ubiquitin-Like Modifiers: Emerging Regulators of Protozoan Parasites. *Biomolecules 2020, Vol. 10, Page 1403*, *10*(10), 1403. https://doi.org/10.3390/BIOM10101403

Kats, L. M., Fernandez, K. M., Glenister, F. K., Herrmann, S., Buckingham, D. W., Siddiqui, G., Sharma, L., Bamert, R., Lucet, I., Guillotte, M., Mercereau-Puijalon, O., & Cooke, B. M. (2014). An exported kinase (FIKK4.2) that mediates virulence-associated changes in Plasmodium falciparum-infected red blood cells. *International Journal for Parasitology*, *44*(5), 319–328. https://doi.org/10.1016/J.IJPARA.2014.01.003

Kemp, L. E., Yamamoto, M., & Soldati-Favre, D. (2013). Subversion of host cellular functions by the apicomplexan parasites. *FEMS Microbiology Reviews*, *37*(4), 607–631. https://doi.org/10.1111/1574-6976.12013

Khelifa, A. S., Boissavy, T., Mouveaux, T., Silva, T. A., Chhuon, C., Attias, M., Guerrera, I. C., Souza, W. De, Dauvillee, D., Roger, E., & Gissot, M. (2023). The PP1 phosphatase exhibits pleiotropic roles controlling both the tachyzoite cell cycle and amylopectin-steady state levels in Toxoplasma gondii. *BioRxiv*, 2023.08.10.552784. https://doi.org/10.1101/2023.08.10.552784

Knight, Z. A., & Shokat, K. M. (2005). Features of Selective Kinase Inhibitors. *Chemistry & Biology*, *12*(6), 621–637. https://doi.org/10.1016/J.CHEMBIOL.2005.04.011

Kobe, B., & Deisenhofer, J. (1995). A structural basis of the interactions between leucine-rich repeats and protein ligands. *Nature 1995 374:6518*, *374*(6518), 183–186. https://doi.org/10.1038/374183a0

Kobe, B., & Kajava, A. V. (2001). The leucine-rich repeat as a protein recognition motif. *Current Opinion in Structural Biology*, *11*(6), 725–732. https://doi.org/10.1016/S0959-440X(01)00266-4

Kofler, M., Motzny, K., Beyermann, M., & Freund, C. (2005). Novel Interaction Partners of the CD2BP2-GYF Domain. *Journal of Biological Chemistry*, *280*(39), 33397–33402. https://doi.org/10.1074/JBC.M503989200

Kofler, M., Schuemann, M., Merz, C., Kosslick, D., Schlundt, A., Tannert, A., Schaefer, M., Lührmann, R., Krause, E., & Freund, C. (2009). Proline-rich sequence recognition: I. Marking GYF and WW domain assembly sites in early spliceosomal complexes. *Molecular & Cellular Proteomics : MCP*, *8*(11), 2461–2473. https://doi.org/10.1074/MCP.M900191-MCP200

Korrodi-Gregório, L., Esteves, S. L. C., & Fardilha, M. (2014). Protein phosphatase 1 catalytic isoforms: specificity toward interacting proteins. *Translational Research : The Journal of Laboratory and Clinical Medicine*, *164*(5), 366–391. https://doi.org/10.1016/J.TRSL.2014.07.001

Kotloff, K. L., Nataro, J. P., Blackwelder, W. C., Nasrin, D., Farag, T. H., Panchalingam, S., Wu, Y., Sow, S. O., Sur, D., Breiman, R. F., Faruque, A. S. G., Zaidi, A. K. M., Saha, D., Alonso, P. L., Tamboura, B., Sanogo, D., Onwuchekwa, U., Manna, B., Ramamurthy, T., … Levine, M. M. (2013). Burden and aetiology of diarrhoeal disease in infants and young children in developing countries (the Global Enteric Multicenter Study, GEMS): a prospective, case-control study. *Lancet (London, England)*, *382*(9888), 209–222. https://doi.org/10.1016/S0140-6736(13)60844-2

Koussis, K., Withers-Martinez, C., Baker, D. A., & Blackman, M. J. (2020). Simultaneous multiple allelic replacement in the malaria parasite enables dissection of PKG function. *Life Science Alliance*, *3*(4). https://doi.org/10.26508/LSA.201900626

Krishnan, M., Teply, B. A., Yu, F., & High, R. (2020). Impact of performance status on response and survival among patients receiving checkpoint inhibitors for advanced solid tumors. *Https://Doi.Org/10.1200/JCO.2020.38.15_suppl.12028*, *38*(15_suppl), 12028–12028. https://doi.org/10.1200/JCO.2020.38.15_SUPPL.12028

Krzyzosiak, A., Sigurdardottir, A., Luh, L., Carrara, M., Das, I., Schneider, K., & Bertolotti, A. (2018). Target-Based Discovery of an Inhibitor of the Regulatory Phosphatase PPP1R15B. *Cell*, *174*(5), 1216-1228.e19. https://doi.org/10.1016/J.CELL.2018.06.030

Kudlik, G., Takács, T., Radnai, L., Kurilla, A., Szeder, B., Koprivanacz, K., Merő, B. L., Buday, L., & Vas, V. (2020). Advances in Understanding TKS4 and TKS5: Molecular Scaffolds Regulating Cellular Processes from Podosome and Invadopodium Formation

to Differentiation and Tissue Homeostasis. *International Journal of Molecular Sciences*, *21*(21), 1–28. https://doi.org/10.3390/IJMS21218117

Kudyba, H. M., Cobb, D. W., Vega-Rodríguez, J., & Muralidharan, V. (2021). Some conditions apply: Systems for studying Plasmodium falciparum protein function. *PLoS Pathogens*, *17*(4). https://doi.org/10.1371/JOURNAL.PPAT.1009442

Kumar, R., Adams, B., Oldenburg, A., Musiyenko, A., & Barik, S. (2002). Characterisation and expression of a PP1 serine/threonine protein phosphatase (PfPP1) from the malaria parasite, Plasmodium falciparum: demonstration of its essential role using RNA interference. *Malaria Journal*, *1*(1), 5. https://doi.org/10.1186/1475-2875-1-5

Kupferschmid, M., Aquino-Gil, M. O., Shams-Eldin, H., Schmidt, J., Yamakawa, N., Krzewinski, F., Schwarz, R. T., & Lefebvre, T. (2017). Identification of O-GlcNAcylated proteins in Plasmodium falciparum. *Malaria Journal*, *16*(1). https://doi.org/10.1186/S12936-017-2131-2

Kutay, U., Wild, T., Horvath, P., Wyler, E., Widmann, B., Badertscher, L., Zemp, I., Kozak, K., Csucs, G., & Lund, E. (2010). A Protein Inventory of Human Ribosome Biogenesis Reveals an Essential Function of Exportin 5 in 60S Subunit Export. *PLOS Biology*, *8*(10), e1000522. https://doi.org/10.1371/JOURNAL.PBIO.1000522

Kwon, Y. G., Lee, S. Y., Choi, Y., Greengard, P., & Nairn, A. C. (1997). Cell cycle-dependent phosphorylation of mammalian protein phosphatase 1 by cdc2 kinase. *Proceedings of the National Academy of Sciences of the United States of America*, *94*(6), 2168–2173. https://doi.org/10.1073/PNAS.94.6.2168

Lad, C., Williams, N. H., & Wolfenden, R. (2003). The rate of hydrolysis of phosphomonoester dianions and the exceptional catalytic proficiencies of protein and inositol phosphatases. *Proceedings of the National Academy of Sciences of the United States of America*, *100*(10), 5607. https://doi.org/10.1073/PNAS.0631607100

Laggerbauer, B., Liu, S., Makarov, E., Vornlocher, H. P., Makarova, O., Ingelfinger, D., Achsel, T., & Lührmann, R. (2005). The human U5 snRNP 52K protein (CD2BP2) interacts with U5-102K (hPrp6), a U4/U6.U5 tri-snRNP bridging protein, but dissociates upon tri-snRNP formation. *RNA*, *11*(5), 598. https://doi.org/10.1261/RNA.2300805

Lajarín-Cuesta, R., Arribas, R. L., & De Los Rios, C. (2016). Ligands for Ser/Thr phosphoprotein phosphatases: a patent review (2005-2015). *Expert Opinion on Therapeutic Patents*, *26*(3), 389–407. https://doi.org/10.1517/13543776.2016.1135903

Lasonder, E., Green, J. L., Camarda, G., Talabani, H., Holder, A. A., Langsley, G., & Alano, P. (2012). The plasmodium falciparum schizont phosphoproteome reveals extensive phosphatidylinositol and cAMP-protein kinase A signaling. *Journal of Proteome Research*, *11*(11), 5323–5337. https://doi.org/10.1021/PR300557M/SUPPL_FILE/PR300557M_SI_009.XLSX

Lasonder, E., Rijpma, S. R., Van Schaijk, B. C. L., Hoeijmakers, W. A. M., Kensche, P. R., Gresnigt, M. S., Italiaander, A., Vos, M. W., Woestenenk, R., Bousema, T., Mair, G. R., Khan, S. M., Janse, C. J., Bártfai, R., & Sauerwein, R. W. (2016). Integrated transcriptomic and proteomic analyses of P. falciparum gametocytes: molecular insight into sex-specific processes and translational repression. *Nucleic Acids Research*, *44*(13), 6087. https://doi.org/10.1093/NAR/GKW536

Lasonder, E., Treeck, M., Alam, M., & Tobin, A. B. (2012). Insights into the Plasmodium falciparum schizont phospho-proteome. *Microbes and Infection*, *14*(10), 811–819. https://doi.org/10.1016/J.MICINF.2012.04.008

Leach, C., Shenolikar, S., & Brautigan, D. L. (2003). Phosphorylation of Phosphatase Inhibitor-2 at Centrosomes during Mitosis. *Journal of Biological Chemistry*, *278*(28), 26015–26020. https://doi.org/10.1074/JBC.M300782200

Lei, X., Ning, Y., Eid Elesawi, I., Yang, K., Chen, C., Wang, C., & Liu, B. (2020). Heat stress interferes with chromosome segregation and cytokinesis during male meiosis in Arabidopsis thaliana. *Plant Signaling & Behavior*, *15*(5). https://doi.org/10.1080/15592324.2020.1746985

Lemonnier, T., Daldello, E. M., Poulhe, R., Le, T., Miot, M., Lignières, L., Jessus, C., & Dupré, A. (2021). The M-phase regulatory phosphatase PP2A-B55δ opposes protein kinase A on Arpp19 to initiate meiotic division. *Nature Communications*, *12*(1). https://doi.org/10.1038/S41467-021-22124-0

Lenne, A., De Witte, C., Tellier, G., Hollin, T., Aliouat, E. M., Martoriati, A., Cailliau, K., Saliou, J. M., Khalife, J., & Pierrot, C. (2018). Characterization of a Protein Phosphatase Type-1 and a Kinase Anchoring Protein in Plasmodium falciparum. *Frontiers in Microbiology*, *9*. https://doi.org/10.3389/FMICB.2018.02617

Le Roch, K. G., Zhou, Y., Blair, P. L., Grainger, M., Moch, J. K., Haynes, J. D., De la Vega, P., Holder, A. A., Batalov, S., Carucci, D. J., & Winzeler, E. A. (2003). Discovery of gene function by expression profiling of the malaria parasite life cycle. *Science (New York, N.Y.)*, *301*(5639), 1503–1508. https://doi.org/10.1126/SCIENCE.1087025

Lesage, B., Beullens, M., Pedelini, L., Garcia-Gimeno, M. A., Waelkens, E., Sanz, P., & Bollen, M. (2007). A complex of catalytically inactive protein phosphatase-1 sandwiched between Sds22 and inhibitor-3. *Biochemistry*, *46*(31), 8909–8919. https://doi.org/10.1021/BI7003119

Liang, X., Hart, K. J., Dong, G., Siddiqui, F. A., Sebastian, A., Li, X., Albert, I., Miao, J., Lindner, S. E., & Cui, L. (2018). Puf3 participates in ribosomal biogenesis in malaria parasites. *Journal of Cell Science*, *131*(6). https://doi.org/10.1242/JCS.212597

Li, M., Satinover, D. L., & Brautigan, D. L. (2007). Phosphorylation and functions of inhibitor-2 family of proteins. *Biochemistry*, *46*(9), 2380–2389. https://doi.org/10.1021/BI602369M

Lin, T. H., Chen, Y. C., Chyan, C. L., Tsay, L. H., Tang, T. C., Jeng, H. H., Lin, F. M., & Huang, H. Bin. (2003). Phosphorylation by glycogen synthase kinase of inhibitor-2 does not change its structure in free state. *FEBS Letters*, *554*(3), 253–256. https://doi.org/10.1016/S0014-5793(03)01097-4

López-Barragán, M. J., Lemieux, J., Quiñones, M., Williamson, K. C., Molina-Cruz, A., Cui, K., Barillas-Mury, C., Zhao, K., & Su, X. zhuan. (2011). Directional gene expression and antisense transcripts in sexual and asexual stages of Plasmodium falciparum. *BMC Genomics*, *12*. https://doi.org/10.1186/1471-2164-12-587

Ludlow, R. F., Verdonk, M. L., Saini, H. K., Tickle, I. J., & Jhoti, H. (2015). Detection of secondary binding sites in proteins using fragment screening. *Proceedings of the National Academy of Sciences of the United States of America*, *112*(52), 15910–15915. https://doi.org/10.1073/PNAS.1518946112

Mahindra, A., Janha, O., Mapesa, K., Sanchez-Azqueta, A., Alam, M. M., Amambua-Ngwa, A., Nwakanma, D. C., Tobin, A. B., & Jamieson, A. G. (2020). Development of Potent Pf CLK3 Inhibitors Based on TCMDC-135051 as a New Class of Antimalarials. *Journal of Medicinal Chemistry*, *63*(17), 9300–9315. https://doi.org/10.1021/ACS.JMEDCHEM.0C00451

Maier, A. G., Matuschewski, K., Zhang, M., & Rug, M. (2019). Plasmodium falciparum. *Trends in Parasitology*, *35*(6), 481–482. https://doi.org/10.1016/j.pt.2018.11.010

Mair, G. R., Braks, J. A. M., Garver, L. S., Wiegant, J. C. A. G., Hall, N., Dirks, R. W., Khan, S. M., Dimopoulos, G., Janse, C. J., & Waters, A. P. (2006). Regulation of sexual development of Plasmodium by translational repression. *Science (New York, N.Y.)*, *313*(5787), 667–669. https://doi.org/10.1126/SCIENCE.1125129

Malleret, B., Li, A., Zhang, R., Tan, K. S. W., Suwanarusk, R., Claser, C., Cho, J. S., Koh, E. G. L., Chu, C. S., Pukrittayakamee, S., Ng, M. L., Ginhoux, F., Ng, L. G., Lim, C. T., Nosten, F., Snounou, G., Rénia, L., & Russell, B. (2015). Plasmodium vivax: restricted tropism and rapid remodeling of CD71-positive reticulocytes. *Blood*, *125*(8), 1314–1324. https://doi.org/10.1182/BLOOD-2014-08-596015

Manna, P. R., Dyson, M. T., & Stocco, D. M. (2009). Regulation of the steroidogenic acute regulatory protein gene expression: present and future perspectives. *Molecular Human Reproduction*, *15*(6), 321. https://doi.org/10.1093/MOLEHR/GAP025

Manzano-Román, R., & Fuentes, M. (2020). Relevance and proteomics challenge of functional posttranslational modifications in Kinetoplastid parasites. *Journal of Proteomics*, *220*, 103762. https://doi.org/10.1016/J.JPROT.2020.103762

Martin, F. A., Murphy, R. P., & Cummins, P. M. (2013). Thrombomodulin and the vascular endothelium: insights into functional, regulatory, and therapeutic aspects. *American Journal of Physiology. Heart and Circulatory Physiology*, *304*(12). https://doi.org/10.1152/AJPHEART.00096.2013

Meiselbach, H., Sticht, H., & Enz, R. (2006). Structural analysis of the protein phosphatase 1 docking motif: molecular description of binding specificities identifies interacting proteins. *Chemistry & Biology*, *13*(1), 49–59. https://doi.org/10.1016/J.CHEMBIOL.2005.10.009

Mercier, C., Adjogble, K. D. Z., Däubener, W., & Delauw, M. F. C. (2005). Dense granules: are they key organelles to help understand the parasitophorous vacuole of all apicomplexa parasites? *International Journal for Parasitology*, *35*(8), 829–849. https://doi.org/10.1016/J.IJPARA.2005.03.011

Miao, W., Zhang, Y., & Li, H. (2013). Bispectral index predicts deaths within 2 weeks in coma patients, a better predictor than serum neuron-specific enolase or S100 protein. *Journal of Anesthesia*, *27*(6), 855–861. https://doi.org/10.1007/S00540-013-1654-0

Miller, M. S., Thompson, P. E., & Gabelli, S. B. (2019). Structural Determinants of Isoform Selectivity in PI3K Inhibitors. *Biomolecules*, *9*(3). https://doi.org/10.3390/BIOM9030082

Miranda-Saavedra, D., Gabaldón, T., Barton, G. J., Langsley, G., & Doerig, C. (2012). The kinomes of apicomplexan parasites. *Microbes and Infection*, *14*(10), 796–810. https://doi.org/10.1016/J.MICINF.2012.04.007

Mochida, S., & Hunt, T. (2012). Protein phosphatases and their regulation in the control of mitosis. *EMBO Reports*, *13*(3), 197. https://doi.org/10.1038/EMBOR.2011.263

Modrzynska, K., Pfander, C., Chappell, L., Yu, L., Suarez, C., Dundas, K., Gomes, A. R., Goulding, D., Rayner, J. C., Choudhary, J., & Billker, O. (2017). A Knockout Screen of ApiAP2 Genes Reveals Networks of Interacting Transcriptional Regulators Controlling the Plasmodium Life Cycle. *Cell Host & Microbe*, *21*(1), 11–22. https://doi.org/10.1016/J.CHOM.2016.12.003

Molineaux, L., Storey, J., Cohen, J. E., & Thomas, A. (1980). A longitudinal study of human malaria in the West African Savanna in the absence of control measures: relationships between different Plasmodium species, in particular P. falciparum and P. malariae. *The American Journal of Tropical Medicine and Hygiene*, *29*(5). https://doi.org/10.4269/AJTMH.1980.29.725

MOORE, D. V., & LANIER, J. E. (1961). Observations on two Plasmodium falciparum infections with an abnormal response to chloroquine. *The American Journal of Tropical Medicine and Hygiene*, *10*, 5–9. https://doi.org/10.4269/AJTMH.1961.10.5

Morais, P., Adachi, H., & Yu, Y. T. (2021). The Critical Contribution of Pseudouridine to mRNA COVID-19 Vaccines. *Frontiers in Cell and Developmental Biology*, *9*. https://doi.org/10.3389/FCELL.2021.789427

Mota, M. M., Pradel, G., Vanderberg, J. P., Hafalla, J. C. R., Frevert, U., Nussenzweig, R. S., Nussenzweig, V., & Rodriguez, A. (2001). Migration of Plasmodium sporozoites

through cells before infection. *Science (New York, N.Y.)*, *291*(5501), 141–144. https://doi.org/10.1126/SCIENCE.291.5501.141

Muralidharan, V., & Goldberg, D. E. (2013). Asparagine repeats in Plasmodium falciparum proteins: good for nothing? *PLoS Pathogens*, *9*(8). https://doi.org/10.1371/JOURNAL.PPAT.1003488

Muralidharan, V., Oksman, A., Iwamoto, M., Wandless, T. J., & Goldberg, D. E. (2011). Asparagine repeat function in a Plasmodium falciparum protein assessed via a regulatable fluorescent affinity tag. *Proceedings of the National Academy of Sciences of the United States of America*, *108*(11), 4411–4416. https://doi.org/10.1073/PNAS.1018449108

Nasa, I., Rusin, S. F., Kettenbach, A. N., & Moorhead, G. B. (2018). Aurora B opposes PP1 function in mitosis by phosphorylating the conserved PP1-binding RVxF motif in PP1 regulatory proteins. *Science Signaling*, *11*(530). https://doi.org/10.1126/SCISIGNAL.AAI8669

Nerlich, A. G., Schraut, B., Dittrich, S., Jelinek, T., & Zink, A. R. (2008). Plasmodium falciparum in Ancient Egypt. *Emerging Infectious Diseases*, *14*(8), 1317. https://doi.org/10.3201/EID1408.080235

Nilsson, J. (2019). Protein phosphatases in the regulation of mitosis. *Journal of Cell Biology*, *218*(2), 395–409. https://doi.org/10.1083/JCB.201809138

Nishizawa, K., Freund, C., Li, J., Wagner, G., & Reinherz, E. L. (1998). Identification of a proline-binding motif regulating CD2-triggered T lymphocyte activation. *Proceedings of the National Academy of Sciences of the United States of America*, *95*(25), 14897–14902. https://doi.org/10.1073/PNAS.95.25.14897/ASSET/B644B207-1956-48C9-A394-A23AD5650EE5/ASSETS/GRAPHIC/PQ2583258005.JPEG

Noedl, H., Se, Y., Schaecher, K., Smith, B. L., Socheat, D., & Fukuda, M. M. (2008). Evidence of Artemisinin-Resistant Malaria in Western Cambodia. *New England Journal of Medicine*, *359*(24), 2619–2620. https://doi.org/10.1056/NEJMC0805011/SUPPL_FILE/NEJM_NOEDL_2619SA1.PDF

Nunes-Xavier, C. E., Tárrega, C., Cejudo-Marín, R., Frijhoff, J., Sandin, Å., Östman, A., & Pulido, R. (2010). Differential up-regulation of MAP kinase phosphatases MKP3/DUSP6 and DUSP5 by Ets2 and c-Jun converge in the control of the growth arrest versus proliferation response of MCF-7 breast cancer cells to phorbol ester. *The Journal of Biological Chemistry*, *285*(34), 26417–26430. https://doi.org/10.1074/JBC.M110.121830

Oberstaller, J., Zoungrana, L., Bannerman, C. D., Jahangiri, S., Dwivedi, A., Silva, J. C., Adams, J. H., & Takala-Harrison, S. (2021). Integration of population and functional genomics to understand mechanisms of artemisinin resistance in Plasmodium

falciparum. *International Journal for Parasitology: Drugs and Drug Resistance*, *16*, 119. https://doi.org/10.1016/J.IJPDDR.2021.05.006

Oehring, S. C., Woodcroft, B. J., Moes, S., Wetzel, J., Dietz, O., Pulfer, A., Dekiwadia, C., Maeser, P., Flueck, C., Witmer, K., Brancucci, N. M. B., Niederwieser, I., Jenoe, P., Ralph, S. A., & Voss, T. S. (2012). Organellar proteomics reveals hundreds of novel nuclear proteins in the malaria parasite Plasmodium falciparum. *Genome Biology*, *13*(11). https://doi.org/10.1186/GB-2012-13-11-R108

Ohkura, H., & Yanagida, M. (1991). S. pombe gene sds22+ essential for a midmitotic transition encodes a leucine-rich repeat protein that positively modulates protein phosphatase-1. *Cell*, *64*(1), 149–157. https://doi.org/10.1016/0092-8674(91)90216-L

Olszewski, K. L., & Llinás, M. (2011). Central carbon metabolism of Plasmodium parasites. *Molecular and Biochemical Parasitology*, *175*(2), 95. https://doi.org/10.1016/J.MOLBIOPARA.2010.09.001

Osawa, Y., Nakagama, H., Shima, H., Sugimura, T., & Nagao, M. (1996). Identification and characterization of three isotypes of protein phosphatase inhibitor-2 and their expression profiles during testis maturation in rats. *European Journal of Biochemistry*, *242*(3), 793–798. https://doi.org/10.1111/J.1432-1033.1996.0793R.X

Pace, D. A., McKnight, C. A., Liu, J., Jimenez, V., & Moreno, S. N. J. (2014). Calcium entry in Toxoplasma gondii and its enhancing effect of invasion-linked traits. *The Journal of Biological Chemistry*, *289*(28), 19637–19647. https://doi.org/10.1074/JBC.M114.565390

Packard, R. M. (2014). The origins of antimalarial-drug resistance. *The New England Journal of Medicine*, *371*(5), 397–399. https://doi.org/10.1056/NEJMP1403340

Pandey, R., Mohmmed, A., Pierrot, C., Khalife, J., Malhotra, P., & Gupta, D. (2014). Genome wide in silico analysis of Plasmodium falciparum phosphatome. *BMC Genomics*, *15*(1). https://doi.org/10.1186/1471-2164-15-1024

Park, E., Patel, S., Wang, Q., Andhey, P., Zaitsev, K., Porter, S., Hershey, M., Bern, M., Plougastel-Douglas, B., Collins, P., Colonna, M., Murphy, K. M., Oltz, E., Artyomov, M., Sibley, L. D., & Yokoyama, W. M. (2019). Toxoplasma gondii infection drives conversion of NK cells into ILC1-like cells. *ELife*, *8*. https://doi.org/10.7554/ELIFE.47605

Paul, A. S., Miliu, A., Paulo, J. A., Goldberg, J. M., Bonilla, A. M., Berry, L., Seveno, M., Braun-Breton, C., Kosber, A. L., Elsworth, B., Arriola, J. S. N., Lebrun, M., Gygi, S. P., Lamarque, M. H., & Duraisingh, M. T. (2020). Co-option of Plasmodium falciparum PP1 for egress from host erythrocytes. *Nature Communications 2020 11:1*, *11*(1), 1–13. https://doi.org/10.1038/s41467-020-17306-1

Paul, D., Bargale, A. B., Rapole, S., Shetty, P. K., & Santra, M. K. (2019). Protein Phosphatase 1 Regulatory Subunit SDS22 Inhibits Breast Cancer Cell Tumorigenesis by

Functioning as a Negative Regulator of the AKT Signaling Pathway. *Neoplasia (New York, N.Y.)*, *21*(1), 30–40. https://doi.org/10.1016/J.NEO.2018.10.009

Pease, B. N., Huttlin, E. L., Jedrychowski, M. P., Talevich, E., Harmon, J., Dillman, T., Kannan, N., Doerig, C., Chakrabarti, R., Gygi, S. P., & Chakrabarti, D. (2013). Global analysis of protein expression and phosphorylation of three stages of Plasmodium falciparum intraerythrocytic development. *Journal of Proteome Research*, *12*(9), 4028–4045. https://doi.org/10.1021/PR400394G

Pedelini, L., Marquina, M., Ariño, J., Casamayor, A., Sanz, L., Bollen, M., Sanz, P., & Garcia-Gimeno, M. A. (2007). YPI1 and SDS22 proteins regulate the nuclear localization and function of yeast type 1 phosphatase Glc7. *The Journal of Biological Chemistry*, *282*(5), 3282–3292. https://doi.org/10.1074/JBC.M607171200

Peggie, M. W., MacKelvie, S. H., Bloecher, A., Knatko, E. V., Tatchell, K., & Stark, M. J. R. (2002). Essential functions of Sds22p in chromosome stability and nuclear localization of PP1. *Journal of Cell Science*, *115*(Pt 1), 195–206. https://doi.org/10.1242/JCS.115.1.195

Pérez-Toledo, K., Rojas-Meza, A. P., Mancio-Silva, L., Hernández-Cuevas, N. A., Delgadillo, D. M., Vargas, M., Martínez-Calvillo, S., Scherf, A., & Hernandez-Rivas, R. (2009). Plasmodium falciparum heterochromatin protein 1 binds to tri-methylated histone 3 lysine 9 and is linked to mutually exclusive expression of var genes. *Nucleic Acids Research*, *37*(8), 2596–2606. https://doi.org/10.1093/NAR/GKP115

Peti, W., Nairn, A. C., & Page, R. (2013). Structural basis for protein phosphatase 1 regulation and specificity. *The FEBS Journal*, *280*(2), 596–611. https://doi.org/10.1111/J.1742-4658.2012.08509.X

Philip, N., Vaikkinen, H. J., Tetley, L., & Waters, A. P. (2012). A Unique Kelch Domain Phosphatase in Plasmodium Regulates Ookinete Morphology, Motility and Invasion. *PLOS ONE*, *7*(9), e44617. https://doi.org/10.1371/JOURNAL.PONE.0044617

Pierrot, C., Zhang, X., Zhangi, G., Fréville, A., Rebollo, A., & Khalife, J. (2018). Peptides derived from <em>Plasmodium falciparum</em> leucine-rich repeat 1 bind to serine/threonine phosphatase type 1 and inhibit parasite growth in vitro. *Drug Design, Development and Therapy*, *12*, 85–88. https://doi.org/10.2147/DDDT.S153095

Pisciotta, J. M., Scholl, P. F., Shuman, J. L., Shualev, V., & Sullivan, D. J. (2017). Quantitative characterization of hemozoin in Plasmodium berghei and vivax. *International Journal for Parasitology. Drugs and Drug Resistance*, *7*(1), 110–119. https://doi.org/10.1016/J.IJPDDR.2017.02.001

Poirot, E., Skarbinski, J., Sinclair, D., Kachur, S. P., Slutsker, L., & Hwang, J. (2013). Mass drug administration for malaria. *The Cochrane Database of Systematic Reviews*, *2013*(12). https://doi.org/10.1002/14651858.CD008846.PUB2

Punta, M., & Ofran, Y. (2008). The Rough Guide to In Silico Function Prediction, or How To Use Sequence and Structure Information To Predict Protein Function. *PLOS Computational Biology*, *4*(10), e1000160. https://doi.org/10.1371/JOURNAL.PCBI.1000160

Ragusa, M. J., Dancheck, B., Critton, D. A., Nairn, A. C., Page, R., & Peti, W. (2010). Spinophilin directs Protein Phosphatase 1 specificity by blocking substrate binding sites. *Nature Structural & Molecular Biology*, *17*(4), 459. https://doi.org/10.1038/NSMB.1786

Rajaram, K., Liu, H. B., & Prigge, S. T. (2020). Redesigned TetR-Aptamer System To Control Gene Expression in Plasmodium falciparum. *MSphere*, *5*(4). https://doi.org/10.1128/MSPHERE.00457-20

Ramaswamy, N. T., Li, L., Khalil, M., & Cannon, J. F. (1998). Regulation of yeast glycogen metabolism and sporulation by Glc7p protein phosphatase. *Genetics*, *149*(1), 57–72. https://doi.org/10.1093/GENETICS/149.1.57

Rashidi, S., Tuteja, R., Mansouri, R., Ali-Hassanzadeh, M., Shafiei, R., Ghani, E., Karimazar, M., Nguewa, P., & Manzano-Román, R. (2021). The main post-translational modifications and related regulatory pathways in the malaria parasite Plasmodium falciparum: An update. *Journal of Proteomics*, *245*. https://doi.org/10.1016/J.JPROT.2021.104279

Rath, A., Glibowicka, M., Nadeau, V. G., Chen, G., & Deber, C. M. (2009). Detergent binding explains anomalous SDS-PAGE migration of membrane proteins. *Proceedings of the National Academy of Sciences of the United States of America*, *106*(6), 1760–1765. https://doi.org/10.1073/PNAS.0813167106

Resh, M. D. (2012). Targeting Protein Lipidation in Disease. *Trends in Molecular Medicine*, *18*(4), 206. https://doi.org/10.1016/J.MOLMED.2012.01.007

Rodrigues, N. T. L., Lekomtsev, S., Jananji, S., Kriston-Vizi, J., Hickson, G. R. X., & Baum, B. (2015). Kinetochore-localized PP1-Sds22 couples chromosome segregation to polar relaxation. *Nature*, *524*(7566), 489–492. https://doi.org/10.1038/NATURE14496

Russo, S. J., Dietz, D. M., Dumitriu, D., Morrison, J. H., Malenka, R. C., & Nestler, E. J. (2010). The addicted synapse: mechanisms of synaptic and structural plasticity in nucleus accumbens. *Trends in Neurosciences*, *33*(6), 267–276. https://doi.org/10.1016/J.TINS.2010.02.002

Saitou, N., & Nei, M. (1987). The neighbor-joining method: a new method for reconstructing phylogenetic trees. *Molecular Biology and Evolution*, *4*(4), 406–425. https://doi.org/10.1093/OXFORDJOURNALS.MOLBEV.A040454

Saraf, A., Cervantes, S., Bunnik, E. M., Ponts, N., Sardiu, M. E., Chung, D. W. D., Prudhomme, J., Varberg, J. M., Wen, Z., Washburn, M. P., Florens, L., & Le Roch, K. G. (2016). Dynamic and Combinatorial Landscape of Histone Modifications during the

Intraerythrocytic Developmental Cycle of the Malaria Parasite. *Journal of Proteome Research*, *15*(8), 2787–2801. https://doi.org/10.1021/ACS.JPROTEOME.6B00366

Schlüter, D., Däubener, W., Schares, G., Groß, U., Pleyer, U., & Lüder, C. (2014). Animals are key to human toxoplasmosis. *International Journal of Medical Microbiology : IJMM*, *304*(7), 917–929. https://doi.org/10.1016/J.IJMM.2014.09.002

Schmidt, C., Grønborg, M., Deckert, J., Bessonov, S., Conrad, T., Lührmann, R., & Urlaub, H. (2014). Mass spectrometry-based relative quantification of proteins in precatalytic and catalytically active spliceosomes by metabolic labeling (SILAC), chemical labeling (iTRAQ), and label-free spectral count. *RNA (New York, N.Y.)*, *20*(3), 406–420. https://doi.org/10.1261/RNA.041244.113

Serrano-Durán, R., López-Farfán, D., & Gómez-Díaz, E. (2022). Epigenetic and Epitranscriptomic Gene Regulation in Plasmodium falciparum and How We Can Use It against Malaria. *Genes*, *13*(10). https://doi.org/10.3390/GENES13101734

Sharma, V., Nag, T. C., Wadhwa, S., & Roy, T. S. (2009). Temporal distribution of mRNA expression levels of various genes in the developing human inferior colliculus. *Neuroscience Letters*, *461*(3), 229–234. https://doi.org/10.1016/J.NEULET.2009.06.049

Shaw, M. K., Tilney, L. G., & Musoke, A. J. (1991). The entry of Theileria parva sporozoites into bovine lymphocytes: evidence for MHC class I involvement. *The Journal of Cell Biology*, *113*(1), 87–101. https://doi.org/10.1083/JCB.113.1.87

Shi, Y. (2009). Serine/threonine phosphatases: mechanism through structure. *Cell*, *139*(3), 468–484. https://doi.org/10.1016/J.CELL.2009.10.006

Sierra-Miranda, M., Vembar, S. S., Delgadillo, D. M., Ávila-López, P. A., Herrera-Solorio, A. M., Lozano Amado, D., Vargas, M., & Hernandez-Rivas, R. (2017). PfAP2Tel, harbouring a non-canonical DNA-binding AP2 domain, binds to Plasmodium falciparum telomeres. *Cellular Microbiology*, *19*(9), e12742. https://doi.org/10.1111/CMI.12742

Sinha, A., Hughes, K. R., Modrzynska, K. K., Otto, T. D., Pfander, C., Dickens, N. J., Religa, A. A., Bushell, E., Graham, A. L., Cameron, R., Kafsack, B. F. C., Williams, A. E., Llinás, M., Berriman, M., Billker, O., & Waters, A. P. (2014). A cascade of DNA-binding proteins for sexual commitment and development in Plasmodium. *Nature*, *507*(7491), 253–257. https://doi.org/10.1038/NATURE12970

Smith, J. D., Rowe, J. A., Higgins, M. K., & Lavstsen, T. (2013). Malaria's deadly grip: cytoadhesion of Plasmodium falciparum-infected erythrocytes. *Cellular Microbiology*, *15*(12), 1976–1983. https://doi.org/10.1111/CMI.12183

Sologub, L., Kuehn, A., Kern, S., Przyborski, J., Schillig, R., & Pradel, G. (2011). Malaria proteases mediate inside-out egress of gametocytes from red blood cells following parasite transmission to the mosquito. *Cellular Microbiology*, *13*(6), 897–912. https://doi.org/10.1111/J.1462-5822.2011.01588.X

Solyakov, L., Halbert, J., Alam, M. M., Semblat, J. P., Dorin-Semblat, D., Reininger, L., Bottrill, A. R., Mistry, S., Abdi, A., Fennell, C., Holland, Z., Demarta, C., Bouza, Y., Sicard, A., Nivez, M. P., Eschenlauer, S., Lama, T., Thomas, D. C., Sharma, P., … Doerig, C. (2011). Global kinomic and phospho-proteomic analyses of the human malaria parasite Plasmodium falciparum. *Nature Communications*, *2*(1). https://doi.org/10.1038/NCOMMS1558

Song, X. W., Yuan, Q. N., Tang, Y., Cao, M., Shen, Y. F., Zeng, Z. Y., Lei, C. H., Li, S. H., Zhao, X. X., & Yang, Y. J. (2018). Conditionally targeted deletion of PSEN1 leads to diastolic heart dysfunction. *Journal of Cellular Physiology*, *233*(2), 1548–1557. https://doi.org/10.1002/JCP.26057

Sorber, K., Dimon, M. T., & Derisi, J. L. (2011). RNA-Seq analysis of splicing in Plasmodium falciparum uncovers new splice junctions, alternative splicing and splicing of antisense transcripts. *Nucleic Acids Research*, *39*(9), 3820. https://doi.org/10.1093/NAR/GKQ1223

Spinello, Z., Fregnani, A., Tubi, L. Q., Trentin, L., Piazza, F., & Manni, S. (2021). Targeting Protein Kinases in Blood Cancer: Focusing on CK1α and CK2. *International Journal of Molecular Sciences*, *22*(7). https://doi.org/10.3390/IJMS22073716

Sturm, A., Amino, R., Van De Sand, C., Regen, T., Retzlaff, S., Rennenberg, A., Krueger, A., Pollok, J. M., Menard, R., & Heussler, V. T. (2006). Manipulation of host hepatocytes by the malaria parasite for delivery into liver sinusoids. *Science (New York, N.Y.)*, *313*(5791), 1287–1290. https://doi.org/10.1126/SCIENCE.1129720

Swapna, L. S., & Parkinson, J. (2017). Genomics of apicomplexan parasites. *Critical Reviews in Biochemistry and Molecular Biology*, *52*(3), 254–273. https://doi.org/10.1080/10409238.2017.1290043

Takemiya, A., Ariyoshi, C., & Shimazaki, K. I. (2009). Identification and functional characterization of inhibitor-3, a regulatory subunit of protein phosphatase 1 in plants. *Plant Physiology*, *150*(1), 144–156. https://doi.org/10.1104/PP.109.135335

Tamura, K., Stecher, G., & Kumar, S. (2021). MEGA11: Molecular Evolutionary Genetics Analysis Version 11. *Molecular Biology and Evolution*, *38*(7), 3022–3027. https://doi.org/10.1093/MOLBEV/MSAB120

Tavares, J., Formaglio, P., Thiberge, S., Mordelet, E., Van Rooijen, N., Medvinsky, A., Ménard, R., & Amino, R. (2013). Role of host cell traversal by the malaria sporozoite during liver infection. *The Journal of Experimental Medicine*, *210*(5), 905–915. https://doi.org/10.1084/JEM.20121130

Taylor, H. M., McRobert, L., Grainger, M., Sicard, A., Dluzewski, A. R., Hopp, C. S., Holder, A. A., & Baker, D. A. (2010). The malaria parasite cyclic GMP-dependent protein kinase plays a central role in blood-stage schizogony. *Eukaryotic Cell*, *9*(1), 37–45. https://doi.org/10.1128/EC.00186-09

Tellier, G., Lenne, A., Cailliau-Maggio, K., Cabezas-Cruz, A., Valdés, J. J., Martoriati, A., Aliouat, E. M., Gosset, P., Delaire, B., Fréville, A., Pierrot, C., & Khalife, J. (2016). Identification of Plasmodium falciparum Translation Initiation eIF2β Subunit: Direct Interaction with Protein Phosphatase Type 1. *Frontiers in Microbiology*, *7*(MAY). https://doi.org/10.3389/FMICB.2016.00777

Templeton, G. W., & Moorhead, G. B. G. (2004). A Renaissance of Metabolite Sensing and Signaling: From Modular Domains to Riboswitches. *The Plant Cell*, *16*(9), 2252. https://doi.org/10.1105/TPC.104.160930

Terrak, M., Kerff, F., Langseimo, K., Tao, T., & Dominguez, R. (2004). Structural basis of protein phosphatase 1 regulation. *Nature*, *429*(6993), 780–784. https://doi.org/10.1038/NATURE02582

Thimasarn, K., Jatapadma, S., Vijaykadga, S., Sirichaisinthop, J., & Wongsrichanalai, C. (1995). Epidemiology of Malaria in Thailand. *Journal of Travel Medicine*, *2*(2), 59–65. https://doi.org/10.1111/J.1708-8305.1995.TB00627.X

Thompson, G. M., Pacheco, E., Melo, E. O., & Castilho, B. A. (2000). Conserved sequences in the beta subunit of archaeal and eukaryal translation initiation factor 2 (eIF2), absent from eIF5, mediate interaction with eIF2gamma. *Biochemical Journal*, *347*(Pt 3), 703. https://doi.org/10.1042/0264-6021:3470703

Tizifa, T. A., Kabaghe, A. N., McCann, R. S., van den Berg, H., Van Vugt, M., & Phiri, K. S. (2018). Prevention Efforts for Malaria. *Current Tropical Medicine Reports*, *5*(1), 41–50. https://doi.org/10.1007/S40475-018-0133-Y

Toenhake, C. G., Fraschka, S. A. K., Vijayabaskar, M. S., Westhead, D. R., van Heeringen, S. J., & Bártfai, R. (2018). Chromatin Accessibility-Based Characterization of the Gene Regulatory Network Underlying Plasmodium falciparum Blood-Stage Development. *Cell Host & Microbe*, *23*(4), 557-569.e9. https://doi.org/10.1016/J.CHOM.2018.03.007

Tomita, H., Cornejo, F., Aranda-Pino, B., Woodard, C. L., Rioseco, C. C., Neel, B. G., Alvarez, A. R., Kaplan, D. R., Miller, F. D., & Cancino, G. I. (2020). The Protein Tyrosine Phosphatase Receptor Delta Regulates Developmental Neurogenesis. *Cell Reports*, *30*(1), 215-228.e5. https://doi.org/10.1016/J.CELREP.2019.11.033

Torgerson, P. R., & Mastroiacovo, P. (2013). The global burden of congenital toxoplasmosis: a systematic review. *Bulletin of the World Health Organization*, *91*(7), 501–508. https://doi.org/10.2471/BLT.12.111732

Trager, W., & Jensen, J. B. (1976). Human malaria parasites in continuous culture. *Science (New York, N.Y.)*, *193*(4254), 673–675. https://doi.org/10.1126/SCIENCE.781840

*Traité des fièvres palustres : avec la description des microbes du paludisme : Laveran, Alphonse, 1849-1922 : Free Download, Borrow, and Streaming : Internet Archive*. (n.d.).

Retrieved September 27, 2023, from
https://archive.org/details/traitdesfivr00lave/page/n7/mode/2up

Treeck, M., Sanders, J. L., Elias, J. E., & Boothroyd, J. C. (2011). The phosphoproteomes of Plasmodium falciparum and Toxoplasma gondii reveal unusual adaptations within and beyond the parasites' boundaries. *Cell Host & Microbe*, *10*(4), 410–419. https://doi.org/10.1016/J.CHOM.2011.09.004

Tsalkova, T., Kramer, G., & Hardesty, B. (1999). The effect of a hydrophobic N-terminal probe on translational pausing of chloramphenicol acetyl transferase and rhodanese. *Journal of Molecular Biology*, *286*(1), 71–81. https://doi.org/10.1006/JMBI.1998.2481

Tung, H. Y. L., Wang, W., & Chan, C. S. M. (1995). Regulation of chromosome segregation by Glc8p, a structural homolog of mammalian inhibitor 2 that functions as both an activator and an inhibitor of yeast protein phosphatase 1. *Molecular and Cellular Biology*, *15*(11), 6064–6074. https://doi.org/10.1128/MCB.15.11.6064

Tyanova, S., Temu, T., Sinitcyn, P., Carlson, A., Hein, M. Y., Geiger, T., Mann, M., & Cox, J. (2016). The Perseus computational platform for comprehensive analysis of (prote)omics data. *Nature Methods*, *13*(9), 731–740. https://doi.org/10.1038/NMETH.3901

Ukaegbu, U. E., Kishore, S. P., Kwiatkowski, D. L., Pandarinath, C., Dahan-Pasternak, N., Dzikowski, R., & Deitsch, K. W. (2014). Recruitment of PfSET2 by RNA polymerase II to variant antigen encoding loci contributes to antigenic variation in P. falciparum. *PLoS Pathogens*, *10*(1). https://doi.org/10.1371/JOURNAL.PPAT.1003854

Valdés, J. J., Cabezas-Cruz, A., Sima, R., Butterill, P. T., Růžek, D., & Nuttall, P. A. (2016). Substrate prediction of Ixodes ricinus salivary lipocalins differentially expressed during Borrelia afzelii infection. *Scientific Reports*, *6*. https://doi.org/10.1038/SREP32372

Vella, S. A., Moore, C. A., Li, Z. H., Hortua Triana, M. A., Potapenko, E., & Moreno, S. N. J. (2021). The role of potassium and host calcium signaling in Toxoplasma gondii egress. *Cell Calcium*, *94*. https://doi.org/10.1016/J.CECA.2020.102337

Venugopal, K., Hentzschel, F., Valkiūnas, G., & Marti, M. (2020). Plasmodium asexual growth and sexual development in the haematopoietic niche of the host. *Nature Reviews. Microbiology*, *18*(3), 177–189. https://doi.org/10.1038/S41579-019-0306-2

Verbinnen, I., Ferreira, M., & Bollen, M. (2017). Biogenesis and activity regulation of protein phosphatase 1. *Biochemical Society Transactions*, *45*(1), 89–99. https://doi.org/10.1042/BST20160154

Vernes, A., Haynes, J. D., Tapchaisri, P., Williams, J. L., Dutoit, E., & Diggs, C. L. (1984). Plasmodium Falciparum Strain-Specific Human Antibody Inhibits Merozoite Invasion of Erythrocytes. *The American Journal of Tropical Medicine and Hygiene*, *33*(2), 197–203. https://doi.org/10.4269/AJTMH.1984.33.197

Virshup, D. M., & Shenolikar, S. (2009). From promiscuity to precision: protein phosphatases get a makeover. *Molecular Cell*, *33*(5), 537–545. https://doi.org/10.1016/J.MOLCEL.2009.02.015

Wakula, P., Beullens, M., Ceulemans, H., Stalmans, W., & Bollen, M. (2003). Degeneracy and function of the ubiquitous RVXF motif that mediates binding to protein phosphatase-1. *The Journal of Biological Chemistry*, *278*(21), 18817–18823. https://doi.org/10.1074/JBC.M300175200

Wakula, P., Beullens, M., Van Eynde, A., Ceulemans, H., Stalmans, W., & Bollen, M. (2006). The translation initiation factor eIF2β is an interactor of protein phosphatase-1. *Biochemical Journal*, *400*(Pt 2), 377. https://doi.org/10.1042/BJ20060758

Wang, J. L., Li, T. T., Elsheikha, H. M., Liang, Q. L., Zhang, Z. W., Wang, M., Sibley, L. D., & Zhu, X. Q. (2022). The protein phosphatase 2A holoenzyme is a key regulator of starch metabolism and bradyzoite differentiation in Toxoplasma gondii. *Nature Communications*, *13*(1). https://doi.org/10.1038/S41467-022-35267-5

Wang, W., Cronmiller, C., & Brautigan, D. L. (2008). Maternal Phosphatase Inhibitor-2 Is Required for Proper Chromosome Segregation and Mitotic Synchrony During Drosophila Embryogenesis. *Genetics*, *179*(4), 1823. https://doi.org/10.1534/GENETICS.108.091959

Wang, W., Todd Stukenberg, P., & Brautigan, D. L. (2008). Phosphatase inhibitor-2 balances protein phosphatase 1 and aurora B kinase for chromosome segregation and cytokinesis in human retinal epithelial cells. *Molecular Biology of the Cell*, *19*(11), 4852–4862. https://doi.org/10.1091/MBC.E08-05-0460

Ward, P., Equinet, L., Packer, J., & Doerig, C. (2004). Protein kinases of the human malaria parasite Plasmodium falciparum: the kinome of a divergent eukaryote. *BMC Genomics*, *5*. https://doi.org/10.1186/1471-2164-5-79

Wasmuth, J., Daub, J., Peregrín-Alvarez, J. M., Finney, C. A. M., & Parkinson, J. (2009). The origins of apicomplexan sequence innovation. *Genome Research*, *19*(7), 1202–1213. https://doi.org/10.1101/GR.083386.108

White, N. J. (2008). Qinghaosu (artemisinin): the price of success. *Science (New York, N.Y.)*, *320*(5874), 330–334. https://doi.org/10.1126/SCIENCE.1155165

Wilkes, J. M., & Doerig, C. (2008). The protein-phosphatome of the human malaria parasite Plasmodium falciparum. *BMC Genomics*, *9*. https://doi.org/10.1186/1471-2164-9-412

Wińska, P., Widło, L., Senkara, E., Koronkiewicz, M., Cieśla, J. M., Krzyśko, A., Skierka, K., & Cieśla, J. (2022). Inhibition of Protein Kinase CK2 Affects Thymidylate Synthesis Cycle Enzyme Level and Distribution in Human Cancer Cells. *Frontiers in Molecular Biosciences*, *9*. https://doi.org/10.3389/FMOLB.2022.847829/FULL

*World malaria report 2022*. (n.d.). Retrieved September 27, 2023, from https://www.who.int/publications/i/item/9789240064898

Wu, J. Q., Guo, J. Y., Tang, W., Yang, C. S., Freel, C. D., Chen, C., Nairn, A. C., & Kornbluth, S. (2009). PP1-mediated dephosphorylation of phosphoproteins at mitotic exit is controlled by inhibitor-1 and PP1 phosphorylation. *Nature Cell Biology*, *11*(5), 644–651. https://doi.org/10.1038/NCB1871

Wyatt, L., Wadham, C., Crocker, L. A., Lardelli, M., & Khew-Goodall, Y. (2007). The protein tyrosine phosphatase Pez regulates TGFbeta, epithelial-mesenchymal transition, and organ development. *The Journal of Cell Biology*, *178*(7), 1223–1235. https://doi.org/10.1083/JCB.200705035

Yakubu, R. R., Weiss, L. M., & Silmon de Monerri, N. C. (2018). Post-translational modifications as key regulators of apicomplexan biology: insights from proteome-wide studies. *Molecular Microbiology*, *107*(1), 1–23. https://doi.org/10.1111/MMI.13867

Yang, A. S. P., & Boddey, J. A. (2017). Molecular mechanisms of host cell traversal by malaria sporozoites. *International Journal for Parasitology*, *47*(2–3), 129–136. https://doi.org/10.1016/J.IJPARA.2016.09.002

Yang, H., Hou, H., Pahng, A., Gu, H., Nairn, A. C., Tang, Y. P., Colombo, P. J., & Xia, H. (2015). Protein Phosphatase-1 Inhibitor-2 Is a Novel Memory Suppressor. *The Journal of Neuroscience : The Official Journal of the Society for Neuroscience*, *35*(45), 15082–15087. https://doi.org/10.1523/JNEUROSCI.1865-15.2015

YOUNG, M. D., CONTACOS, P. G., STITCHER, J. E., & MILLAR, J. W. (1963). DRUG RESISTANCE IN PLASMODIUM FALCIPARUM FROM THAILAND. *The American Journal of Tropical Medicine and Hygiene*, *12*, 305–314. https://doi.org/10.4269/AJTMH.1963.12.305

Yuda, M., Iwanaga, S., Kaneko, I., & Kato, T. (2015). Global transcriptional repression: An initial and essential step for Plasmodium sexual development. *Proceedings of the National Academy of Sciences of the United States of America*, *112*(41), 12824–12829. https://doi.org/10.1073/PNAS.1504389112

Yuda, M., Iwanaga, S., Shigenobu, S., Kato, T., & Kaneko, I. (2010). Transcription factor AP2-Sp and its target genes in malarial sporozoites. *Molecular Microbiology*, *75*(4), 854–863. https://doi.org/10.1111/J.1365-2958.2009.07005.X

Yuda, M., Iwanaga, S., Shigenobu, S., Mair, G. R., Janse, C. J., Waters, A. P., Kato, T., & Kaneko, I. (2009). Identification of a transcription factor in the mosquito-invasive stage of malaria parasites. *Molecular Microbiology*, *71*(6), 1402–1414. https://doi.org/10.1111/J.1365-2958.2009.06609.X

Zeeshan, M., Pandey, R., Subudhi, A. K., Ferguson, D. J. P., Kaur, G., Rashpa, R., Nugmanova, R., Brady, D., Bottrill, A. R., Vaughan, S., Brochet, M., Bollen, M., Pain,

A., Holder, A. A., Guttery, D. S., & Tewari, R. (2021). Protein phosphatase 1 regulates atypical mitotic and meiotic division in Plasmodium sexual stages. *Communications Biology*, *4*(1). https://doi.org/10.1038/S42003-021-02273-0

Zhang, C., Li, Z., Cui, H., Jiang, Y., Yang, Z., Wang, X., Gao, H., Liu, C., Zhang, S., Su, X. Z., & Yuana, J. (2017). Systematic CRISPR-Cas9-Mediated Modifications of Plasmodium yoelii ApiAP2 Genes Reveal Functional Insights into Parasite Development. *MBio*, *8*(6). https://doi.org/10.1128/MBIO.01986-17

Zhang, C., Tang, J., Xie, J., Zhang, H., Li, Y., Zhang, J., Verpooten, D., He, B., & Cao, Y. (2008). A conserved domain of herpes simplex virus ICP34.5 regulates protein phosphatase complex in mammalian cells. *FEBS Letters*, *582*(2), 171–176. https://doi.org/10.1016/J.FEBSLET.2007.11.082

Zhang, H., Zhang, Q., Tu, J., You, Q., & Wang, L. (2023). Dual function of protein phosphatase 5 (PPP5C): An emerging therapeutic target for drug discovery. *European Journal of Medicinal Chemistry*, *254*. https://doi.org/10.1016/J.EJMECH.2023.115350

Zhang, J., Ma, Y., Taylor, S. S., & Tsien, R. Y. (2001). Genetically encoded reporters of protein kinase A activity reveal impact of substrate tethering. *Proceedings of the National Academy of Sciences of the United States of America*, *98*(26), 14997–15002. https://doi.org/10.1073/PNAS.211566798/SUPPL_FILE/MOVIE.GIF

Zhang, J., Zhang, L., Zhao, S., & Lee, E. Y. C. (1998). Identification and characterization of the human HCG V gene product as a novel inhibitor of protein phosphatase-1. *Biochemistry*, *37*(47), 16728–16734. https://doi.org/10.1021/BI981169G

Zhang, M., Mishra, S., Sakthivel, R., Fontoura, B. M. A., & Nussenzweig, V. (2016). UIS2: A Unique Phosphatase Required for the Development of Plasmodium Liver Stages. *PLOS Pathogens*, *12*(1), e1005370. https://doi.org/10.1371/JOURNAL.PPAT.1005370

Zhang, M., Wang, C., Otto, T. D., Oberstaller, J., Liao, X., Adapa, S. R., Udenze, K., Bronner, I. F., Casandra, D., Mayho, M., Brown, J., Li, S., Swanson, J., Rayner, J. C., Jiang, R. H. Y., & Adams, J. H. (2018). Uncovering the essential genes of the human malaria parasite Plasmodium falciparum by saturation mutagenesis. *Science (New York, N.Y.)*, *360*(6388). https://doi.org/10.1126/SCIENCE.AAP7847

Zhou, H., & Skolnick, J. (2010). Improving threading algorithms for remote homology modeling by combining fragment and template comparisons. *Proteins*, *78*(9), 2041–2048. https://doi.org/10.1002/PROT.22717

Zimmerman, P. A., & Howes, R. E. (2015). Malaria diagnosis for malaria elimination. *Current Opinion in Infectious Diseases*, *28*(5), 446–454. https://doi.org/10.1097/QCO.0000000000000191

# Annexes I

# Annexes I

**Supplementary Table 1. Identified proteins after PfGEXP15-GFP immunoprecipitation in *P. falciparum* trophozoites and schizonts.** The table shows the name of identified proteins and the number of peptides identified for each experiment are indicated. Three experiments were performed with GFP nanobodies on WT schizonts as negative control and PfGEXP15-GFP schizonts. Here, we highlight in green the protein co-immunoprecipitated with PfGEXP15-GFP in at least two experiments with peptides ≥ 2 and with peptides and spectra ≥ 2 fold compared with the control strain. Blank cells represent 0 peptide/spectrum identified.

| C: Student's T-test Significant WT_GEXP15 | C: Student's T-test significant | N: Peptides | Protein Name |
|---|---|---|---|
| + | WT_GEXP15 | 7 | Dihydrofolate reductase OS=Escherichia coli (strain B / BL21-DE3) OX=469008 GN=ECBD_3567 PE=3 SV=1 |
| + | WT_GEXP15 | 46 | protein GEXP15 |
| + | WT_GEXP15 | 2 | WD and tetratricopeptide repeats protein 1, putative |
| + | WT_GEXP15 | 8 | small nuclear ribonucleoprotein-associated protein B, putative |
| + | WT_GEXP15 | 11 | 60S ribosomal protein L28 |
|  |  | 8 | 60S ribosomal protein L36 |
| + | WT_GEXP15 | 1 | lipoamide acyltransferase component of branched-chain alpha-keto acid dehydrogenase complex |
|  |  | 6 | eukaryotic translation initiation factor 4E, putative |
| + | WT_GEXP15 | 13 | 60S ribosomal protein L38 |
|  |  | 4 | 40S ribosomal protein S30 |
|  |  | 12 | 60S ribosomal protein L35, putative |
| + | WT_GEXP15 | 12 | 40S ribosomal protein S24 |
|  |  | 3 | small nuclear ribonucleoprotein Sm D1, putative |
|  |  | 1 | reticulocyte binding protein 2 homologue a |
| + | WT_GEXP15 | 2 | RNA-binding protein, putative |
|  |  | 10 | 40S ribosomal protein S25 |

| | | | |
|---|---|---|---|
| + | WT_GEXP15 | 37 | pre-mRNA-processing-splicing factor 8, putative |
| | | 1 | mRNA-binding protein PUF3 |
| | | 3 | conserved Plasmodium protein, unknown function |
| | | 3 | small nuclear ribonucleoprotein Sm D3, putative |
| | | 1 | kelch domain-containing protein, putative |
| | | 1 | homeobox domain-containing protein, putative |
| + | WT_GEXP15 | 14 | 40S ribosomal protein S15 |
| + | WT_GEXP15 | 4 | histidine phosphatase, putative |
| | | 6 | 60S ribosomal protein L6, putative |
| + | WT_GEXP15 | 9 | 60S ribosomal protein L32 |
| | | 22 | U5 small nuclear ribonucleoprotein component, putative |
| | | 7 | 60S ribosomal protein L37ae, putative |
| | | 14 | 40S ribosomal protein S6 |
| | | 1 | leucine-rich repeat protein |
| | | 4 | histone H2A |
| | | 4 | nucleolar protein 5, putative |
| | | 13 | 60S ribosomal protein L27 |
| | | 3 | 60S ribosomal protein L7-2, putative |
| | | 2 | pre-rRNA-processing protein PNO1, putative |
| | | 5 | 60S ribosomal protein L7, putative |
| | | 1 | conserved Plasmodium protein, unknown function |
| + | WT_GEXP15 | 4 | FoP domain-containing protein, putative |
| | | 10 | U5 small nuclear ribonucleoprotein 40 kDa protein, putative |
| | | 9 | 60S ribosomal protein L44 |
| | | 9 | histone H2B |
| | | 4 | 60S ribosomal protein L22, putative |
| | | 2 | conserved Plasmodium protein, unknown function |
| + | WT_GEXP15 | 6 | 60S ribosomal protein L26, putative |
| + | WT_GEXP15 | 1 | conserved Plasmodium protein, unknown function |
| | | 11 | 60S ribosomal protein L23 |
| | | 9 | BRIX domain, putative |
| | | 2 | MSP7-like protein |
| + | WT_GEXP15 | 13 | RNA-binding protein, putative |
| | | 5 | 40S ribosomal protein S19 |

| | | | | |
|---|---|---|---|---|
| | | | 11 | 60S ribosomal protein L7-3, putative |
| | | | 4 | 60S ribosomal protein L35ae, putative |
| | | | 2 | conserved Plasmodium protein, unknown function |
| | | | 4 | vacuolar protein sorting-associated protein 45 |
| | | | 2 | U6 snRNA-associated Sm-like protein LSm4, putative |
| | | | 4 | histone H2A.Z |
| | | | 1 | thioredoxin 2 |
| | | | 8 | 40S ribosomal protein S16, putative |
| | | | 2 | U3 small nucleolar ribonucleoprotein protein MPP10, putative |
| | | | 13 | 60S ribosomal protein L13-2, putative |
| | | | 1 | Nicotinate-nucleotide--dimethylbenzimidazole phosphoribosyltransferase OS=Escherichia coli (strain B / BL21-DE3) OX=469008 GN=cobT PE=3 SV=1 |
| | | | 3 | conserved Plasmodium protein, unknown function |
| | | | 1 | bromodomain protein 2, putative |
| | | | 2 | plasmoredoxin |
| | | | 5 | AP2 domain transcription factor AP2-EXP |
| | | | 3 | 60S ribosomal protein L29, putative |
| | | | 1 | zinc finger protein, putative |
| | | | 1 | conserved Plasmodium protein, unknown function |
| | | | 1 | EH domain-containing protein |
| | | | 7 | ribosomal protein S27a, putative |
| | | | 1 | kinetochore protein SPC25, putative |
| | | | 5 | topoisomerase I |
| | | | 3 | 60S ribosomal protein L30e, putative |
| | | | 25 | 40S ribosomal protein S4, putative |
| | | | 1 | elongator complex protein 3, putative |
| | | | 8 | 60S ribosomal protein L14, putative |
| | | | 1 | E3 SUMO-protein ligase PIAS, putative |
| | | | 17 | peroxiredoxin |
| | | | 1 | ribosomal RNA-processing protein 8, putative |
| | | | 2 | asparagine-rich protein, putative |

| | | | |
|---|---|---|---|
| | | 3 | ookinete surface and oocyst capsule protein OSCP, putative |
| | | 2 | acyl-CoA binding protein, isoform 2, ACBP2 |
| | | 2 | transporter, putative |
| | | 7 | cytoadherence linked asexual protein 8 |
| | | 4 | ATP-dependent RNA helicase DBP10, putative |
| | | 1 | Plasmodium exported protein, unknown function |
| | | 7 | 60S ribosomal protein L24, putative |
| | | 1 | small nuclear ribonucleoprotein E, putative |
| | | 1 | dynein light chain 1, putative |
| | | 5 | small nuclear ribonucleoprotein F, putative |
| | | 8 | 40S ribosomal protein S17, putative |
| | | 2 | mediator of RNA polymerase II transcription subunit 18, putative |
| | | 4 | apical membrane antigen 1 |
| | | 1 | mitochondrial import receptor subunit TOM40, putative |
| | | 5 | ribosome biogenesis protein TSR1, putative |
| | | 1 | methyltransferase AAMT |
| | | 8 | 60S ribosomal protein L2 |
| | | 1 | conserved Plasmodium protein, unknown function |
| | | 2 | acyl-CoA-binding protein, putative |
| | | 2 | protein transport protein SEC61 subunit beta, putative |
| | | 4 | 40S ribosomal protein S18, putative |
| | | 2 | AAR2 protein, putative |
| | | 2 | DnaJ protein, putative |
| | | 4 | conserved protein, unknown function |
| | | 1 | cation diffusion facilitator family protein, putative |
| | | 4 | importin subunit beta, putative |
| | | 7 | translation-enhancing factor |
| | | 2 | conserved Plasmodium protein, unknown function |
| | | 2 | Bifunctional ligase/repressor BirA OS=Escherichia coli (strain B / BL21-DE3) OX=469008 GN=birA PE=3 SV=1 |
| | | 1 | mitochondrial phosphate carrier protein |

| | | | | |
|---|---|---|---|---|
| | | | 1 | histone RNA hairpin-binding protein, putative |
| | | | 11 | glycerol-3-phosphate dehydrogenase [NAD(+)], putative |
| | | | 7 | polyadenylate-binding protein 2, putative |
| | | | 1 | pre-mRNA-splicing factor CEF1, putative |
| | | | 4 | 60S ribosomal protein L18-2, putative |
| | | | 1 | PDCD2 domain-containing protein, putative |
| | | | 2 | zinc finger protein, putative |
| | | | 3 | transcription factor BTF3, putative |
| | | | 1 | 40S ribosomal protein S23, putative |
| | | | 2 | erythrocyte membrane protein 1, PfEMP1 |
| | | | 2 | pre-mRNA-processing factor 19, putative |
| | | | 5 | calcyclin binding protein, putative |
| | | | 4 | chaperone protein ClpB1 |
| | | | 1 | nuclear polyadenylated RNA-binding protein NAB2, putative |
| | | | 4 | ATP-dependent RNA helicase DDX41, putative |
| | | | 16 | 60S ribosomal protein L4 |
| | | | 2 | ADP-ribosylation factor GTPase-activating protein 1 |
| | | | 1 | monocarboxylate transporter, putative |
| | | | 1 | cysteine-rich PDZ-binding protein, putative |
| | | | 3 | protein phosphatase PPM7, putative |
| | | | 8 | 60S ribosomal protein L18, putative |
| | | | 4 | 60S ribosomal protein L37 |
| | | | 3 | phosducin-like protein 1, putative |
| | | | 1 | UDP-N-acetylglucosamine transferase subunit ALG13, putative |
| | | | 4 | antigen UB05 |
| | | | 2 | bromodomain protein 5 |
| | | | 6 | AP2 domain transcription factor, putative |
| | | | 3 | tetratricopeptide repeat protein, putative |
| | | | 13 | dynamin-like protein, putative |
| | | | 2 | tRNA-2-methylthio-N(6)-dimethylallyladenosine synthase |
| | | | 1 | protein transport protein SEC22 |

| | | | |
|---|---|---|---|
| | | | 3 | high mobility group protein B2 |
| | | | 2 | eukaryotic translation initiation factor 3 subunit H, putative |
| | | | 4 | small nuclear ribonucleoprotein G, putative |
| | | | 3 | protein CINCH |
| | | | 2 | methyltransferase, putative |
| | | | 1 | conserved Plasmodium protein, unknown function |
| | | | 3 | serine/arginine-rich splicing factor 1 |
| | | | 23 | 40S ribosomal protein S3A, putative |
| | | | 2 | phosphoglycerate mutase, putative |
| | | | 7 | haloacid dehalogenase-like hydrolase |
| | | | 16 | receptor for activated c kinase |
| | | | 3 | RNA-binding protein Nova-1, putative |
| | | | 2 | conserved Plasmodium protein, unknown function |
| | | | 4 | conserved protein, unknown function |
| | | | 9 | histone H4 |
| | | | 8 | DNA/RNA-binding protein Alba 3 |
| | | | 10 | signal recognition particle subunit SRP19 |
| | | | 2 | tRNA N6-adenosine threonylcarbamoyltransferase |
| | | | 6 | 60S ribosomal protein L15, putative |
| | | | 6 | purine nucleoside phosphorylase |
| | | | 2 | ubiquitin domain-containing protein DSK2, putative |
| | | | 2 | mitochondrial import receptor subunit TOM22, putative |
| | | | 2 | copper transporter |
| | | | 1 | small nuclear ribonucleoprotein Sm D2, putative |
| | | | 2 | DIX domain-containing protein, putative |
| | | | 1 | conserved Plasmodium protein, unknown function |
| | | | 10 | 40S ribosomal protein S11 |
| | | | 4 | vacuolar iron transporter |
| | | | 3 | conserved protein, unknown function |
| | | | 5 | 60S ribosomal protein L11a, putative |
| | | | 1 | conserved Plasmodium protein, unknown function |

| | | | |
|---|---|---|---|
| | | 7 | 26S protease regulatory subunit 4, putative |
| | | 14 | rhoptry neck protein 3 |
| | | 1 | conserved Plasmodium protein, unknown function |
| | | 5 | merozoite surface protein 2 |
| | | 4 | V-type proton ATPase subunit E, putative |
| | | 4 | Sec1 family protein, putative |
| | | 8 | 40S ribosomal protein S19 |
| | | 3 | allantoicase, putative |
| | | 2 | exosome complex component RRP4 |
| | | 1 | elongation factor 1-delta, putative |
| | | 17 | ATP-dependent RNA helicase DDX17 |
| | | 1 | pseudo protein kinase 1, putative |
| | | 2 | inner membrane complex sub-compartment protein 3 |
| | | 7 | 40S ribosomal protein S7, putative |
| | | 2 | glutamine--fructose-6-phosphate aminotransferase [isomerizing], putative |
| | | 3 | nuclear GTP-binding protein, putative |
| | | 8 | 6-phosphogluconate dehydrogenase, decarboxylating |
| | | 2 | dynein heavy chain, putative |
| | | 1 | zinc finger protein, putative |
| | | 2 | translation initiation factor eIF-2B subunit alpha, putative |
| | | 10 | conserved Plasmodium protein, unknown function |
| | | 2 | ER membrane protein complex subunit 3, putative |
| | | 4 | flavoprotein subunit of succinate dehydrogenase |
| | | 5 | nuclear cap-binding protein subunit 2, putative |
| | | 6 | DNA-directed RNA polymerases I and III subunit RPAC1, putative |
| | | 1 | 6-cysteine protein P41 |
| | | 18 | methionine--tRNA ligase |
| | | 1 | U3 small nucleolar ribonucleoprotein protein IMP3, putative |
| | | 4 | protein transport protein SEC61 subunit alpha |
| | | 10 | clustered-asparagine-rich protein |
| | | 12 | RNA-binding protein, putative |

| | | | |
|---|---|---|---|
| | | | 10 | eukaryotic translation initiation factor 5A |
| | | | 2 | FAD synthetase, putative |
| | | | 8 | V-type proton ATPase subunit G, putative |
| | | | 5 | 60S ribosomal protein L17, putative |
| | | | 2 | photosensitized INA-labeled protein PHIL1 |
| | | | 1 | ubiquitin-conjugating enzyme E2, putative |
| | | | 5 | glideosome-associated protein 50 |
| | | | 1 | ATP-dependent protease subunit ClpQ |
| | | | 1 | conserved Plasmodium protein, unknown function |
| | | | 5 | conserved Plasmodium protein, unknown function |
| | | | 31 | glyceraldehyde-3-phosphate dehydrogenase |
| | | | 1 | DNA-binding protein, putative |
| | | | 4 | histone H3 |
| | | | 7 | 40S ribosomal protein S8e, putative |
| | | | 1 | ubiquitin-conjugating enzyme E2 |
| | | | 2 | alkaline phosphatase, putative |
| | | | 1 | major facilitator superfamily-related transporter, putative |
| | | | 3 | serine/threonine protein phosphatase 8, putative |
| | | | 2 | conserved Plasmodium protein, unknown function |
| | | | 3 | mitochondrial-processing peptidase subunit alpha, putative |
| | | | 7 | phosphoglucomutase, putative |
| | | | 4 | syntaxin, Qa-SNARE family |
| | | | 12 | 60S ribosomal protein L27a, putative |
| | | | 4 | DnaJ protein, putative |
| | | | 4 | eukaryotic translation initiation factor subunit eIF2A, putative |
| | | | 12 | proliferation-associated protein 2g4, putative |
| | | | 2 | mitochondrial import inner membrane translocase subunit TIM17, putative |
| | | | 6 | 40S ribosomal protein S9, putative |
| | | | 5 | N-ethylmaleimide-sensitive fusion protein |
| | | | 3 | AP2 domain transcription factor AP2-O5, putative |

| | | | | |
|---|---|---|---|---|
| | | | 6 | 40S ribosomal protein S29, putative |
| | | | 10 | chromodomain-helicase-DNA-binding protein 1 homolog, putative |
| | | | 5 | ras-related protein RAB7 |
| | | | 9 | DnaJ protein, putative |
| | | | 1 | RNA cytosine C(5)-methyltransferase, putative |
| | | | 7 | CUGBP Elav-like family member 1 |
| | | | 12 | ribose-phosphate pyrophosphokinase, putative |
| | | | 2 | U4/U6.U5 tri-snRNP-associated protein 2, putative |
| | | | 14 | MORN repeat-containing protein 1 |
| | | | 1 | flap endonuclease 1 |
| | | | 4 | AP-4 complex subunit epsilon, putative |
| | | | 2 | protein GCN20 |
| | | | 1 | vacuole membrane protein 1, putative |
| | | | 1 | conserved protein, unknown function |
| | | | 2 | DNA-directed RNA polymerase II subunit RPB9, putative |
| | | | 3 | protein phosphatase PPM10, putative |
| | | | 4 | conserved Plasmodium protein, unknown function |
| | | | 4 | conserved Plasmodium protein, unknown function |
| | | | 17 | histidine--tRNA ligase, putative |
| | | | 1 | conserved Plasmodium protein, unknown function |
| | | | 3 | N-terminal acetyltransferase A complex catalytic subunit ARD1, putative |
| | | | 2 | DNA polymerase alpha catalytic subunit A |
| | | | 5 | parasite-infected erythrocyte surface protein |
| | | | 2 | dihydrouridine synthase, putative |
| | | | 4 | MCL1 domain-containing protein, putative |
| | | | 2 | bromodomain protein 1 |
| | | | 4 | bacterial histone-like protein |
| | | | 14 | conserved Plasmodium protein, unknown function |
| | | | 12 | 60S ribosomal protein L5, putative |
| | | | 2 | DNA-3-methyladenine glycosylase |
| | | | 16 | ethanolamine kinase |

| | | | | |
|---|---|---|---|---|
| | | | 11 | ATP-dependent RNA helicase DBP1, putative |
| | | | 4 | histone H3 variant |
| | | | 1 | syntaxin-binding protein, putative |
| | | | 1 | O-phosphoseryl-tRNA(Sec) selenium transferase, putative |
| | | | 4 | THUMP domain-containing protein, putative |
| | | | 7 | 40S ribosomal protein S15A, putative |
| | | | 5 | voltage-dependent anion-selective channel protein, putative |
| | | | 5 | PPPDE peptidase domain-containing protein, putative |
| | | | 13 | PHAX domain-containing protein, putative |
| | | | 10 | 60S ribosomal protein L21 |
| | | | 28 | heat shock protein 60 |
| | | | 2 | GDP dissociation inhibitor, putative |
| | | | 11 | 40S ribosomal protein S3 |
| | | | 16 | ATP-dependent RNA helicase UAP56 |
| | | | 3 | malate:quinone oxidoreductase |
| | | | 1 | PP-loop family protein, putative |
| | | | 2 | conserved protein, unknown function |
| | | | 6 | diacylglycerol kinase, putative |
| | | | 3 | RNA-binding protein 8A, putative |
| | | | 15 | GMP synthase [glutamine-hydrolyzing] |
| | | | 14 | eukaryotic translation initiation factor 2 subunit gamma, putative |
| | | | 8 | eukaryotic translation initiation factor 4E |
| | | | 4 | 60S ribosomal protein L19 |
| | | | 25 | DNA replication licensing factor MCM5, putative |
| | | | 8 | calcium/calmodulin-dependent protein kinase, putative |
| | | | 4 | conserved Plasmodium protein, unknown function |
| | | | 5 | nuclear transport factor 2, putative |
| | | | 2 | exported protein 1 |
| | | | 1 | 1-cys-glutaredoxin-like protein-1 |
| | | | 7 | 26S protease regulatory subunit 10B, putative |

| | | | |
|---|---|---|---|
| | | 11 | nicotinate phosphoribosyltransferase, putative |
| | | 7 | 26S proteasome regulatory subunit RPN10, putative |
| | | 2 | pre-mRNA-processing ATP-dependent RNA helicase PRP5, putative |
| | | 4 | succinate--CoA ligase [ADP-forming] subunit alpha, putative |
| | | 3 | high mobility group protein B1 |
| | | 2 | conserved Plasmodium protein, unknown function |
| | | 2 | DnaJ protein, putative |
| | | 2 | autophagy-related protein 18 |
| | | 2 | GTPase-activating protein, putative |
| | | 52 | merozoite surface protein 1 |
| | | 33 | heat shock protein 70 |
| | | 1 | actin-depolymerizing factor 1 |
| | | 6 | ras-related protein Rab-18 |
| | | 2 | conserved protein, unknown function |
| | | 3 | mRNA-decapping enzyme subunit 1, putative |
| | | 13 | DNA/RNA-binding protein Alba 1 |
| | | 2 | conserved Plasmodium protein, unknown function |
| | | 3 | alternative splicing factor ASF-1, putative |
| | | 3 | dihydroorotate dehydrogenase |
| | | 8 | RNA-binding protein, putative |
| | | 5 | tRNA-splicing ligase RtcB, putative |
| | | 7 | ubiquitin-conjugating enzyme MMS2, putative |
| | | 6 | tryptophan--tRNA ligase |
| | | 48 | M1-family alanyl aminopeptidase |
| | | 2 | conserved Plasmodium protein, unknown function |
| | | 5 | polypyrimidine tract-binding protein, putative |
| | | 2 | HotDog domain-containing protein, putative |
| | | 4 | 60S ribosomal protein L34 |
| | | 10 | glutathione synthetase |
| | | 18 | conserved Plasmodium protein, unknown function |
| | | 9 | protein transport protein Sec24A |
| | | 13 | CUGBP Elav-like family member 2, putative |

| | | | | |
|---|---|---|---|---|
| | | | 1 | merozoite organizing protein |
| | | | 12 | protein SEY1, putative |
| | | | 2 | 60S ribosomal protein L31 |
| | | | 1 | rhoptry associated adhesin |
| | | | 6 | conserved protein, unknown function |
| | | | 12 | Obg-like ATPase 1, putative |
| | | | 8 | ADP,ATP carrier protein 1 |
| | | | 1 | AP-3 complex subunit beta, putative |
| | | | 1 | Niemann-Pick type C1-related protein |
| | | | 2 | inorganic pyrophosphatase |
| | | | 1 | conserved Plasmodium protein, unknown function |
| | | | 3 | G-strand-binding protein 2 |
| | | | 1 | splicing factor 3A subunit 3, putative |
| | | | 6 | rhoptry neck protein 4 |
| | | | 4 | 40S ribosomal protein S21 |
| | | | 12 | CTP synthase |
| | | | 3 | heterochromatin protein 1 |
| | | | 8 | KH domain-containing protein, putative |
| | | | 1 | queuine tRNA-ribosyltransferase, putative |
| | | | 4 | 26S proteasome regulatory subunit RPN13, putative |
| | | | 3 | transcription initiation TFIID-like, putative |
| | | | 21 | ornithine aminotransferase |
| | | | 3 | conserved Plasmodium protein, unknown function |
| | | | 13 | 26S protease regulatory subunit 7, putative |
| | | | 1 | prohibitin 2, putative |
| | | | 5 | histone H2B variant |
| | | | 15 | T-complex protein 1 subunit delta |
| | | | 7 | DNA-directed RNA polymerase II subunit RPB3, putative |
| | | | 2 | 6-cysteine protein |
| | | | 1 | WD repeat-containing protein, putative |
| | | | 8 | heat shock protein DNAJ homologue Pfj4 |
| | | | 12 | 40S ribosomal protein S11, putative |
| | | | 4 | GTP-binding protein, putative |
| | | | 3 | phosphatidylglycerophosphate synthase |
| | | | 1 | chorismate synthase |
| | | | 4 | Glyceraldehyde-3-phosphate dehydrogenase |

| | | | |
|---|---|---|---|
| | | | OS=Escherichia coli (strain B / BL21-DE3) OX=469008 GN=ECBD_1865 PE=3 SV=1 |
| | | 3 | inner membrane complex protein 1c, putative |
| | | 24 | protein disulfide-isomerase, putative |
| | | 1 | multidrug resistance protein 2 |
| | | 4 | arginase |
| | | 11 | 26S proteasome regulatory subunit RPN11, putative |
| | | 1 | conserved Plasmodium protein, unknown function |
| | | 6 | spindle and kinetochore-associated protein 2, putative |
| | | 6 | ras-related protein Rab-11B |
| | | 2 | pre-mRNA-splicing factor PRP46, putative |
| | | 10 | AP2 domain transcription factor AP2-I |
| | | 20 | DNA-directed RNA polymerase II subunit RPB2, putative |
| | | 5 | glycogen synthase kinase 3 |
| | | 3 | conserved Plasmodium protein, unknown function |
| | | 2 | MYND-type zinc finger protein, putative |
| | | 6 | 60S ribosomal protein L1, putative |
| | | 4 | phosphoenolpyruvate carboxylase |
| | | 2 | skeleton-binding protein 1 |
| | | 13 | transketolase |
| | | 9 | proline--tRNA ligase |
| | | 12 | regulator of chromosome condensation, putative |
| | | 2 | prefoldin subunit 3, putative |
| | | 3 | ATP-dependent RNA helicase DDX1, putative |
| | | 11 | hydroxymethyldihydropterin pyrophosphokinase-dihydropteroate synthase |
| | | 1 | protein KIC3 |
| | | 1 | conserved Plasmodium protein, unknown function |
| | | 10 | rhoptry neck protein 2 |
| | | 2 | SAP domain-containing protein, putative |
| | | 1 | 4-hydroxy-3-methylbut-2-enyl diphosphate reductase |
| | | 31 | DNA replication licensing factor MCM3, putative |
| | | 2 | eukaryotic translation initiation factor 6, putative |

| | | | |
|---|---|---|---|
| | | 2 | conserved Plasmodium membrane protein, unknown function |
| | | 5 | 60S ribosomal protein L13, putative |
| | | 4 | signal recognition particle receptor subunit alpha, putative |
| | | 4 | ubiquitin carboxyl-terminal hydrolase UCH54 |
| | | 2 | selenide water dikinase, putative |
| | | 10 | serine/threonine protein phosphatase UIS2, putative |
| | | 47 | heat shock protein 90 |
| | | 2 | ring-exported protein 2 |
| | | 17 | ATP-dependent zinc metalloprotease FTSH, putative |
| | | 3 | DNA-directed RNA polymerases I, II, and III subunit RPABC1, putative |
| | | 3 | translation initiation factor SUI1, putative |
| | | 1 | lipin, putative |
| | | 3 | DNA repair protein RAD51 |
| | | 4 | serine/arginine-rich splicing factor 4 |
| | | 4 | SWIB/MDM2 domain-containing protein |
| | | 9 | acyl-CoA synthetase |
| | | 8 | cysteine--tRNA ligase |
| | | 11 | apoptosis-inducing factor, putative |
| | | 6 | RNA (uracil-5-)methyltransferase, putative |
| | | 10 | FACT complex subunit SSRP1, putative |
| | | 6 | zinc finger protein, putative |
| | | 1 | 60S ribosomal protein L39 |
| | | 10 | eukaryotic translation initiation factor 3 subunit D, putative |
| | | 3 | kelch protein K13 |
| | | 10 | early transcribed membrane protein 10.2 |
| | | 6 | conserved protein, unknown function |
| | | 2 | 3-phosphoinositide-dependent protein kinase 1 |
| | | 16 | deoxyribodipyrimidine photo-lyase, putative |
| | | 6 | nascent polypeptide-associated complex subunit alpha, putative |
| | | 15 | ring-infected erythrocyte surface antigen |

| | | | | |
|---|---|---|---|---|
| | | | 1 | mediator of RNA polymerase II transcription subunit 6, putative |
| | | | 16 | inosine-5-monophosphate dehydrogenase |
| | | | 31 | S-adenosylmethionine decarboxylase/ornithine decarboxylase |
| | | | 8 | conserved Apicomplexan protein, unknown function |
| | | | 3 | multifunctional methyltransferase subunit TRM112, putative |
| | | | 3 | conserved Plasmodium protein, unknown function |
| | | | 1 | zinc finger protein, putative |
| | | | 11 | rab specific GDP dissociation inhibitor |
| | | | 1 | protein AAP6 |
| | | | 5 | conserved Plasmodium protein, unknown function |
| | | | 1 | essential nuclear protein 1, putative |
| | | | 10 | karyopherin alpha |
| | | | 18 | V-type proton ATPase catalytic subunit A |
| | | | 48 | heat shock protein 70 |
| | | | 6 | V-type H(+)-translocating pyrophosphatase, putative |
| | | | 24 | polyadenylate-binding protein 1, putative |
| | | | 1 | heat shock protein 86 family protein |
| | | | 3 | tRNAHis guanylyltransferase, putative |
| | | | 1 | splicing factor 3B subunit 6, putative |
| | | | 13 | StAR-related lipid transfer protein |
| | | | 12 | 40S ribosomal protein S5 |
| | | | 1 | general transcription factor IIH subunit 2 |
| | | | 14 | phosphoribosylpyrophosphate synthetase |
| | | | 8 | casein kinase 2, alpha subunit |
| | | | 23 | heat shock protein 90, putative |
| | | | 2 | ATP-dependent RNA helicase MTR4 |
| | | | 3 | ATP-dependent zinc metalloprotease FTSH 1 |
| | | | 2 | conserved Plasmodium protein, unknown function |
| | | | 14 | peptidyl-prolyl cis-trans isomerase FKBP35 |
| | | | 4 | E3 ubiquitin-protein ligase ZNF598, putative |
| | | | 8 | V-type proton ATPase subunit C, putative |

223

| | | | |
|---|---|---|---|
| | | 16 | DNA-directed RNA polymerase II subunit RPB1 |
| | | 5 | calcium-transporting ATPase |
| | | 2 | conserved protein, unknown function |
| | | 23 | fructose-bisphosphate aldolase |
| | | 3 | thioredoxin peroxidase 2 |
| | | 8 | heat shock protein J2 |
| | | 6 | phenylalanine--tRNA ligase alpha subunit |
| | | 14 | DNA/RNA-binding protein Alba 4 |
| | | 10 | chromatin remodeling protein |
| | | 1 | dolichol-phosphate mannosyltransferase |
| | | 14 | DNA methyltransferase 1-associated protein 1, putative |
| | | 3 | single-stranded DNA-binding protein, putative |
| | | 12 | hypoxanthine-guanine phosphoribosyltransferase |
| | | 2 | ADP-ribosylation factor, putative |
| | | 2 | 60S acidic ribosomal protein P1, putative |
| | | 2 | transcription initiation factor IIF subunit beta, putative |
| | | 3 | 60S ribosomal protein L6, putative |
| | | 2 | rhoptry-associated protein 3 |
| | | 4 | DNA primase small subunit |
| | | 41 | PRE-binding protein |
| | | 9 | eukaryotic translation initiation factor 3 subunit C, putative |
| | | 4 | AP-1 complex subunit mu-1 |
| | | 7 | proteasome subunit alpha type-5, putative |
| | | 5 | calmodulin |
| | | 9 | ADP-ribosylation factor 1 |
| | | 9 | DnaJ protein, putative |
| | | 33 | erythrocyte membrane-associated antigen |
| | | 15 | adenosine deaminase |
| | | 10 | 26S proteasome regulatory subunit RPN9, putative |
| | | 3 | rhoptry neck protein 5 |
| | | 5 | CX3CL1-binding protein 2 |
| | | 7 | haloacid dehalogenase-like hydrolase, putative |
| | | 2 | ras-related protein Rab-11A |
| | | 2 | coatomer subunit epsilon, putative |
| | | 2 | glycerol kinase |

| | | | | |
|---|---|---|---|---|
| | | | 2 | E3 ubiquitin-protein ligase, putative |
| | | | 2 | pseudouridylate synthase, putative |
| | | | 6 | para-aminobenzoic acid synthetase |
| | | | 3 | protein-L-isoaspartate(D-aspartate) O-methyltransferase, putative |
| | | | 6 | RNA-binding protein musashi, putative |
| | | | 18 | T-complex protein 1 subunit theta |
| | | | 13 | eukaryotic translation initiation factor eIF2A, putative |
| | | | 3 | 40S ribosomal protein S27 |
| | | | 1 | Lysine decarboxylase OS=Escherichia coli (strain B / BL21-DE3) OX=469008 GN=ECBD_3899 PE=3 SV=1 |
| | | | 9 | 40S ribosomal protein S20e, putative |
| | | | 12 | dihydroorotase, putative |
| | | | 1 | nucleic acid binding protein, putative |
| | | | 7 | protein phosphatase containing kelch-like domains |
| | | | 2 | ATP synthase subunit alpha, mitochondrial |
| | | | 14 | 60S ribosomal protein P0 |
| | | | 3 | actin-like protein, putative |
| | | | 3 | queuine tRNA-ribosyltransferase, putative |
| | | | 6 | Plasmodium exported protein, unknown function |
| | | | 1 | conserved Plasmodium protein, unknown function |
| | | | 2 | 60S ribosomal protein L23, putative |
| | | | 2 | conserved Plasmodium protein, unknown function |
| | | | 24 | asparagine--tRNA ligase |
| | | | 4 | SWI/SNF-related matrix-associated actin-dependent regulator of chromatin |
| | | | 6 | polyadenylate-binding protein 3, putative |
| | | | 10 | eukaryotic translation initiation factor 2 subunit beta |
| | | | 5 | dicarboxylate/tricarboxylate carrier |
| | | | 3 | eukaryotic peptide chain release factor GTP-binding subunit, putative |
| | | | 4 | conserved Plasmodium protein, unknown function |
| | | | 52 | heat shock protein 70 |

| | | | | |
|---|---|---|---|---|
| | | | 13 | dynamin-like protein |
| | | | 1 | S-antigen |
| | | | 1 | conserved Plasmodium protein, unknown function |
| | | | 11 | rRNA 2-O-methyltransferase fibrillarin, putative |
| | | | 19 | T-complex protein 1 subunit gamma |
| | | | 11 | actin-related protein ARP4 |
| | | | 11 | exported protein 2 |
| | | | 13 | 26S protease regulatory subunit 8, putative |
| | | | 4 | phosphatidylserine decarboxylase |
| | | | 34 | elongation factor 2 |
| | | | 21 | alanine--tRNA ligase |
| | | | 7 | spermidine synthase |
| | | | 7 | ABC transporter E family member 1, putative |
| | | | 7 | conserved protein, unknown function |
| | | | 4 | ATP-dependent protease ATPase subunit ClpY |
| | | | 4 | rhoptry protein, putative |
| | | | 3 | RNA-binding protein, putative |
| | | | 3 | chromatin assembly factor 1 subunit B, putative |
| | | | 6 | heat shock protein 90, putative |
| | | | 23 | hexokinase |
| | | | 8 | ubiquitin carboxyl-terminal hydrolase, putative |
| | | | 2 | histone deacetylase 1 |
| | | | 24 | pyruvate kinase |
| | | | 15 | T-complex protein 1 subunit alpha |
| | | | 3 | structural maintenance of chromosomes protein 1, putative |
| | | | 7 | WD repeat-containing protein, putative |
| | | | 2 | conserved protein, unknown function |
| | | | 12 | exportin-T, putative |
| | | | 3 | conserved Plasmodium protein, unknown function |
| | | | 14 | proliferating cell nuclear antigen 1 |
| | | | 21 | asparagine synthetase [glutamine-hydrolyzing], putative |
| | | | 11 | tRNA import protein tRIP |
| | | | 19 | BFR1 domain-containing protein, putative |
| | | | 2 | PHD finger protein PHD1 |

| | | | |
|---|---|---|---|
| | | 9 | 26S protease regulatory subunit 6B, putative |
| | | 3 | RNA-binding protein, putative |
| | | 16 | Plasmodium exported protein (PHISTc), unknown function |
| | | 5 | proteasome subunit beta type-1, putative |
| | | 3 | AMMECR1 domain-containing protein, putative |
| | | 4 | tRNA nucleotidyltransferase, putative |
| | | 7 | replication factor C subunit 2, putative |
| | | 2 | peroxisome assembly protein 22, putative |
| | | 7 | ethanolamine-phosphate cytidylyltransferase |
| | | 15 | mini-chromosome maintenance complex-binding protein |
| | | 3 | prodrug activation and resistance esterase |
| | | 12 | serine--tRNA ligase, putative |
| | | 11 | exportin-7, putative |
| | | 2 | tetQ family GTPase, putative |
| | | 1 | prolyl 4-hydroxylase subunit alpha, putative |
| | | 8 | pyrroline-5-carboxylate reductase, putative |
| | | 14 | pyruvate kinase 2 |
| | | 5 | conserved Plasmodium protein, unknown function |
| | | 2 | kinetochore protein NDC80, putative |
| | | 9 | 60 kDa chaperonin |
| | | 16 | 60S ribosomal protein L3 |
| | | 10 | 26S proteasome regulatory subunit RPN7, putative |
| | | 19 | glutamine--tRNA ligase, putative |
| | | 3 | ubiquitin conjugation factor E4 B, putative |
| | | 10 | 1-cys peroxiredoxin |
| | | 4 | replication factor C subunit 5, putative |
| | | 7 | adenylosuccinate synthetase |
| | | 11 | ras-related protein Rab-2 |
| | | 7 | succinate--CoA ligase [ADP-forming] subunit beta |
| | | 14 | 40S ribosomal protein S2 |
| | | 5 | conserved Plasmodium protein, unknown function |
| | | 1 | conserved protein, unknown function |
| | | 2 | peptidyl-prolyl cis-trans isomerase |

| | | | | |
|---|---|---|---|---|
| | | | 8 | V-type proton ATPase subunit H, putative |
| | | | 6 | AP2 domain transcription factor, putative |
| | | | 3 | histidine triad nucleotide-binding protein 1 |
| | | | 9 | ring-infected erythrocyte surface antigen |
| | | | 2 | HSP90 co-chaperone p23 |
| | | | 5 | replication factor C subunit 3, putative |
| | | | 5 | plasmepsin II |
| | | | 2 | proteasome subunit beta type-5 |
| | | | 16 | GTP-binding nuclear protein RAN/TC4 |
| | | | 32 | endoplasmin, putative |
| | | | 11 | N-alpha-acetyltransferase 15, NatA auxiliary subunit, putative |
| | | | 15 | T-complex protein 1 subunit beta |
| | | | 13 | pyridoxine biosynthesis protein PDX1 |
| | | | 1 | 40S ribosomal protein S28e, putative |
| | | | 10 | arginyl-tRNA--protein transferase |
| | | | 8 | MORC family protein |
| | | | 1 | conserved Plasmodium protein, unknown function |
| | | | 2 | dihydrofolate synthase/folylpolyglutamate synthase |
| | | | 2 | conserved Plasmodium protein, unknown function |
| | | | 3 | mitochondrial-processing peptidase subunit beta, putative |
| | | | 15 | bifunctional dihydrofolate reductase-thymidylate synthase |
| | | | 2 | vacuolar protein sorting-associated protein 9, putative |
| | | | 2 | signal recognition particle subunit SRP54 |
| | | | 6 | Plasmodium exported protein, unknown function |
| | | | 5 | coatomer subunit zeta, putative |
| | | | 9 | M18 aspartyl aminopeptidase |
| | | | 3 | conserved protein, unknown function |
| | | | 3 | conserved Plasmodium protein, unknown function |
| | | | 14 | translation initiation factor IF-2, putative |
| | | | 21 | high molecular weight rhoptry protein 3 |

| | | | |
|---|---|---|---|
| | | 8 | eukaryotic translation initiation factor 3 subunit F, putative |
| | | 4 | filament assembling protein, putative |
| | | 3 | proteasome subunit beta type-2, putative |
| | | 28 | isocitrate dehydrogenase [NADP], mitochondrial |
| | | 32 | inositol-3-phosphate synthase |
| | | 1 | heptatricopeptide repeat and RAP domain-containing protein, putative |
| | | 16 | rhoptry-associated protein 1 |
| | | 17 | 26S proteasome regulatory subunit RPN3, putative |
| | | 3 | pre-mRNA-splicing regulator WTAP, putative |
| | | 3 | inner membrane complex protein |
| | | 9 | GYF domain-containing protein, putative |
| | | 2 | AP-1 complex subunit sigma, putative |
| | | 2 | protein phosphatase, putative |
| | | 4 | WD repeat-containing protein |
| | | 3 | ubiquitin-conjugating enzyme E2 13 |
| | | 13 | ribonucleoside-diphosphate reductase small chain, putative |
| | | 2 | choline-phosphate cytidylyltransferase |
| | | 20 | T-complex protein 1 subunit epsilon |
| | | 1 | tyrosine kinase-like protein |
| | | 3 | ras-related protein Rab-5A |
| | | 2 | orotate phosphoribosyltransferase |
| | | 11 | alpha tubulin 1 |
| | | 2 | alpha/beta-hydrolase, putative |
| | | 1 | conserved protein, unknown function |
| | | 11 | tudor staphylococcal nuclease |
| | | 7 | proteasome subunit beta type-7, putative |
| | | 6 | conserved Plasmodium protein, unknown function |
| | | 1 | AP-4 complex accessory subunit Tepsin, putative |
| | | 9 | FAD-dependent glycerol-3-phosphate dehydrogenase, putative |
| | | 3 | plasma membrane protein 1, putative |

| | | | | |
|---|---|---|---|---|
| | | | 7 | erythrocyte membrane protein 1, PfEMP1 |
| | | | 5 | conserved protein, unknown function |
| | | | 11 | heat shock protein 101 |
| | | | 2 | DNA-directed RNA polymerase II subunit RPB11, putative |
| | | | 4 | suppressor of kinetochore protein 1, putative |
| | | | 9 | tubulin gamma chain |
| | | | 2 | thioredoxin reductase |
| | | | 3 | conserved protein, unknown function |
| | | | 2 | glutaredoxin 1 |
| | | | 3 | Plasmodium exported protein, unknown function |
| | | | 10 | NPL domain-containing protein, putative |
| | | | 2 | leucine-rich repeat protein |
| | | | 1 | zinc finger protein, putative |
| | | | 3 | conserved protein, unknown function |
| | | | 11 | 26S proteasome regulatory subunit RPN6 |
| | | | 7 | ubiquitin carboxyl-terminal hydrolase 13, putative |
| | | | 11 | casein kinase 1 |
| | | | 1 | conserved Plasmodium protein, unknown function |
| | | | 11 | DNA mismatch repair protein MSH6, putative |
| | | | 13 | 26S proteasome regulatory subunit RPN2, putative |
| | | | 1 | ataxin-3, putative |
| | | | 22 | glutamate--tRNA ligase, putative |
| | | | 2 | tRNA (adenine(58)-N(1))-methyltransferase catalytic subunit TRM61, putative |
| | | | 2 | met-10+ like protein, putative |
| | | | 4 | conserved Plasmodium protein, unknown function |
| | | | 10 | eukaryotic translation initiation factor 3 subunit I, putative |
| | | | 2 | conserved protein, unknown function |
| | | | 5 | proteasome subunit beta type-6, putative |
| | | | 21 | elongation factor 1-gamma, putative |
| | | | 13 | eukaryotic peptide chain release factor subunit 1, putative |
| | | | 3 | DNA polymerase delta small subunit, putative |

| | | | |
|---|---|---|---|
| | | 12 | transportin |
| | | 5 | prefoldin subunit 2, putative |
| | | 53 | ATP-dependent 6-phosphofructokinase |
| | | 8 | non-SERCA-type Ca2+ -transporting P-ATPase |
| | | 1 | Na+/H+ antiporter OS=Escherichia coli (strain B / BL21-DE3) OX=469008 GN=ECBD_3967 PE=3 SV=1 |
| | | 4 | replication factor C subunit 4, putative |
| | | 2 | ankyrin-repeat protein, putative |
| | | 8 | eukaryotic initiation factor 4A-III, putative |
| | | 9 | actin-like protein, putative |
| | | 10 | eukaryotic translation initation factor 4 gamma |
| | | 23 | ubiquitin-activating enzyme E1 |
| | | 7 | DNA mismatch repair protein MSH2, putative |
| | | 2 | ubiquitin-like protein, putative |
| | | 2 | ubiquitin fusion degradation protein 1, putative |
| | | 7 | eukaryotic translation initiation factor 3 subunit L, putative |
| | | 7 | cAMP-dependent protein kinase regulatory subunit |
| | | 18 | threonine--tRNA ligase |
| | | 6 | chaperone binding protein, putative |
| | | 5 | pantothenate kinase 1 |
| | | 5 | conserved protein, unknown function |
| | | 41 | high molecular weight rhoptry protein 2 |
| | | 11 | protein phosphatase PPM2 |
| | | 2 | SAC3 domain-containing protein, putative |
| | | 6 | surface protein P113 |
| | | 2 | zinc finger protein, putative |
| | | 3 | pre-mRNA-splicing factor CWC2, putative |
| | | 19 | glycine--tRNA ligase |
| | | 28 | S-adenosylmethionine synthetase |
| | | 4 | TLD domain-containing protein |
| | | 8 | small heat shock protein, putative |
| | | 5 | deoxyuridine 5-triphosphate nucleotidohydrolase |
| | | 3 | calcium-dependent protein kinase 1 |

| | | | |
|---|---|---|---|
| | | 33 | cell division cycle protein 48 homologue, putative |
| | | 8 | replication factor C subunit 1 |
| | | 19 | heat shock protein 70 |
| | | 18 | HSP40, subfamily A |
| | | 2 | CCR4-NOT transcription complex subunit NOT1-G, putative |
| | | 6 | DNA/RNA-binding protein Alba 2 |
| | | 13 | 26S proteasome regulatory subunit RPN1, putative |
| | | 3 | RNA-binding protein, putative |
| | | 6 | lysine--tRNA ligase |
| | | 5 | thioredoxin-related protein, putative |
| | | 4 | conserved Plasmodium protein, unknown function |
| | | 6 | AP-1 complex subunit gamma, putative |
| | | 6 | 60S ribosomal protein L12, putative |
| | | 4 | dolichyl-phosphate-mannose--protein mannosyltransferase, putative |
| | | 17 | enolase |
| | | 4 | vacuolar protein sorting-associated protein 46, putative |
| | | 2 | splicing factor U2AF large subunit, putative |
| | | 31 | phosphoglycerate kinase |
| | | 17 | gamma-glutamylcysteine synthetase |
| | | 3 | CCR4-associated factor 1 |
| | | 8 | T-complex protein 1 subunit eta |
| | | 4 | translocation protein SEC63, putative |
| | | 20 | protein transport protein SEC23 |
| | | 3 | histone acetyltransferase, putative |
| | | 2 | arginine--tRNA ligase |
| | | 10 | glutamine synthetase, putative |
| | | 37 | elongation factor 1-alpha |
| | | 4 | splicing factor 3B subunit 5, putative |
| | | 2 | U6 snRNA-associated Sm-like protein LSm7, putative |
| | | 4 | cysteine desulfurase IscS |
| | | 6 | 26S proteasome regulatory subunit p55, putative |
| | | 4 | thiamine pyrophosphokinase |

| | | | | |
|---|---|---|---|---|
| | | | 24 | eukaryotic initiation factor 4A |
| | | | 7 | PI31 domain-containing protein, putative |
| | | | 5 | dipeptidyl aminopeptidase 3 |
| | | | 9 | H/ACA ribonucleoprotein complex subunit 4, putative |
| | | | 2 | signal recognition particle receptor subunit beta, putative |
| | | | 7 | nucleolar protein 56, putative |
| | | | 14 | ATP-dependent RNA helicase DDX60, putative |
| | | | 9 | nicotinamidase, putative |
| | | | 9 | sortilin |
| | | | 6 | rhomboid protease ROM4 |
| | | | 4 | RNA-binding protein, putative |
| | | | 12 | protein transport protein SEC31 |
| | | | 30 | karyopherin beta |
| | | | 11 | tubulin beta chain |
| | | | 9 | polyadenylate-binding protein-interacting protein 1, putative |
| | | | 14 | protein phosphatase PPM11, putative |
| | | | 3 | signal peptidase complex catalytic subunit SEC11 |
| | | | 3 | dihydrolipoyllysine-residue succinyltransferase component of 2-oxoglutarate dehydrogenase complex |
| | | | 6 | NLI interacting factor-like phosphatase, putative |
| | | | 10 | parasitophorous vacuolar protein 1 |
| | | | 7 | tyrosine--tRNA ligase |
| | | | 2 | ubiquitin-conjugating enzyme E2, putative |
| | | | 3 | phosphoinositide-binding protein, putative |
| | | | 2 | nuclear import protein MOG1, putative |
| | | | 4 | AP2 domain transcription factor |
| | | | 10 | coronin |
| | | | 2 | peptidyl-prolyl cis-trans isomerase |
| | | | 2 | serine/threonine protein phosphatase 6, putative |
| | | | 1 | conserved Plasmodium protein, unknown function |
| | | | 5 | coatomer subunit delta |
| | | | 6 | transcription elongation factor SPT5, putative |
| | | | 8 | exosome complex component RRP40, putative |

| | | | |
|---|---|---|---|
| | | 4 | acylphosphatase, putative |
| | | 4 | fam-a protein |
| | | 8 | Plasmodium exported protein (PHISTc) |
| | | 3 | early transcribed membrane protein 5 |
| | | 11 | copper-transporting ATPase |
| | | 8 | proteasome subunit alpha type-6, putative |
| | | 7 | protein DJ-1 |
| | | 9 | importin alpha re-exporter, putative |
| | | 2 | N6-adenosine-methyltransferase, putative |
| | | 13 | 26S protease regulatory subunit 6A, putative |
| | | 4 | myosin A |
| | | 4 | 40S ribosomal protein S10, putative |
| | | 6 | vacuolar protein sorting-associated protein 35, putative |
| | | 6 | parasite-infected erythrocyte surface protein |
| | | 9 | replication protein A1, small fragment |
| | | 7 | bifunctional farnesyl/geranylgeranyl diphosphate synthase |
| | | 5 | DNA polymerase alpha subunit B, putative |
| | | 10 | U4/U6 small nuclear ribonucleoprotein PRP4, putative |
| | | 13 | RNA cytosine C(5)-methyltransferase, putative |
| | | 5 | proteasome subunit alpha type-1, putative |
| | | 2 | glycine cleavage system H protein |
| | | 12 | Plasmodium exported protein (PHISTb) |
| | | 8 | eukaryotic translation initiation factor 3 subunit E, putative |
| | | 3 | V-type proton ATPase subunit F, putative |
| | | 3 | phosphoenolpyruvate carboxykinase |
| | | 8 | protein arginine N-methyltransferase 5, putative |
| | | 5 | proteasome activator 28 |
| | | 9 | histone-arginine methyltransferase CARM1, putative |
| | | 23 | acyl-CoA synthetase |
| | | 2 | protein P22, putative |
| | | 1 | falstatin |

| | | | | |
|---|---|---|---|---|
| | | | 3 | ATP-dependent RNA helicase DDX42, putative |
| | | | 5 | ribonucleoside-diphosphate reductase small chain, putative |
| | | | 2 | conserved protein, unknown function |
| | | | 12 | glucose-6-phosphate isomerase |
| | | | 2 | serine/threonine protein phosphatase 4, putative |
| | | | 24 | glideosome-associated connector |
| | | | 3 | CRWN-like protein, putative |
| | | | 26 | isoleucine--tRNA ligase, putative |
| | | | 4 | AP2 domain transcription factor, putative |
| | | | 2 | ribosome associated membrane protein RAMP4, putative |
| | | | 2 | conserved Plasmodium protein, unknown function |
| | | | 3 | uracil-DNA glycosylase |
| | | | 15 | T-complex protein 1 subunit zeta |
| | | | 2 | ubiquitin specific protease, putative |
| | | | 13 | phosphoethanolamine N-methyltransferase |
| | | | 6 | multidrug resistance protein 1 |
| | | | 14 | V-type proton ATPase subunit B |
| | | | 4 | parasite-infected erythrocyte surface protein |
| | | | 9 | valine--tRNA ligase, putative |
| | | | 9 | TatD-like deoxyribonuclease |
| | | | 5 | ras-related protein Rab-5C |
| | | | 3 | 26S proteasome regulatory subunit RPN8, putative |
| | | | 15 | rhoptry-associated leucine zipper-like protein 1 |
| | | | 13 | exportin-1, putative |
| | | | 7 | coatomer subunit gamma, putative |
| | | | 8 | DNA-binding chaperone, putative |
| | | | 3 | single-stranded DNA-binding protein |
| | | | 2 | cleavage and polyadenylation specificity factor subunit 5, putative |
| | | | 2 | conserved Plasmodium protein, unknown function |
| | | | 4 | conserved protein, unknown function |
| | | | 6 | choline kinase |

| | | | | |
|---|---|---|---|---|
| | | | 2 | U6 snRNA-associated Sm-like protein LSm3, putative |
| | | | 15 | cAMP-dependent protein kinase catalytic subunit |
| | | | 15 | heat shock protein 110 |
| | | | 18 | nuclear protein localization protein 4, putative |
| | | | 13 | structural maintenance of chromosomes protein 3 |
| | | | 9 | KH domain-containing protein, putative |
| | | | 26 | cytoadherence linked asexual protein 3.1 |
| | | | 19 | 14-3-3 protein |
| | | | 5 | hydroxyethylthiazole kinase |
| | | | 5 | proliferating cell nuclear antigen 2 |
| | | | 14 | aspartate--tRNA ligase |
| | | | 1 | ATPase GET3 |
| | | | 6 | inner membrane complex protein 1g, putative |
| | | | 3 | UMP-CMP kinase, putative |
| | | | 2 | peptidyl-prolyl cis-trans isomerase |
| | | | 2 | conserved Plasmodium protein, unknown function |
| | | | 2 | Maltodextrin-binding protein OS=Escherichia coli (strain B / BL21-DE3) OX=469008 GN=ECBD_4002 PE=1 SV=1 |
| | | | 2 | autophagy-related protein 8 |
| | | | 17 | myosin F, putative |
| | | | 15 | Hsp70/Hsp90 organizing protein |
| | | | 12 | eukaryotic translation initiation factor 2 subunit alpha |
| | | | 11 | eukaryotic translation initiation factor 3 subunit A, putative |
| | | | 8 | conserved protein, unknown function |
| | | | 6 | proteasome subunit alpha type-2, putative |
| | | | 3 | cytosolic glyoxalase II |
| | | | 7 | Plasmodium exported protein (PHISTa), unknown function |
| | | | 3 | N2227-like protein, putative |
| | | | 2 | PhIL1-interacting candidate PIC5 |
| | | | 9 | thioredoxin peroxidase 1 |
| | | | 6 | asparagine and aspartate rich protein 1 |
| | | | 9 | serine/threonine protein phosphatase 5 |

| | | | |
|---|---|---|---|
| | | 17 | glucose-6-phosphate dehydrogenase-6-phosphogluconolactonase |
| | | 5 | proteasome subunit alpha type-4, putative |
| | | 1 | SUZ domain-containing protein, putative |
| | | 1 | conserved Plasmodium protein, unknown function |
| | | 12 | ATP-dependent RNA helicase DBP5 |
| | | 14 | acetyl-CoA synthetase |
| | | 7 | V-type proton ATPase subunit D, putative |
| | | 5 | GRIP domain-containing protein, putative |
| | | 10 | DNA-(apurinic or apyrimidinic site) endonuclease |
| | | 1 | replication factor A protein 3, putative |
| | | 2 | conserved protein, unknown function |
| | | 6 | activator of Hsp90 ATPase, putative |
| | | 24 | DNA replication licensing factor MCM6 |
| | | 4 | vesicle-associated membrane protein, putative |
| | | 12 | DNA helicase 60 |
| | | 4 | exosome complex component RRP45, putative |
| | | 2 | pre-rRNA-processing protein TSR2, putative |
| | | 1 | conserved Plasmodium protein, unknown function |
| | | 7 | XTBD domain-containing protein, putative |
| | | 3 | conserved Plasmodium protein, unknown function |
| | | 3 | ubiquitin-60S ribosomal protein L40 |
| | | 1 | exosome complex component RRP42, putative |
| | | 2 | TOG domain-containing protein, putative |
| | | 1 | centrin-1 |
| | | 7 | W2 domain-containing protein, putative |
| | | 6 | prefoldin subunit 5, putative |
| | | 22 | leucine--tRNA ligase, putative |
| | | 15 | falcilysin |
| | | 8 | nucleoside diphosphate kinase |
| | | 8 | 40S ribosomal protein S5, putative |
| | | 1 | transmembrane emp24 domain-containing protein, putative |
| | | 26 | actin I |

| | | | | |
|---|---|---|---|---|
| | | | 6 | nucleosome assembly protein |
| | | | 4 | nuclear movement protein, putative |
| | | | 2 | Plasmodium exported protein (hyp16), unknown function |
| | | | 3 | conserved protein, unknown function |
| | | | 4 | oxysterol-binding protein, putative |
| | | | 33 | glutamate dehydrogenase, putative |
| | | | 10 | elongation factor 1-beta |
| | | | 9 | merozoite surface protein 7 |
| | | | 1 | rhoptry protein RHOP148 |
| | | | 4 | protein kinase, putative |
| | | | 2 | pantothenate kinase 2 |
| | | | 3 | hydrolase, putative |
| | | | 22 | DNA replication licensing factor MCM7 |
| | | | 17 | ISWI chromatin-remodeling complex ATPase |
| | | | 3 | AP-1/2 complex subunit beta, putative |
| | | | 27 | mannose-6-phosphate isomerase, putative |
| | | | 3 | transcriptional coactivator ADA2 |
| | | | 5 | deoxyribose-phosphate aldolase, putative |
| | | | 2 | E3 ubiquitin-protein ligase, putative |
| | | | 5 | methionine aminopeptidase 2 |
| | | | 13 | dipeptidyl aminopeptidase 1 |
| | | | 3 | HECT-type E3 ubiquitin ligase UT |
| | | | 5 | dual specificity protein phosphatase |
| | | | 2 | conserved Plasmodium protein, unknown function |
| | | | 12 | RuvB-like helicase 2 |
| | | | 9 | transcription elongation factor SPT6, putative |
| | | | 9 | ras-related protein Rab-6 |
| | | | 9 | M17 leucyl aminopeptidase |
| | | | 4 | H/ACA ribonucleoprotein complex subunit 3, putative |
| | | | 2 | mediator of RNA polymerase II transcription subunit 17, putative |
| | | | 6 | RNA-binding protein, putative |
| | | | 9 | serine/threonine protein kinase, FIKK family |
| | | | 4 | protein disulfide-isomerase |

| | | | | |
|---|---|---|---|---|
| | | | 2 | conserved Plasmodium protein, unknown function |
| | | | 32 | DNA replication licensing factor MCM4 |
| | | | 17 | phosphoglycerate mutase, putative |
| | | | 6 | vacuolar protein sorting-associated protein 26, putative |
| | | | 4 | vacuolar protein sorting-associated protein 29 |
| | | | 9 | HECT-like E3 ubiquitin ligase, putative |
| | | | 1 | pre-mRNA-processing factor 40, putative |
| | | | 2 | N-acetyltransferase, GNAT family, putative |
| | | | 12 | centrin-2 |
| | | | 5 | conserved protein, unknown function |
| | | | 6 | aspartate transaminase |
| | | | 5 | plasmepsin III |
| | | | 3 | proteasome subunit alpha type-3, putative |
| | | | 24 | clathrin heavy chain, putative |
| | | | 2 | pyridoxine biosynthesis protein PDX2 |
| | | | 3 | 60S acidic ribosomal protein P2 |
| | | | 20 | adenosylhomocysteinase |
| | | | 1 | lysine-rich membrane-associated PHISTb protein |
| | | | 9 | protein transport protein SEC13 |
| | | | 2 | regulator of chromosome condensation, putative |
| | | | 10 | geranylgeranyl transferase type-2 subunit beta, putative |
| | | | 15 | cytoadherence linked asexual protein 9 |
| | | | 20 | DNA replication licensing factor MCM2 |
| | | | 6 | conserved protein, unknown function |
| | | | 1 | chloroquine resistance transporter |
| | | | 2 | conserved Plasmodium protein, unknown function |
| | | | 21 | antigen 332, DBL-like protein |
| | | | 3 | conserved Plasmodium protein, unknown function |
| | | | 31 | carbamoyl phosphate synthetase |
| | | | 13 | RNA lariat debranching enzyme, putative |
| | | | 3 | glutathione S-transferase |
| | | | 2 | rab GTPase activator, putative |
| | | | 4 | methyltransferase, putative |

| | | | | |
|---|---|---|---|---|
| | | | 10 | eukaryotic translation initiation factor 3 subunit M, putative |
| | | | 3 | conserved Plasmodium protein, unknown function |
| | | | 4 | serine/threonine protein phosphatase CPPED1, putative |
| | | | 10 | thioredoxin-like mero protein |
| | | | 1 | H/ACA ribonucleoprotein complex subunit 1, putative |
| | | | 4 | CCR4 domain-containing protein 4, putative |
| | | | 8 | YEATS domain-containing protein, putative |
| | | | 3 | proteasome subunit beta type-3, putative |
| | | | 10 | conserved Plasmodium protein, unknown function |
| | | | 4 | nucleic acid binding protein, putative |
| | | | 47 | mature parasite-infected erythrocyte surface antigen |
| | | | 1 | conserved Plasmodium protein, unknown function |
| | | | 13 | ubiquitin carboxyl-terminal hydrolase 2, putative |
| | | | 11 | GBP130 protein |
| | | | 13 | splicing factor 3B subunit 3, putative |
| | | | 2 | actin-like protein, putative |
| | | | 2 | protein arginine N-methyltransferase 1 |
| | | | 4 | histone acetyltransferase GCN5 |
| | | | 10 | coatomer subunit beta, putative |
| | | | 14 | importin-7, putative |
| | | | 2 | ubiquitin carboxyl-terminal hydrolase 14 |
| | | | 7 | histone-binding protein RBBP7, putative |
| | | | 2 | proteasome activator complex subunit 4, putative |
| | | | 5 | protein SIS1 |
| | | | 7 | lysine decarboxylase-like protein, putative |
| | | | 4 | elongation factor Tu, putative |
| | | | 4 | NLI interacting factor-like phosphatase, putative |
| | | | 5 | prefoldin subunit 6 |
| | | | 21 | ribonucleoside-diphosphate reductase large subunit, putative |
| | | | 2 | cdc2-related protein kinase 3 |
| | | | 2 | U6 snRNA-associated Sm-like protein LSm2, putative |
| | | | 2 | translation initiation factor eIF-1A, putative |

| | | | | |
|---|---|---|---|---|
| | | | 5 | elongation factor Tu, putative |
| | | | 4 | glyoxalase I |
| | | | 3 | deubiquitinating enzyme MINDY, putative |
| | | | 5 | signal recognition particle subunit SRP68, putative |
| | | | 2 | Plasmodium exported protein (PHISTc), unknown function |
| | | | 22 | insulinase, putative |
| | | | 5 | Eps15-like protein |
| | | | 8 | Hsc70-interacting protein |
| | | | 4 | ATPase |
| | | | 6 | ATP-dependent RNA helicase DHX57, putative |
| | | | 3 | cysteine proteinase falcipain 3 |
| | | | 8 | activator of Hsp90 ATPase |
| | | | 3 | phosphomethylpyrimidine kinase, putative |
| | | | 1 | glideosome associated protein with multiple membrane spans 2 |
| | | | 10 | coatomer alpha subunit, putative |
| | | | 20 | conserved Plasmodium protein, unknown function |
| | | | 10 | actin II |
| | | | 8 | rhoptry-associated protein 2 |
| | | | 5 | UVB-resistance protein UVR8 homologue |
| | | | 4 | transcription elongation factor s-II, putative |
| | | | 3 | DNA primase large subunit, putative |
| | | | 5 | trophozoite exported protein 1 |
| | | | 3 | tRNA (adenine(58)-N(1))-methyltransferase non-catalytic subunit TRM6, putative |
| | | | 9 | thioesterase/thiol ester dehydrase-isomerase, putative |
| | | | 6 | conserved Plasmodium protein, unknown function |
| | | | 4 | 40S ribosomal protein S12, putative |
| | | | 13 | conserved protein, unknown function |
| | | | 6 | chromatin assembly factor 1 subunit C, putative |
| | | | 3 | protein kinase 6 |
| | | | 13 | L-lactate dehydrogenase |
| | | | 2 | cleavage stimulation factor subunit 1, putative |
| | | | 6 | serine hydroxymethyltransferase |

| | | | |
|---|---|---|---|
| | | 6 | small GTP-binding protein sar1 |
| | | 6 | conserved Plasmodium protein, unknown function |
| | | 2 | Maf-like protein, putative |
| | | 11 | RuvB-like helicase 3 |
| | | 2 | conserved protein, unknown function |
| | | 4 | conserved Plasmodium protein, unknown function |
| | | 1 | proteasome assembly chaperone 4, putative |
| | | 6 | cyclin-dependent kinases regulatory subunit, putative |
| | | 2 | U4/U6 small nuclear ribonucleoprotein PRP3, putative |
| | | 15 | glutamine-dependent NAD(+) synthetase, putative |
| | | 4 | NYN domain-containing protein, putative |
| | | 2 | conserved Plasmodium protein, unknown function |
| | | 1 | protein transport protein SEC16, putative |
| | | 10 | acyl-CoA synthetase |
| | | 1 | AP-3 complex subunit mu, putative |
| | | 3 | conserved protein, unknown function |
| | | 5 | polyubiquitin binding protein, putative |
| | | 1 | conserved Plasmodium membrane protein, unknown function |
| | | 2 | conserved Plasmodium protein, unknown function |
| | | 4 | translation initiation factor eIF-2B subunit gamma, putative |
| | | 5 | SUMO-activating enzyme subunit 1 |
| | | 1 | dynamin-like protein |
| | | 1 | RWD domain-containing protein, putative |
| | | 2 | glutamate-rich protein GLURP |
| | | 3 | conserved Plasmodium protein, unknown function |
| | | 11 | phenylalanine--tRNA ligase beta subunit |
| | | 5 | plasmepsin IV |
| | | 1 | conserved Plasmodium protein, unknown function |
| | | 10 | triosephosphate isomerase |
| | | 2 | Plasmodium exported protein (PHISTb), unknown function |
| | | 2 | trafficking protein particle complex subunit 8, putative |

242

| | | | | |
|---|---|---|---|---|
| | | | 7 | pseudouridine synthase, putative |
| | | | 10 | nucleosome assembly protein |
| | | | 13 | Plasmodium exported protein (PHISTb), unknown function |
| | | | 2 | superoxide dismutase [Fe] |
| | | | 2 | conserved protein, unknown function |
| | | | 4 | peptidyl-prolyl cis-trans isomerase |
| | | | 2 | conserved protein, unknown function |
| | | | 3 | translation machinery-associated protein 46, putative |
| | | | 1 | ubiquitin fusion degradation protein 1, putative |
| | | | 3 | acyl-CoA synthetase |
| | | | 3 | ras-related protein Rab-1B |
| | | | 1 | HSP20-like chaperone, putative |
| | | | 14 | serine repeat antigen 5 |
| | | | 1 | conserved Plasmodium protein, unknown function |
| | | | 18 | protein disulfide-isomerase |
| | | | 3 | 40S ribosomal protein S26 |
| | | | 6 | tetratricopeptide repeat protein, putative |
| | | | 3 | YOP1-like protein, putative |
| | | | 6 | replication protein A1, large subunit |
| | | | 18 | protein phosphatase PPM8, putative |
| | | | 2 | elongation factor Tu, putative |
| | | | 1 | aminomethyltransferase, mitochondrial, putative |
| | | | 2 | ubiquitin-conjugating enzyme E2 PEX4, putative |
| | | | 24 | aminopeptidase P |
| | | | 2 | DNA-directed RNA polymerases I, II, and III subunit RPABC3, putative |
| | | | 1 | conserved Plasmodium protein, unknown function |
| | | | 4 | kinetochore protein NUF2, putative |
| | | | 7 | small exported membrane protein 1 |
| | | | 2 | conserved protein, unknown function |
| | | | 6 | cysteine proteinase falcipain 2b |
| | | | 7 | FACT complex subunit SPT16, putative |
| | | | 2 | BolA-like protein, putative |
| | | | 3 | elongation factor, putative |

| | | | | |
|---|---|---|---|---|
| | | | 2 | CCR4-NOT transcription complex subunit NOT1, putative |
| | | | 6 | endoplasmic reticulum chaperone GRP170 |
| | | | 1 | WD repeat-containing protein 70, putative |
| | | | 2 | 26S proteasome non-ATPase regulatory subunit 9, putative |
| | | | 1 | AP-4 complex subunit mu, putative |
| | | | 6 | proteasome subunit alpha type-7, putative |
| | | | 5 | Plasmodium exported protein, unknown function |
| | | | 4 | conserved Plasmodium protein, unknown function |
| | | | 4 | proteasome subunit beta type-4 |
| | | | 3 | mediator of RNA polymerase II transcription subunit 11, putative |
| | | | 9 | merozoite surface protein 9 |
| | | | 14 | 7-helix-1 protein |
| | | | 1 | conserved Plasmodium protein, unknown function |
| | | | 1 | Btz domain-containing protein, putative |
| | | | 1 | kinesin-13, putative |
| | | | 6 | 60S ribosomal protein L10, putative |
| + | WT_GEXP15 | | 7 | EMP1-trafficking protein |
| | | | 2 | DNA helicase, putative |
| | | | 3 | ribosome assembly protein RRB1, putative |
| | | | 2 | bromodomain protein 3, putative |
| | | | 3 | mitochondrial acidic protein MAM33, putative |
| | | | 1 | splicing factor 3B subunit 4, putative |
| | | | 2 | methionine aminopeptidase 1b, putative |
| | | | 2 | CRAL/TRIO domain-containing protein, putative |
| | | | 4 | ran-specific GTPase-activating protein 1, putative |
| | | | 6 | MA3 domain-containing protein, putative |
| | | | 2 | protein LTV1, putative |
| | | | 1 | CSTF domain-containing protein, putative |
| | | | 1 | serine repeat antigen 6 |
| | | | 2 | superoxide dismutase [Fe] |
| | | | 2 | exoribonuclease, putative |
| | | | 5 | glutathione peroxidase-like thioredoxin peroxidase |

| | | | | |
|---|---|---|---|---|
| | | | 5 | conserved Plasmodium protein, unknown function |
| | | | 2 | histone chaperone ASF1 |
| | | | 5 | ATP-dependent RNA helicase DDX23, putative |
| | | | 2 | ras-related protein Rab-1A |
| | | | 2 | profilin |
| | | | 1 | thioredoxin-like protein, putative |
| | | | 1 | phosphoacetylglucosamine mutase, putative |
| | | | 1 | cytidine diphosphate-diacylglycerol synthase |
| | | | 2 | conserved Plasmodium protein, unknown function |
| | | | 1 | SAE2 domain-containing protein, putative |
| | | | 11 | leucine-rich repeat protein |
| | | | 2 | EKC/KEOPS complex subunit CGI121 |
| | | | 21 | deoxyhypusine synthase |
| | | | 1 | SNARE protein, putative |
| | | | 2 | nuclear export mediator factor NEMF, putative |
| | | | 12 | geranylgeranyl transferase type-2 subunit alpha, putative |
| | | | 11 | adenylosuccinate lyase |
| | | | 1 | RNA-binding protein, putative |
| | | | 2 | SUMO-activating enzyme subunit 2 |
| | | | 1 | conserved Plasmodium protein, unknown function |
| | | | 1 | conserved Plasmodium protein, unknown function |
| | | | 3 | aminomethyltransferase, putative |
| | | | 2 | MSP7-like protein |
| | | | 3 | conserved Plasmodium protein, unknown function |
| | | | 6 | U3 small nucleolar ribonucleoprotein protein IMP4, putative |
| | | | 4 | acid phosphatase, putative |
| | | | 1 | phosphatidylinositol 4-kinase beta |
| | | | 2 | chaperone protein DnaJ |
| | | | 1 | CCR4-associated factor 16, putative |
| | | | 3 | small ubiquitin-related modifier |
| | | | 3 | signal recognition particle subunit SRP72, putative |
| | | | 1 | sphingomyelin phosphodiesterase |

| | | | | |
|---|---|---|---|---|
| | | | 13 | endoplasmic reticulum-resident calcium binding protein |
| | | | 2 | 10 kDa chaperonin |
| | | | 2 | phosphoglucomutase-2 |
| | | | 1 | translation machinery-associated protein 7, putative |
| | | | 6 | PUB domain-containing protein, putative |
| | | | 2 | PDCD2 domain-containing protein, putative |
| | | | 1 | beta-catenin-like protein 1, putative |
| | | | 3 | exosome complex component MTR3, putative |
| | | | 2 | RNA polymerase II transcription factor B subunit 2, putative |
| | | | 1 | conserved Plasmodium protein, unknown function |
| | | | 1 | leucine carboxyl methyltransferase, putative |
| | | | 2 | coatomer subunit beta, putative |
| | | | 1 | AN1-type zinc finger protein, putative |
| | | | 3 | adenylate kinase |
| | | | 4 | NADP-specific glutamate dehydrogenase |
| | | | 1 | aspartate carbamoyltransferase |
| | | | 1 | ribonuclease P protein subunit p29, putative |
| | | | 2 | proteasome maturation factor UMP1, putative |
| | | | 7 | macrophage migration inhibitory factor |
| | | | 2 | membrane associated histidine-rich protein 1 |
| | | | 4 | peptidase, putative |
| | | | 2 | phosphopantothenoylcysteine decarboxylase, putative |
| | | | 4 | Chaperone protein ClpB OS=Escherichia coli (strain B / BL21-DE3) OX=469008 GN=clpB PE=3 SV=1 |
| | | | 2 | 60S ribosomal protein L7ae/L30e, putative |
| | | | 2 | conserved Plasmodium protein, unknown function |
| | | | 8 | conserved protein, unknown function |
| | | | 1 | RNA-binding protein, putative |
| | | | 3 | spindle assembly abnormal protein 6, putative |
| | | | 1 | protein phosphatase inhibitor 2 |
| | | | 2 | serine/threonine protein phosphatase PP1 |

| | | | | |
|---|---|---|---|---|
| | | | 5 | ring-exported protein 1 |
| | | | 6 | lipocalin |
| | | | 3 | 6-cysteine protein P92 |
| | | | 2 | conserved protein, unknown function |
| | | | 5 | PhIL1-interacting candidate PIC1 |
| | | | 1 | U6 snRNA-associated Sm-like protein LSm1, putative |
| | | | 2 | trafficking protein particle complex subunit 13, putative |
| | | | 5 | GrpE protein homolog, mitochondrial, putative |
| | | | 2 | Plasmodium exported protein (PHISTb), unknown function |
| | | | 1 | pyridoxal 5-phosphate synthase, putative |
| | | | 2 | ELM2 domain-containing protein, putative |
| | | | 1 | PCI domain-containing protein, putative |
| | | | 2 | cation transporting ATPase, putative |
| | | | 2 | protein phosphatase PPM6, putative |
| | | | 3 | thioredoxin 1 |
| | | | 2 | Voldacs domain-containing protein, putative |
| | | | 2 | transcription elongation factor SPT4, putative |
| | | | 1 | signal peptide peptidase |
| | | | 3 | centrin-3 |
| | | | 5 | GTPase-activating protein, putative |
| | | | 2 | transcription initiation factor IIA subunit 2, putative |
| | | | 1 | ribosome-interacting GTPase 1, putative |
| | | | 1 | COBW domain-containing protein 1, putative |
| | | | 2 | Pfmc-2TM Maurers cleft two transmembrane protein |
| | | | 7 | eukaryotic translation initiation factor 3 subunit B, putative |
| | | | 2 | U3 small nucleolar RNA-associated protein 21, putative |
| | | | 1 | mago-binding protein, putative |
| + | WT_GEXP15 | | 1 | telomere repeat-binding zinc finger protein |
| | | | 3 | VPS13 domain-containing protein, putative |
| | | | 2 | conserved Plasmodium protein, unknown function |

**Supplementary Table 2. Identified proteins after RVxF, UCD, GYF and tetR containing proteins pulldown in *P. falciparum* extracts.** The table shows the name/accession number of identified proteins. Three experiments were performed with nickel agarose beads on WT trophozoites and schizonts. Here, we mention + for the protein immunoprecipitated in at least two experiments with peptides ≥ 2 and with peptides and spectra ≥ 2 fold compared with the control strain.

| GYF: Significant Class A | GYF: Difference | RVxF: Significant Class B | RVxF: Difference | UD: Significant Class B | UD: Difference | Protein annotation |
|---|---|---|---|---|---|---|
| + | 12,9985374 | | -0,22888724 | | 0,32973035 | PF3D7_1308700 |
| + | 9,57448928 | | -0,30352783 | | 0,58421612 | Early transcribed membrane protein 2 |
| + | 9,13377253 | | -0,83106661 | | -0,28226248 | Dynamin-like protein |
| + | 8,81650956 | | -0,45667394 | | 0,52165031 | 60S ribosomal protein L34 |
| + | 8,51759911 | | -0,31552601 | | -0,52967421 | PF3D7_1319900 |
| + | 8,41810385 | | -0,17542362 | | 0,56650639 | Membrane associated histidine-rich protein 1 |
| + | 8,23792871 | | 0,63668569 | | 0,91308212 | 60S ribosomal protein L13 |
| + | 8,16959413 | | -0,02914906 | | 1,10328515 | Receptor for activated c kinase |
| + | 8,02622286 | + | 8,85241954 | | 8,82465744 | GEXP15 |
| + | 7,74916871 | | 0,76115894 | | 0,02200413 | 60S ribosomal protein L37ae |

| | | | | | |
|---|---|---|---|---|---|
| + | 7,67428589 | | 0,02912807 | -0,50060972 | 60S ribosomal protein L30e |
| + | 7,511 | | -2,60081784 | 0,39835421 | 60S ribosomal protein L37 |
| + | 7,45493031 | | 1,2191124 | 1,85791524 | 60S ribosomal protein L31 |
| + | 7,37267049 | | 2,19933891 | 1,65299733 | DNA-directed RNA polymerase II subunit RPB2 |
| + | 7,35988617 | | 0,01919238 | -0,78175449 | Early transcribed membrane protein 14.1 |
| + | 7,2990907 | + | -1,63642883 | -0,53984547 | 60S ribosomal protein L14 |
| + | 7,26907031 | | -0,56157907 | -0,082901 | 60S ribosomal protein L10 |
| + | 7,05625566 | | -1,30183506 | 2,17159684 | 60S ribosomal protein L15 |
| + | 6,95318762 | | 0,91839854 | 0,52097575 | 40S ribosomal protein S9 |
| + | 6,69147491 | | -0,95315933 | -0,04397297 | 60S ribosomal protein L26 |
| + | 6,64732806 | | -0,67478625 | 0,46363386 | 40S ribosomal protein S8e |
| + | 6,54275894 | | -0,14363035 | 0,70409679 | Eukaryotic translation initiation factor 3 subunit A |
| + | 6,28102016 | | -1,48563925 | 0,31660239 | 60S ribosomal protein L27a |
| + | 6,2300326 | | 1,42081197 | 0,8692468 | Plasmodium exported protein |
| + | 6,192132 | | 0,05463123 | 0,84877014 | Protein transport protein SEC61 subunit alpha |
| + | 6,17350388 | | -0,16602484 | -0,41476409 | 60S ribosomal protein L4 |
| + | 6,10081228 | | -0,8554519 | 0,05679607 | Ubiquitin specific protease |
| + | 6,08022213 | | 3,33239746 | 2,59398015 | 40S ribosomal protein S16 |
| + | 6,0660251 | | -0,44993305 | 1,22384199 | RNA-binding protein |
| + | 5,98597368 | | -0,01859411 | 0,62799581 | Chloroquine resistance transporter |
| + | 5,91626644 | + | -1,03457801 | -0,57537047 | Membrane associated histidine-rich protein 2 |
| | 5,87351831 | | -3,74026839 | -0,83737723 | |
| + | 5,83046818 | | 1,44882393 | 1,22291597 | Calcium-transporting ATPase |
| + | 5,78145568 | | -0,17504978 | 1,47328027 | 60S ribosomal protein L2 |
| + | 5,77754402 | | -2,51520602 | 2,50226816 | 40S ribosomal protein S23 |
| + | 5,69904741 | | -0,09663296 | 0,10135492 | Nucleolar protein 56 |
| + | 5,66950862 | | -1,33294868 | -0,72435792 | 60S ribosomal protein L24 |
| + | 5,65970325 | + | -1,2457641 | -1,03928471 | Ras-related protein Rab-1B |
| + | 5,58084202 | | -1,2805802 | 1,20054722 | Methionine-tRNA ligase |
| + | 5,57834244 | | 2,89887174 | 2,60820675 | 60S ribosomal protein L3 |
| + | 5,46835423 | | -0,29940255 | -0,52841314 | PF3D7_1237700 |
| + | 5,3951664 | | 2,10819372 | -1,73930709 | PF3D7_1447700 |

| | | | | | | |
|---|---|---|---|---|---|---|
| + | 5,37185415 | | 0,26532396 | | -0,58159542 | PF3D7_0305300 |
| + | 5,36398093 | + | -3,47776413 | | -0,70779483 | Knob-associated histidine-rich protein |
| + | 5,35540613 | | -0,53561783 | | -0,65598202 | Glutamate-tRNA ligase |
| + | 5,33381526 | | -0,72251479 | | -0,02080313 | Tudor staphylococcal nuclease |
| + | 5,28325876 | | -0,51260217 | | -0,40557448 | Autophagy-related protein 18 |
| + | 5,14563942 | | -1,33600648 | | 1,38347848 | 60S ribosomal protein L21 |
| + | 5,12739468 | | 0,13103167 | | 1,24305852 | 60S ribosomal protein L44 |
| + | 5,10867437 | | 1,15212568 | | 1,47658189 | 40S ribosomal protein S15 |
| + | 5,09728654 | | 1,65059471 | | 1,29507796 | Ribonucleoside-diphosphate reductase small chain |
| + | 5,07631938 | | 0,24740473 | | -0,5671463 | Succinate-CoA ligase [ADP-forming] subunit alpha |
| | 5,04595089 | + | 5,58454386 | | 2,88881652 | 60S ribosomal protein L39 |
| | 4,81045564 | | 2,83060455 | | -2,40086714 | |
| | 4,78548622 | | 3,05269305 | | -2,3655014 | |
| | 4,71837362 | | -1,6524814 | | -1,59880956 | |
| | 4,66097418 | | 2,40582053 | | 1,11837228 | |
| + | 4,64358966 | | -0,87054571 | | -0,55967935 | Rhoptry neck protein 2 |
| + | 4,59404214 | | -2,67656803 | | -2,24112304 | V-type H(+)-translocating pyrophosphatase |
| + | 4,50597032 | | 0,24870141 | | -1,1189146 | Plasmodium exported protein |
| + | 4,47528521 | + | 1,39362367 | | 0,63873418 | Ras-related protein Rab-2 |
| + | 4,43310865 | + | 2,61064434 | | -1,2240785 | DnaJ protein |
| + | 4,38136609 | | -1,01969973 | | -0,18532117 | Amino acid transporter AAT1 |
| + | 4,3523337 | | -4,14132436 | | -3,64116065 | High mobility group protein B2 |
| | 4,21919854 | | -2,42787774 | | -0,40061633 | |
| + | 4,21302573 | | 0,43914859 | | 1,69382222 | RNA-binding protein |
| + | 4,1998148 | | 0,74168809 | | 2,17636998 | Spermidine synthase |
| + | 4,13910357 | | -1,74636205 | | 0,77887535 | MSP7-like protein |
| + | 4,10598787 | | 2,26584689 | | -2,1850179 | High molecular weight rhoptry protein 2 |
| | 3,96644529 | | -3,0113608 | | -2,69277668 | |
| + | 3,95258935 | | 0,47417609 | | -0,82920869 | 60S ribosomal protein L32 |
| | 3,9397548 | | -1,0091753 | | -0,97828325 | |
| | 3,79060491 | | 2,70847321 | | -1,9169995 | |
| | 3,74449158 | | -1,50026639 | | -1,29925919 | |

| | | | | | | |
|---|---|---|---|---|---|---|
| + | 3,68021584 | | 2,09223525 | | -1,93655936 | L-lactate dehydrogenase |
| | 3,57600753 | | -1,86677202 | | -1,99585787 | |
| + | 3,45819664 | | -2,25335471 | | -1,65221055 | 60S ribosomal protein L5 |
| + | 3,45377286 | | -2,47424444 | | -3,55895297 | Heat shock protein 101 |
| + | 3,40555731 | | 0,11967182 | | 1,01941617 | 40S ribosomal protein S25 |
| + | 3,39203993 | + | 4,89622561 | + | 5,25682004 | 40S ribosomal protein S3 |
| | 3,39190992 | | -4,45365429 | | -4,09707324 | |
| + | 3,36337566 | | -1,2142849 | | 2,06676928 | PF3D7_1306200 |
| | 3,31727441 | | 2,94618448 | | 3,33409437 | |
| + | 3,29283969 | | -1,28556665 | | -1,19267686 | Translocation protein SEC63 |
| + | 3,25971794 | | -1,91769091 | | -1,16121197 | Dynein light chain 1 |
| | 3,1691157 | | -2,9562664 | | -2,50342941 | |
| | 3,12267399 | | -1,79556529 | | -1,91441536 | |
| | 3,08316898 | | -3,86693414 | | 0,04404354 | |
| | 2,96008301 | | 1,97604243 | + | 9,29394436 | Exportin-7 |
| | 2,79591052 | | -3,29045725 | | -3,09830316 | |
| + | 2,79498545 | + | -4,51650206 | + | -4,65738583 | Phosphoenolpyruvate carboxykinase |
| + | 2,76728948 | | 0,69753647 | | 0,83755875 | Histone H2B |
| | 2,76706696 | | -3,9707071 | | 4,3806057 | |
| | 2,63812478 | | -3,54074605 | | -2,28186035 | |
| | 2,51679866 | | -2,29689566 | | -3,21287187 | |
| + | 2,49175707 | | -2,48522123 | | -1,73218664 | Acyl-CoA synthetase |
| + | 2,29038048 | + | 8,41443443 | + | 10,5255375 | PF3D7_1444100 |
| | 2,28525575 | | -2,88487275 | | -2,2376744 | |
| + | 2,21456559 | + | -2,77232265 | | -0,61501439 | PF3D7_1036900 |
| | 2,17517122 | | -4,27563794 | | -4,91058318 | |
| | 2,14609814 | | -3,74791876 | | 0,59923204 | |
| | 2,1340847 | | -2,35701942 | | 1,04786714 | |
| | 2,11960379 | + | -4,22084936 | | 1,96727816 | |
| + | 2,11349233 | + | -3,51083088 | + | -2,36639023 | Histone H2A |
| + | 1,97750473 | | -4,05066713 | + | -2,24044291 | Ubiquitin-60S ribosomal protein L40 |
| + | 1,9454422 | + | -1,98421764 | | -1,12161573 | Endoplasmin |
| | 1,8896815 | | -1,98371315 | | -2,10253588 | |

| | | | | | | |
|---|---|---|---|---|---|---|
| | 1,88383452 | | -2,71356678 | | -2,9447972 | |
| + | 1,71180662 | + | -7,37003899 | | -2,26498286 | Alpha tubulin 1 |
| | 1,65628211 | | -0,37826888 | | -0,80724748 | |
| | 1,5925471 | | -3,2449789 | | -1,13197581 | |
| | 1,57546107 | | -3,80063852 | | -3,03615634 | |
| | 1,54254468 | | -2,90913995 | + | 4,67059422 | |
| + | 1,52043025 | | -1,25557804 | | -0,56278865 | Elongation factor 2 |
| | 1,48493767 | | -2,91249243 | | 1,34612306 | |
| | 1,40026093 | | -1,54630311 | | -1,07755979 | |
| | 1,25636578 | + | 11,4586611 | | -0,65952269 | PF3D7_1313100 |
| | 1,24000804 | + | -6,13414224 | | -2,07839266 | |
| | 1,1841135 | | -2,58203252 | | -3,28043461 | |
| | 1,18087578 | | -4,07246685 | | -2,80988216 | |
| | 1,15911261 | | -2,12580204 | | -2,48575592 | |
| | 1,15311495 | + | -4,6077919 | | 4,41054885 | |
| | 1,14951579 | | -2,13530954 | | -1,28174082 | |
| | 1,11654154 | | -1,37741311 | | -0,82225672 | |
| | 1,1070474 | + | -2,67020067 | | -3,92107773 | |
| | 1,07853762 | | -2,16607412 | | -1,05426788 | |
| + | 1,06652133 | + | -1,03155835 | | -0,69621627 | Multidrug resistance protein 1 |
| | 1,06485939 | + | -1,92718506 | | -0,82664553 | |
| | 1,06155968 | + | 10,1756856 | | 0,2609024 | Pseudouridylate synthase |
| | 1,03481929 | | -0,72308731 | | -0,39382807 | |
| | 0,94542535 | + | 9,4206384 | | -0,60403283 | ABC transporter I family member 1 |
| | 0,90742493 | | -1,96103096 | | -0,88982137 | |
| | 0,88697529 | + | 11,4705966 | | -0,14952119 | Dynein heavy chain |
| + | 0,87235769 | + | 5,55898539 | | 4,29591719 | Eukaryotic translation initiation factor 3 subunit C |
| | 0,6980168 | + | -3,44913038 | | -1,58084456 | |
| | 0,68884595 | + | -7,19289939 | | -2,57340177 | |
| | 0,65335433 | + | -4,91481113 | | -1,59361013 | |
| | 0,5630455 | + | -3,07939561 | | -1,79271762 | |

| | | | | | | |
|---|---|---|---|---|---|---|
| | 0,54321639 | + | -6,40414747 | | -2,52974033 | |
| | 0,44089413 | + | 7,2254432 | | -0,44359366 | 26S proteasome regulatory subunit RPN3 |
| | 0,43857511 | | -3,11408297 | | -0,87845262 | |
| | 0,40638796 | | -0,85324192 | + | 5,01736641 | Erythrocyte membrane-associated antigen |
| | 0,39155865 | + | 7,52375094 | | 1,20308145 | Peptidase family C50 |
| | 0,37654686 | | -1,4745903 | | 1,30427233 | |
| | 0,27093093 | | -3,11860212 | | -4,23599052 | |
| | 0,21648057 | | -3,62313684 | | -4,23669243 | |
| | 0,15676181 | | -3,62421131 | | -0,43497721 | |
| | 0,14082146 | + | -1,64595032 | | -0,83385531 | |
| | 0,06670189 | | -3,58999793 | | -3,52799797 | |
| | -0,08583705 | | -1,9669253 | | 1,57270495 | |
| | -0,13054053 | | 4,03549004 | | -2,4784433 | |
| | -0,19278971 | + | -1,98683135 | | -0,58999952 | |
| | -0,28953743 | | -3,70339457 | | -0,00255553 | |
| | -0,45605818 | + | -1,74685287 | | 0,22588158 | |
| | -0,46178214 | | -5,03303941 | | -4,85691643 | |
| | -0,46525192 | | -3,13885816 | + | 5,36914444 | |
| | -0,49704774 | | 0,53384495 | | 1,70895735 | |
| | -0,54660606 | + | -1,54502296 | | 1,37618637 | |
| | -0,66417535 | | 2,71144327 | | -0,60660744 | |
| | -0,72885831 | | 3,46413104 | | 3,55690702 | |
| | -0,86023776 | | -1,16872787 | | 0,13340314 | |
| | -0,91206233 | | -1,70835972 | | -3,11039829 | |
| | -0,92561499 | + | -3,14286327 | | -2,08311494 | |
| | -1,14422544 | | 2,29778417 | | 2,10777632 | |
| | -1,20512358 | | 4,51004791 | | 0,15265083 | |
| | -1,29698499 | | -3,57127094 | | 5,91543833 | |
| | -1,33724181 | | -4,9586846 | | -1,73138777 | |
| + | -1,3544178 | + | -1,48871295 | | 0,09955597 | |
| + | -1,36133258 | | -0,9559447 | | -0,70072428 | |

| | | | | | | |
|---|---|---|---|---|---|---|
| | -1,37724686 | + | 2,00768153 | | -2,23064677 | |
| | -1,38539346 | + | -6,220239 | | -2,56459427 | |
| | -1,38581657 | + | -4,05854575 | | -0,45124658 | |
| + | -1,3939743 | | -1,08474859 | | -1,65904808 | |
| | -1,47789351 | + | -5,06043243 | | -3,4338932 | |
| + | 1,50329653 | + | -1,50038401 | | 0,53343582 | |
| + | 1,58399264 | + | 0,94873937 | | 0,64219411 | |
| | -1,59786924 | | 0,11840057 | | 0,37373288 | |
| | -1,61561712 | | 5,10158761 | | 2,08364391 | |
| | -1,66371727 | + | -4,34032122 | + | -5,39401531 | |
| + | -1,68260765 | | -0,79277547 | | -0,29973412 | |
| + | -1,7196935 | | -0,96662839 | | 0,86033058 | |
| | -1,78322601 | + | -5,37128639 | + | -5,51776695 | |
| + | -1,80570539 | + | -2,2270635 | | 1,60719681 | |
| | -1,80879847 | | 3,82364178 | | 1,28146458 | |
| | -1,83109029 | + | -6,10925388 | | -4,43186124 | |
| + | -1,87857087 | | -0,66150475 | | 0,04559263 | |
| + | -1,93798033 | + | -4,40207767 | + | -4,38227145 | |
| | -2,0308431 | | -2,96159871 | | 1,41415787 | |
| + | -2,05118624 | | -1,05272547 | | 0,69065666 | |
| + | -2,10511398 | | -0,7122167 | | -0,72600047 | |
| | -2,12794463 | + | -5,00949574 | + | -4,55045064 | |
| + | -2,13710467 | | -0,73629761 | | 0,80231094 | |
| | -2,18764973 | | -0,54228083 | | -0,13831647 | |
| + | -2,21419493 | | -0,29826641 | | -1,47856236 | |
| | -2,21584034 | + | -5,34894053 | | -3,35211849 | |
| + | -2,26448123 | | -1,38527171 | | 0,99112574 | |
| | -2,26960564 | + | -5,2417326 | | 1,45241992 | |
| | -2,45261065 | + | -6,70487944 | + | -5,83209006 | |
| | -2,47802766 | | 2,08588346 | | -0,4931558 | |
| | -2,48499362 | | -0,07007726 | | 1,70063305 | |

| | | | | | | |
|---|---|---|---|---|---|---|
| | -2,5087204 | | -0,28215122 | | 1,51108901 | |
| + | -2,52544594 | | -0,95712725 | | 1,13171196 | |
| + | -2,60615095 | | -1,57288996 | | -2,41926734 | |
| + | -2,65720844 | | -0,27517573 | | -0,16385078 | |
| | -2,77196185 | + | 1,71149826 | | -0,5479997 | |
| + | -2,78688876 | | 0,72832108 | | 0,84085528 | |
| | -2,8014911 | | 0,71005185 | | -0,01122793 | |
| + | -2,83224583 | | -3,26849651 | + | -4,49856472 | |
| + | -2,86592452 | + | 1,23008855 | | -0,73186239 | |
| + | -2,99165503 | | -3,12998962 | | -1,81186167 | |
| + | -3,06540203 | + | -4,8304793 | + | -5,16221078 | |
| + | -3,09773318 | | -0,13906161 | | -1,15289084 | |
| + | -3,09943326 | | -0,94800504 | | 0,57728767 | |
| | -3,11692079 | | 1,55541801 | | -1,78016504 | |
| + | -3,14137268 | | 4,55627251 | | -2,43225797 | |
| | -3,18835704 | + | 5,52591515 | | -1,56076686 | |
| | -3,28605779 | | 0,42055543 | | 0,81302102 | |
| | -3,31986205 | + | 6,44694869 | | -2,36364492 | |
| | -3,36069584 | + | 6,63321018 | | -2,38089466 | |
| + | -3,39401499 | | -1,58786964 | | -0,53441938 | |
| + | -3,40860494 | + | -3,52785969 | | -0,33652369 | |
| | -3,53267161 | + | 5,31687482 | | -2,63818423 | |
| + | -3,54586951 | + | 3,56220818 | | -0,1145153 | |
| + | -3,55098279 | | 0,74860287 | | 0,61291854 | |
| + | -3,55181376 | | -3,2980334 | | -3,69478035 | |
| + | -3,57035669 | | -2,92266909 | | -1,41330338 | |
| + | -3,58161354 | | 0,05647691 | | -1,16262817 | |
| + | -3,60543855 | + | 5,12511094 | | 0,39328798 | |
| | -3,62334633 | | 0,07347298 | | 0,23556773 | |
| + | -3,66227913 | | -2,31321224 | | -2,19950326 | |
| + | -3,67139626 | | -1,88228194 | | 0,08670076 | |

| | | | | | | |
|---|---|---|---|---|---|---|
| + | -3,68346024 | | -1,68098291 | | -0,01612886 | |
| + | -3,70632235 | + | -1,41380246 | | -0,69697094 | |
| | -3,70759805 | | 0,10324923 | | -0,20489883 | |
| + | -3,71482372 | + | -5,34999847 | + | -5,31517569 | |
| + | -3,84740353 | + | -5,42183081 | | -1,93195883 | |
| + | -3,92785263 | + | -2,46296501 | | -0,16630459 | PF3D7_0716300 |
| + | -3,95005894 | + | -4,48289967 | | -1,99415461 | |
| + | -3,96405315 | | -1,52793376 | | 3,46130308 | |
| + | -4,00142097 | | -4,0475626 | | -2,53052743 | |
| + | -4,03648567 | + | -4,59754244 | | -2,56302293 | |
| + | -4,11923758 | + | -1,01300557 | | -1,82352575 | |
| + | -4,1206557 | | 0,61822351 | | -0,07289823 | |
| + | -4,20549138 | | -0,55183983 | | -0,33470408 | |
| + | -4,20618089 | + | -6,52313296 | | -4,82318338 | |
| + | -4,26805592 | | -2,34081268 | | -1,65576045 | |
| + | -4,27102566 | | -0,62130102 | | -0,61061287 | |
| + | -4,30246035 | | -3,35049375 | | -2,12553151 | |
| + | -4,33141327 | + | -5,51909351 | | -2,32290808 | |
| + | -4,33522733 | | -3,08270168 | | -0,01856486 | |
| + | -4,34043948 | | -2,57633686 | | -0,42707666 | |
| + | -4,36042786 | | -4,32862091 | | -3,98633226 | |
| + | -4,3913765 | | -3,99161307 | | -2,4953076 | |
| + | -4,48182074 | | -0,36238988 | | -0,4402984 | |
| + | -4,50978343 | + | -3,9655873 | | -2,77706973 | |
| + | -4,52567895 | + | -1,45697244 | | -0,96494738 | |
| + | -4,52741337 | | -1,62375832 | | -0,74167538 | |
| + | -4,52971045 | | -0,07788467 | | -1,92865531 | |
| + | -4,53282897 | | -1,27787622 | | -0,81980832 | |
| + | -4,55277411 | | -4,07992013 | | -3,50922585 | |
| + | -4,58139865 | | -2,23489634 | | -1,62344329 | |
| + | -4,60104942 | | -0,23333963 | | -0,64612548 | |

| | | | | | |
|---|---|---|---|---|---|
| + | -4,61579164 | | -0,96745141 | | -2,72802067 |
| + | -4,62175433 | | -1,74990877 | | -1,32561525 |
| + | -4,64617697 | + | -3,58049933 | | -1,70661736 |
| + | -4,72553698 | + | -6,06686497 | + | -5,50757599 |
| + | -4,74225044 | | -2,52151934 | | -0,14596685 |
| + | -4,83793799 | + | -1,74786154 | + | -2,27218024 |
| + | -4,85464668 | + | -2,8367246 | | -1,63248412 |
| + | -4,85670439 | | -2,42950471 | + | -5,83303865 |
| + | -4,86329428 | | -0,70591704 | | -0,07525285 |
| + | -4,86478202 | | -3,62748051 | | -2,95452277 |
| + | -4,8779939 | | -4,7068669 | | -2,05662855 |
| + | -4,9179678 | | 0,21076361 | | -0,4263773 |
| + | -4,97516314 | | -1,31946564 | | -1,01404476 |
| + | -5,0123256 | | 3,09626293 | | -0,14375877 |
| + | -5,0192976 | + | 1,23293845 | | -2,9370451 |
| + | -5,02370389 | | -4,59245396 | | -0,4633309 |
| + | -5,06368256 | | -0,82739449 | | -0,77867826 |
| + | -5,08642292 | + | -7,03828128 | | -3,11945152 |
| + | -5,1088829 | + | -5,20077387 | | -3,00499805 |
| + | -5,15113449 | + | -6,68257427 | | -4,35165532 |
| + | -5,17549356 | | -0,2344141 | | -1,04317093 |
| + | -5,21259721 | + | -1,13826243 | | -0,76453209 |
| + | -5,2371343 | + | -2,27396615 | | -2,83423742 |
| + | -5,24159686 | | -2,58566634 | | -2,3698794 |
| + | -5,2417949 | | 0,63542875 | | -0,03226757 |
| + | -5,26035627 | | -2,73716354 | | -1,69747225 |
| + | -5,29110082 | + | -6,46543566 | | -2,82468605 |
| + | -5,30063947 | | 0,29128329 | | -1,36825307 |
| + | -5,3022515 | | 0,03085327 | | 0,08091291 |
| + | -5,30646229 | | -2,98129845 | | -0,95672385 |
| + | -5,32179674 | | -0,89573352 | | -3,08385944 |

| | | | | | | |
|---|---|---|---|---|---|---|
| + | -5,33599567 | | -0,47626305 | | -2,19567045 | |
| + | -5,34036382 | | -0,35584005 | | -0,19737943 | |
| + | -5,35512384 | | -4,47134972 | | -2,01428064 | |
| + | -5,370725 | + | -2,44159635 | + | -2,27899901 | |
| + | -5,40154362 | | -3,6850783 | | -1,5775013 | |
| | -5,88484796 | | 2,26099237 | | 1,99092452 | |
| + | -6,05303065 | | -4,9974788 | | -1,31163724 | |
| + | -6,10124048 | | 1,11159643 | | -2,64977837 | |
| + | -6,24773471 | | -2,73247687 | | -1,24188964 | |
| + | -6,24863815 | | -3,05791314 | | -2,65559387 | |
| + | -6,2749548 | | -2,6764218 | | -3,01673476 | |
| + | -6,45080503 | + | -2,16705608 | | -4,11868191 | |
| + | -6,46171347 | | -0,48289903 | | -0,28032684 | |
| + | -6,55007458 | | -0,49663734 | | -0,01038551 | |
| + | -6,56429927 | | -3,60214806 | | -2,79139264 | |
| + | -6,71087265 | | 1,09410095 | | -0,19287936 | |
| + | -7,6757733 | | 0,40568479 | | 0,3399512 | |
| + | -8,79756769 | | -3,60604922 | | -2,16276805 | |
| | 0,71815713 | + | ==4,34491634== | | -0,57708645 | PP1 |

# Annexes II

*Article*

# Characterization of GEXP15 as a Potential Regulator of Protein Phosphatase 1 in *Plasmodium falciparum*

**Hala Mansour** [1]**, Alejandro Cabezas-Cruz** [2]**, Véronique Peucelle** [1]**, Amaury Farce** [3]**, Sophie Salomé-Desnoulez** [4]**, Ines Metatla** [5]**, Ida Chiara Guerrera** [5]**, Thomas Hollin** [1,6,*] **and Jamal Khalife** [1,*]

[1] Univ. Lille, CNRS, Inserm, CHU Lille, Institut Pasteur de Lille, U1019-UMR 9017-CIIL-Center for Infection and Immunity of Lille, 59000 Lille, France; hala.mansour@lau.edu (H.M.); veronique.peucelle@pasteur-lille.fr (V.P.)

[2] ANSES, INRAE, Ecole Nationale Vétérinaire d'Alfort, UMR BIPAR, Laboratoire de Santé Animale, 94700 Maisons-Alfort, France; alejandro.cabezas@vet-alfort.fr

[3] Univ. Lille, Inserm, CHU Lille, U1286–Infinite–Institute for Translational Research in Inflammation, 59000 Lille, France; amaury.farce@univ-lille.fr

[4] Univ. Lille, CNRS, Inserm, CHU Lille, Institut Pasteur de Lille, US 41–UAR 2014–PLBS, 59000 Lille, France; sophie.desnoulez@inserm.fr

[5] Proteomics Platform Necker, Université Paris Cité–Structure Fédérative de Recherche Necker, INSERM US24/CNRS UAR3633, 75015 Paris, France; ines.metatla@inserm.fr (I.M.); chiara.guerrera@inserm.fr (I.C.G.)

[6] Department of Molecular, Cell and Systems Biology, University of California Riverside, Riverside, CA 92521, USA

\* Correspondence: thollin@ucr.edu (T.H.); jamal.khalife@pasteur-lille.fr (J.K.)

**Abstract:** The Protein Phosphatase type 1 catalytic subunit (PP1c) (PF3D7_1414400) operates in combination with various regulatory proteins to specifically direct and control its phosphatase activity. However, there is little information about this phosphatase and its regulators in the human malaria parasite, *Plasmodium falciparum*. To address this knowledge gap, we conducted a comprehensive investigation into the structural and functional characteristics of a conserved *Plasmodium*-specific regulator called Gametocyte EXported Protein 15, GEXP15 (PF3D7_1031600). Through in silico analysis, we identified three significant regions of interest in GEXP15: an N-terminal region housing a PP1-interacting RVxF motif, a conserved domain whose function is unknown, and a GYF-like domain that potentially facilitates specific protein–protein interactions. To further elucidate the role of GEXP15, we conducted in vitro interaction studies that demonstrated a direct interaction between GEXP15 and PP1 via the RVxF-binding motif. This interaction was found to enhance the phosphatase activity of PP1. Additionally, utilizing a transgenic GEXP15-tagged line and live microscopy, we observed high expression of GEXP15 in late asexual stages of the parasite, with localization predominantly in the nucleus. Immunoprecipitation assays followed by mass spectrometry analyses revealed the interaction of GEXP15 with ribosomal- and RNA-binding proteins. Furthermore, through pull-down analyses of recombinant functional domains of His-tagged GEXP15, we confirmed its binding to the ribosomal complex via the GYF domain. Collectively, our study sheds light on the PfGEXP15–PP1–ribosome interaction, which plays a crucial role in protein translation. These findings suggest that PfGEXP15 could serve as a potential target for the development of malaria drugs.

**Keywords:** Protein Phosphatase 1; Plasmodium; malaria; GEXP15; CD2BP2; GYF domain; ribosome biogenesis

## 1. Introduction

*Plasmodium falciparum* (Pf) is a unicellular parasite responsible for the deadliest form of human malaria. It poses a significant threat to global health, particularly in regions where the disease is endemic [1]. The function of Pf proteins is regulated by various post-translational modifications, with reversible protein phosphorylation being the most

common protein modification observed in the parasite. Protein phosphorylation allows cells to adapt their functions rapidly in response to internal and external changes [2].

Among the Serine (Ser)/Threonine (Thr) phosphatases, Protein Phosphatase 1 (PP1c) (PF3D7_1414400) plays a crucial role in diverse cellular functions in *Plasmodium* and other organisms [3]. PP1c is a highly conserved enzyme in eukaryotes, and *Plasmodium* PP1c (PfPP1c) shares approximately 80% identity with its counterparts in mammals. Its phosphatase activity on phosphopeptides and small substrates is conserved across PP1c homologs in many species [4].

PP1c functions by associating with various regulatory partners to form holoenzymes, which specifically dephosphorylate a wide range of substrates in different cellular locations. Mammalian cells have 200 identified regulatory subunits that contribute to the specificity, location, and level of phosphatase activity of PP1c [5,6]. In Pf and in *Plasmodium berghei* (Pb), PP1c has been shown to have numerous potential regulatory partners, with hundreds of interacting proteins identified through yeast two-hybrid (Y2H) and immunoprecipitation experiments combined with mass spectrometry analysis [7–9].

Among the PP1c-interacting proteins, three conserved regulators (Inhibitor 2, Inhibitor 3, and LRR1) and a *Plasmodium*-specific protein Gametocyte EXported Protein 15 (GEXP15) (PF3D7_1031600) were detected as top interactors [10,11]. Biochemical studies have shown a direct interaction between PbGEXP15 and PbPP1c, increasing the phosphatase activity of PP1c in vitro [7]. Knockout of PbGEXP15 in Pb showed the vital role for the protein during the asexual life cycle and the mosquito stages, where no oocysts and sporozoites were found [7]. This phenotype could be attributed to a decrease in protein dephosphorylation due to the absence of PP1c control in the PbGEXP15 knockout line. Additionally, the crucial role of PbGEXP15 may be related to its interactome, as it was found to be associated with protein complexes involved in essential biological pathways, such as mRNA splicing and the proteasome pathway [7].

In addition to the RVxF motif located at the N-terminus of PbGEXP15, a GYF domain was identified at its C-terminal [12]. The GYF domain, characterized by the consensus sequence GP[YF]xxxx[MV]xxWxxx[GN]YF (IPR003169), is known to play a role in protein–protein interactions and is present in numerous proteins in mammals [13]. The GYF domain was initially described in the CD2 Cytoplasmic Tail-Binding Protein 2 (CD2BP2) expressed in human T cells, where it interacts with the cytoplasmic tail of the CD2 receptor, contributing to T cell activation [13]. Further studies have indicated that CD2BP2 is also present in the nucleus and may be part of the pre-spliceosomal complex [14]. Conditional gene targeting in mice revealed the essential role of CD2BP2 in embryonic development [15]. Based on reciprocal best hits (RBH) analysis, GEXP15 in *Plasmodium* is suggested to be an ortholog of human CD2BP2 [16].

Although studies on proteins functions in Pb, the most tractable of the most rodent malaria models for experimental genetics, can provide valuable insights into fundamental aspects of *Plasmodium* biology, there are limits to how much can be extrapolated to Pf [17]. For instance, targeted gene-by-gene functional studies showed that the gene encoding Schewanella-like phosphatase (shlp1) in Pf was described as likely essential for erythrocyte development by a functional screen analysis [18]. On the contrary, in Pb, shlp1 is dispensable for the development of blood stage parasites [19].

In Pf, genome-wide saturation mutagenesis suggested GEXP15 as an essential gene in the intraerythrocytic developmental cycle. However, the specific roles of this protein throughout the lifecycle of Pf are still not fully characterized. In this study, we aimed to investigate the structural and functional characteristics of GEXP15 in Pf. We employed various approaches, including comparative genomics, structural and evolutionary analyses, in vivo studies using an inducible GEXP15 knockdown line to examine cellular localization and function, and protein–protein interaction analyses to explore GEXP15's interactors and interactome. Through these methods, we uncovered the critical interactome and potential role of GEXP15 in Pf.

## 2. Results

### 2.1. Plasmodium GEXP15 Protein Sequence Analysis

The primary structure of PfGEXP15 was compared to *Homo sapiens* (Hs) CD2BP2 (UniProt_O95400), and the alignment of their full-length protein sequences showed 23% identity (Supplementary Figure S1). This low identity may be attributed to the presence of several low complexity regions (LCRs) in PfGEXP15. Pf proteins are known to have an unusually high abundance of repetitive LCRs, which often consist of amino acid repeats such as asparagine (N), lysine (K), glutamic acid (E), and aspartic acid (D). These LCRs are thought to lack any specific function [20]. Previous studies have shown that the deletion of a poly-asparagine tract in PfRPN6 did not affect protein lifetime, cellular localization, protein–protein interaction, or progression of the IDC cycle [21]. In the case of PfGEXP15, these low homology regions account for the majority of the sequence differences and the low identity between the two proteins.

Next, we compared PfGEXP15 and its potential homologs in Pb (PBANKA_0515400), *Toxoplasma gondii* (Tg) (TGGT1_217010), *Saccharomyces cerevisiae* (Sc) (known as "LIN1" in yeast, NP_012026), and Hs (UniProt_O95400). The alignment of these five proteins confirmed the presence of two conserved regions (Figure 1A). The central region of PfGEXP15 (residues 315–425) showed 25–37% identity and 39–65% similarity to the corresponding regions in PbGEXP15, HsCD2BP2, TgCD2BP2, and ScLIN1 (Figure 1B). Although the function of this central region (unknown domain, UD) is unknown, it contains conserved residues, including glycines (G315, G330 and G336) and leucines (L402, L405 and L408). The second conserved region includes the GYF domain found at the C-terminus of PbGEXP15 (residues 516–568) and PfGEXP15 (residues 713–765), as well as in Sc and Tg homologs (Figure 1C). The alignment revealed 27% identity and 52% similarity in the GYF domain between the two *Plasmodium* species. While the *Plasmodium* domain deviates from the canonical GYF consensus sequence, the substitutions involve amino acids with similar physicochemical properties (i.e., hydrophobic) to those found in the human homolog. However, two glycines, a proline (P), and a tyrosine (Y) within this domain are well conserved. The observed variations in the amino acid consensus sequence may have functional implications for the GYF-like domains.

Further analysis of PfGEXP15 identified a PP1-binding motif located in the N-terminus of the protein, similar to PbGEXP15 and human CD2BP2 (Figure 1D). This motif, KKVQF, corresponds to a canonical RVxF motif with the consensus sequence [K/R][K/R][V/I][x][F/W] [5,22] (Figure 1D). The motif is conserved in Tg but not in Sc, suggesting a loss of interaction or a different mechanism of interaction with PP1 in yeasts. Additionally, a second minimal PP1-binding RVxF motif was found in the C-terminus of PfGEXP15 (KNVYF, residues 688–692), which matches a less specific and minimal consensus sequence. The interaction of human CD2BP2 with PP1 is exclusively linked to the RVxF motif in the N-terminal end [15]. Similarly, only the first RVxF motif of PbGEXP15 was able to bind to and enhance PP1 activity, indicating a conserved PP1-binding mode between *Plasmodium* GEXP15 and CD2BP2 [7].

The identified motifs and domains were further validated using MEME Suite (Figure 2). The presence of the UD (motif 1) containing conserved glycine residues and the sequences PFN and GNY was confirmed (Figure 2). Two additional motifs were detected upstream (motif 4, residues 715–720) and downstream (motif 2, residues 729–746) of the GYF domain, but they showed high variability consistent with the degenerate consensus sequence, except for two well-conserved tryptophans and one glycine across the species (motifs 2 and 4, Figure 2). Interestingly, motif 5, composed of highly conserved amino acids, was only detected in PfGEXP15 and PbGEXP15, suggesting a potential unique function in the parasite.
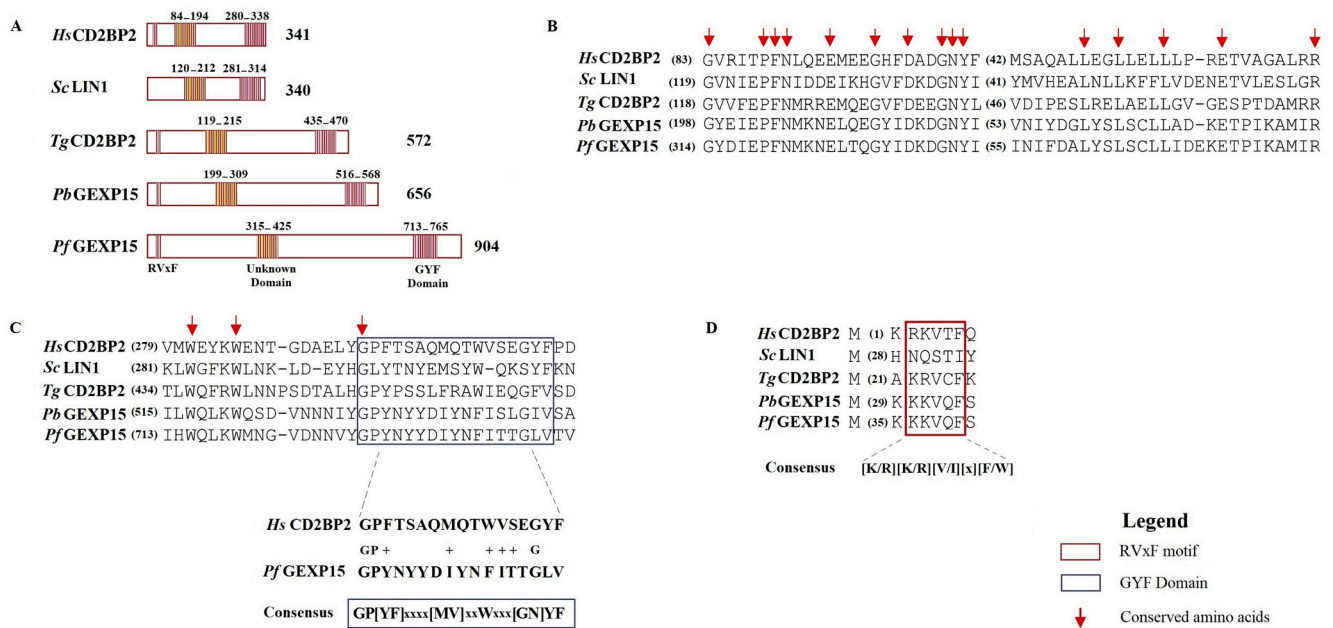
**Figure 1.** In silico analysis of *Plasmodium* GEXP15 and CD2BP2 homologs. (**A**) GEXP15 amino acid sequences from Pb and Pf were aligned with CD2BP2 from *H. sapiens*, *S. cerevisiae* and *T. gondii* using the MAFFT alignment program. A schematic representation of relevant motifs alongside their positions. (**B**) Multiple protein sequence alignment of an unknown conserved domain (UD). (**C**) GYF and GYF-like domain alignment with the consensus sequence. (**D**) Multiple alignments of the conserved RVxF motif, represented above its consensus sequence. Arrows show the conserved amino acid residues.

### 2.2. GEXP15 3D Structure Modeling

The three-dimensional (3D) structures of PfGEXP15, PbGEXP15, and HsCD2BP2 were predicted using AlphaFold. The generated models for these three proteins exhibited well-defined structured domains along with long unfolded regions, represented as straight chains of varying lengths (Supplementary Figure S2).

To enhance the accuracy of 3D predictions and address the challenges posed by unfolded regions, we conducted separated modeling for the UD and the GYF-like domains. In the UD, the presence of disordered regions hindered a complete superposition between the two *Plasmodium* proteins. However, both 3D models featured six alpha helices with a short two-stranded beta-sheet, consistent with the I-TASSER (5.1) prediction, which revealed a compact structure comprising six helices without beta sheets (Supplementary Figure S3).

Regarding the GYF-like domain, both PfGEXP15 and PbGEXP15 displayed the same domain organization but with different spatial architecture (Supplementary Figure S3), supporting the available NMR experimental data on the GYF-containing protein of CD2BP2 (residues 280–338) [23]. In Pb, a right angle was observed between the N-terminal helix and the beta-sheet, resulting in an almost straight orientation between the two elements. This variation may be attributed to the less structured C-terminal part of the predicted GYF domain in Pb, which may have influenced the orientation of the beta-sheet group during the optimization steps of the AlphaFold model-building process.

As for the RVxF motif, no model was generated since it often resides in unstructured regions of PP1 regulators [24]. The lack of conformation of this motif contributes to PP1 binding through a phenomenon known as "structure upon binding". The ability of the RVxF motif to transition from an unstructured state to a structured conformation upon binding is a specific characteristic that plays a crucial role in the regulation of PP1 activity [25].
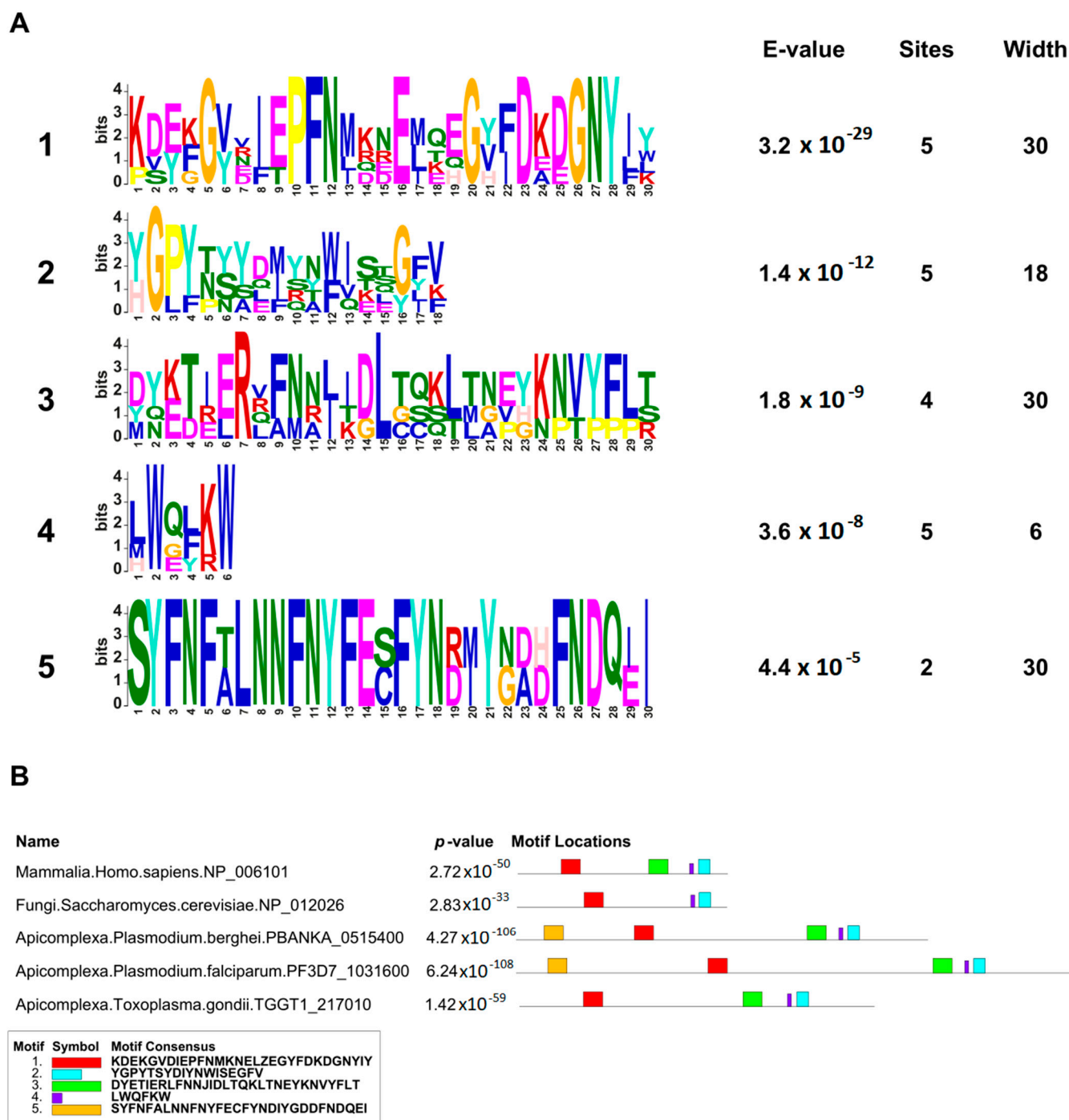
**Figure 2.** MEME motif search of GEXP15 and CD2BP2 proteins. (**A**) The 5 most significant sequence logos identified by MEME are represented, as well as their respective E-values, number of sites and widths. The height and size of the letters represent the amino acid frequency. (**B**) Distribution of these motifs across HsCD2BP2, ScLIN1, PbGEXP15, PfGEXP15, and TgCD2BP2. The color of each motif is indicated in part A. *p*-value and consensus sequence are also reported.

### 2.3. Distribution and Phylogenetic Analysis of CD2BP2

We investigate the distribution of CD2BP2 homologs and CD2BP2-like proteins across different Metazoan species. A total of 84 protein sequences (Supplementary data sheet S1) were retrieved using HsCD2BP2 as a query. Sequences showing >30% overall identity with HsCD2BP2, along with the conserved UD domain and the GYF domain, were considered CD2BP2 homologs. CD2BP2-like proteins were identified as proteins with an

identity lower than 30% but possessing the UD domain and the GYF domain. CD2BP2 homologs were found in various Metazoan species, while CD2BP2-like proteins occurred in 20 phyla, including dictyostelids, fungi, choanoflagellates, rhodophytes, chlorophytes, dinoflagellates, apicomplexan parasites, and oomycetes (Figure 3). All CD2BP2 homologs had the RVxF motif and the GYF or GYF-like domains. However, CD2BP2-like proteins in Rhizaria, Plantae, and Amoebozoa lacked the RVxF motif, suggesting no PP1-binding ability. PfGEXP15 was classified as CD2BP2-like due to <30% identity but possessing the RVxF motif, UD domain, and GYF-like domain. Conservation of these domains was analyzed using MEME Suite on 84 CD2BP2 orthologs (Figure 3). Supplementary Figure S4 shows motifs in the UD and GYF domains. Proline, phenylalanine, glycine, asparagine (N), aspartic (D), and glutamic acid (E) residues were conserved in the UD, while motif 4 was absent in apicomplexan parasites, fungi, and oomycetes. The GYF domain has conserved N-terminal amino-acid residues (G, P, F) and C terminal residues (G, Y, F), along with other regions like WExKW (motif 7). Apicomplexa had only one of the three motifs, indicating a GYF-like domain. Using FIMO, we searched for the RVxF motif and found it in most species except platyhelminths, chlorophytes, and dinoflagellates. The motif KVTF was highly conserved in mammals, amphibians, and nematodes (Supplementary Table S1).
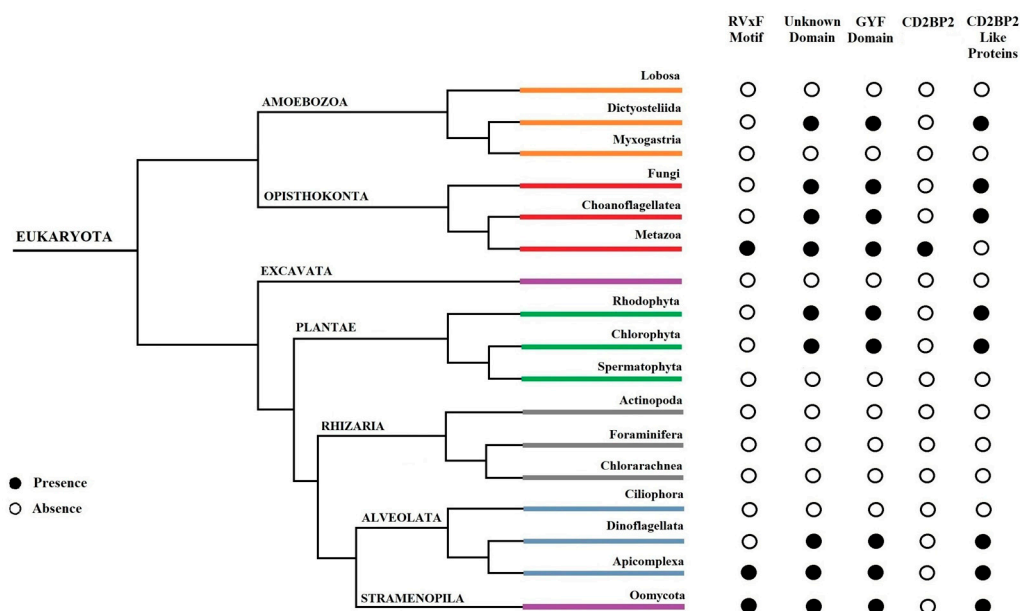


**Figure 3.** Distribution of CD2BP2 homologs and their domains in eukaryotes. The figure displays the distribution of CD2BP2 in the phylogenetic tree of life. Open and closed circles represent absence and presence of the RVxF motif, unknown domain, GYF domain, CD2BP2 homologs, and CD2BP2-like proteins, respectively. For fungi, *Saccharomyces* species were the main ones considered.

To assess the evolution of conserved regions between CD2BP2 and CD2BP2-like proteins, we constructed a phylogenetic tree using 66 CD2BP2 and CD2BP2-like proteins, three *Plasmodium* GEXP15 sequences, and six homologs from other Apicomplexa parasites (Supplementary data sheet S2). The tree revealed two major clusters. Cluster I contained vertebrate and invertebrate CD2BP2 sequences, while Cluster II included Apicomplexa, Arthropods, Mollusca, Nematodes and Cnidarians (Figure 4). Vertebrate CD2BP2 formed Cluster Ia, distinct from invertebrate CD2BP2 in Cluster Ib. Arthropod CD2BP2 sequences spanned multiple clusters, suggesting gene duplications. Cluster II consisted of Apicomplexa CD2BP2-like sequences, indicating a shared a common ancestor. Divergent tree clustering, along with shared structural features (e.g., conserved motifs and domains) and functional similarities, suggest convergent evolution between CD2BP2 and CD2BP2-like proteins.
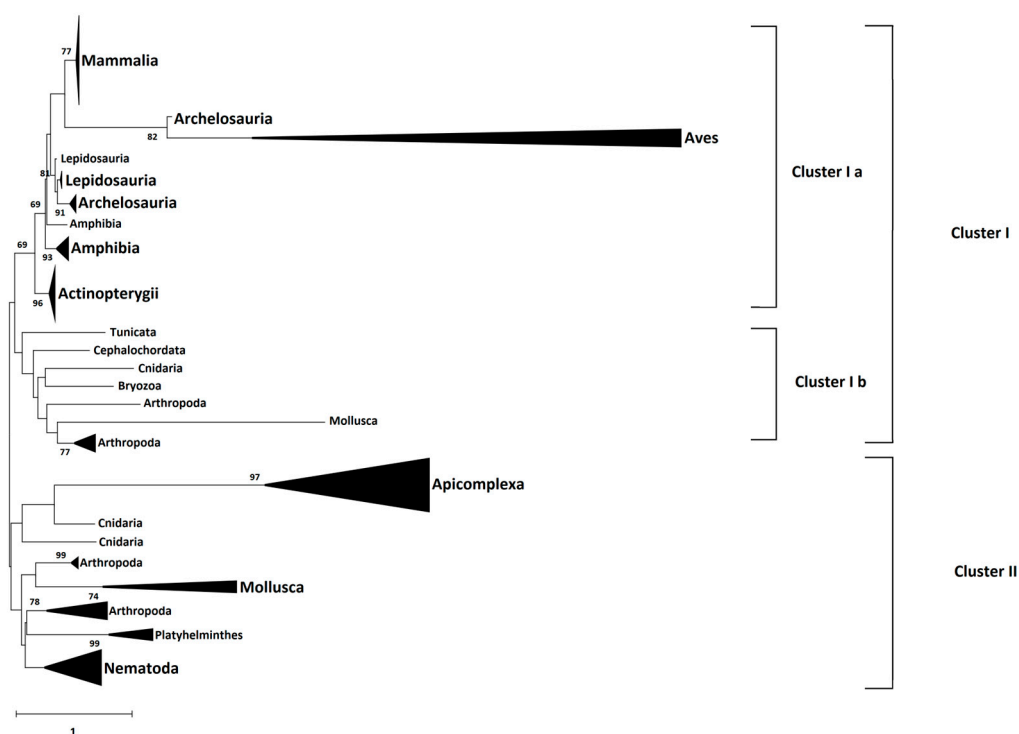
**Figure 4.** Phylogenetic tree of CD2BP2 and GEXP15 proteins. The evolutionary history was inferred using the Neighbor-Joining method [26]. The optimal tree is shown. The percentage of replicate trees in which the associated taxa clustered together in the bootstrap test (500 replicates) are shown next to the branches [27]. The tree is drawn to scale, with branch lengths in the same units as those of the evolutionary distances used to infer the phylogenetic tree. The evolutionary distances were computed using the JTT matrix-based method [28] and are in the units of the number of amino acid substitutions per site. The rate variation among sites was modeled with a gamma distribution (shape parameter = 1). This analysis involved 66 amino acid sequences. All positions with less than 95% site coverage were eliminated, i.e., fewer than 5% alignment gaps, missing data, and ambiguous bases were allowed at any position (partial deletion option). There was a total of 213 positions in the final dataset. Evolutionary analyses were conducted in MEGA 11 [29].

*2.4. Binding and Activation of PfPP1 by PfGEXP15*

In a previous study, three clones corresponding to PfGEXP15 and containing the RVxF motif were identified via a Y2H screening with PfPP1c as bait [8]. In this study, a plasmid encoding a fragment of PfGEXP15 containing the first RVxF motif (8–182 residues) was used to test its ability to bind to PP1c. Only diploid cells expressing PfGEXP15 RVxF and PfPP1c were able to grow on selective media, while no yeast growth was observed with different control plasmids. This suggests a specific interaction between PfGEXP15 and PfPP1c (Figure 5A). The RVxF-dependent binding between PfGEXP15 and PfPP1c was confirmed by mutations in the binding region of PP1c (residues F255A and F256A), which prevented yeast growth under high-stringency selection.

To further confirm the direct nature of this interaction, a GST pull-down assay was performed using GST-PfPP1c and three recombinant His-tagged proteins containing the RVxF motif, UD or GYF domains produced and purified as described in Materials and Methods (Supplementary Figure S5). Immunoblot analysis showed that RVxF-containing proteins bound to GST-PfPP1c but not to the GST alone (Figure 5B). An artificially dimerized form of PfGEXP15, able to bind to PfPP1c (Figure 5B), was detected and could be due to the overexpression or misfolding of the recombinant fragment produced. Neither UD-containing nor GYF-containing proteins showed binding to GST-PfPP1c, confirming the previous observation that the RVxF motif is the main contributor to the PfGEXP15–PfPP1c interaction, similar to the observation with PbGEXP15 [7].
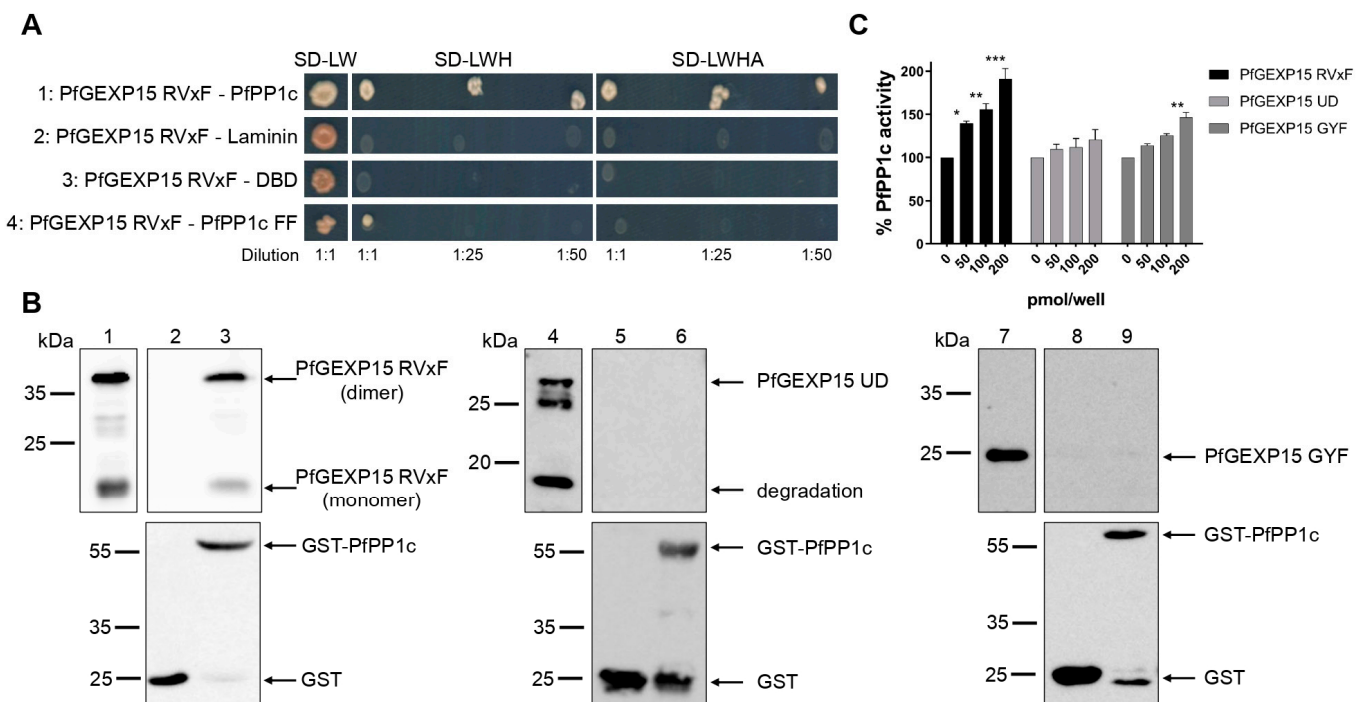
**Figure 5.** Interaction of PfGEXP15 with PfPP1c and its regulatory effect on the phosphatase activity. (**A**) Yeast two-hybrid assay. pGADT7-PfGEXP15 RVxF was mated with pGBKT7-PfPP1c (lane 1), pGBKT7-Laminin (lane 2), pGBKT7-DBD (lane 3), and pGBKT7-PfPP1c F255A F256A (FF) (lane 4). Yeast diploids were plated on SD-LW, SD-LWH, and SD-LWHA selective media and interactions were identified by growth of undiluted and diluted (1:25 and 1:50) cultures. (**B**) GST pull-down assay. Lane 1 shows the input of 6-His PfGEXP15 RVxF (500 ng) and, in lanes 2 and 3, the eluted proteins (2 μg) after incubation with GST alone or GST-PfPP1c, respectively. The recombinant proteins 6-His PfGEXP15 UD and 6-His PfGEXP15 GYF are loaded in the same conditions in lanes 4–5–6 and 7–8–9, respectively. Immunoblots are revealed with mAb anti-His (upper panel) and anti-GST (lower panel). (**C**) pNPP-phosphatase assay. The recombinant proteins 6-His PfGEXP15 RVxF, 6-His PfGEXP15 UD, and 6-His PfGEXP15 GYF were incubated at different concentrations with PfPP1c for 30 min at 37 °C before the addition of para-nitrophenyl phosphate (pNPP). The linear formation of the dephosphorylated product, para-nitrophenol, was measured by optical density after 1h at 37 °C. Results are reported as mean ± SD of the percent relative activity ($n$ = 2 in duplicate). Significance was determined by Kruskal–Wallis with Dunn's post-hoc test: * $p < 0.05$, ** $p < 0.01$, *** $p < 0.001$. The detection of free GST in lanes 3, 6, and 9 could be attributed to non-specific cleavage or protease activity.

We further examined whether the binding of PfGEXP15 affected the activity of PP1. The addition of PfGEXP15 RVxF significantly increased the dephosphorylation of p-nitrophenyl phosphate (pNPP) by PfPP1c in a concentration-dependent manner to a level similar to that of PbGEXP15 (Figure 5C). However, neither PfGEXP15 UD nor PfG-EXP15 GYF showed a dose-dependent increase in PP1c activity. Only PfGEXP15 GYF at a concentration of 200 pmol/well was associated with a significant increase in PP1c activity.

Altogether, these findings demonstrate that PfGEXP15 directly and specifically inter-acts with PfPP1c, primarily through its RVxF motif. This binding enhances the phosphatase activity of PfPP1c in vitro.

## 2.5. Conditional Mutants, Expression, and Localization of PfGEXP15

Previous findings by Zhang et al. [18] through genome-wide saturation mutagenesis indicated that PfGEXP15 could have essential functions in the asexual stages of Pf, as no viable parasites were detected. To further investigate the role of PfGEXP15, we generated transgenic Pf parasites using an all-inclusive construction called PfGEXP15-GFP-DDD-

HA (Figure 6A), based on the plasmid previously described [21]. This system enables the degradation of the tagged protein of interest in the absence of the folate analog trimethoprim (TMP). We confirmed the correct integration of the transfected plasmid at the PfGEXP15 locus by performing integration-specific PCR on the cloned population (Figure 6B), with wild-type parasites as a control (Figure 6C). The expression of PfGEXP15-GFP-DDD-HA was also detected using western blot analysis of parasite extracts probed with an anti-HA antibody, which revealed a main band at the expected size of the fusion protein (Figure 6D).
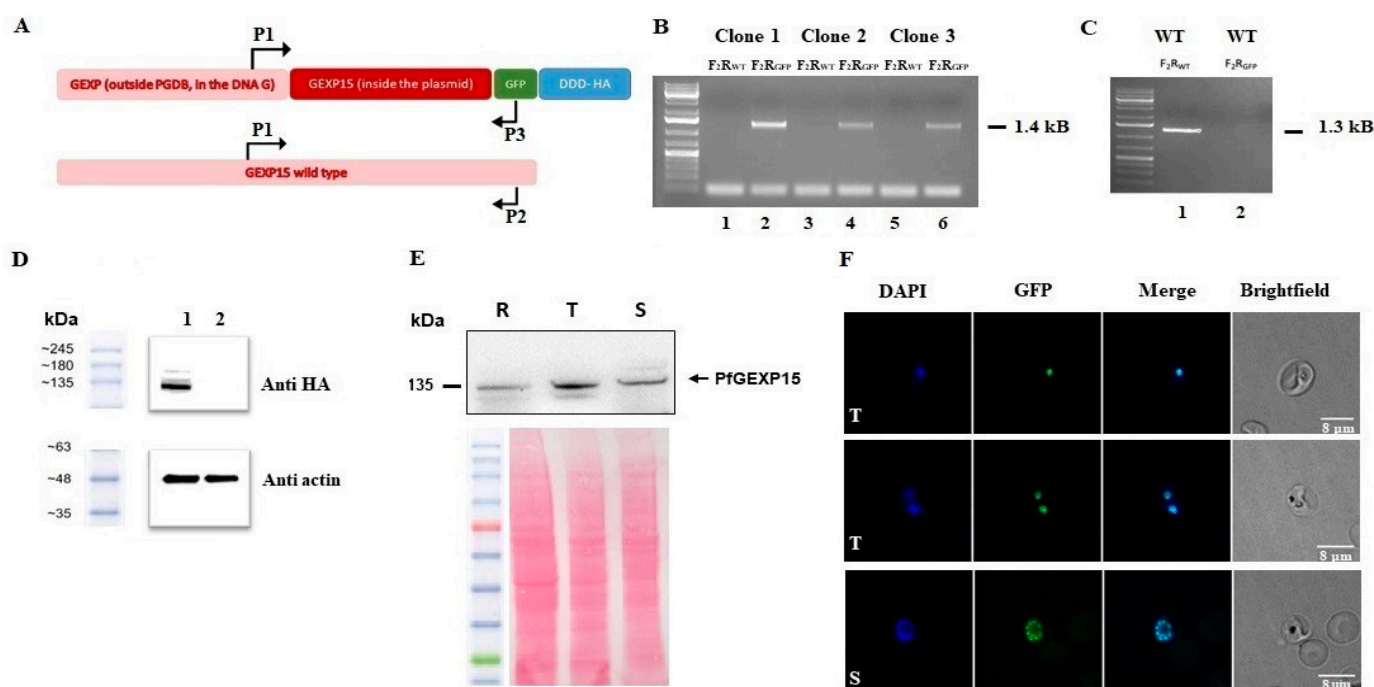


**Figure 6.** Expression and localization of PfGEXP15-GFP-DDD-HA. (**A**) Schematic representation of the pGDB construct and the primers used to check plasmid integration. The GEXP15 is tagged with DDD, GFP, and HA tags. (**B**) Diagnostic PCR analysis of tagged GEXP15 clones. Lanes 1–6 correspond to gDNA extracted from transfected parasites. Lanes 1, 3, and 5 represent the detection of the wild-type (WT) locus; lanes 2, 4, and 6 correspond to the integration of the construct. (**C**) Diagnostic PCR analysis of WT parasites. Lane 1 represents the detection of the WT locus; lane 2 corresponds to the integration of the construct. (**D**) Western blot analysis representing the soluble protein extract from transgenic PfGEXP15 in lane 1 and WT parasites as negative control in lane 2. They were revealed with mAb anti-HA rabbit. In the lower panel, anti-actin was used as a positive loading control. Forty million parasites were used. (**E**) Western blot analysis representing the soluble protein extract from transgenic iKd PfGEXP15 of ring (R), trophozoite (T), and schizont (S) stages. In the lower panel, total protein detected by Ponceau Red staining as loading control. (**F**) Confocal laser scanning microscopy showing GFP-expressing parasites in transfected cultures. Parasite nuclei were stained with DAPI and transgenic parasites express PfGEXP15-GFP-DDD-HA. Merged images showed protein colocalization.

Next, we utilized the generated transgenic strain to examine the expression of PfG-EXP15 throughout the asexual cycle. Western blot analysis showed that PfGEXP15 highest expression was predominantly observed during the trophozoite stage (Figure 6E). This observation aligns with RNA-seq analysis, showing a peak transcript expression during late trophozoites and early schizonts [30]. Live fluorescence microscopy analysis showed that PfGEXP15 was primarily localized in the nucleus of late trophozoite and schizont stages, with foci overlapping DNA staining (Figure 6F). This location pattern is supported by proteomic studies that detected PfGEXP15 in nuclear extracts of schizonts [31]. In the

case of Pb, however, GEXP15 was also clearly detected in the parasite cytosol, suggesting species-specific functions of GEXP15 [7].

Finally, we verified the efficiency of our inducible system by western blot analysis and live fluorescence. Unexpectedly, after TMP removal, western blot examination of parasite lysates revealed that PfGEXP15 protein levels remain stable over time. Evaluation of parasite growth over several days with at least three replication cycles shows that that parasite proliferation was unaffected by the absence of TMP (Supplementary Figure S6). Live fluorescence confirms that TMP had no influence on PfGEXP15 localization in the nucleus (Supplementary Figure S6). The persistence of PfGEXP15, in the absence of TMP for up than four months, indicates that this method is not suitable for its degradation. These unexpected data are in line with previous studies of protein chaperones [32].

### 2.6. Identification of PfGEXP15-Interacting Proteins

To gain a better understanding of the biological roles of GEXP15 in the asexual stages of Pf, it was necessary to investigate the complexes formed by PfGEXP15. We conducted a global immunoprecipitation (IP) of PfGEXP15-HA-GFP using anti-GFP nanobodies on soluble extracts from late trophozoite and schizont stages, followed by mass spectrometry analysis (IP/MS). The parental strain was used as a control. Three biological replicates were analyzed, resulting in the identification of 1200 Pf proteins recovered from the beads (Supplementary Table S2). To refine the results, we ensured that proteins were identified in at least two out of three biological replicates, with a $p$-value ($p < 0.05$) and difference (log 2 FC) compared to the control parental strain. A total of 16 proteins were recognized, with the majority associated with the ribosomal complex (seven proteins) or RNA-binding (three proteins). STRING analysis of this interactome confirmed the enrichment of ribosome biogenesis and the translation process. However, PfPP1 did not meet the cut-off criteria in this analysis (Figure 7).

To further investigate the protein profile and determine the specific regions of GEXP15 involved in these interactions, we employed a complementary approach using pull-down experiments with recombinant proteins containing different protein domains. His-tagged proteins containing the RVxF motif, the UD, and the GYF domain were produced and coupled to nickel agarose beads, while a tetR bacterial protein served as a negative control. Soluble proteins from three independent biological replicates were incubated with the different recombinant proteins bound to beads. Prior to pull-down experiments, the presence of the tagged fragments adsorbed on the beads was confirmed by immunoblot (Supplementary Figure S7). The eluted proteins were directly analyzed by MS to identify GEXP15-associated partners. A total of 312 interacting proteins were identified through the different domains (Supplementary Table S3). PF3D7_1444100, which was detected with all GEXP15 domains, and PF3D7_1206200, common between RVxF and GYF fragments, were excluded from the analysis. Principal component analysis (PCA) of the different protein domains showed distinct clusters, particularly for GYF pull-down, indicating a specific and divergent set of interactants different from RVXF and UD (Figure 8A). After filtering the proteins based on their $p$-value ($p < 0.05$) and difference (log 2 FC), nine, two, and eighty proteins were found to be significantly enriched with RVxF, UD, and GYF-containing proteins, respectively. As expected, PP1 was detected as the main interactor of the RVxF-containing protein, validating the approach (Figure 8B). Although STRING analysis of the other potential RVxF partners did not show any significant enrichment, they were associated with DNA/RNA/ATP binding and translation initiation activity.

The UD pull-down revealed only two unique proteins (Figure 8C). One of them, erythrocyte membrane-associated antigen, is present in the membrane and was excluded from analysis since GEXP15 is a nuclear protein. Therefore, exportin-7 was the only specific protein pulled down with the UD-containing protein. Exportin-7 is conserved among eukaryotes and plays a role in mediating the nuclear export of proteins into the cytoplasm. A similar function may occur in Plasmodium for the transport of GEXP15, but further investigation is needed.
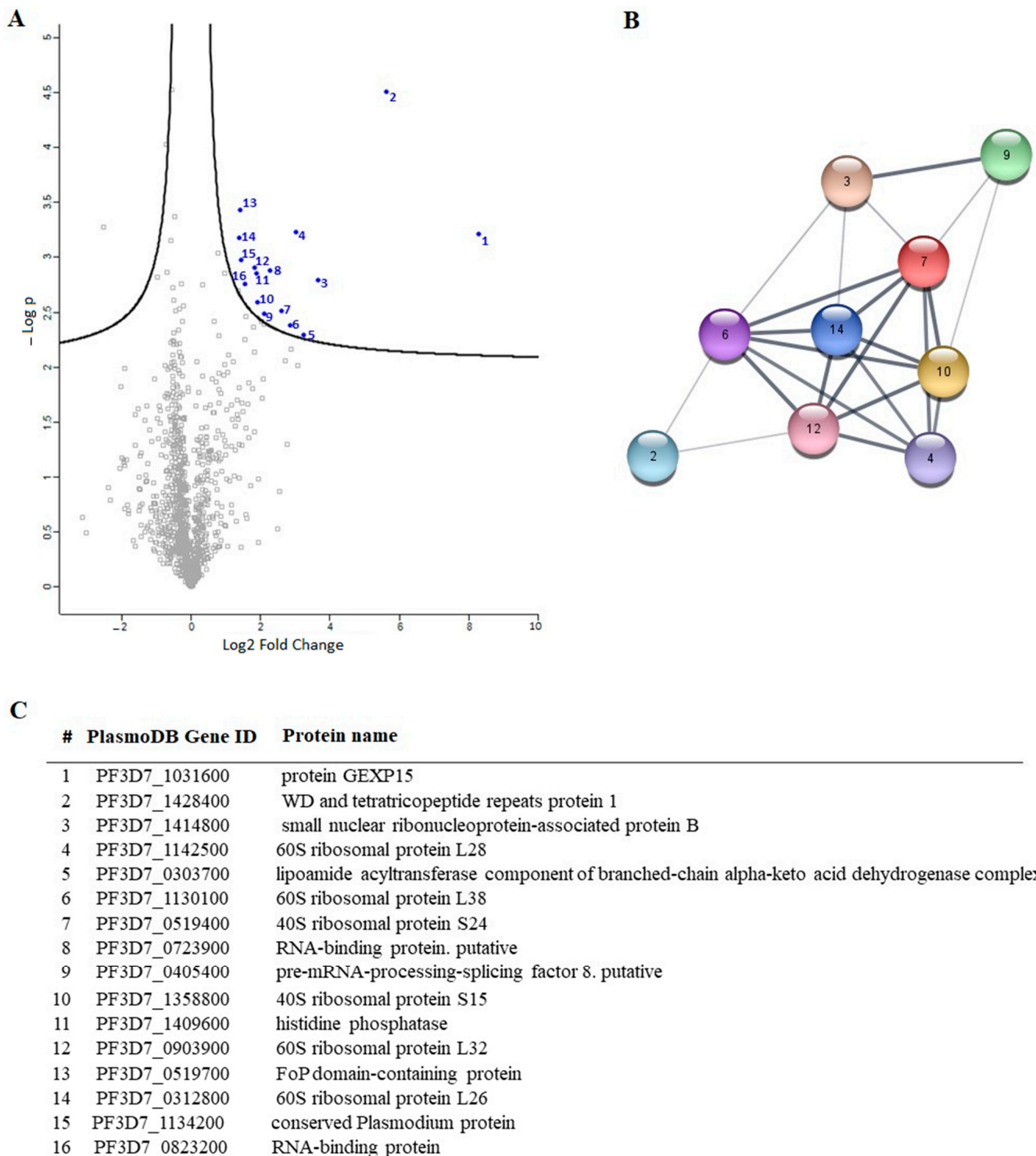
**Figure 7.** PfGEXP15 interactome analysis. (**A**) Volcano plot representation of PfGEXP15 immunoprecipitation. Blue and gray dots represent statistically significant and non-significant detected proteins respectively. (**B**) STRING network visualization of PfGEXP15-interacting proteins using Cytoscape software (3.9.1). (**C**) List of PfGEXP15 interacting partners. Proteins were ranked according to their Student's *t*-test difference PfGEXP15–WT in the schizont stage.
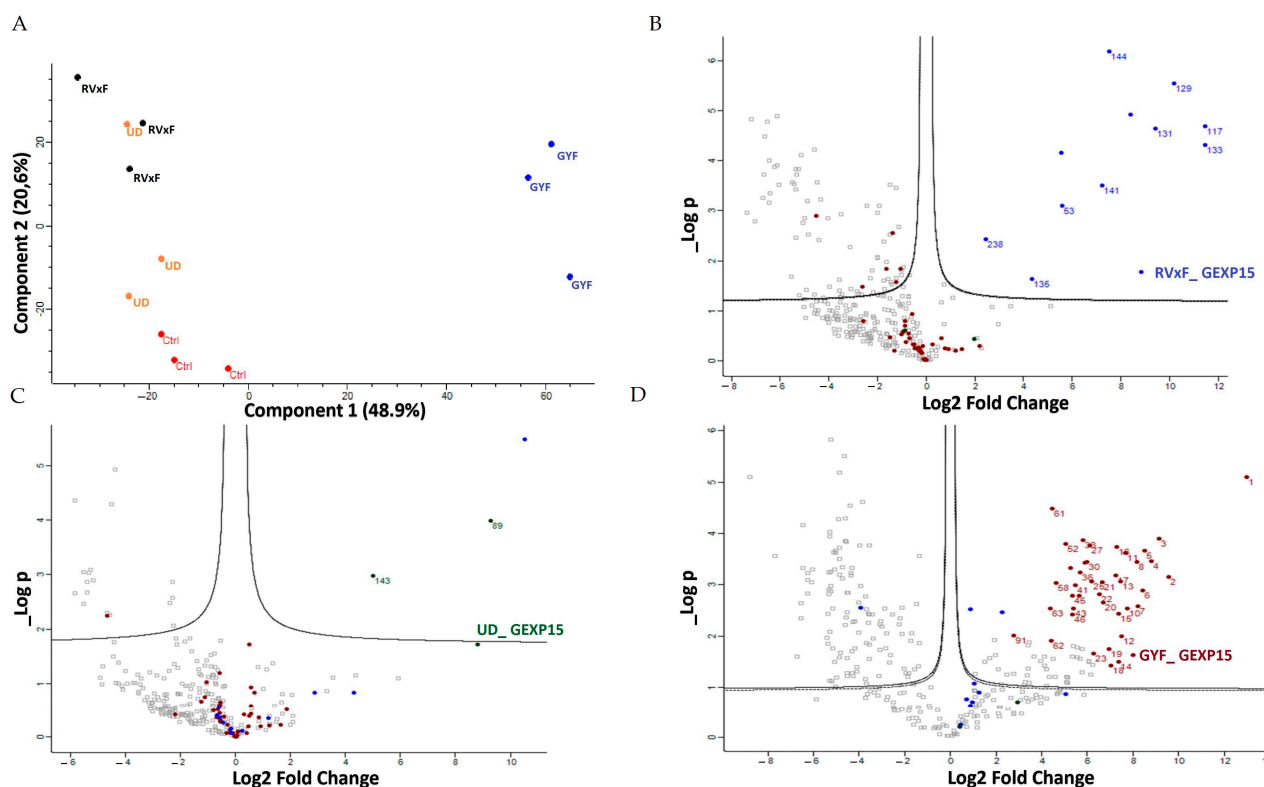
**Figure 8.** PfGEXP15 pull-down analysis. (**A**) PCA analysis of the outcome of the pull-downs of PfGEXP15 RVxF (black), UD (orange) and GYF (blue) in three different replicates. The control samples (Ctrl) are indicated in red. Gray dots represent proteins detected with no statistical significance. Volcano plot representation of the outcome of the RVxF (**B**), UD (**C**), and GYF (**D**) pull-downs. The proteins significantly co-purified are indicated in blue, green and purple, respectively.

For the GYF domain, 36% of the significant proteins (29/80) were found to be ribosomal subunits or ribosome-associated proteins, suggesting that this domain co-precipitated a large part of the 60S and 40S ribosomal complexes (Figure 8D). STRING analysis confirmed this observation, with enrichment of structural constituents of ribosomes (FDR = $1.73 \times 10^{-17}$) as well as rRNA binding. Additionally, 19 biological processes were enriched, including translation (FDR = $1.33 \times 10^{-13}$) and biosynthetic processes (Supplementary Figure S8).

When comparing the results of the two approaches, three common proteins were shared between the GYF pull-down and the global PfGEXP15 IP: the 60S ribosomal proteins L26, L32, and the 40S ribosomal protein S15. However, other partners should also be considered since they share similar functions, such as small ribonucleoproteins and RNA-binding proteins. These data revealed that the most dominant network involving GEXP15 corresponds to the 40S and 60S ribosomal proteins. RVxF was found to be mainly involved in PP1 interaction, while the GYF domain played a role in the recognizing of the ribosomal machinery, unlike UD, which did not appear to be a protein-binding domain.

## 3. Discussion

In this work, we provided a better understanding of the structure and evolution of GEXP15 and its homologs in various organisms. A closer examination of these proteins highlighted three regions of particular interest. First, an RVxF motif was detected by manual inspection in the N-terminal region of PfGEXP15, PbGEXP15, TgCD2BP2, and HsCD2BP2. Using the FIMO tool, we confirmed the presence of this motif in various phyla including Apicomplexa, Metazoa, and Nematoda. This motif is known to be implicated in PP1 interaction in eukaryotes and our previous work conducted in *Plasmodium* had already established the capacity of PbGEXP15 as well as other regulators to modulate the activity

of PP1 [7,10]. Here, we validated by Y2H and GST pull-down that PfGEXP15 bound to PP1, and that this interaction is RVxF-specific since the PP1 mutant and other GEXP15 regions were not able to interact. Furthermore, we demonstrated the ability of PfGEXP15 to regulate the dephosphorylation activity of PP1 through its N-terminal region containing the RVxF-binding motif. These findings confirmed the preponderant role of the RVxF motif in the interaction and regulation of PP1 by GEXP15.

Second, a conserved domain with an unknown function was identified through the in silico comparative study conducted on the different species as well as with the MEME analysis. Although our pull-down and interactome analyses showed that this domain is unlikely to be involved as a platform for protein interactions, the conservation of critical residues across distant species suggests that this UD region may play a crucial unknown role. From the MS analysis of the pull-down performed with this domain, we found only the exportin 7 (PF3D7_0910100) as a potential binder, which was detected in the nuclear fraction of Pf, suggesting its potential role in PfGEXP15 nuclear trafficking [31]. In this context, it should be noted that a previous study reported that exportin 5 is required in nuclear export of 60S ribosome subunits in human cells [33]. Further studies will be necessary for *Plasmodium* to elucidate the contribution of this domain to GEXP15 function.

Finally, our in silico study highlighted the presence of a GYF-like domain in GEXP15. The GYF domain is present in a diverse array of proteins, known to interact with proline-rich peptides, including those found in RNA-binding proteins, cytoskeletal proteins, and transcription factors [14]. Notably, the function of the GYF domain can be modulated by subtle changes in its amino acid sequence, making it a flexible region for regulating protein–protein interactions in a context-dependent manner [14]. This observation may explain why among the sequences of CB2BP2 and GEXP15 analyzed in this study, only the metazoan proteins had a GYF domain matching the currently described consensus sequence. However, despite the observed differences, the MEME analysis and 3D modeling confirmed some degree of conservation of the GYF-like domains identified in the other species, which may confer adaptation to mediate distinct protein–protein interactions.

To further investigate the functional role of GEXP15, we attempted to conditionally knock down PfGEXP15 using a degradation domain since the protein was previously suggested as essential for the development of blood-stage parasites [18]. Despite the integration of the degradation domain, confirmed by genotyping and immunoblotting, phenotypic analysis was not possible as the protein remained stable, suggesting that GEXP15 may be part of a large and stable complex. A previous study proposed that proteins not accessible to the proteasome for degradation could be a challenge for knockdown experiments [34]. Other systems can be considered, such as the Cre-LoxP system, which can be used to excise the gene of interest [35] or the *TetR*-DOZI–aptamer module repressing translation [36].

Next, we took advantage of the GFP and HA tagging of GEXP15 to follow up its localization throughout its intraerythrocytic stages. Confocal microscopy revealed that GEXP15 is highly expressed in late asexual stages, in agreement with previous transcriptomics data [12], and is localized in the parasite nucleus. In contrast to the localization of PbGEXP15 in both the nucleus and cytoplasm [7], this finding is similar to the human CD2BP2 localization [37]. This potential difference between the two *Plasmodium* species requires further investigation using electron microscopy or subcellular fractionation in order to confirm that the localization of GEXP15 is species-specific.

To gain a deeper understanding of the function of PfGEXP15, we profiled the GEXP15 interactome. A first approach based on immunoprecipitation experiments of endogenous tagged PfGEXP15-DDD-GFP-HA present in protein extracts by MS was applied to identify binding partners. This allowed the identification of 10 proteins related to one main functional group corresponding to the ribosomal complex and RNA-binding proteins.

Although PfPP1 was not detected in the PfGEXP15 IP/MS, the likelihood of this interaction via the RVxF motif was demonstrated by the use of complementary approaches such as Y2H, GST pull-down, and pull-down experiments (this study), confirming previous

findings [8,9]. Supporting this is the fact that in *P. berghei* parasites, PbGEXP15 was also detected among the top PP1-interacting proteins in both schizont and gametocyte stages [9]. Further, the reciprocal IP/MS identified PbPP1 after PbGEXP15 immunoprecipitation [7]. Using this approach, the lack of PfPP1 can be due to the fact that the complex PfGEXP15-PP1 is unstable at the time point examined and/or its association is transient at this stage.

A second approach, using pull-down experiments with recombinant GYF-domain bound to beads and soluble protein extracts, revealed 29 proteins that belong to ribosomal subunits and ribosomal-associated proteins and of which three are shared with the ribosomal proteins detected in the IP-MS experiments. The limited subset of partners identified by IP and not by pull-down is not surprising as they represent different methods for interactome studies. It is known that the quantity of immunoprecipitated tagged protein, expected to be different from the quantity engaged in pull-down experiments, greatly affects MS identification. Hence, the results obtained herein can be complementary and, taken together, strongly suggest that PfGEXP15 is a ribosome-associated protein. More important is the fact that our data clearly revealed that the GYF-domain-containing protein of PfGEXP15 binds to ribosomal complex proteins, unlike the GYF domain of human CD2BP2 that has been shown to bind to spliceosomal proteins [14]. This unexpected observation suggests that the GYF-containing proteins might have diverse interactomes according to their subcellular localization, the presence and availability of species-specific partners, and/or the subtle differences in amino acids within or around the GYF domain per se. This is supported by the fact that the binding partners of GEXP15 of Pb obtained by IP experiments are different from those of Pf as they belong to spliceosomal and proteasomal core complexes which could be, at least in part, attributed to the different localization of GEXP15 in both parasites.

A closer examination of the identified proteins in the PfGEXP15 interactome showed the presence of the ribosomal RNA processing 1 homolog b (PF3D7_1414800). Interestingly, an earlier study using quantitative affinity purification followed by mass spectrometry demonstrated that human RRP1B was the most abundant partner of PP1 [38]. Moreover, it has been reported that nucleolar complexes contain both RRP1B and PP1 as components of pre-ribosomal subunit processing complexes [39]. The potential involvement of PfGEXP15 in this RRP1B-PP1 complex could therefore be envisaged. Altogether, these findings are consistent with the fact that reversible phosphorylation events via PfPP1 likely contribute to fine-tuning ribosomal biogenesis.

Despite the fact that we have not obtained direct evidence on the impact of PfGEXP15 on intraerythrocytic parasite development as the knockdown approach based on protein degradation failed, our data showing the capacity of PfGEXP15 (1) to bind and regulate PfPP1c activity, essential for *Plasmodium* survival, through its N-terminal side and (2) to interact with the ribosomal protein complex via its C-terminal side, crucial for protein translation, strongly support the essentiality of PfGEXP15. Given the functional difference between human CD2BP2 and PfGEXP15, and particularly the specific partners of the latter, identified through the GYF domain-containing protein, it would be important to determine how they interact in order to exploit specific parasite PfGEXP15–ribosome interaction for malaria drug development.

In this context, we have already shown that peptides interrupting the interaction of PP1 to its regulators via the RVxF-binding motif were able to inhibit Pf growth in vitro [40]. This proof of concept and validation of the binding of PfGEXP15 with PP1 and the ribosomal complex will open new opportunities to identify small inhibitors to disrupt this interaction network and the development of Pf.

## 4. Materials and Methods

### 4.1. Plasmid

Plasmid pGDB was a kind gift from Vasant Muralidharan. The integration plasmid, pGEXP15GDB, was synthetized by introducing a 984 bp fragment from the 3′ end of the GEXP15 ORF into pGDB between the XhoI/AvrII (New England Biolabs, Ipswich, MA, USA). PetDuet-1 was purchased from Novagen (Darmstadt, Germany).

### 4.2. Parasite Culture

The Pf3D7 strain was grown according to Trager and Jensen in RPMI 1640 medium with 10% human AB$^+$ serum, in the presence of O$^+$ erythrocytes [41]. Cultures were maintained at 37 °C in a humidified atmosphere (5% CO$_2$, 5% O$_2$, and 90% N$_2$). Parasites were synchronized by successive rounds of 5% sorbitol treatment as described previously [42]. In order to isolate total proteins, parasites from infected red blood cells were purified as previously described [43].

### 4.3. MEME and FIMO Analysis

MEME Suite v5.5.1 (https://meme-suite.org/meme/tools/meme accessed on 16 March 2023) was used on the full-length sequences of GEXP15 and CD2BP2 proteins to identify conserved motifs. A maximum of 5 motifs were searched for Pf, Pb, Tg, Sc, and human sequences with maximum widths of 30 and default parameters. For the 84 CD2BP2 proteins identified, a maximum of 7 motifs were searched with the same settings. FIMO v5.5.1 (https://meme-suite.org/meme/doc/fimo.html accessed on 5 April 2023) was used to scan the RVxF motif among the 84 sequences using the consensus sequence [RK][RK][VI]X[FW] and default parameters.

### 4.4. 3D Modeling

The modeling of the PF3D7_1031600, NP_006101, and PBANKA_0515400 were carried out using Alphafold (https://alphafold.ebi.ac.uk/ accessed on 24 November 2022). I-TASSER (https://zhanggroup.org/I-TASSER/ accessed on 21 November 2022) was used additionally for the modelling of the two domains: UD (145 a.a.) and GYF (100 a.a.).

### 4.5. Phylogeny Analysis

The amino acid sequences of 66 identified CD2BP2 proteins were downloaded from the NCBI database (https://www.ncbi.nlm.nih.gov/ accessed on 12 September 2022) as well as three Plasmodium GEXP15 sequences and six homologs from Apicomplexa parasites. The species and accession numbers of each sequence is provided in Supplementary data sheet S2. Multiple sequence alignment of these full-length sequences was performed by Clustal Omega (https://www.ebi.ac.uk/Tools/msa/clustalo/ accessed on 11 October 2022). Then, the Neighbor-Joining method and JTT matrix-based model, implemented in MEGA X software (Version 10.2.6), were used to build a phylogenetic tree from the sequence alignment. A gamma distribution equal to one with partial deletion was used. Reliability of internal branches was assessed using the bootstrapping method (500 bootstrap replicates).

### 4.6. Yeast Two-Hybrid Assays

pGADT7-PfGEXP15 RVxF was isolated from our initial yeast-two hybrid screening [8]. Gal4-DBD-Laminin, Gal4-DBD-PfPP1c, and PfPP1c F255A/F256A were previously cloned in pGBKT7 [40]. Y2H Gold (pGADT7-PfGEXP15 RVxF) and Y187 (pGBKT7 constructs) yeast strains (Clontech, California, USA) were mated on SD-LW media. Diploids were then selected on plates lacking leucine, tryptophan and histidine (SD-LWH), and adenine (SD-LWHA) after dilutions at 1:1, 1:25, and 1:50. Plates were incubated for 4–6 days at 30 °C.

### 4.7. GST Pull-Down Assays

The coding region of the three recombinant protein fragments were PCR amplified using genomic DNA with the following primers: (1) P4–P5 for the N-terminal fragment (21–546 bp); (2) P6–P7 for the central region (625–1242 bp); and (3) P8–P9 for the C terminal portion (1878–2445 bp) (Supplementary Table S4). They were cloned into pETDuet-1 (Novagen, Darmstadt, Germany) using the In-Fusion HD Cloning system (Clontech, Mountain View, CA, USA) and transformed into One Shot® BL21 Star™ (DE3) Chemically Competent *E. coli* cells (Life Technologies, Carlsbad, CA, USA) (Supplementary Table S5). The recombinant proteins were expressed in the presence of 0.5 mM IPTG at 16 °C overnight. Cells were harvested in non-denaturing buffer (20 mM Tris, 500 mM NaCl, 20 mM Imidazole,

and protease inhibitor cocktail (Roche, Basel, Switzerland), pH 7.5) prior to sonication and ultracentrifugation. Then, the different pellets were resuspended for 30 min in denaturing buffer (20 mM Tris, 500 mM NaCl, 6 M Guanidine, 20 mM Imidazole, and protease inhibitor cocktail (Roche, Basel, Switzerland), pH 7.5). Recombinant proteins were purified by $Ni^{2+}$-NTA agarose beads (Macherey Nagel, Düren, Germany) and washed with 20 mM Tris, 500 mM NaCl, and 20 mM Imidazole, pH 7.5. His-tagged proteins were eluted from beads with buffer containing 20 mM Tris, 500 mM NaCl, and 600 mM Imidazole, pH 7.5, and then the imidazole was eliminated by dialysis. The purified recombinant proteins were analyzed by western blot with anti-His antibody (1:2000 dilution) (Qiagen, Hilden, Germany) followed by HRP-labeled anti-mouse IgG (1:50,000 dilution) and quantified with a Pierce™ BCA Protein Assay Kit (Life Technologies, Carlsbad, CA, USA). GST-PfPP1c and PfPP1c were produced as previously described [7].

GST or GST-PfPP1c coupled with Glutathione-Sepharose beads (Sigma-Aldrich, Darmstadt, Germany) were saturated with 25 μg of BSA and incubated overnight at 4 °C with 2 μg of PfGEXP15 RVxF, UD, and GYF in binding buffer (20 mM Tris, 150 mM NaCl, 0.2 mM EDTA, 20 mM HEPES, 1 mM $MnCl_2$, 1 mM DTT, 0.1% Triton X-100, 10% glycerol, protease inhibitor cocktail (Roche, Basel, Switzerland), and pH 7.5). After washes, proteins were analyzed by western blot, as well as 500 ng of PfGEXP15 RVxF, UD, and GYF used as inputs.

### 4.8. pNPP Phosphatase Assays

Different amounts of PfGEXP15 RVxF-, UD-, and GYF-containing proteins, described above, were preincubated with 40 pmol of PfPP1c for 30 min at 37 °C. Addition of p-nitrophenyl phosphate (pNPP) substrate (Sigma-Aldrich, Darmstadt, Germany) initiated the enzymatic reaction and after 1h of incubation, absorbance was measured at 405 nm (Thermo Scientific Multiskan FC, Marsiling Industrial Estate, Singapore). No phosphatase activity was detected with the different PfGEXP15 proteins in the absence of PP1. Two independent experiments were carried out in duplicate.

### 4.9. Transfection

To generate the PfGEXP15-HA-GFP parasite line, uninfected RBCs were transfected with 100 μg pGEXP15GDB vector then fed to wild type parasites. Drug pressure was applied 48 h after transfection, selecting for integration using 5 μM TMP (Sigma, Darmstadt, Germany) and 2.5 μg/mL Blasticidin (Calbiochem). Integration was detected after two rounds of BSD cycling after transfection. TMP was always present in the medium. Integrant clones were isolated by limiting dilution.

### 4.10. Genotype and Phenotype Analysis of Pf Transfectants

To confirm that transfected parasites contained the right integration, genomic DNA extracted (KAPA Express Extract, Kapa BioSystems, Dunedin, New Zealand) from wild or transfected parasites were analyzed by PCR using standard procedures with the primers P1–P3. Expression of the iKd PfGEXP15 protein was checked by western blotting using anti-HA (1/1000, Cell signaling C29F4, Massachusetts, USA) followed by anti-Rabbit IgG (1/20,000, Sigma, Darmstadt, Germany). Live parasites expressing PfGEXP15-GFP were analyzed by fluorescence microscopy as described below. To address the phenotype of transgenic parasites, cultures highly enriched with late trophozoites (>80%) were washed 6 times then set up ± TMP at 1% of infected red blood cells. The parasitemia were monitored up for 12 days (covering 6 life cycle) on a daily basis. After 3 and 5 cycles, viable parasites were checked for PfGEXP15 expression by live microscopy and immunoblot assays.

### 4.11. Immunoblot Assays

Parasites were suspended in Laemmli buffer and total proteins were subjected to electrophoresis in a 10% polyacrylamide gel. The proteins were transferred onto a nitrocellulose membrane (Amersham Protran 0.45 μm NC). The membrane was blocked with 5% milk (non-fat milk powder dissolved in PBS) and probed with primary antibodies (rabbit

anti-HA, 1/1000 or mouse anti-His, 1/2000) diluted in the blocking buffer. The primary antibodies were followed by respective species-specific secondary antibodies conjugated to HRP (anti-rabbit, 1/20,000, Sigma) or (anti-mouse, 1/20,000, Rockland). The antibody incubations were followed by thorough washing using PBS tween 0.4%. The membranes were visualized using Dura/ Femto western blotting substrate.

### 4.12. Fluorescence Microscopy

Transgenic and parental parasites were washed then fixed with 4% paraformaldehyde and 0.0075% glutaraldehyde for 15 min at 4 °C. After PBS washing, cells were settled on Poly-L-lysine coated coverslips. The coverslips were mounted in Mowiol with DAPI (1 µg/mL) and multipoint-confocal imaging was performed with a spinning disk Live SR (stand Nikon Ti-2 combined with Live-SR module Gataca Systems, Massy, France). Figures were produced using ImageJ/Fiji software (ImageJ 1.54f, National Institutes of Health, USA).

### 4.13. Pull-Down Assays

For pull-down experiments, the RVxF-containing protein, described above, was used. For the other two recombinant proteins, shorter fragments were synthesized in order to retain the minimal functional domains based on sequence and structure analyses (UD:853–1266 bp; GYF:2053–2347 bp) (Supplementary Table S5).

The expression of His6-motifs was carried out in the *E. coli* BL21 strain in the presence of 0.5 mM IPTG at 37 °C for 2 h. Cells were harvested in lysis buffer (20 mM Tris, 150 mM NaCl, 20 mM Imidazole, Triton 1%, Lysozyme 1 mg/50 mL, DNase I, and protease inhibitor cocktail (Roche, Basel, Switzerland), pH 7.5). Recombinant proteins were purified according to manufacturer's instructions by Ni$^{2+}$-NTA agarose beads (QIAGEN, Hilden, Germany). Washing steps were performed with a buffer containing 20 mM Tris, 150 mM NaCl, and 20 mM imidazole, pH 7.5. Three additional washing steps with a buffer containing 20 mM Tris, 150 mM NaCl, 0.5% Triton X-100, and protease inhibitor cocktail (Roche, Basel, Switzerland), pH 7.5 were done before adding the soluble proteins to parasite extracts.

For the pull-down experiment, trophozoites/schizonts of parental wild-type parasites were suspended in 50 mM Tris, 0.5% Triton X-100, 150 mm NaCl, and protease inhibitor cocktail (Roche), pH 7.5. After ten consecutive freezing–thawing cycles and sonication, soluble fractions were obtained after repeated centrifugations at 13,000 rpm at 4 °C.

The agarose nickel beads coated with the recombinant proteins were mixed overnight at 4 °C with parasite soluble extracts in 20 mM Tris, 150 mM NaCl, 0.5% Triton X-100, and protease inhibitor cocktail (Roche, Basel, Switzerland), pH 7.5.

The beads were washed and elution was performed in Laemmli buffer. Then, after 3 min at 95 °C, samples were loaded on a 4–20% SDS-PAGE for western blot or mass spectrometry analyses. Western blots were carried out probed with anti-His mAb (1:1000, Invitrogen, Waltham, MA, USA) followed by anti-mice IgG-HRP (1:20,000, Sigma-Aldrich).

### 4.14. Sample Preparation and Immunoprecipitation

Pf-enriched trophozoite and schizont cultures of PfGEXP15-GFP-DDD-HA or parental wildtype strain (control) were used for protein extracts as described above.

Immunoprecipitation experiments were performed using 3 biological replicates of each strain. Each biological replicate contained 10 isolated pellets of trophozoites and schizonts, each purified from one culture flask of 75 cm$^2$. Soluble protein extractions and immunoprecipitation assays were performed as previously described [7]. Purified parasites of each strain were suspended in 50 mM Tris, 0.5% Triton X-100, 150 mm NaCl, and protease inhibitor cocktail (Roche, Basel, Switzerland), pH 7.5. After ten consecutive freezing–thawing cycles and sonication, soluble fractions were obtained after repeated centrifugations at 13,000 rpm at 4 °C. These soluble fractions were incubated with GFP-Trap magnetic agarose (ChromoTek, Martinsried, Germany) overnight at 4 °C on a rotating wheel. The beads were washed 10 times with washing buffer containing 20 mM Tris,

150 mM NaCl, 0.5% Triton X-100, and protease inhibitor cocktail (Roche, Basel, Switzerland) at pH 7.5. Elution was performed in Laemmli buffer.

### 4.15. Sample Preparation for Mass Spectrometry

S-Trap[TM] micro spin column (Protifi, Huntington, WV, USA) digestion was performed on immunoprecipitation eluates and pull-down eluates according to the manufacturer's instructions. Briefly, samples were supplemented with 20% SDS to a final concentration of 5%, reduced with 20 mM TCEP (Tris(2-carboxyethyl) phosphine hydrochloride), and alkylated with 50 mM CAA (chloroacetamide) for 5 min at 95 °C. Aqueous phosphoric acid was then added to a final concentration of 2.5% followed by the addition of S-Trap binding buffer (90% aqueous methanol, 100mM TEAB, pH 7.1). The mixtures were then loaded on S-Trap columns. Five washes were performed for thorough SDS elimination. Samples were digested with 2 μg of trypsin (Promega, Madison, WI, USA) at 47 °C for 2 h. After elution, peptides were vacuum dried and resuspended in 2% ACN, 0.1% formic acid in HPLC-grade water prior to MS analysis.

### 4.16. NanoLC-MS/MS Protein Identification and Quantification

The tryptic peptides were resuspended in 30 μL and an amount of 400 ng was injected on a nanoElute (Bruker Daltonics, Bremen, Germany) HPLC (high-performance liquid chromatography) system coupled to a timsTOF Pro (Bruker Daltonics, Bremen, Germany) mass spectrometer. HPLC separation (Solvent A: 0.1% formic acid in water; Solvent B: 0.1% formic acid in acetonitrile) was carried out at 250 nL/min using a packed emitter column (C18, 25 cm × 75 μm 1.6 μm) (Ion Optics, Melbourne, Australia) using a 40 min gradient elution (2 to 11% solvent B during 19 min; 11 to 16% during 7 min; 16% to 25% during 4 min; 25% to 80% for 3 min; and, finally, 80% for 7 min to wash the column). Mass spectrometric data were acquired using the parallel accumulation serial fragmentation (PASEF) acquisition method in DDA (data-dependent analysis) mode. The measurements were carried out over the m/z range from 100 to 1700 Th. The range of ion mobilities values were from 0.7 to 1.1 V s/cm$^2$ (1/k0). The total cycle time was set to 1.2 s and the number of PASEF MS/MS scans was set to 6.

Data analysis was performed using MaxQuant software version 2.1.3.0 and searched with the Andromeda search engine against the TrEMBL/Swiss-Prot Pf 3D7 database downloaded from Uniprot on 10 October 2022 (5392 entries) and the *E. coli* BL21-DE3 database downloaded from Uniprot on 10 October 2022 (4173 entries). To search parent mass and fragment ions, we set a mass deviation of 10 ppm for the main search and 40 ppm, respectively. The minimum peptide length was set to 7 amino acids and strict specificity for trypsin cleavage was required, allowing up to 2 missed cleavage sites. Carbamidomethylation (Cys) was set as fixed modification, whereas oxidation (Met) and N-term acetylation (Prot N-term) were set as variable modifications. The false discovery rates (FDRs) at the peptide and protein levels were set to 1%. Scores were calculated in MaxQuant as described previously [44]. The reverse and common contaminants hits were removed from MaxQuant output as well as the protein only identified by site. Proteins were quantified according to the MaxQuant label-free algorithm using LFQ intensities, and protein quantification was obtained using at least 1 peptide per protein. Matching between runs was allowed only with IP samples.

Statistical and bioinformatic analysis, including heatmaps, profile plots, and clustering, were performed with Perseus software (version 1.6.15.0) freely available at www.perseus-framework.org accessed on 10 October 2022 [45]. For statistical comparison, we set four groups, each containing up to 3 biological replicates for the pull-down samples (Control, RVxF, UD, GYF). For the IP samples, we set two groups with 3 biological replicates each (Control, GEXP15). We then filtered the data to keep only proteins with at least 3 and 2 valid values in at least one group for pull-down and IP experiments, respectively. Next, the data were imputed to fill missing data points by creating a Gaussian distribution of random numbers with a standard deviation of 33% relative to the standard deviation

of the measured values and using 3 and 1.8 SD downshift of the mean to simulate the distribution of low signal values for pull-down and IP datasets, respectively. We then performed an ANOVA test (FDR < 0.05, S0 = 1) for the pull-down samples and a statistical *t*-test (FDR < 0.05, S0 = 0.1) for IP samples. Hierarchical clustering of proteins that survived the test was performed in Perseus on LFQ intensities expressed on a logarithmic scale after z-score normalization of the data using Euclidean distances.

## References

1. World Malaria Report 2022. Available online: https://www.who.int/teams/global-malaria-programme/reports/world-malaria-report-2022 (accessed on 3 May 2023).
2. Brautigan, D.L.; Shenolikar, S. Protein Serine/Threonine Phosphatases: Keys to Unlocking Regulators and Substrates. *Annu. Rev. Biochem.* **2018**, *87*, 921–964. [CrossRef] [PubMed]
3. Khalife, J.; Fréville, A.; Gnangnon, B.; Pierrot, C. The Multifaceted Role of Protein Phosphatase 1 in Plasmodium. *Trends Parasitol.* **2020**, *37*, 154–164. [CrossRef] [PubMed]
4. Peti, W.; Nairn, A.C.; Page, R. Structural basis for protein phosphatase 1 regulation and specificity. *FEBS J.* **2012**, *280*, 596–611. [CrossRef] [PubMed]
5. Hendrickx, A.; Beullens, M.; Ceulemans, H.; Abt, T.D.; Van Eynde, A.; Nicolaescu, E.; Lesage, B.; Bollen, M. Docking Motif-Guided Mapping of the Interactome of Protein Phosphatase-1. *Chem. Biol.* **2009**, *16*, 365–371. [CrossRef]
6. Lyons, S.P.; Jenkins, N.P.; Nasa, I.; Choy, M.S.; Adamo, M.E.; Page, R.; Peti, W.; Moorhead, G.B.; Kettenbach, A.N. A Quantitative Chemical Proteomic Strategy for Profiling Phosphoprotein Phosphatases from Yeast to Humans. *Mol. Cell. Proteom.* **2018**, *17*, 2448–2461. [CrossRef]
7. Hollin, T.; De Witte, C.; Fréville, A.; Guerrera, I.C.; Chhuon, C.; Saliou, J.M.; Herbert, F.; Pierrot, C.; Khalife, J. Essential role of GEXP15, a specific Protein Phosphatase type 1 partner, in Plasmodium berghei in asexual erythrocytic proliferation and transmission. *PLoS Pathog.* **2019**, *15*, e1007973. [CrossRef]
8. Hollin, T.; De Witte, C.; Lenne, A.; Pierrot, C.; Khalife, J. Analysis of the interactome of the Ser/Thr Protein Phosphatase type 1 in Plasmodium falciparum. *BMC Genom.* **2016**, *17*, 246. [CrossRef] [PubMed]
9. De Witte, C.; Aliouat, E.M.; Chhuon, C.; Guerrera, I.C.; Pierrot, C.; Khalife, J. Mapping PP1c and Its Inhibitor 2 Interactomes Reveals Conserved and Specific Networks in Asexual and Sexual Stages of Plasmodium. *Int. J. Mol. Sci.* **2022**, *23*, 1069.
10. Fréville, A.; Tellier, G.; Vandomme, A.; Pierrot, C.; Vicogne, J.; Cantrelle, F.X.; Martoriati, A.; Cailliau-Maggio, K.; Khalife, J.; Landrieu, I. Identification of a Plasmodium falciparum inhibitor-2 motif involved in the binding and regulation activity of protein phosphatase type 1. *FEBS J.* **2014**, *281*, 4519–4534. [CrossRef]
11. Daher, W.; Browaeys, E.; Pierrot, C.; Jouin, H.; Dive, D.; Meurice, E.; Dissous, C.; Capron, M.; Tomavo, S.; Doerig, C.; et al. Regulation of protein phosphatase type 1 and cell cycle progression by PfLRR1, a novel leucine-rich repeat protein of the human malaria parasite Plasmodium falciparum. *Mol. Microbiol.* **2006**, *60*, 578–590. [CrossRef]
12. PlasmoDB. Available online: https://plasmodb.org/plasmo/app (accessed on 3 July 2023).
13. Nishizawa, K.; Freund, C.; Li, J.; Wagner, G.; Reinherz, E.L. Identification of a proline-binding motif regulating CD2-triggered T lymphocyte activation. *Proc. Natl. Acad. Sci. USA* **1998**, *95*, 14897–14902. [PubMed]

14. Kofler, M.; Schuemann, M.; Merz, C.; Kosslick, D.; Schlundt, A.; Tannert, A.; Schaefer, M.; Lührmann, R.; Krause, E.; Freund, C. Proline-rich sequence recognition: I. Marking GYF and WW domain assembly sites in early spliceosomal complexes. *Mol. Cell. Proteom.* **2009**, *8*, 2461–2473.

15. Albert, G.I.; Schell, C.; Kirschner, K.M.; Schäfer, S.; Naumann, R.; Müller, A.; Kretz, O.; Kuropka, B.; Girbig, M.; Hübner, N.; et al. The GYF domain protein CD2BP2 is critical for embryogenesis and podocyte function. *J. Mol. Cell Biol.* **2015**, *7*, 402–414. [CrossRef]

16. Sorber, K.; Dimon, M.T.; DeRisi, J.L. RNA-Seq analysis of splicing in Plasmodium falciparum uncovers new splice junctions, alternative splicing and splicing of antisense transcripts. *Nucleic Acids Res.* **2011**, *39*, 3820–3835. [CrossRef]

17. Oberstaller, J.; Otto, T.D.; Rayner, J.C.; Adams, J.H. Essential Genes of the Parasitic Apicomplexa. *Trends Parasitol.* **2021**, *37*, 304–316. [CrossRef]

18. Zhang, M.; Wang, C.; Otto, T.D.; Oberstaller, J.; Liao, X.; Adapa, S.R.; Udenze, K.; Bronner, I.F.; Casandra, D.; Mayho, M.; et al. Uncovering the essential genome of the human malaria parasite Plasmodium falciparum by saturation mutagenesis. *Science* **2018**, *360*, eaap7847. [CrossRef]

19. Patzewitz, E.-M.; Guttery, D.S.; Poulin, B.; Ramakrishnan, C.; Ferguson, D.J.; Wall, R.J.; Brady, D.; Holder, A.A.; Szöodoubleacuter, B.; Tewari, R. An Ancient Protein Phosphatase, SHLP1, Is Critical to Microneme Development in Plasmodium Ookinetes and Parasite Transmission. *Cell Rep.* **2013**, *3*, 622–629. [CrossRef]

20. Muralidharan, V.; Goldberg, D.E. Asparagine Repeats in Plasmodium falciparum Proteins: Good for Nothing? *PLoS Pathog.* **2013**, *9*, e1003488.

21. Muralidharan, V.; Oksman, A.; Iwamoto, M.; Wandless, T.J.; Goldberg, D.E. Asparagine repeat function in a Plasmodium falciparum protein assessed via a regulatable fluorescent affinity tag. *Proc. Natl. Acad. Sci. USA* **2011**, *108*, 4411–4416. [CrossRef] [PubMed]

22. Wakula, P.; Beullens, M.; Ceulemans, H.; Stalmans, W.; Bollen, M. Degeneracy and Function of the Ubiquitous RVXF Motif That Mediates Binding to Protein Phosphatase-1. *J. Biol. Chem.* **2003**, *278*, 18817–18823. [CrossRef]

23. Kofler, M.; Motzny, K.; Beyermann, M.; Freund, C. Novel Interaction Partners of the CD2BP2-GYF Domain. *J. Biol. Chem.* **2005**, *280*, 33397–33402. [CrossRef]

24. Terrak, M.; Kerff, F.; Langsetmo, K.; Tao, T.; Dominguez, R. Structural basis of protein phosphatase 1 regulation. *Nature* **2004**, *429*, 780–784. [CrossRef] [PubMed]

25. Ceulemans, H.; Bollen, M. Functional Diversity of Protein Phosphatase-1, a Cellular Economizer and Reset Button. *Physiol. Rev.* **2004**, *84*, 1–39. [CrossRef]

26. Saitou, N.; Nei, M. The neighbor-joining method: A new method for reconstructing evolutionary trees. *Mol. Biol. Evol.* **1987**, *4*, 406–425. [PubMed]

27. Felsenstein, J. Confidence Limits on Phylogenies: An Approach Using the Bootstrap. *Evolution* **1985**, *39*, 783. [PubMed]

28. Jones, D.T.; Taylor, W.R.; Thornton, J.M. The rapid generation of mutation data matrices from protein sequences. *Comput. Appl. Biosci.* **1992**, *8*, 275–282. [PubMed]

29. Tamura, K.; Stecher, G.; Kumar, S. MEGA11: Molecular Evolutionary Genetics Analysis Version 11. *Mol. Biol. Evol.* **2021**, *38*, 3022–3027. [CrossRef]

30. Toenhake, C.G.; Fraschka, S.A.K.; Vijayabaskar, M.S.; Westhead, D.R.; van Heeringen, S.J.; Bártfai, R. Chromatin Accessibility-Based Characterization of the Gene Regulatory Network Underlying Plasmodium falciparum Blood-Stage Development. *Cell Host Microbe* **2018**, *23*, 557.

31. Oehring, S.C.; Woodcroft, B.J.; Moes, S.; Wetzel, J.; Dietz, O.; Pulfer, A.; Dekiwadia, C.; Maeser, P.; Flueck, C.; Witmer, K.; et al. Organellar proteomics reveals hundreds of novel nuclear proteins in the malaria parasite Plasmodium falciparum. *Genome Biol.* **2012**, *13*, R108. [CrossRef]

32. Cobb, D.W.; Florentin, A.; Fierro, M.; Krakowiak, M.; Moore, J.M.; Muralidharan, V. The Exported Chaperone PfHsp70x Is Dispensable for the Plasmodium falciparum Intraerythrocytic Life Cycle. *Msphere* **2017**, *2*, e00363-17. [CrossRef] [PubMed]

33. Wild, T.; Horvath, P.; Wyler, E.; Widmann, B.; Badertscher, L.; Zemp, I.; Kozak, K.; Csucs, G.; Lund, E.; Kutay, U. A Protein Inventory of Human Ribosome Biogenesis Reveals an Essential Function of Exportin 5 in 60S Subunit Export. *PLoS Biol.* **2010**, *8*, e1000522.

34. Russo, S.J.; Dietz, D.M.; Dumitriu, D.; Morrison, J.H.; Malenka, R.C.; Nestler, E.J. The addicted synapse: Mechanisms of synaptic and structural plasticity in nucleus accumbens. *Trends Neurosci.* **2010**, *33*, 267–276. [PubMed]

35. Kudyba, H.M.; Cobb, D.W.; Vega-Rodríguez, J.; Muralidharan, V. Some conditions apply: Systems for studying Plasmodium falciparum protein function. *PLoS Pathog.* **2021**, *17*, e1009442.

36. Rajaram, K.; Liu, H.B.; Prigge, S.T. Redesigned TetR-Aptamer System To Control Gene Expression in Plasmodium falciparum. *mSphere* **2020**, *5*, e00457-20. [CrossRef]

37. Heinze, M.; Kofler, M.; Freund, C. Investigating the functional role of CD2BP2 in T cells. *Int. Immunol.* **2007**, *19*, 1313–1318. [CrossRef]

38. Srivastava, G.; Bajaj, R.; Kumar, G.S.; Gaudreau-Lapierre, A.; Nicolas, H.; Chamousset, D.; Kreitler, D.; Peti, W.; Trinkle-Mulcahy, L.; Page, R. The ribosomal RNA processing 1B:protein phosphatase 1 holoenzyme reveals non-canonical PP1 interaction motifs. *Cell Rep.* **2022**, *41*, 111726. [CrossRef]

39.  Chamousset, D.; De Wever, V.; Moorhead, G.B.; Chen, Y.; Boisvert, F.-M.; Lamond, A.I.; Trinkle-Mulcahy, L. RRP1B Targets PP1 to Mammalian Cell Nucleoli and Is Associated with Pre-60S Ribosomal Subunits. *Mol. Biol. Cell* **2010**, *21*, 4212–4226. [CrossRef]

40.  Fréville, A.; Cailliau-Maggio, K.; Pierrot, C.; Tellier, G.; Kalamou, H.; Lafitte, S.; Martoriati, A.; Pierce, R.J.; Bodart, J.-F.; Khalife, J. Plasmodium falciparum encodes a conserved active inhibitor-2 for Protein Phosphatase type 1: Perspectives for novel anti-plasmodial therapy. *BMC Biol.* **2013**, *11*, 80.

41.  Trager, W.; Jensen, J.B. Human Malaria Parasites in Continuous Culture. *Science* **1976**, *193*, 673–675. [CrossRef]

42.  Vernes, A.; Williams, J.L.; Diggs, C.L.; Tapchaisri, P.; Dutoit, E.; Haynes, J.D. Plasmodium Falciparum Strain-Specific Human Antibody Inhibits Merozoite Invasion of Erythrocytes. *Am. J. Trop. Med. Hyg.* **1984**, *33*, 197–203. [CrossRef]

43.  Umlas, J.; Fallon, J.N. New thick-film technique for malaria diagnosis. Use of saponin stromatolytic solution for lysis. *Am. J. Trop. Med. Hyg.* **1971**, *20*, 527–529. [CrossRef] [PubMed]

44.  Cox, J.; Mann, M. MaxQuant enables high peptide identification rates, individualized p.p.b.-range mass accuracies and proteome-wide protein quantification. *Nat. Biotechnol.* **2008**, *26*, 1367–1372. [CrossRef] [PubMed]

45.  Tyanova, S.; Temu, T.; Sinitcyn, P.; Carlson, A.; Hein, M.Y.; Geiger, T.; Mann, M.; Cox, J. The Perseus computational platform for comprehensive analysis of (prote)omics data. *Nat. Methods* **2016**, *13*, 731–740. [CrossRef] [PubMed]